



## **Pacer Calibration of F-16D USAF Serial Number 87-0391 (Project Pace Maker)**

**JIMMY A. JONES, Maj, USAF**  
**MICHAEL B. BAKER, Capt, USAF**  
Project Pilots

**ANDREW D. ANDERSON, Capt, USAF**  
Project Manager / Project Engineer  
**JONATHAN P. MAJO, Capt, USAF**  
**JAMES A. PATE, Capt, USAF**  
**CHARLES M. MCNIEL, Capt, USAF**  
Project Engineers

**June 2010**

### **FINAL TECHNICAL INFORMATION MEMORANDUM**


**Approved for public release; distribution is unlimited**

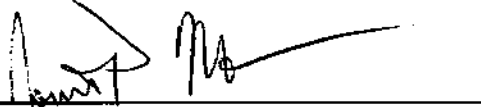
**USAF TEST PILOT SCHOOL  
AIR FORCE FLIGHT TEST CENTER  
EDWARDS AIR FORCE BASE, CALIFORNIA  
AIR FORCE MATERIEL COMMAND  
UNITED STATES AIR FORCE**

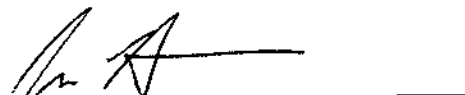
**U  
S  
A  
F  
  
T  
P  
S**


This Technical Information Memorandum (AFFTC-TIM-10-02), Pacer Calibration F-16D USAF serial number 87-0391 (project Pace Maker), was submitted under job order number MT09B300 by the Commandant, USAF Test Pilot School, Edwards AFB, California 93524-6485.


**Prepared by:**


  
ANDREW D. ANDERSON, Capt, USAF  
Project Manager / Flight Test Engineer

  
JONATHAN P. MAJO, Capt, USAF  
Flight Test Engineer

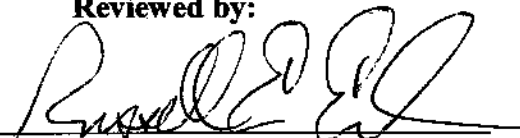
  
JAMES A. PATE, Capt, USAF  
Flight Test Weapons System Officer

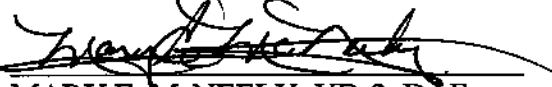
  
CHARLES M. MCNIEL, Capt, USAF  
Flight Test Engineer

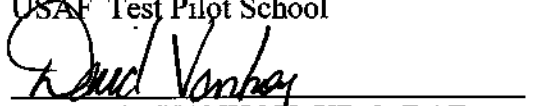
  
JIMMY A. JONES, Maj, USAF  
Flight Test Pilot

  
MICHAEL B. BAKER, Capt, USAF  
Flight Test Pilot


**Reviewed by:**

  
RUSSELL E. ERB, YD-2, DAF  
Performance Branch Master Instructor  
USAF Test Pilot School

  
MARY E. McNEELY, YD-2, DAF  
Test Management Master Instructor  
USAF Test Pilot School

  
DAVID L. VANHOY, YD-3, DAF  
Technical Director  
USAF Test Pilot School

This test plan has been approved for publication.

  
NOEL ZAMOT, Colonel, USAF  
Commandant, USAF Test Pilot School

JAN 19 2011

<b>REPORT DOCUMENTATION PAGE</b>			<i>Form Approved</i> OMB No. 0704-0188	
Public reporting burden for this collection of information is estimated to average 1 hour per response, including the time for reviewing instructions, searching existing data sources, gathering and maintaining the data needed, and completing and reviewing this collection of information. Send comments regarding this burden estimate or any other aspect of this collection of information, including suggestions for reducing this burden to Department of Defense, Washington Headquarters Services, Directorate for Information Operations and Reports (0704-0188), 1215 Jefferson Davis Highway, Suite 1204, Arlington, VA 22202-4302. Respondents should be aware that notwithstanding any other provision of law, no person shall be subject to any penalty for failing to comply with a collection of information if it does not display a currently valid OMB control number. <b>PLEASE DO NOT RETURN YOUR FORM TO THE ABOVE ADDRESS.</b>				
<b>1. REPORT DATE (DD-MM-YYYY)</b> 12-06-2010		<b>2. REPORT TYPE</b> Technical Information Memorandum		<b>3. DATES COVERED (From - To)</b> 8 Mar 10 – 31 Mar 10
<b>4. TITLE AND SUBTITLE</b> Pacer Calibration of F-16D USAF Serial Number 87-0391 (Project Pace Maker)		<b>5a. CONTRACT NUMBER</b>		
		<b>5b. GRANT NUMBER</b>		
		<b>5c. PROGRAM ELEMENT NUMBER</b>		
<b>6. AUTHOR(S)</b> Maj Jimmy A. Jones, USAF, Test Pilot Capt Michael B. Baker, USAF, Test Pilot Capt Andrew D. Anderson, USAF, Flight Test Engineer Capt Jonathan P. Majo, USAF, Flight Test Engineer Capt James A. Pate, USAF, Flight Test Weapons System Officer Capt Charles M. McNeil, Flight Test Engineer		<b>5d. PROJECT NUMBER</b>		
		<b>5e. TASK NUMBER</b>		
		<b>5f. WORK UNIT NUMBER</b>		
<b>7. PERFORMING ORGANIZATION NAME(S) AND ADDRESS(ES)</b> Air Force Flight Test Center 412th Test Wing USAF Test Pilot School 220 South Wolfe Ave Edwards AFB CA 93524-6485		<b>8. PERFORMING ORGANIZATION REPORT NUMBER</b>  AFFTC-TIM-10-02		
		<b>10. SPONSOR/MONITOR'S ACRONYM(S)</b>		
<b>9. SPONSORING / MONITORING AGENCY NAME(S) AND ADDRESS(ES)</b> USAF Test Pilot School 220 South Wolfe Ave Edwards AFB CA 93524-6485		<b>11. SPONSOR/MONITOR'S REPORT NUMBER(S)</b>		
<b>12. DISTRIBUTION / AVAILABILITY STATEMENT</b> Approved for public release; distribution is unlimited				
<b>13. SUPPLEMENTARY NOTES</b> CA: Air Force Flight Test Center Edwards AFB CA CC: 012100				
<b>14. ABSTRACT</b> This report presents the results of test efforts to calibrate F-16D USAF serial number 87-0391 Pitot-static system (Project Pace Maker). The objectives of this project were to determine the calibration of the test aircraft with a flight test noseboom and to calibrate the trailing cone system. The USAF Test Pilot School, Class 09B, conducted eight sorties in an F-16D Block 40 aircraft totaling 13.4 hours at Edwards AFB, CA from 8 March to 31 March 2010. The temperature probe recovery factor for the test aircraft was not determined. All other test objectives were met.				
<b>15. SUBJECT TERMS</b> Pitot-static calibration                      Upwash determination Trailing cone                                      F-16 aircraft				
<b>16. SECURITY CLASSIFICATION OF:</b>		<b>17. LIMITATION OF ABSTRACT</b>	<b>18. NUMBER OF PAGES</b>	<b>19a. NAME OF RESPONSIBLE PERSON</b>
<b>a. REPORT</b> UNCLASSIFIED	<b>b. ABSTRACT</b> UNCLASSIFIED	<b>c. THIS PAGE</b> UNCLASSIFIED	SAME AS REPORT	Russell E. Erb
			142	<b>19b. TELEPHONE NUMBER</b> (661) 277-8829

## **ACKNOWLEDGEMENTS**

The test team wishes to express sincere appreciation to Mr. Vinh Pham for his invaluable technical advice during the planning and execution of this project, and Mr. Chad Bellay for his exceptional photography service. Additionally, the team members wish to thank their families. Without their support, the Pace Maker Test Program would not have been possible.

## EXECUTIVE SUMMARY

This technical information memorandum presents results obtained while executing the Pace Maker test plan. The responsible test organization (RTO) was the 412th Test Wing, Air Force Flight Test Center (AFFTC), Edwards AFB, California. The executing organization was the USAF Test Pilot School. Testing was conducted under job order number (JON) MT09B300. All testing was conducted at AFFTC, Edwards Air Force Base from 8-31 March 2010 and consisted of eight flights totaling 13.4 flight test hours and two chase sorties for an additional 2.9 flight hours.

Pace Maker was a student test management project (TMP) designed and completed by members of Class 09B. F-16D USAF serial number 87-0391 was used for this TMP and calibrated as the test aircraft. It was a Block 40 aircraft equipped with a flight test noseboom, trailing cone system, Data Acquisition System (DAS) and an Advanced Range Data System (ARDS) pod. The primary test objectives were to determine the calibration of the trailing cone system and the calibration of the test aircraft Pitot-static system with a flight test noseboom. Secondary objectives were to determine the effect of the test aircraft angle of attack on the position error corrections of the test aircraft Pitot-static system, determine the temperature probe recovery factor for the test aircraft, and determine the upwash angle at the test noseboom angle of attack vane. The temperature probe recovery factor for the test aircraft was not determined. All other test objectives were met.

A fixed-length trailing cone was used during this test. The trailing cone was designed to measure static air pressure outside of most of the influence of the aircraft using a 62 foot length of pressure tubing trailed behind the aircraft. The tubing was stabilized with a drag cone. A pressure transducer located inside the aircraft measured the static pressure. The trailing cone system and test aircraft Pitot-static system were calibrated at approximately 100 feet above ground level (AGL) using the tower flyby flight test technique (FTT) at Edwards AFB, CA from 11 degrees angle of attack (AOA) to 0.93 Mach number. Weather balloon pressure altitude and ambient air temperature data were used to calibrate the test aircraft Pitot-static system and trailing cone system at 10,000, 20,000, 30,000, 40,000 and 45,000 feet pressure altitude from 11 degrees angle of attack to 1.4 Mach number without the trailing cone and to 0.90 Mach number with the trailing cone attached.

The effect of angle of attack on the aircraft test noseboom Pitot-static position errors was determined. While conducting the FTTs to calibrate the trailing cone system and test aircraft Pitot-static system, different gross weights were tested at different pressure altitudes and airspeeds on multiple sorties. This provided a range of angles of attack, from 11 degrees angle of attack at final approach speeds to near 0 degrees angle of attack at high Mach numbers. Angle of attack effects on the static position error pressure coefficient were characterized.

The Pitot-static position error corrections for the trailing cone system were obtained from the tower flyby FTT and plotted as a function of instrument corrected equivalent airspeed (KEAS). Similar position error correction plots were obtained using the trailing cone at altitudes up to 45,000 feet pressure altitude. Two chase sorties were flown at various test points from 10,000 to 45,000 feet pressure altitude (PA) to collect still photographs to determine trailing cone tube angle of attack at various altitudes and airspeeds. This angle was plotted against KEAS to characterize the relationship between cone tube angle and dynamic pressure.

**This page intentionally left blank.**

## TABLE OF CONTENTS

	<u>Page No</u>
ACKNOWLEDGEMENTS .....	iv
EXECUTIVE SUMMARY .....	v
LIST OF ILLUSTRATIONS .....	viii
LIST OF TABLES .....	xi
INTRODUCTION .....	1
General .....	1
Background .....	1
Test Aircraft Description .....	1
Test Objectives .....	3
TEST AND EVALUATION .....	4
General .....	4
Overall Test Objective .....	4
Procedures .....	4
Calibration of the Trailing Cone System .....	5
Calibration of the Flight Test Noseboom .....	6
Total Air Temperature Probe Recovery Factor .....	9
Upwash at the Test Noseboom AOA Vane .....	10
REFERENCES .....	13
APPENDIX A - DATA FIGURES .....	A-1
APPENDIX B - DATA TABLES .....	B-1
APPENDIX C - DAS DATA PARAMETERS .....	C-1
APPENDIX D - PITOT-STATIC DATA REDUCTION METHODS .....	D-1
APPENDIX E - ABBREVIATIONS AND ACRONYMS .....	E-1
APPENDIX F - DISTRIBUTION LIST .....	F-1

## LIST OF ILLUSTRATIONS

<u>Figure No</u>	<u>Title</u>	<u>Page No</u>
1	Flight Test Noseboom .....	2
2	Temperature Probe .....	2
3	F-16 Reference Points .....	5
4	Measured Trailing Cone Angle .....	5
5	True AOA .....	10

### APPENDIX A

A-1	Trailing Cone Tube AOA (Tower Flyby) .....	A-2
A-2	Trailing Cone Tube AOA (At Altitude) .....	A-3
A-3	Trailing Cone Tube AOA (At Altitude, Expanded View) .....	A-4
A-4	Trailing Cone Tube AOA (All Altitudes) .....	A-5
A-5	Trailing Cone Static Position Error Ratio (All Altitudes) .....	A-6
A-6	Trailing Cone Static Position Error Ratio Best Fits (All Altitudes) .....	A-7
A-7	Trailing Cone Static Position Error Ratio (2,300 feet PA) .....	A-8
A-8	Trailing Cone Static Position Error Ratio (10,000 feet PA) .....	A-9
A-9	Trailing Cone Static Position Error Ratio (20,000 feet PA) .....	A-10
A-10	Trailing Cone Static Position Error Ratio (30,000 feet PA) .....	A-11
A-11	Trailing Cone Static Position Error Ratio (40,000 feet PA) .....	A-12
A-12	Trailing Cone Static Position Error Ratio (40,000 (2) feet PA) .....	A-13
A-13	Trailing Cone Static Position Error Ratio (45,000 PA) .....	A-14
A-14	Trailing Cone Pressure Altitude Position Correction (All Altitudes) .....	A-15
A-15	Trailing Cone Static Position Error Ratio vs. Instrument Corrected Mach Number. .....	A-16
A-16	Trailing Cone Static Position Error Ratio vs. Tube Angle of Attack .....	A-17
A-17	Trailing Cone Static Position Error Ratio vs. Tube Angle of Attack (0.55 Mach) .....	A-18
A-18	Trailing Cone Static Position Error Ratio vs. Tube Angle of Attack (0.72 Mach) .. .....	A-19
A-19	Trailing Cone Static Position Error Ratio vs. Tube Angle of Attack (0.79 Mach) . .....	A-20
A-20	Trailing Cone Tube Angle of Attack vs. Instrument Corrected Mach Number .	A-21
A-21	Static Source Correction .....	A-22
A-22	Noseboom Static Position Error Pressure Coefficient (2,300 ft PA) .....	A-23

## LIST OF ILLUSTRATIONS (Continued)

<u>Figure No</u>	<u>Title</u>	<u>Page No</u>
A-23	Noseboom Static Position Error Pressure Coefficient (10,000 ft PA) .....	A-24
A-24	Noseboom Static Position Error Pressure Coefficient (20,000 ft PA) .....	A-25
A-25	Noseboom Static Position Error Pressure Coefficient (30,000 ft PA) .....	A-26
A-26	Noseboom Static Position Error Pressure Coefficient (40,000 ft PA) .....	A-27
A-27	Noseboom Static Position Error Pressure Coefficient (45,000 ft PA) .....	A-28
A-28	Noseboom Static Position Error Pressure Coefficient Models (2,300 to 45,000 ft PA) .....	A-29
A-29	Noseboom Static Position Error Pressure Coefficient (0.40 Mach).....	A-30
A-30	Noseboom Static Position Error Pressure Coefficient (0.45 Mach).....	A-31
A-31	Noseboom Static Position Error Pressure Coefficient (0.50 Mach).....	A-32
A-32	Noseboom Static Position Error Pressure Coefficient (0.55 Mach).....	A-33
A-33	Noseboom Static Position Error Pressure Coefficient (0.60 Mach).....	A-34
A-34	Noseboom Static Position Error Pressure Coefficient (0.65 Mach).....	A-35
A-35	Noseboom Static Position Error Pressure Coefficient (0.70 Mach).....	A-36
A-36	Noseboom Static Position Error Pressure Coefficient (0.75 Mach).....	A-37
A-37	Noseboom Static Position Error Pressure Coefficient (0.80 Mach).....	A-38
A-38	Noseboom Static Position Error Pressure Coefficient (0.85 Mach).....	A-39
A-39	Noseboom Static Position Error Pressure Coefficient (0.90 Mach).....	A-40
A-40	Noseboom Static Position Error Pressure Coefficient Models (0.40 to 0.90 Mach).. .....	A-41
A-41	Noseboom Static Position Error Pressure Coefficient Models (0.55 to 0.85 Mach).. .....	A-42
A-42	Noseboom Static Position Error Pressure Coefficient (1.10 Mach).....	A-43
A-43	Noseboom Static Position Error Pressure Coefficient (1.15 Mach).....	A-44
A-44	Noseboom Static Position Error Pressure Coefficient (1.20 Mach).....	A-45
A-45	Noseboom Static Position Error Pressure Coefficient (1.25 Mach).....	A-46
A-46	Noseboom Static Position Error Pressure Coefficient Models (1.10 to 1.25 Mach).. .....	A-47
A-47	Noseboom Mach Number Position Correction (2,300 feet PA) .....	A-48
A-48	Noseboom Mach Number Position Correction (10,000 to 45,000 ft PA, below 0.95M) .....	A-49

## LIST OF ILLUSTRATIONS (Continued)

<u>Figure No</u>	<u>Title</u>	<u>Page No</u>
A-49	Noseboom Mach Number Position Correction (10,000 to 45,000 ft PA, ..... above 1.05M) .....	A-50
A-50	Noseboom Mach Number Position Correction Models (2,300 ft to 45,000 ft PA) .....	A-51
A-51	Noseboom Pressure Altitude Position Correction (2,300 ft PA).....	A-52
A-52	Noseboom Pressure Altitude Position Correction (10,000 - 45,000 ft PA,..... below 0.95M) .....	A-53
A-53	Noseboom Pressure Altitude Position Correction (10,000 - 45,000 ft PA,..... above 1.05M) .....	A-54
A-54	Noseboom Pressure Altitude Position Correction Models (2,300 to 45,000 ft PA) .. .....	A-55
A-55 - 73	Temperature Probe Recovery Factor and Bias .....	A-56 - 74
A-74 - 75	Temperature Probe Recovery Factor and Bias Comparison.....	A-75 - 76
A-76 - 90	Temperature Probe Recovery Factor and Ambient Temperature .....	A-77 - 91
A-91	Noseboom Upwash Angle at AOA Vane (2,300 ft to 45,000 ft PA) .....	A-92
<b>APPENDIX D</b>		
D-1	Transducer Trigonometric Relationships .....	D-2

## LIST OF TABLES

<u>Figure No</u>	<u>Title</u>	<u>Page No</u>
<b>APPENDIX B</b>		
B-1	Altitude-Based Noseboom Static Position Error Pressure Coefficient Model (0.3M to 0.48M) .....	B-2
B-2	Altitude-Based Noseboom Static Position Error Pressure Coefficient Model (0.485M to 0.665M) .....	B-3
B-3	Altitude-Based Noseboom Static Position Error Pressure Coefficient Model (0.67M to 0.85M) .....	B-4
B-4	Altitude-Based Noseboom Static Position Error Pressure Coefficient Model (0.855M to 1.035M) .....	B-5
B-5	Altitude-Based Noseboom Static Position Error Pressure Coefficient Model (1.04M to 1.22M) .....	B-6
B-6	Altitude-Based Noseboom Static Position Error Pressure Coefficient Model (1.225M to 1.4M) .....	B-7
B-7	Noseboom Static Position Error Pressure Coefficient vs. AOA Curve Fit Equations .....	B-8
B-8	Tower Fly By Total Air Temperature Probe Recovery Factor and Bias.....	B-9
B-9	At Altitude Temperature Probe Recovery Factor, Bias & Ambient Air Temperature Error .....	B-9
B-10	Total Air Temperature Probe Recovery Factor Comparison .....	B-9
B-11	Calculated versus Weather Balloon Ambient Air Temperatures .....	B-9
<b>APPENDIX C</b>		
C-1	DAS Data Parameters.....	C-2

**This page intentionally left blank.**

# **INTRODUCTION**

## **General**

The objective of the test program was to calibrate F-16D USAF serial number (S/N) 87-0391 as a pacer aircraft for the Air Force Flight Test Center (AFFTC). The temperature probe recovery factor for the test aircraft was not determined. All other test objectives were met. The responsible test organization (RTO) was the 412th Test Wing, AFFTC, Edwards AFB, California. The executing organization was the USAF Test Pilot School. Testing was conducted under job order number (JON) MT09B300. All testing was conducted at AFFTC, Edwards Air Force Base from 8-31 March 2010 and consisted of eight F-16D flights totaling 13.4 flight test hours, and two chase sorties for an additional 2.9 flight hours.

## **Background**

In 2009 the AFFTC had been without a true pacer aircraft for several years. Multiple attempts to calibrate a pacer aircraft had been started but not completed for various reasons. Previous testing and calibration had been accomplished on F-16D USAF S/N 87-0391 by the 445th Flight Test Squadron in 2009; however, insufficient data were collected from 400 KCAS to 0.95 Mach number. USAF TPS was asked to continue the calibration effort of aircraft 87-0391 as part of a student test management project (TMP).

## **Test Aircraft Description**

The aircraft used in this evaluation was a Block 40 F-16D, USAF S/N 87-0391. This aircraft was powered by a single F110-GE-100B afterburning turbofan engine with a maximum uninstalled static thrust of approximately 28,000 pounds. The aircraft was configured with two 370 gallon fuel tanks on stations 4 and 6, LAU-129/A missile rails on stations 1 and 9, and an ARDS pod on the left wingtip (station 1). Stations 2, 3, 7 and 8 were empty. For a complete description of the aircraft, refer to the F-16D Flight Manual and the F-16D Supplemental Flight Manual, references 1 and 2.

## **Trailing Cone System**

A fixed-length trailing cone system was installed on the aircraft. The system consisted of an anchor fixture, a pressure transducer, Nylaflow™ pressure tubing reinforced with a steel cable, a heat-resistant Kevlar fire sleeve, a stainless steel static pressure sensing sleeve, or tube, and a drag cone. The system was attached to the aft tip of the vertical stabilizer in the location of the radar threat warning system, which was removed to accommodate the trailing cone system anchor fixture. A Paroscientific™ 0 to 15 pounds per square inch, absolute (psia) pressure transducer was installed inside the anchor fixture.

The trailing cone assembly had a length of approximately 52 feet between the anchor point and the front of the static sleeve. The overall length of the assembly, from the anchor point to the back of the trailing cone, was approximately 62 feet. The first 30 feet of the Nylaflow™ tubing was covered with 0.125-inch thick Kevlar™ fire sleeve to protect against heat damage from the engine exhaust. The fire sleeve was fastened to the tubing with a hose clamp near the anchor point. The other end of the fire sleeve was sealed with epoxy to prevent fraying. The 10 inch diameter trailing cone was made of carbon fiber and weighed approximately one pound. It was painted flight test orange to enhance visibility. For data quality reasons, flight through visible moisture was prohibited.

### **C2B GLite GPS System**

The C2B GLite was a highly accurate positioning system developed by the Time Space Position Information (TSPI) department of the AFFTC. The system integrates GPS receivers and Ring-Laser-Gyro Inertial Measurement Unit (IMU) sensors to produce a blended, real-time position, velocity, acceleration and attitude solution. C2B GLite measurements, trajectory data and system status information were recorded on an internal flash solid-state recorder for post-flight processing. The C2B GLite system produced a position accuracy of 10.0 feet, velocity accuracy of 0.3 ft/sec, acceleration accuracy of 0.3 ft/s<sup>2</sup>, and attitude accuracy of 0.5 degrees.

### **Flight Test Noseboom Air Data System**

The air data system in aircraft 87-0391 was modified with a Yaw, Angle-of-attack, and Pitot-Static (YAPS) flight test noseboom. This boom included a compensated Pitot-static tube, as well as AOA and angle of sideslip vanes (figure 1). Two probes mounted on the underside of the forebody strake provided total air temperature (figure 2). Static ports were located near the tip of the noseboom. Total and static pressures, AOA, and total air temperature from the exterior air data equipment were provided to a central air data computer (CADC) and the DAS. More information about the air data system can be found in the F-16 Flight Manual (reference 1) and F-16C/D Support Fleet Modification Flight Manual (reference 3).

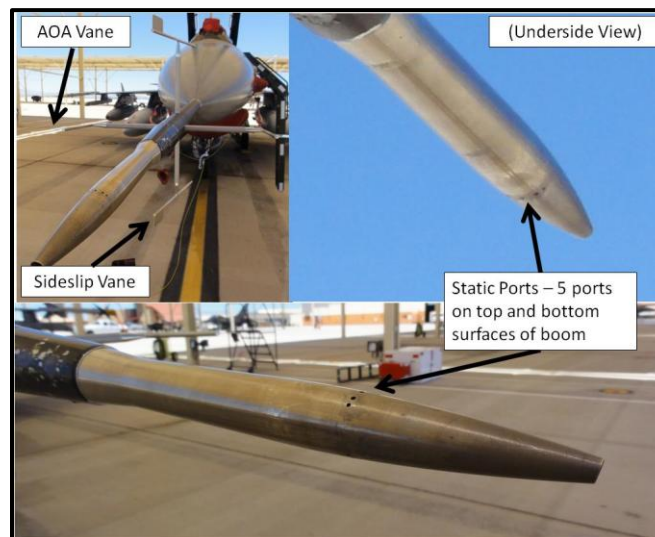


**Figure 1. Flight Test Noseboom**



**Figure 2. Temperature Probe**

### **Data Acquisition System**

Aircraft 87-0391 was modified with a DAS built by Teletronics Technology Corporation. The main components of the system were located in the gun bay area of the F-16. The DAS measured, recorded and transmitted approximately 40 data parameters, listed in appendix C. Internal and external transducers collected data which were then recorded on a solid-state data card for post-flight analysis. The recorder was operated by a control panel located in the aft cockpit. Additionally, an OQO™ cockpit data display was installed in the rear cockpit which displayed DAS data parameters for hand-held data recording. Further details regarding the DAS can be found in the F-16C/D Support Fleet Modification Flight Manual (reference 3).

### **Test Objectives**

The test objectives were to:

1. Determine the calibration of the trailing cone system.
2. Determine the calibration of the test aircraft Pitot-static system with flight test noseboom.
3. Determine the temperature probe recovery factor for the test aircraft.
4. Determine the upwash at the test noseboom AOA vane.

The temperature probe recovery factor for the test aircraft was not determined. All other test objectives were met.

# **TEST AND EVALUATION**

## **General**

The test was conducted with USAF F-16D aircraft 87-0391 during eight sorties totaling 13.4 flight test hours, and two chase sorties for an additional 2.9 flight test hours. All testing was conducted at Edwards Air Force Base, CA from 8-31 March 10 and flown in the R-2508 airspace complex.

## **Overall Test Objective**

The overall test objectives were to determine the calibration of the trailing cone system and the calibration of the test aircraft Pitot-static system with flight test noseboom.

## **Procedures**

### **Overall Administration**

Each flight began with a standard aircraft walk-around. Special interest was paid to the integrity of additional systems on the aircraft such as the trailing cone. Ground checks consisted of standard F-16 aircraft start-up and ground checks as well as a check of the OQO™ cockpit data display. Instrumentation personnel supported the take-off and landing portions of test.

### **Tower Flyby**

The test aircraft was flown across the lakebed tower flyby line at predetermined speeds and a target altitude of 100 feet AGL. Abeam the tower position, the aircrew evented the DAS while flyby tower personnel recorded grid readings of the noseboom transducer, tower ambient temperature and tower ambient pressure. At altitude, aircraft data were recorded on the DAS using trailing cone and noseboom transducer data. As the aircraft passed the tower flyby line, personnel in the tower used the tower gridlines to spot the altitude of the fuselage just forward of and below the canopy leading edge, the approximate location of the test aircraft pressure transducers for the flight test noseboom. At the time of passing, local pressure and temperature measurements were recorded utilizing the Setra™ and Druck™ pressure transducers and calibrated thermocouples supplied by the 773<sup>rd</sup> TS/ENFB. Additionally, these measurements were recorded every 5 minutes between aircraft passes for a history of trend data. Photographs were collected by base photography personnel in the flyby tower and were processed to determine trailing cone tube angle of attack.

### **Altitude Sorties (10,000-45,000 Feet Pressure Altitude)**

All altitude sorties (with the exception of the final sortie) were flown with a trailing cone system attached to the aircraft. These sorties consisted of points where trailing cone and noseboom pressure readings as displayed on the OQO™ computer system in the rear cockpit were stable in altitude. The static pressure at the trailing cone and noseboom static ports was recorded and compared to weather balloon ambient pressure data. Post-flight analysis was used to determine aircraft static position error for various angles of attack, as well as upwash angle at the test noseboom AOA vane. Still photographs from the chase aircraft during altitude/trailing cone sorties were used to determine trailing cone tube angle of attack at various airspeeds and altitudes.

## Calibration of the Trailing Cone System

For a discussion of the trailing cone Pitot-static data reduction methods, reference appendix D.

### RELATIONSHIP BETWEEN TRAILING CONE TUBE AOA AND KEAS

Three plots of the trailing cone's relationship of tube AOA and KEAS are provided in figures A-1, A-2, and A-3. Figure A-1 presents trailing cone tube AOA versus KEAS for tower flyby data. Figure A-2 presents trailing cone tube AOA versus KEAS for altitude data. Figure A-3 presents trailing cone tube AOA versus KEAS at all altitudes.

The trailing cone equipped aircraft was photographed at stabilized test points from the flyby tower or a chase F-16D. The camera recorded GPS time to the nearest second to correlate the picture to the DAS data. The aircraft parameters were retrieved from the recorded DAS data. The trailing cone tube angle was measured between the predetermined F-16 reference line (see figure 3), and the line made by the section of the trailing cone containing the pitot static ports (see figure 4). The trailing cone AOA was calculated by subtracting  $4.503^\circ$  from the trailing cone tube line in figure 4.

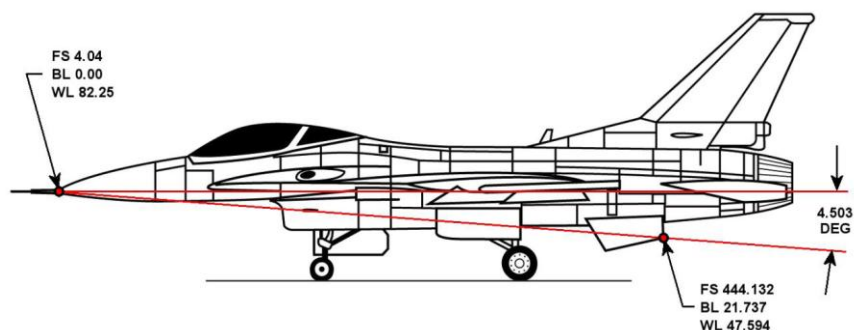


**Figure 3. F-16 Reference Points**

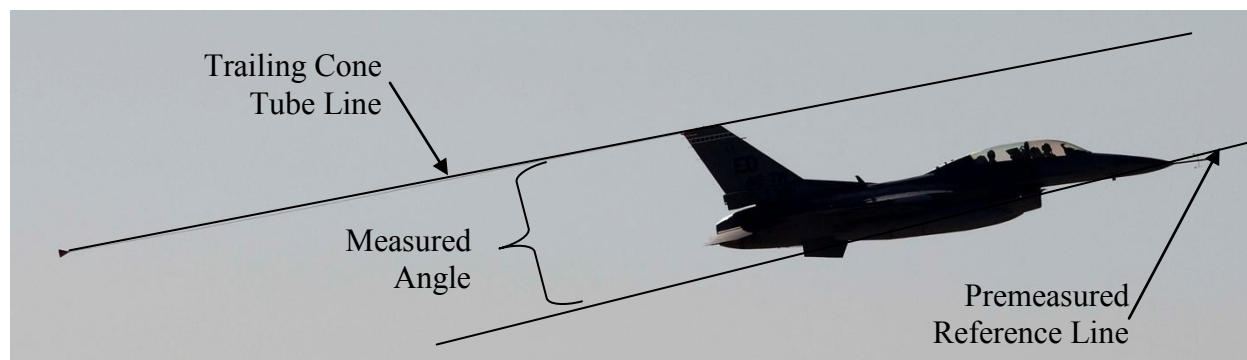


**Figure 4. Measured Trailing Cone Angle**

Data were recorded on each tower flyby run and at 10,000, 20,000, 30,000, 40,000 and 45,000 feet at airspeeds ranging from 11-degrees AOA through 0.90 Mach number.

The relationship between the trailing cone tube AOA and KEAS remained constant ( $\pm 1$  degree data scatter above 300 KEAS), independent of pressure altitude or Mach number<sup>1</sup>. There was a noticeable

<sup>1</sup> At a given KEAS between 200 and 230 KEAS, the tube AOA was approximately 3 to 4 degrees higher at 10,000 feet than at 45,000 feet, Figure A-2. Figure A-3 shows that this was most likely data scatter and not a true trend.

reduction in trailing cone tube AOA as the altitude increased from 10,000 through 45,000 feet PA as a function of KEAS. However, all of the altitude data points overlay with the tower flyby data points. The six airspeed points at two different weights consistently produced lower AOA values for lower aircraft gross weights. The spread in aircraft AOA data at a given KEAS were consistent with change in aircraft gross weight and not with altitude effects.

## **DETERMINATION OF THE TEST TRAILING CONE STATIC POSITION ERROR RATIO**

The trailing cone's static position error ratio ( $\Delta P_p/P_s$ ) was defined as  $(P_s - P_a)/P_s$ , where  $P_s$  was the instrument corrected ambient pressure and  $P_a$  was the truth ambient pressure. No calibration was applied to the pressure transducer measurements based on their temperature; therefore, throughout the analysis,  $P_s$  was equivalent to  $P_{s,ic}$ . Plots of trailing cone static position error ratio data are provided in appendix A (figures A-5 to A-13). Data were collected in both trailing cone tower flyby operations as well as sorties at altitude to calculate the trailing cone static position error ratio. Grid measurements and a GPS-aided C2B G-Lite system served as the truth source for the aircraft geometric altitude (corrected for pitch angle effects). Truth pressure and temperature data at altitude were obtained from Rawinsonde weather balloons. Using geometric altitude as a lookup, the test day ambient air pressure recorded by the balloon was compared to the trailing cone static pressure.

It was predicted that the static position error ratio would increase as Mach number increased, within an interval bound of  $\pm 0.0015$ . Test observations at varying altitudes did not collapse onto a single curve, but they did show deviations within the bounds of predicted values. At instrument corrected equivalent airspeeds (KEAS) from 170 KEAS to 200 KEAS, values ranged from -0.006 to 0.000, with the high altitude data points falling outside the predicted bounds. From 200 to 580 KEAS, some of the test values fell within the predicted bounds with values for  $\Delta P_p/P_s$  ranging between -0.002 and +0.003.

Data from all altitudes were used to fair the best fit line and 95% prediction intervals were plotted to assist in determining the range in which data fell surrounding the best fit line. Data collected at higher altitudes (40,000 feet PA and more notably, 45,000 feet PA) had a higher probability of falling outside of the prediction interval bounds. Analyses indicate that  $\Delta P_p/P_s$  was not solely a function of KEAS and that calibrations based solely on tower flyby data would not be accurate at higher altitudes. It is worth noting that previous test results for the trailing cone differ from the results obtained in this test.

A plot of the trailing cone altitude position correction is included in appendix A (figure A-14). A plot of  $\Delta P_p/P_s$  versus Mach number and tube angle of attack versus Mach number are included in figures A-15 and A-20, respectively. Plots of  $\Delta P_p/P_s$  versus tube angle of attack are included in figures A-16 through A-20.

## **Calibration of the Flight Test Noseboom**

For a discussion of the test noseboom Pitot-static data reduction methods, reference appendix D.

## **FLIGHT TEST NOSEBOOM PITOT-STATIC POSITION ERROR CORRECTIONS**

The two static systems in the pacer aircraft (from the test noseboom) were similar to one another, and with regard to pressure altitude, system two almost always indicated a higher altitude than did system one. The difference between the two was consistent, with the exception of the transonic region between 0.98 Mach number and 1.05 Mach number, where the disparity increased to approximately 55 feet. At 10,000 feet PA, a correction of +1.9 feet was applied to system two to match system one, and at 45,000 feet, a correction of +4.1 feet for system two was required to match system one. Reference figure A-21 for a

depiction of the static system errors and the necessary corrections at the test altitudes. Due to occasional data dropouts in-flight from system two, all data analysis was conducted using the information gathered from system one. **In-flight calibrations and post-flight Pitot-static analysis should use data from system 1. (R1)**

## TEST NOSEBOOM STATIC POSITION ERROR PRESSURE COEFFICIENT

### Mach Number vs. Instrument Corrected Pressure Altitude Analysis

The noseboom static position error pressure coefficient data are presented in appendix A, figures A-22 through A-27. Contrary to predictions, the data from varying altitudes did not collapse onto a single curve (independent of the aircraft AOA), and between 2,300 and 45,000 feet, there were deviations in  $\Delta P_p/q_{cic}$  of up to  $\pm 0.01$  (equivalent to approximately a 100-foot disparity in the altitude position correction,  $\Delta H_{pc}$ ). Above 1.05 Mach number, the data were more consistent, but they still contained a differential in  $\Delta P_p/q_{cic}$  of  $\pm 0.005$  (a shift of approximately 50 feet). The tower flyby data (figure A-16) contained the least internal scatter; although, below 0.40 Mach number (at higher aircraft AOA), dispersion increased by a factor of six. At 10,000 and 20,000 feet PA, data scatter was minimal at all airspeeds (subsonic, transonic, and supersonic). At and above 30,000 feet PA, two unique problems were encountered. First, all data suffered from large dispersion at subsonic speeds, likely due to changes in AOA<sup>2</sup>. In all cases, the data collected on 16 March was the most internally consistent; therefore, it was more heavily weighted during the model-creation process. Second, on 31 March, level acceleration data collected at 30,000 feet PA and above presented strange subsonic “hooks,” which offset the value of  $\Delta P_p/q_{cic}$  by more than 400 percent from baseline values (see figures A-25 to A-27). Potential causes include faulty weather balloon data, lag in the noseboom pressure system due to rapid acceleration, or atmospheric disturbances due a passing weather front. No one case could be uniquely identified as the source of the anomaly; therefore, no correction could be applied. As such, the “hooks” in the  $\Delta P_p/q_{cic}$  data were disregarded during analysis. They are included in the appropriate figures for completeness.

Taken as a whole, no single model based solely on instrument corrected pressure altitude and Mach number could be created for the entire envelope, and unique hand-faired curves were fit to the data at each altitude tested (see figure A-28 and tables B-1 through B-6). Models created for 2,300, 10,000 and 20,000 feet PA had a maximum offset in  $\Delta P_p/q_{cic}$  from actual data of  $\pm 0.005$ ; although, the mean error was approximately  $\pm 0.001$ . At and above 30,000 feet PA, the maximum disparity between model and actual data was  $\pm 0.012$ , and the average was  $\pm 0.003$ . As was previously discussed, in all cases the model was least accurate at low Mach numbers, where AOA effects were believed to have a dominant impact.

### Mach Number vs. True Angle of Attack Analysis

Angle of attack effects on the flight test noseboom pitot-static corrections were analyzed from 11 degrees true AOA to 1.8 degrees true AOA ( $\alpha_T$ ). The AOA was varied by flying at different gross weights at different altitudes and Mach numbers.

Figures A-29 through A-39 are plots of the static position error pressure coefficient ( $\Delta P_p / q_{cic}$ ) as a function of true AOA ( $\alpha_T$ ) for various instrument corrected Mach numbers ( $M_{ic}$ ) from 0.40 to 0.90 Mach number. Figures A-40, A-41 and A-46 are compilations of the hand faired curve fits of the data for 0.40, 0.50, 0.60, 0.70, 0.80 and 0.90 Mach number, 0.55, 0.65, 0.75 and 0.85 Mach number and 1.10, 1.15, 1.20 and 1.25 Mach number, respectively. These sets of families of curves show the data trend for these Mach numbers. Each hand faired curve for the subsonic data points is a second order polynomial that was fit to the data from the lowest to the highest AOA values for the given Mach number. The hand faired curves for the supersonic data points are linear. The data for 0.45 Mach number were limited to only a few points, thus the curve fit for that Mach number was linear instead of polynomial. The equations for the

---

<sup>2</sup> The impact of AOA on the calibration curves is discussed in the following section.

curve fits for static position error pressure coefficients versus AOA are given in table B-7. The data for each discrete Mach number were selected at that Mach number plus or minus 0.01 Mach number. Thus, for example, the 0.70 Mach number plot included data points from 0.69 to 0.71 Mach number. For the gaps in Mach numbers between those that are included in curve fits, the static position error pressure coefficients for each AOA can be determined either by using the curve fit from the nearest Mach number or by interpolating a value between curve fits for Mach numbers on either side.

For a given subsonic Mach number, each plot shows a trend of decreasing static position error pressure coefficient with increasing AOA. The curve fits for each subsonic Mach number establish a family of curves that show a trend toward lower positive AOA's and lower, then negative static position error pressure coefficients as Mach number increases. The curve fits are generally separated by similar spreads. All curve fits started with positive static position error pressure coefficients and transitioned to negative values except for the 0.90 Mach number curve, which had negative static position error pressure coefficients for all AOA's at that test Mach number.

For a given supersonic Mach number, the plots show a trend of decreasing static position error pressure coefficient with increasing AOA as well. All static position error pressure coefficients were negative for the full spectrum of AOA's at these supersonic data points. The family of curves for supersonic conditions shown in figure A-46 shows decreasing magnitude for static position error pressure coefficient as Mach number increases which correlates to the trend seen in the data for static position error pressure coefficient versus Mach number for supersonic data.

### Method Comparison

The static position error pressure coefficient models based on  $M_{ic}$  and pressure altitude are extremely accurate at Mach numbers above 0.80; however, they fail to adequately model  $\Delta P_p / q_{cic}$  at lower airspeeds, where there are non-trivial disparities between the model and test data. Models based on  $M_{ic}$  and  $\alpha_T$  do not perfectly match the test data at any Mach number; however, they provide a more consistent offset across the range of useful airspeeds. Given the expected Mach range that the pacer aircraft will be operating within (0.60 to 0.95 Mach number), AOA is the most logical choice as a reference to determine  $\Delta P_p / q_{cic}$  in that regime. **Below 0.95  $M_{ic}$ , look up  $\Delta P_p / q_{cic}$  based on true angle of attack ( $\alpha_T$ ) and  $M_{ic}$ . Above 0.95  $M_{ic}$  look up  $\Delta P_p / q_{cic}$  based on pressure altitude and  $M_{ic}$ . (R2)**

### MACH NUMBER AND ALTITUDE POSITION CORRECTIONS

During the calculation of the static position error pressure coefficient, Mach number ( $\Delta M_{pc}$ ) and pressure altitude ( $\Delta H_{pc}$ ) position corrections were determined at all altitudes and airspeeds tested. The Mach number position correction was never more than  $\pm 0.0025$ , below 0.95  $M_{ic}$ , and it reached a maximum magnitude of -0.0218 at Mach 1.06 and 45,000 feet PA. At subsonic speeds, the largest disparity in  $\Delta M_{pc}$  at different altitudes occurred at 0.65  $M_{ic}$ , where the spread was 0.008 (see figure A-48). In supersonic flight, the disparity was essentially constant and equal to 0.0055 for all instrument corrected Mach numbers (see figure A-49). Models for  $\Delta M_{pc}$  are shown in figure A-50.

The altitude position correction remained less than  $\pm 57$  feet below 0.95  $M_{ic}$ , achieving a maximum magnitude of -668 feet at 1.045 Mach number and 10,000 feet PA. At subsonic speeds, the largest disparity in  $\Delta H_{pc}$  at different altitudes occurred at 0.70  $M_{ic}$ , where the spread was 155 feet (see figure A-52). At supersonic speeds, the disparity was essentially constant and equal to 100 feet for all instrument corrected Mach numbers (see figure A-53). Models for  $\Delta H_{pc}$  are depicted in figure A-54.

## Total Air Temperature Probe Recovery Factor

Total temperature values were collected from the F-16D DAS during four tower flyby and four “at altitude” sorties. There were two total air temperature probes instrumented on the aircraft. Due to temperature probe one producing unreliable data, only total temperature values collected from sensor two were used to calculate the temperature recovery factor and bias. Truth ambient air temperatures were determined during the tower flyby sorties by taking the average of two thermocouples that were located in the tower. Truth ambient air temperatures for sorties at altitude were determined from two weather balloon data sets through a two-dimensional linear interpolation of both geometric altitude and time-of-day, corresponding to the aircraft’s exact time and geometric altitude during the sortie.

The temperature recovery factor,  $K_t$ , and bias,  $T_{bias}$ , of the DAS were related via the following equation:

$$\frac{T_{ic}}{T_a} - 1 = (K_t \frac{M^2}{5}) + T_{bias}$$

In figures A-55 through A-73, the instrument corrected total air temperature parameter ( $\frac{T_{ic}}{T_a} - 1$ ) was plotted against the position corrected Mach parameter ( $\frac{M_{pc}^2}{5}$ ), where the slope of the data points represented  $K_t$  and the intercept on the vertical axis represents  $T_{bias}$ . For these data, the linear fit revealed values for  $K_t$  and  $T_{bias}$  and are shown in tables B-8 and B-9. Because the difference between the temperature probe recovery factor and bias between the easterly and westerly runs was significant at the same altitude for each pass during the supersonic level acceleration sortie, that particular data was not further analyzed (see figures A-74 and A-75).

A calculated instrument corrected total temperature  $T_{ic, calc}$  was determined using the above expression and setting Mach equal to zero resulting in the following equation.

$$T_{ic, calc} = T_a [T_{bias} + 1]$$

Using this expression along with the temperature bias from table B-9, an ambient air temperature error  $T_{a, error}$  was calculated for each test sortie at each altitude using the expression below.

$$T_{a, error} = T_{ic, calc} - T_a$$

The ambient air temperature ( $T_a$ ) came from the weather balloon data. The error represents the difference between the calculated instrument corrected total temperature and ambient temperature at Mach equal to zero, and the overall results are listed in table B-9. The ambient temperature error was not calculated for the tower flyby sorties due to the temperature change that occurred at 100 ft AGL over the course of the sortie.

Ambient air temperatures were calculated for the up-and-away test points by plotting ( $\frac{1}{T_{ic}}$ ) on the vertical axis versus ( $\frac{M^2}{5 * T_{ic}}$ ) on the horizontal axis. One plot per altitude per flight was generated for each up-and-away altitude and the results are shown in figures A-76 through A-90. The inverse of the vertical axis intercept was the calculated test day ambient air temperature while the slope of the linear fit represented the recovery factor times minus one. The temperature recovery factors for each sortie and altitude using this alternate plotting technique were compared to the temperature recovery factors that were generated

using the traditional method and are shown in B-10. The calculated ambient air temperatures for each sortie and altitude were also compared to the weather balloon ambient air temperatures in table B-11.

The temperature recovery factors and bias for the tower fly by and at altitude sorties showed a relatively large spread in the results. The alternate plotting technique generated a slightly different temperature recovery factor than the traditional method. As compared to the weather balloon data (truth source), the calculated ambient temperatures fell anywhere from 9 degrees too low to 5 degrees too high. Overall, due to the spread in the data in tables B8-B11, a single value for the total air temperature probe recovery factor could not be determined.

## Upwash at the Test Noseboom AOA vane

The test team predicted that despite being well forward of the wings the test noseboom would still be affected as the incoming airstream “saw” the boom, fuselage and wing. The airstream would thus be deflected in pitch before reaching the AOA vanes on the noseboom. The predicted effect was a small but measureable correction to the angle of attack ( $\Delta\alpha_u$ ) as measured by the AOA vane on the boom ( $\alpha_v$ ).

True AOA represents the angular difference between the aircraft’s reference line and the relative wind. It was found by subtracting the airflow flight path angle ( $\gamma$ ) angle from the angle between the aircraft’s reference line and the horizon,  $\theta$ , as measured by the INS (see figure 5). Flight path angle was calculated from true airspeed and C2B G-Lite measured geometric rate-of-climb, assuming no vertical movement in the surrounding air mass.

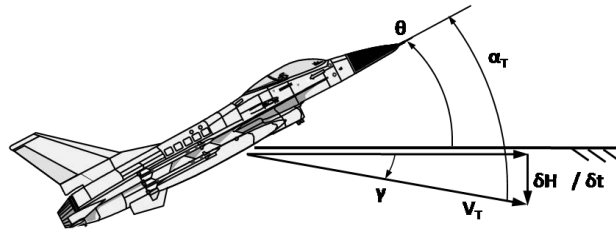


**Figure 5. True AOA**

The true AOA was then calculated by using the following equation:

$$\alpha_t = \theta - \gamma$$

During ground checkout, the test noseboom AOA vane was corrected for alignment errors. DAS measured AOA during flight test was recorded with respect to the fuselage reference line. Vane AOA values were not corrected for fuselage bending or noseboom bending. Vane AOA was adjusted for pitch rate by iterating the following equation:

$$\alpha_{v,q} = \tan^{-1} \left( \tan \alpha_v + \frac{qL_{x\alpha}}{V_t \cos \alpha_{v,q}} \right)$$

where

$\alpha_{v,q}$  = vane angle of attack corrected for pitch rate (radians)

$\alpha_v$  = vane angle of attack (radians)

$q$  = pitch rate (radians per second)

$L_{x\alpha}$  = distance from center of gravity (cg) to angle of attack (AOA) vane (23 feet)

$V_t$  = true airspeed (feet per second)

Magnitudes of pitch rate corrections varied, but were typically less than 0.5 degrees. Upwash angle was then calculated by:

$$\Delta\alpha_u = \alpha_t - \alpha_{v,q}$$

Upwash angle as a function of AOA vane angle of attack is shown in figure A-91. Though scattered, the data show a generally negative trend in upwash angle with increasing AOA. It should be noted that during analysis, vane AOA was observed to shift occasionally by upwards of 0.4 degrees every 0.10 seconds, and that could account for the vast majority of the data scatter. If future testing is conducted, investing in a higher-resolution AOA system and/or modeling the resonance of the AOA vane would likely provide results of improved quality.

**This page intentionally left blank.**

## **REFERENCES**

1. Flight Manual, USAF Series F-16 C/D Aircraft Blocks 40, 42, 50 and 52, Technical Order 1F-16CM-1, Lockheed Martin Corporation, 15 November 2008.
2. Supplemental Flight Manual, USAF Series F-16 C/D Aircraft Blocks 40, 42, 50 and 52, Technical Order 1F-16CM-1-2, 15 October 2008.
3. F-16 C/D Support Fleet Modification Flight Manual, 26 September 2007, Change 5, 31 January 2009.
4. USAF Test Pilot School Pitot-Statics Text (Draft), March 2005.

**This page intentionally left blank.**

## **APPENDIX A – DATA FIGURES**

# Trailing Cone Tube AOA (Tower Flyby)

Aircraft: F-16D, S/N 87-0391 (ARDS Pod on Station 1 and 370 Gallon Fuel Tanks on Stations 4 and 6)

Configuration: Cruise (Gear Up / Flaps Up)

Data Basis: Flight Test (Test Day Data) / 11-31 Mar 2010

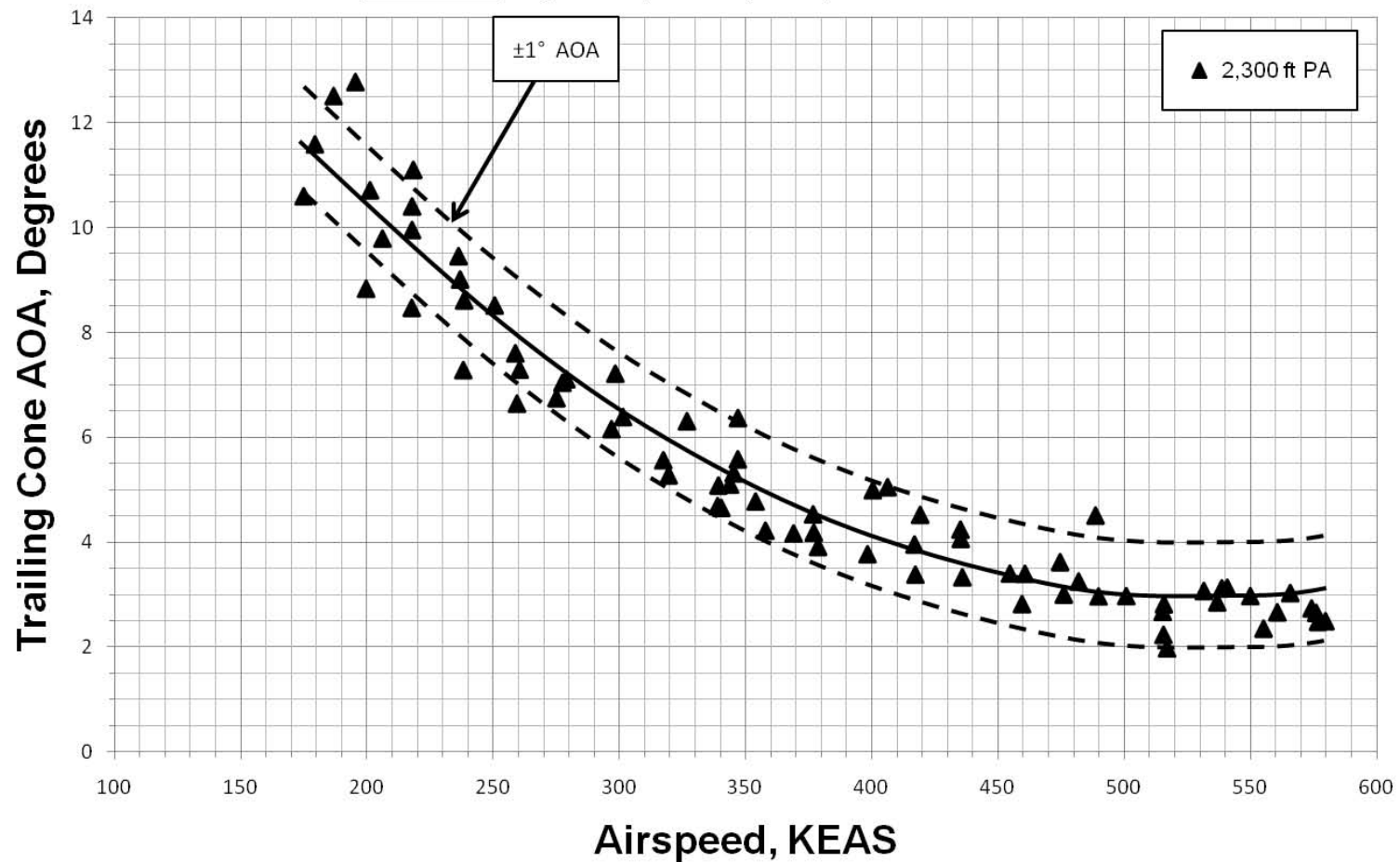


Figure A-1. Trailing Cone Tube AOA (Tower Flyby)

# Trailing Cone Tube AOA (Altitude)

Aircraft: F-16D, S/N 87-0391 (ARDS Pod on Station 1 and 370 Gallon Fuel Tanks on Stations 4 and 6)

Configuration: Cruise (Gear Up / Flaps Up)

Data Basis: Flight Test (Test Day Data) / 11-31 Mar 2010

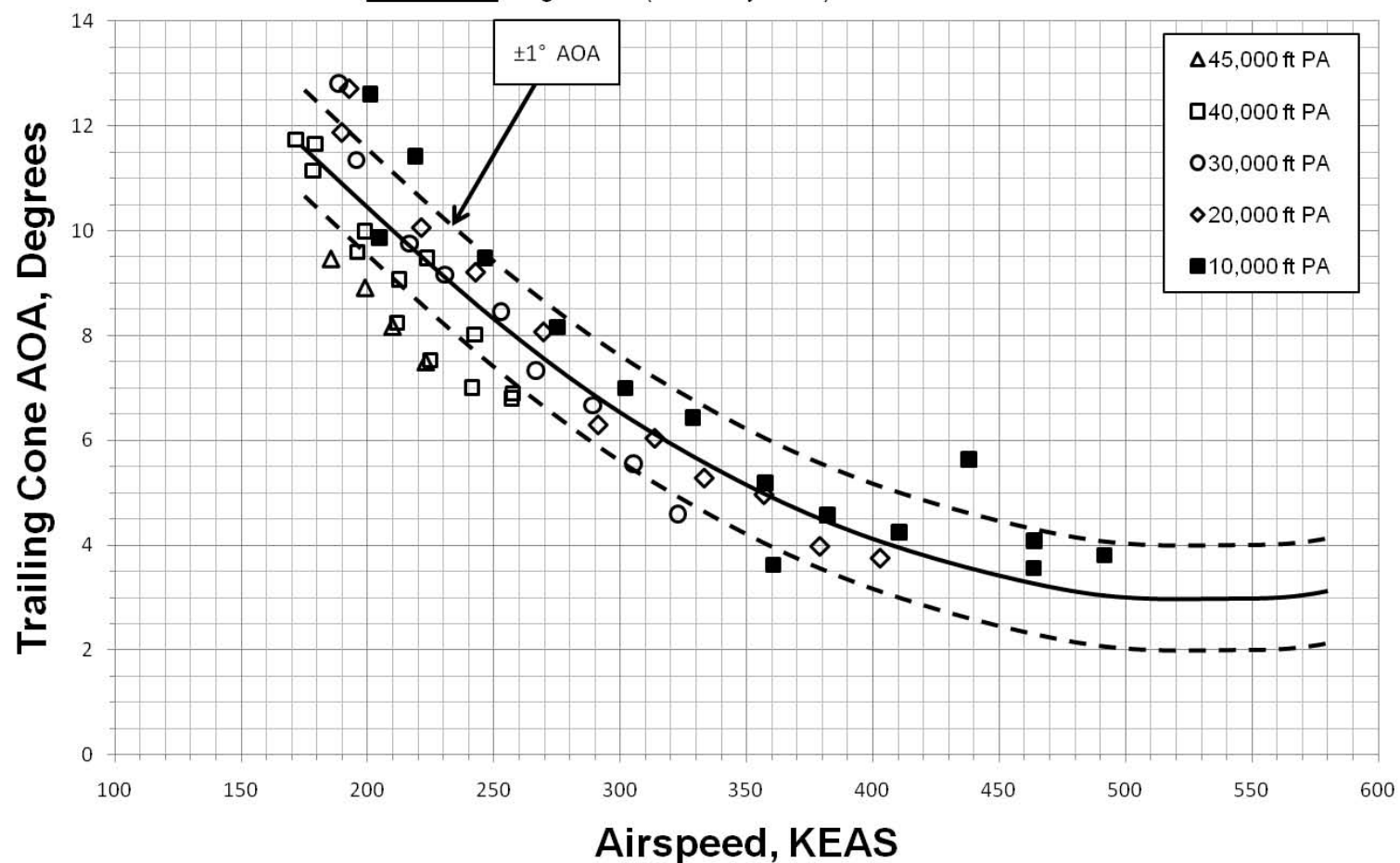


Figure A-2. Trailing Cone Tube AOA (At Altitude)

# Trailing Cone Tube AOA (Altitude)

Aircraft: F-16D, S/N 87-0391 (ARDS Pod on Station 1 and 370 Gallon Fuel Tanks on Stations 4 and 6)

Configuration: Cruise (Gear Up / Flaps Up)

Data Basis: Flight Test (Test Day Data) / 11-31 Mar 2010

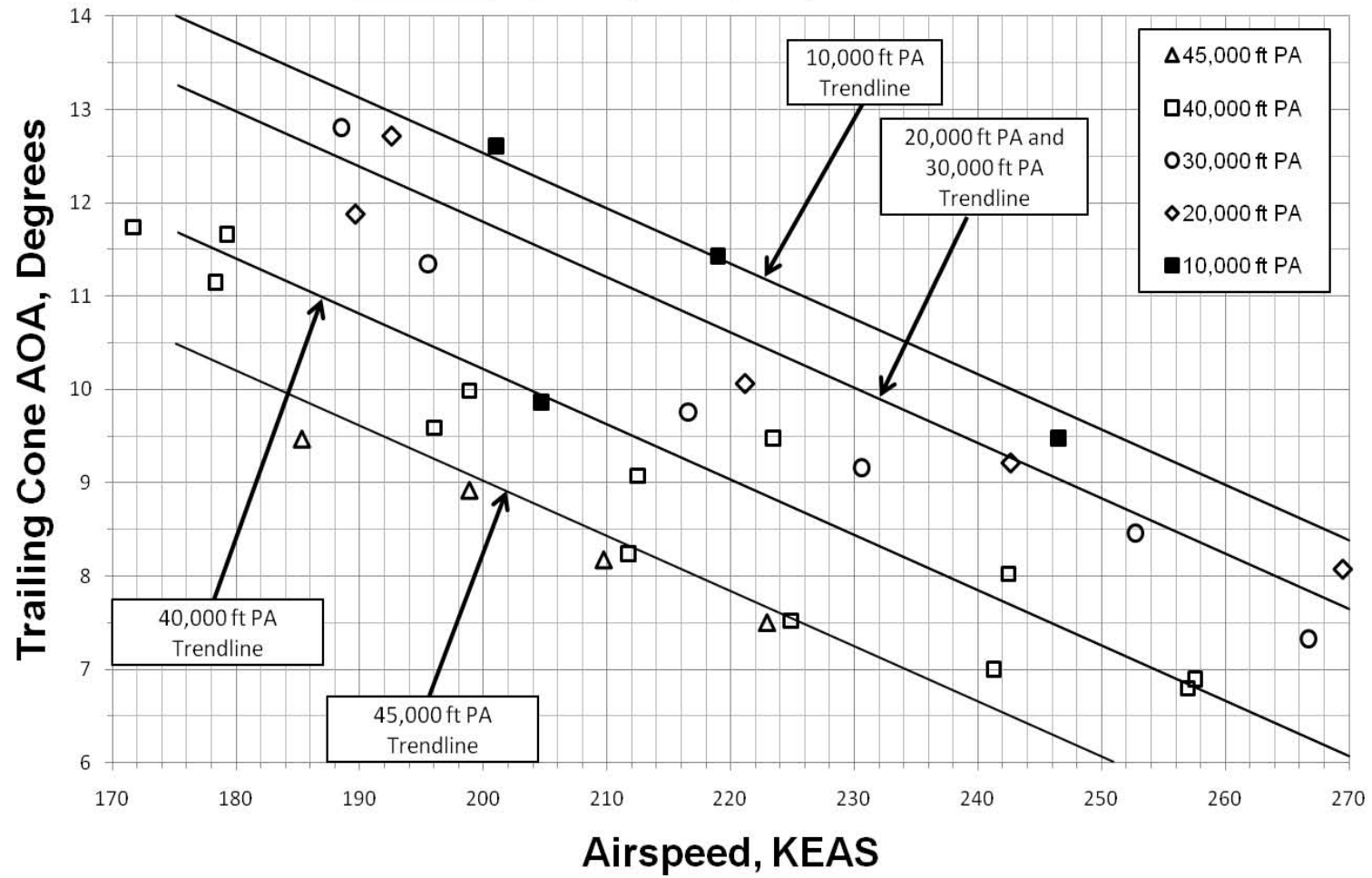


Figure A-3 Trailing Cone Tube AOA (At Altitude, Expanded View)

# Trailing Cone Tube AOA (All Points)

Aircraft: F-16D, S/N 87-0391 (ARDS Pod on Station 1 and 370 Gallon Fuel Tanks on Stations 4 and 6)

Configuration: Cruise (Gear Up / Flaps Up)

Data Basis: Flight Test (Test Day Data) / 11-31 Mar 2010

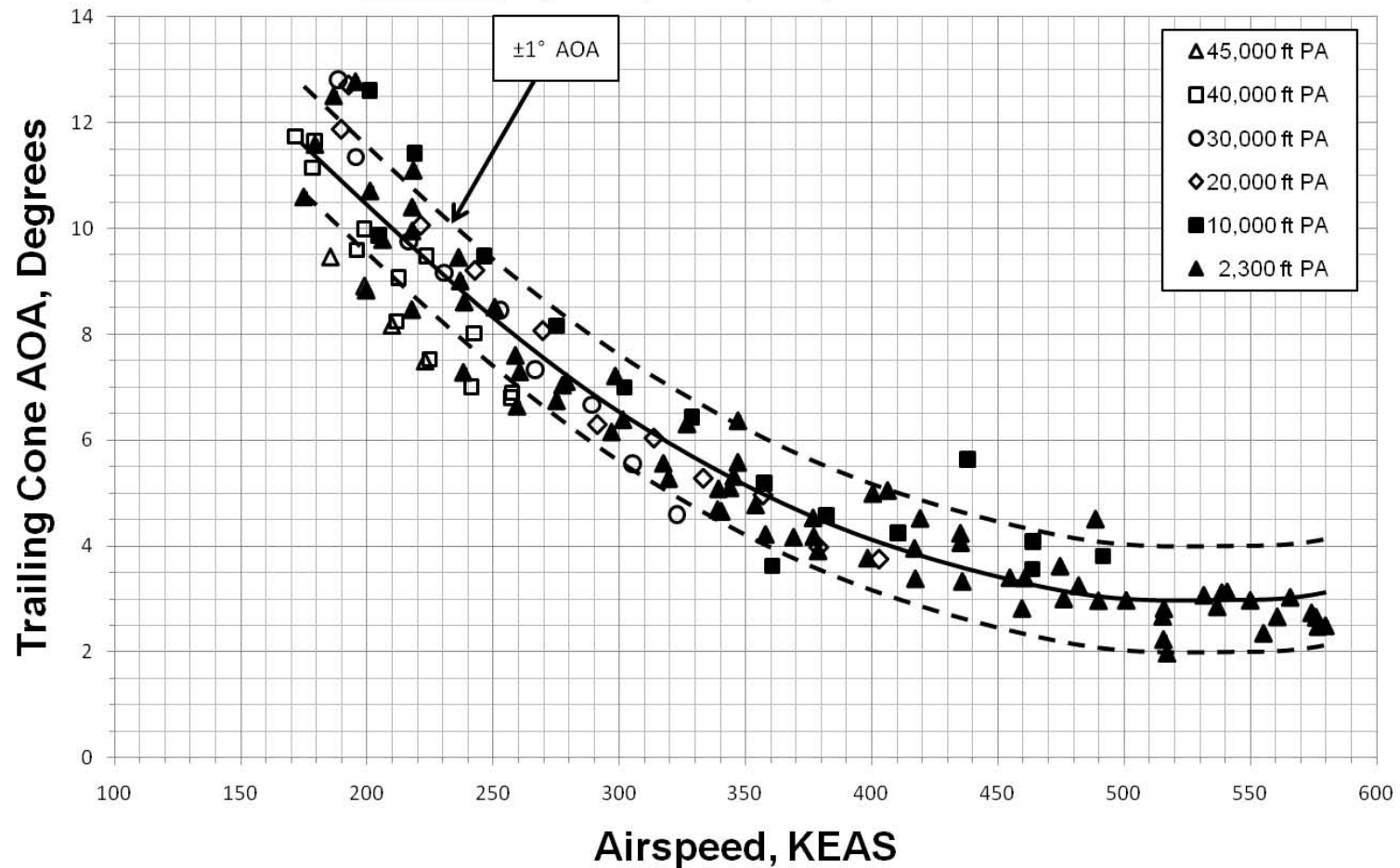


Figure A-4. Trailing Cone Tube AOA (All Altitudes)

# Static Position Error Ratio Trailing Cone

Aircraft: F-16D, S/N 87-0391 (ARDS Pod on Station 1 and 370 Gallon Fuel Tanks on Stations 4 and 6)

Configuration: Cruise (Gear Up / Flaps Up)

Data Basis: Flight Test (Test Day Data) / 11-31 Mar 2010

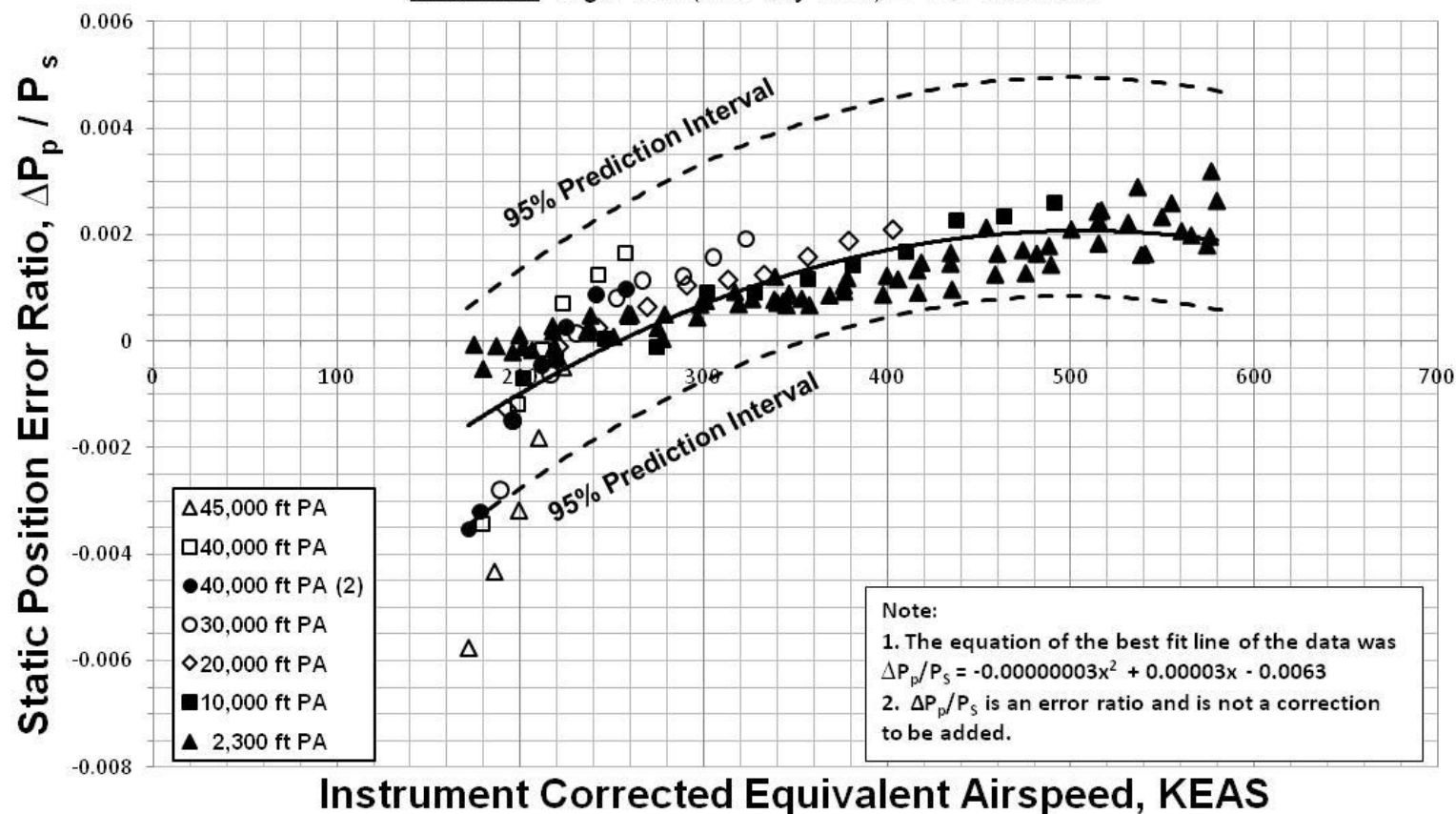


Figure A-5. Trailing Cone Static Position Error Ratio (All Altitudes)

# Static Position Error Ratio Trailing Cone - Best Fits

Aircraft: F-16D, S/N 87-0391 (ARDS Pod on Station 1 and 370 Gallon Fuel Tanks on Stations 4 and 6)

Configuration: Cruise (Gear Up / Flaps Up)

Data Basis: Flight Test (Test Day Data) / 11-31 Mar 2010

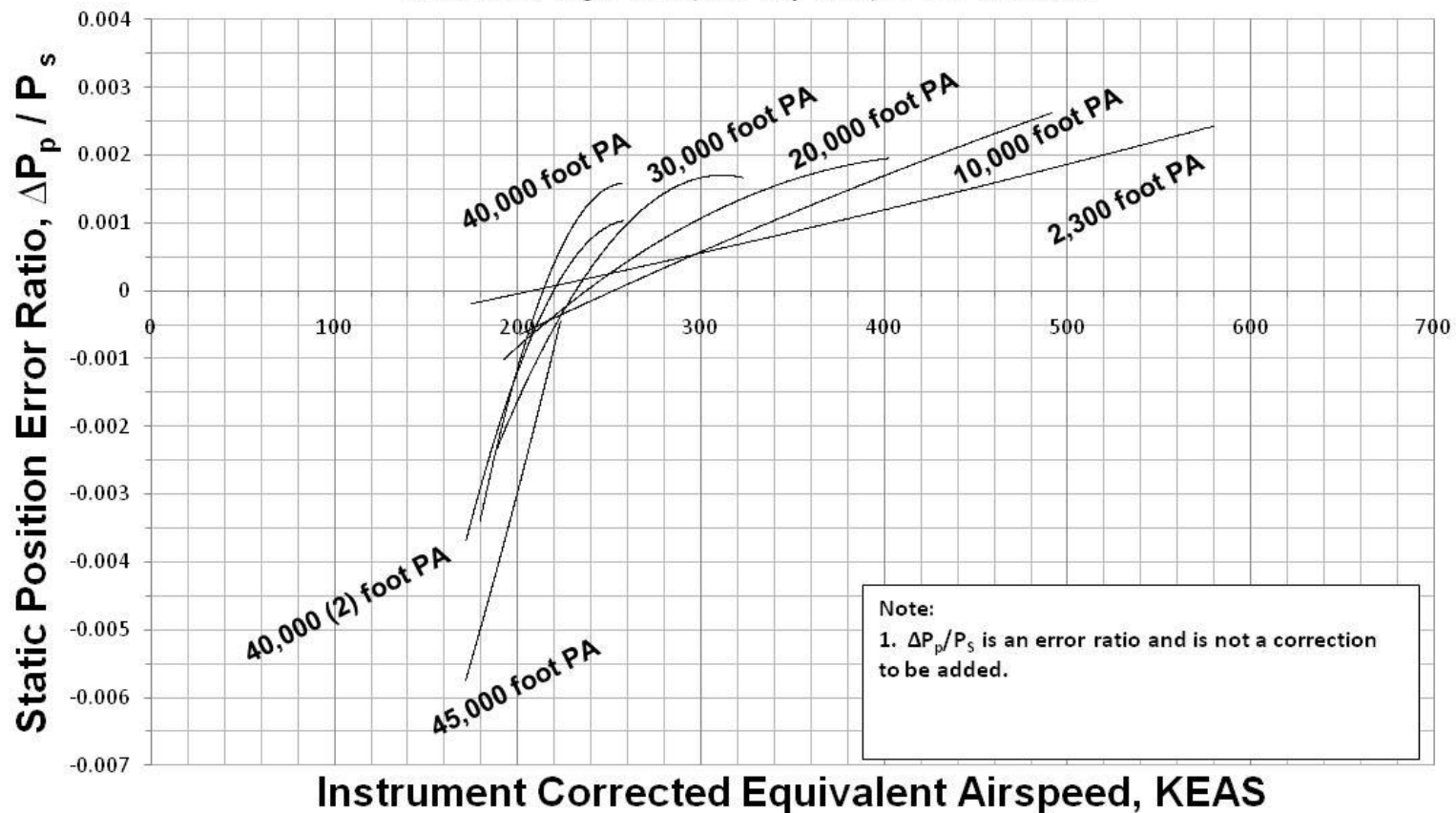


Figure A-6. Trailing Cone Static Position Error Ratio Best Fits (All Altitudes)

# Static Position Error Ratio Trailing Cone

Aircraft: F-16D, S/N 87-0391 (ARDS Pod on Station 1 and 370 Gallon Fuel Tanks on Stations 4 and 6)

Configuration: Cruise (Gear Up / Flaps Up)

Data Basis: Flight Test (Test Day Data) / 11-31 Mar 2010  $y = 2E-09x^2 + 5E-06x - 0.0011$

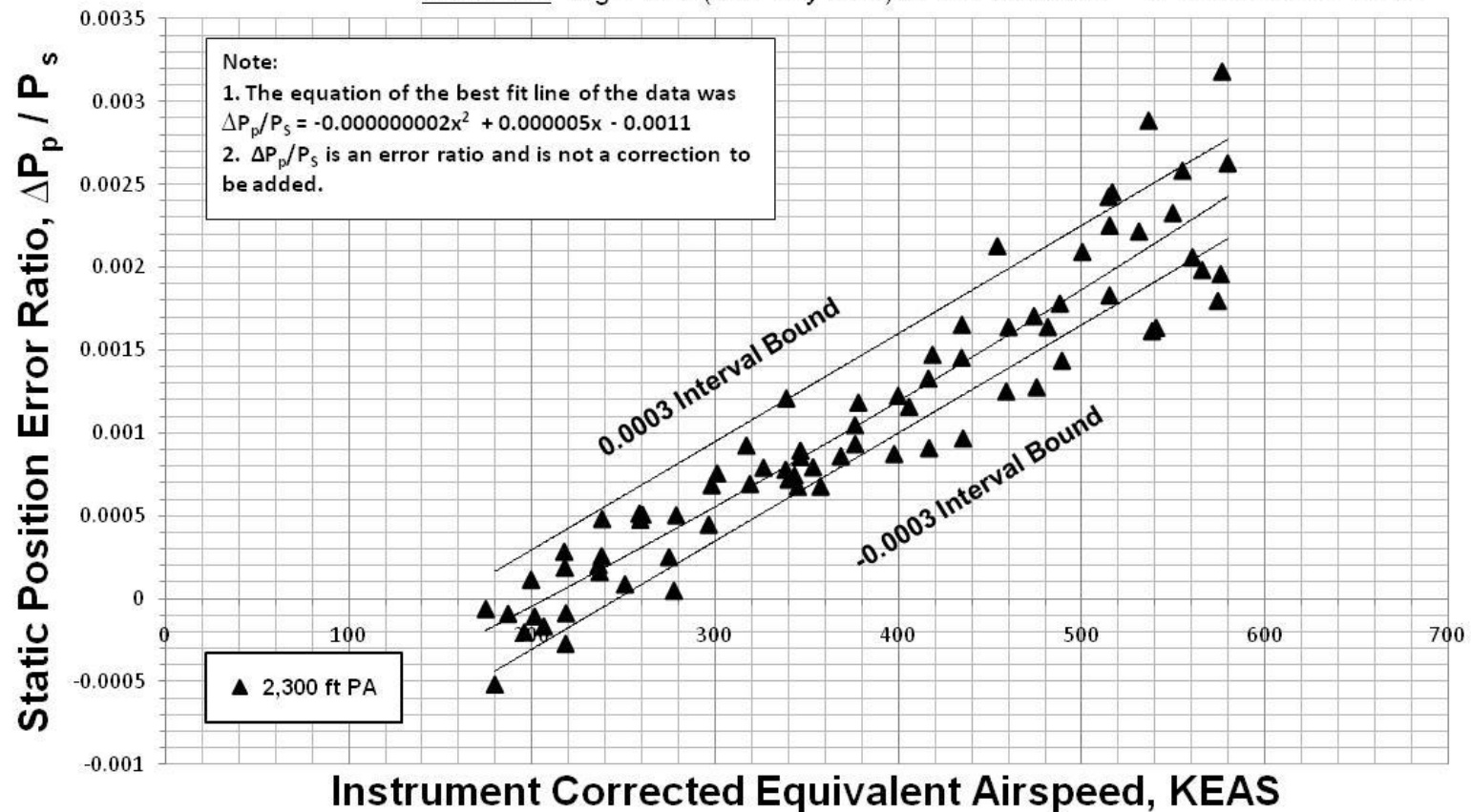


Figure A-7. Trailing Cone Static Position Error Ratio (2,300 feet PA)

# Static Position Error Ratio Trailing Cone

Aircraft: F-16D, S/N 87-0391 (ARDS Pod on Station 1 and 370 Gallon Fuel Tanks on Stations 4 and 6)

Configuration: Cruise (Gear Up / Flaps Up)

Data Basis: Flight Test (Test Day Data) / 11-31 Mar 2010

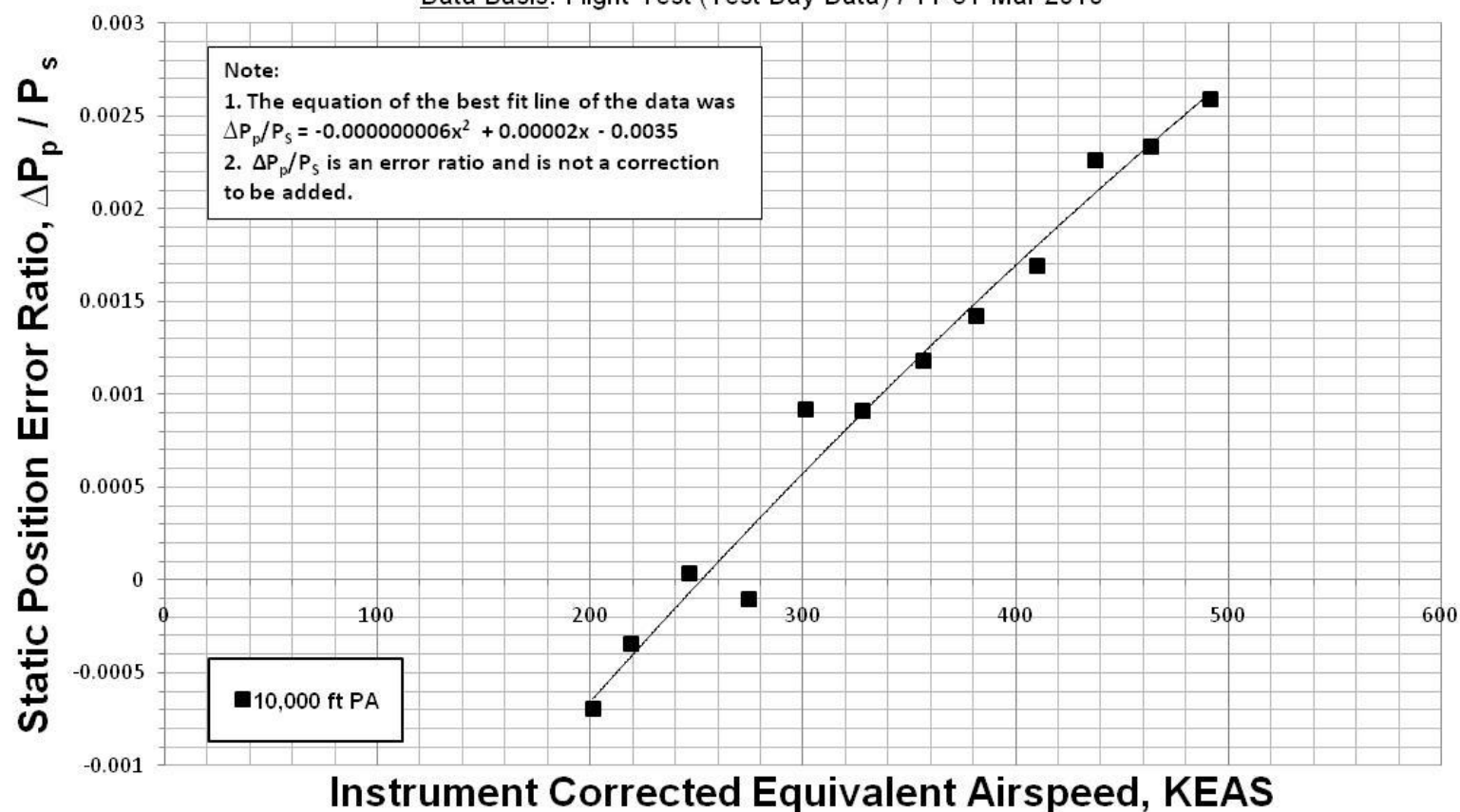


Figure A-8. Trailing Cone Static Position Error Ratio (10,000 feet PA)

# Static Position Error Ratio Trailing Cone

Aircraft: F-16D, S/N 87-0391 (ARDS Pod on Station 1 and 370 Gallon Fuel Tanks on Stations 4 and 6)

Configuration: Cruise (Gear Up / Flaps Up)

Data Basis: Flight Test (Test Day Data) / 11-31 Mar 2010

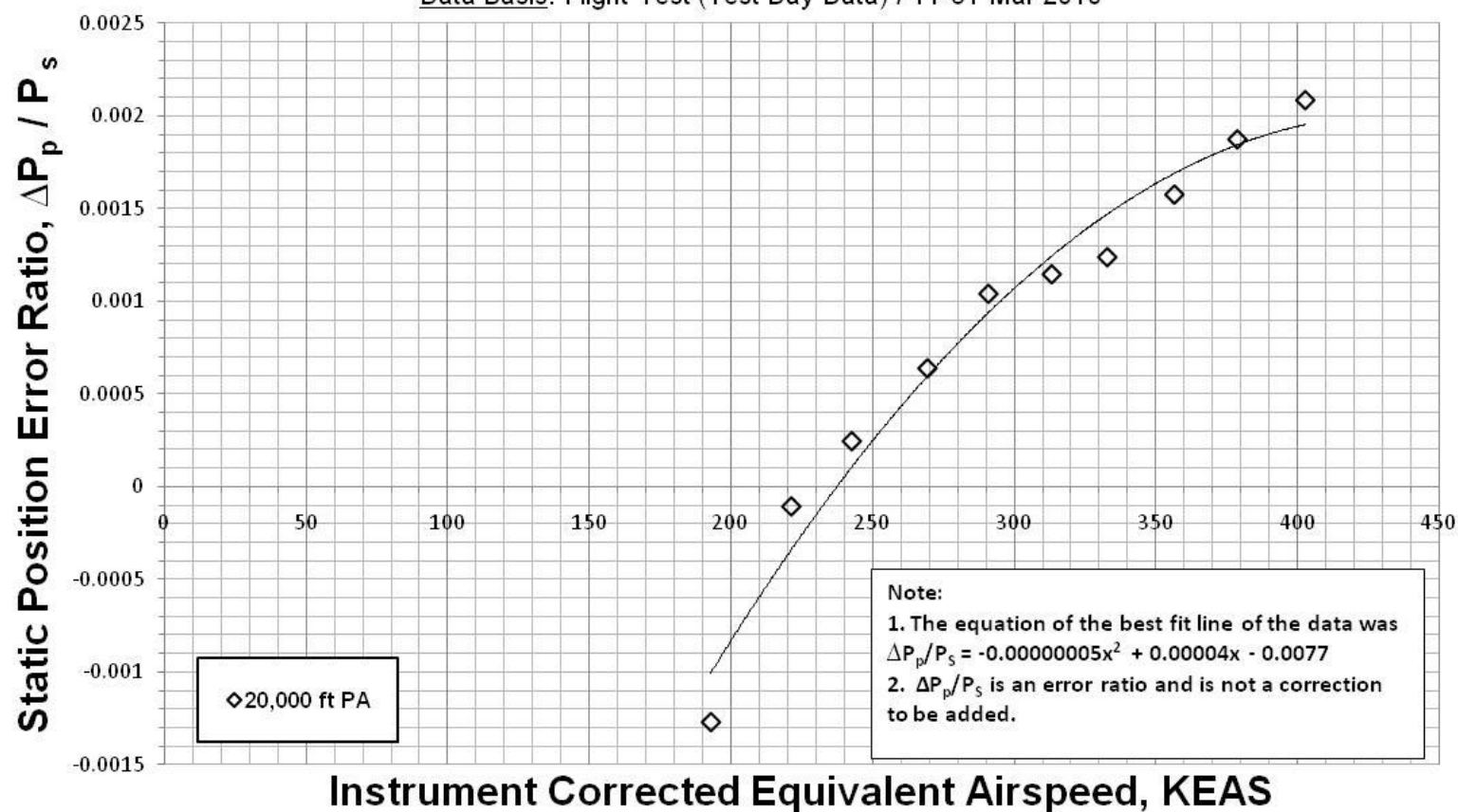


Figure A-9. Trailing Cone Static Position Error Ratio (20,000 feet PA)

# Static Position Error Ratio Trailing Cone

Aircraft: F-16D, S/N 87-0391 (ARDS Pod on Station 1 and 370 Gallon Fuel Tanks on Stations 4 and 6)

Configuration: Cruise (Gear Up / Flaps Up)

Data Basis: Flight Test (Test Day Data) / 11-31 Mar 2010

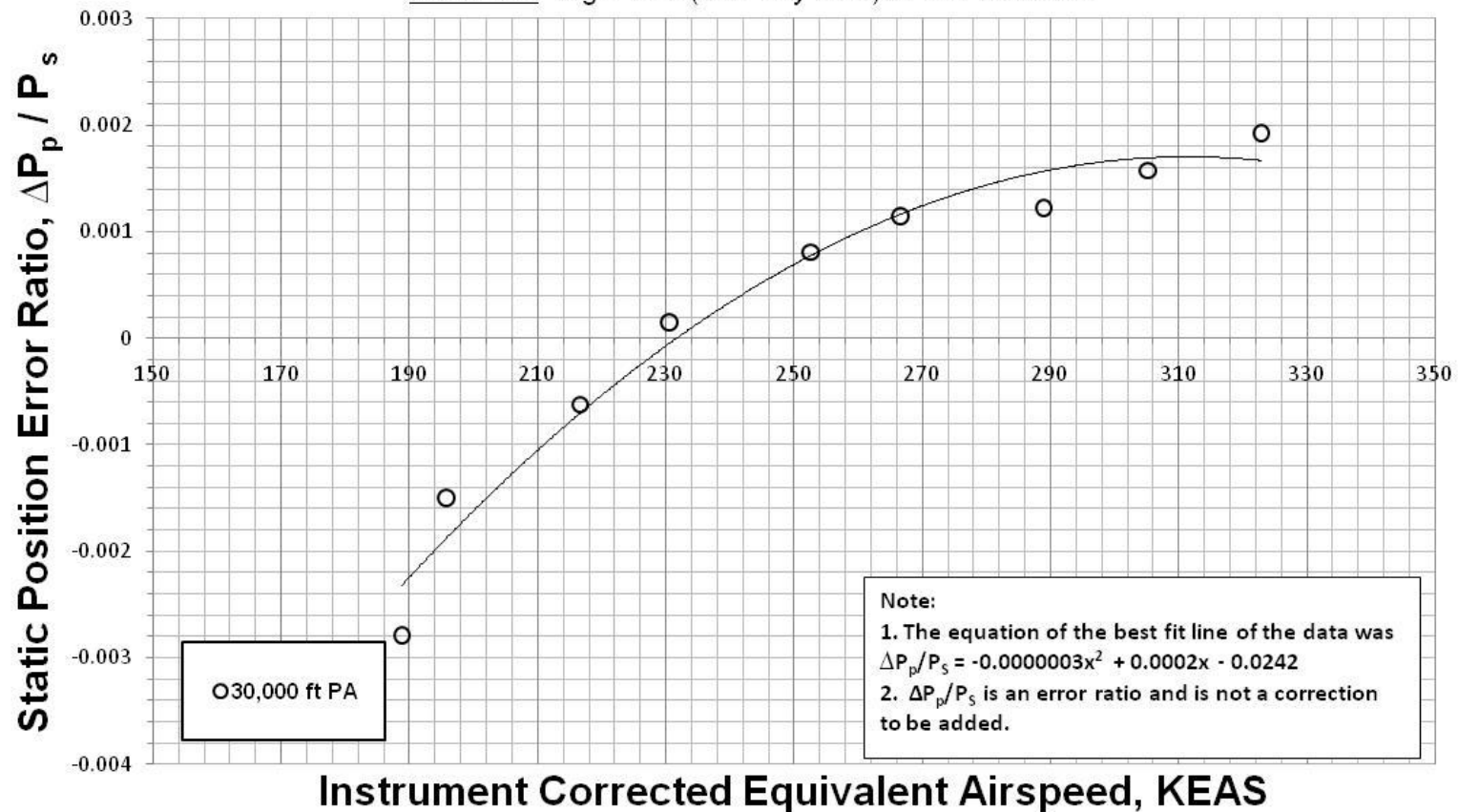


Figure A-10. Trailing Cone Static Position Error Ratio (30,000 feet PA)

# Static Position Error Ratio Trailing Cone

Aircraft: F-16D, S/N 87-0391 (ARDS Pod on Station 1 and 370 Gallon Fuel Tanks on Stations 4 and 6)

Configuration: Cruise (Gear Up / Flaps Up)

Data Basis: Flight Test (Test Day Data) / 11-31 Mar 2010

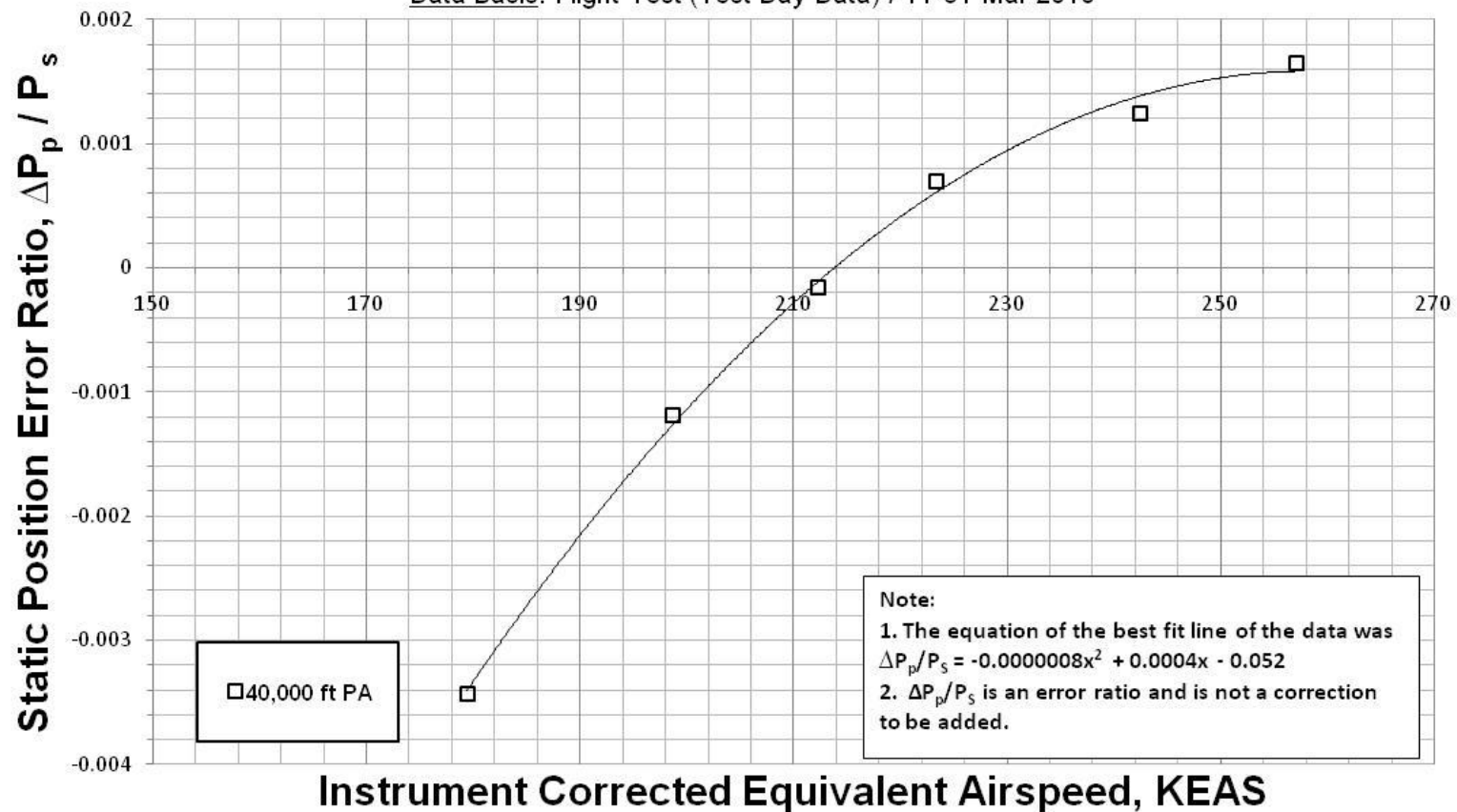


Figure A-11. Trailing Cone Static Position Error Ratio (40,000 feet PA)

# Static Position Error Ratio Trailing Cone

Aircraft: F-16D, S/N 87-0391 (ARDS Pod on Station 1 and 370 Gallon Fuel Tanks on Stations 4 and 6)

Configuration: Cruise (Gear Up / Flaps Up)

Data Basis: Flight Test (Test Day Data) / 11-31 Mar 2010

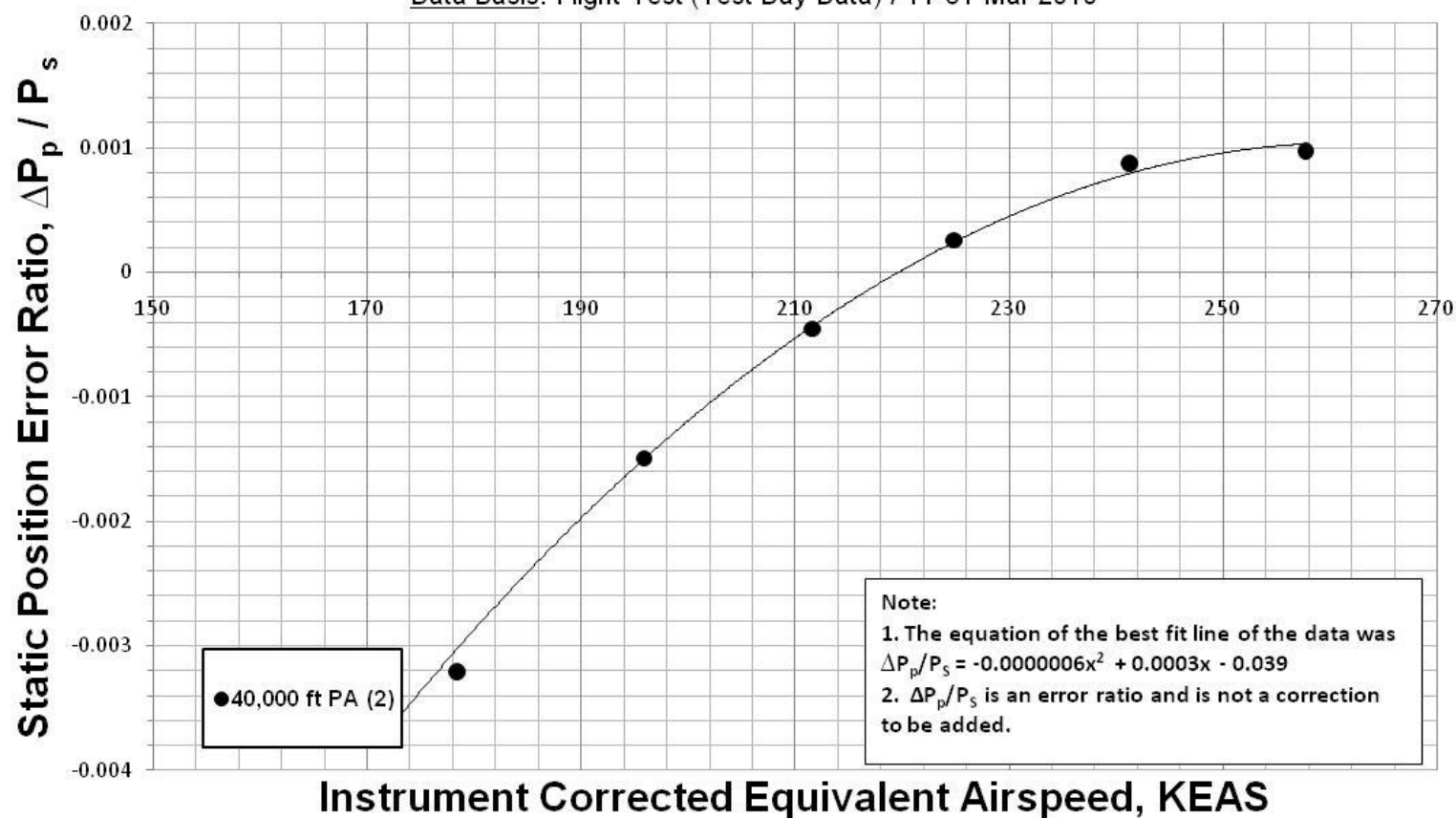


Figure A-12. Trailing Cone Static Position Error Ratio (40,000 (2) feet PA)

## Static Position Error Ratio Trailing Cone

Aircraft: F-16D, S/N 87-0391 (ARDS Pod on Station 1 and 370 Gallon Fuel Tanks on Stations 4 and 6)

Configuration: Cruise (Gear Up / Flaps Up)

Data Basis: Flight Test (Test Day Data) / 11-31 Mar 2010

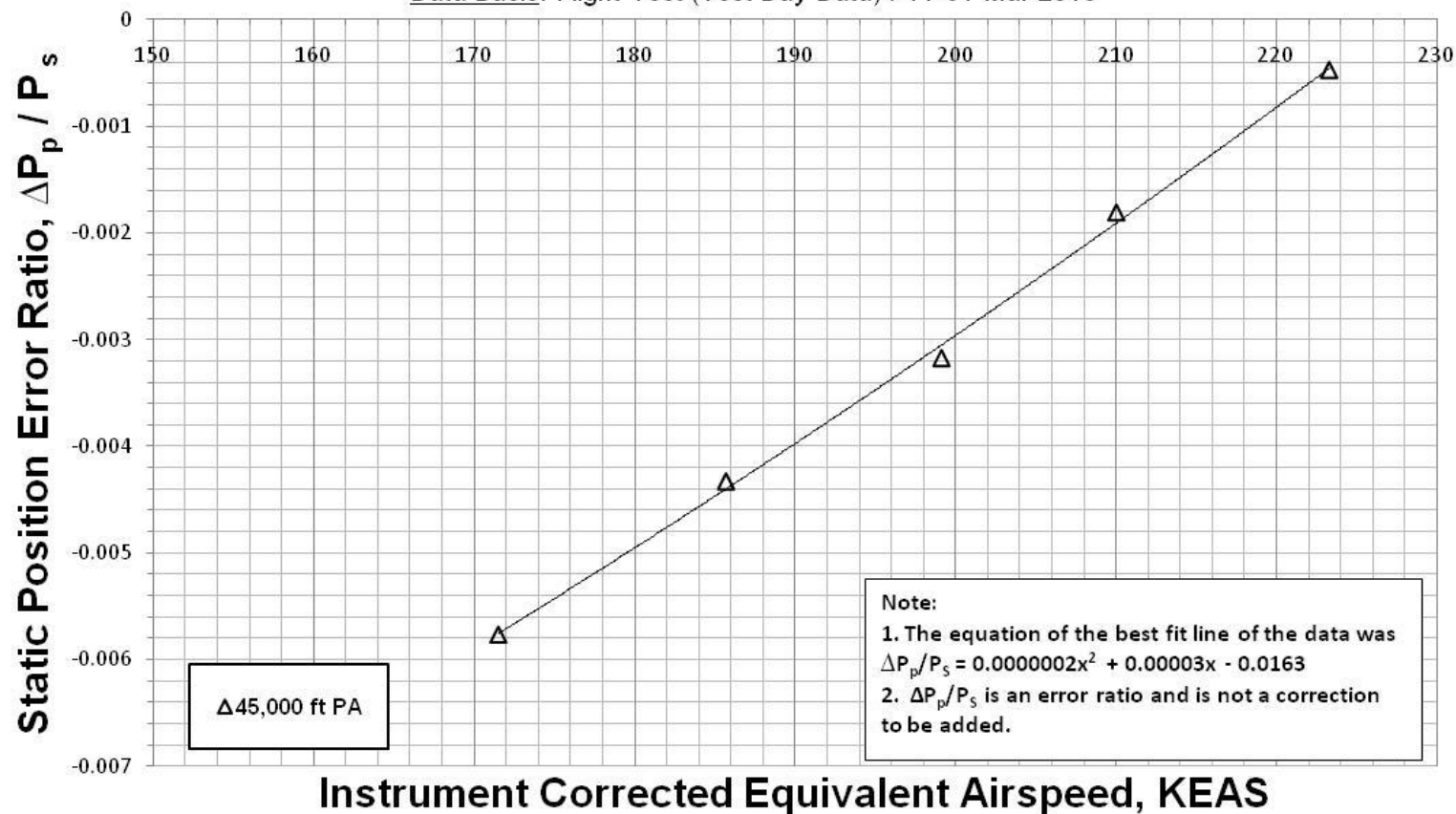


Figure A-13. Trailing Cone Static Position Error Ratio (45,000 PA)

# Pressure Altitude Position Correction Trailing Cone

Aircraft: F-16D, S/N 87-0391 (ARDS Pod on Station 1 and 370 Gallon Fuel Tanks on Stations 4 and 6)

Configuration: Cruise (Gear Up / Flaps Up)

Data Basis: Flight Test (Test Day Data) / 11-31 Mar 2010

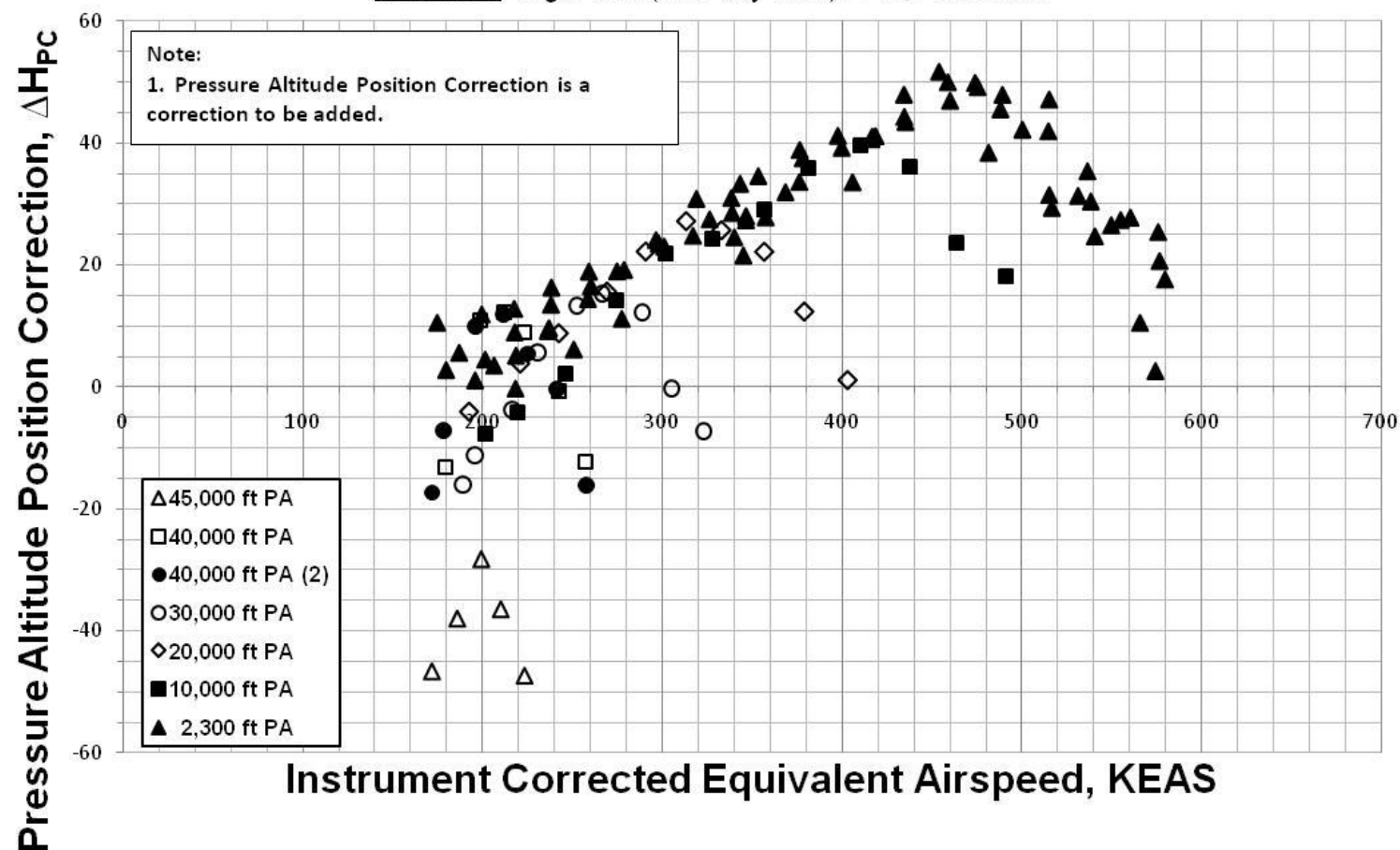


Figure A-14. Trailing Cone Pressure Altitude Position Correction (All Altitudes)

# Static Position Error Ratio Trailing Cone

Aircraft: F-16D, S/N 87-0391 (ARDS Pod on Station 1 and 370 Gallon Fuel Tanks on Stations 4 and 6)

Configuration: Cruise (Gear Up / Flaps Up)

Data Basis: Flight Test (Test Day Data) / 11-31 Mar 2010

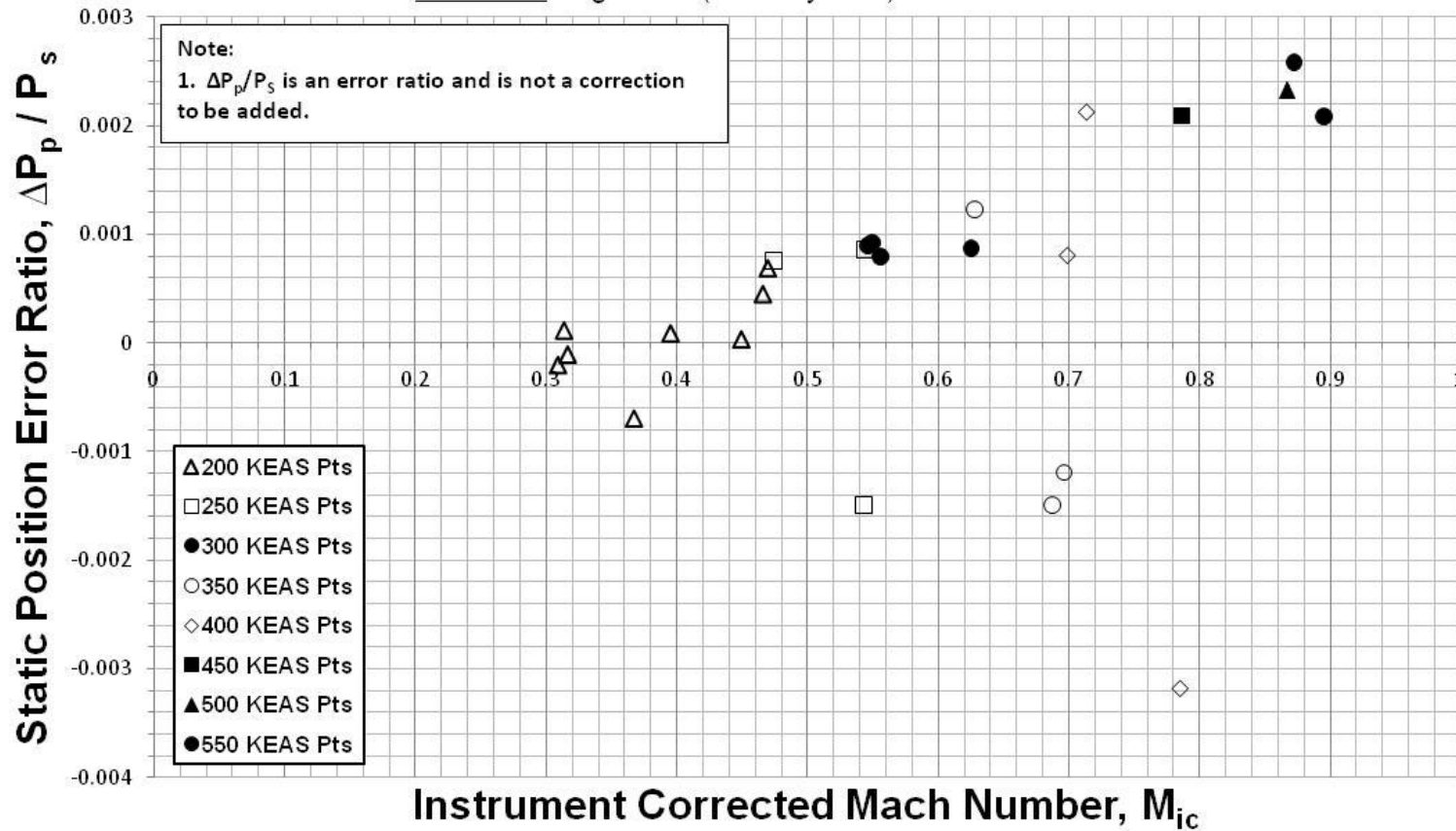


Figure A-15. Trailing Cone Static Position Error Ratio vs. Instrument Corrected Mach Number

## Static Position Error Ratio Trailing Cone

Aircraft: F-16D, S/N 87-0391 (ARDS Pod on Station 1 and 370 Gallon Fuel Tanks on Stations 4 and 6)

Configuration: Cruise (Gear Up / Flaps Up)

Data Basis: Flight Test (Test Day Data) / 11-31 Mar 2010

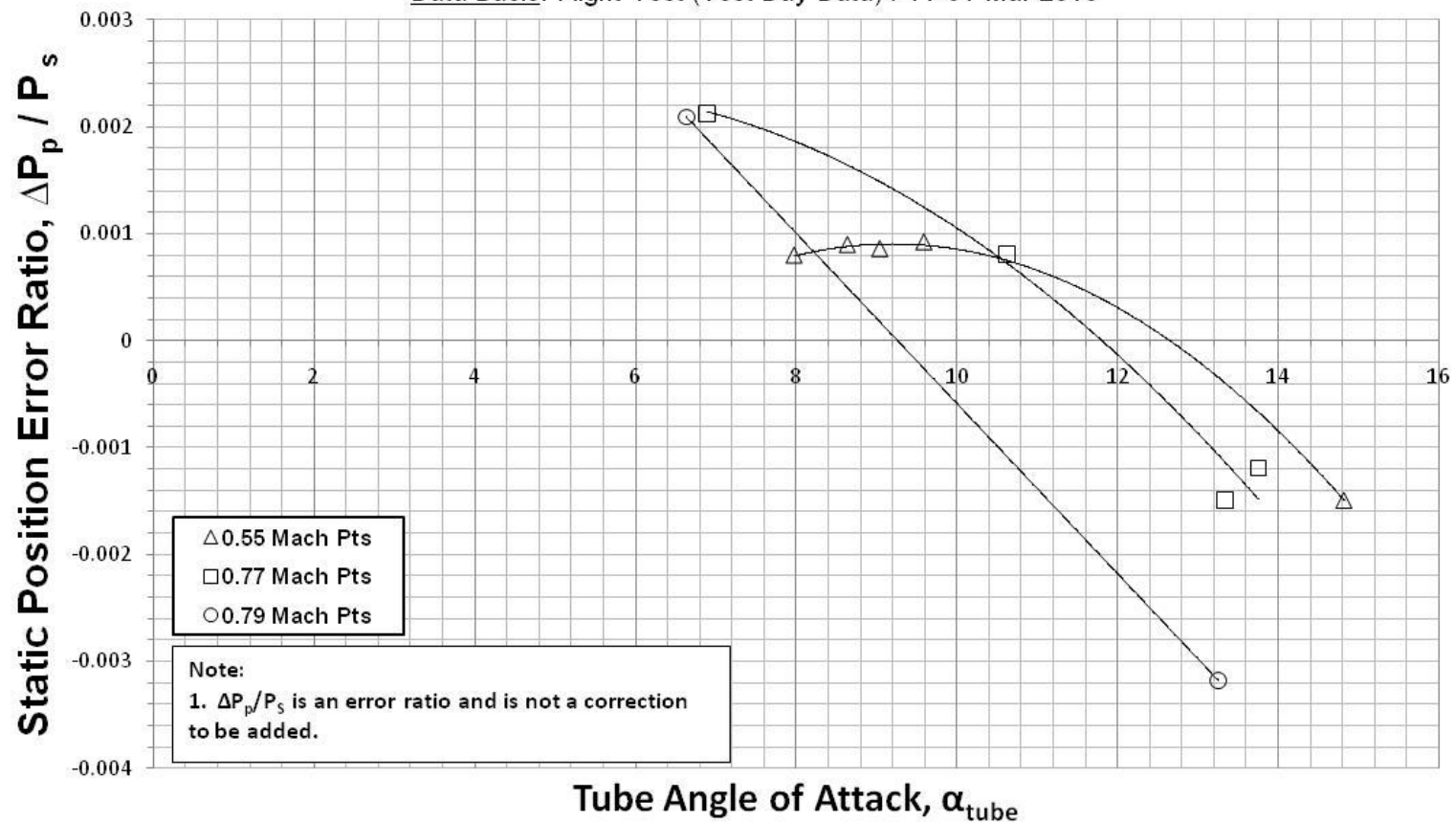


Figure A-16. Trailing Cone Static Position Error Ratio vs. Tube Angle of Attack

# Static Position Error Ratio Trailing Cone

Aircraft: F-16D, S/N 87-0391 (ARDS Pod on Station 1 and 370 Gallon Fuel Tanks on Stations 4 and 6)

Configuration: Cruise (Gear Up / Flaps Up)

Data Basis: Flight Test (Test Day Data) / 11-31 Mar 2010

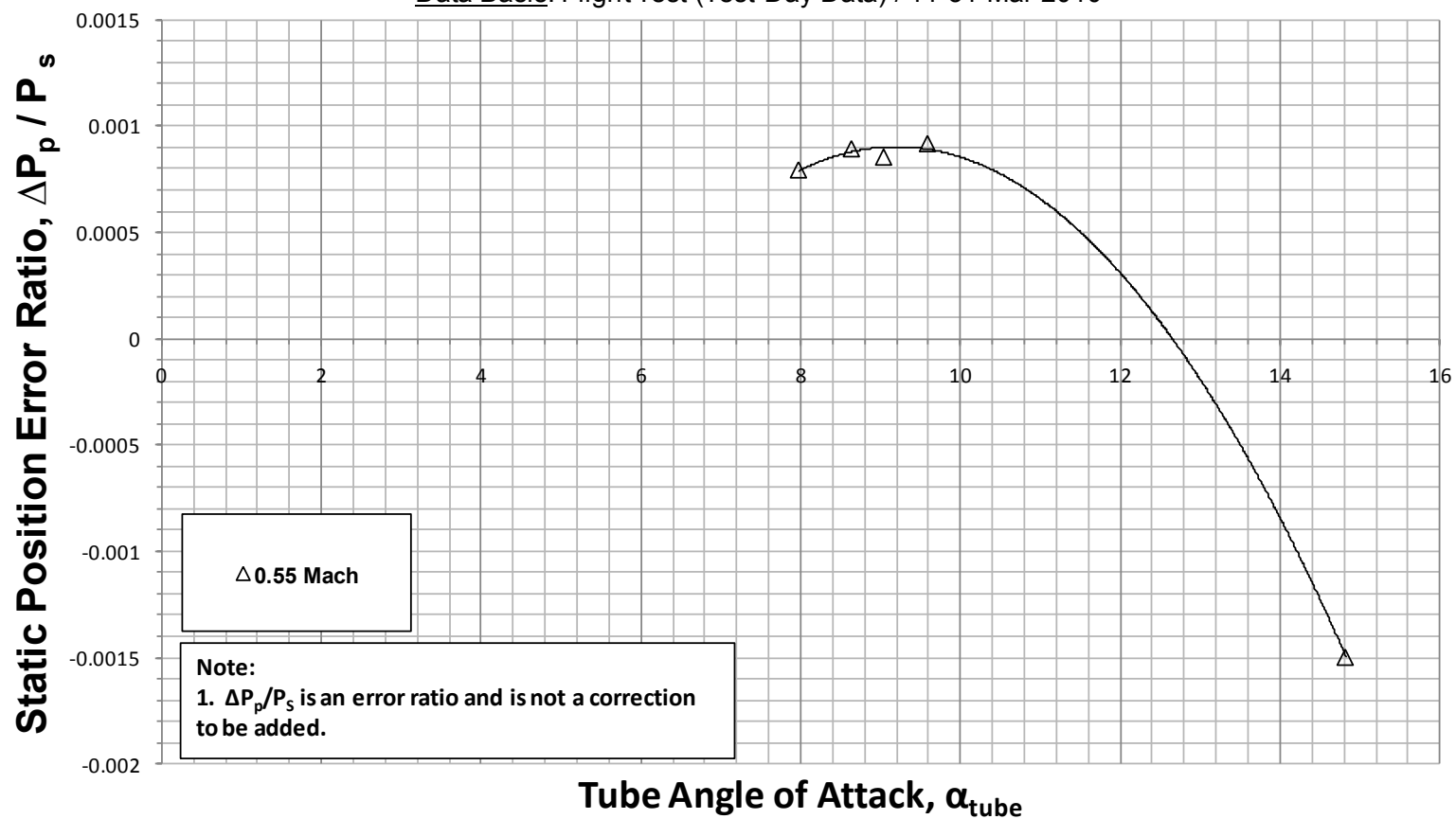


**Figure A-17. Trailing Cone Static Position Error Ratio vs. Tube Angle of Attack (0.55 Mach)**

# Static Position Error Ratio Trailing Cone

Aircraft: F-16D, S/N 87-0391 (ARDS Pod on Station 1 and 370 Gallon Fuel Tanks on Stations 4 and 6)

Configuration: Cruise (Gear Up / Flaps Up)

Data Basis: Flight Test (Test Day Data) / 11-31 Mar 2010

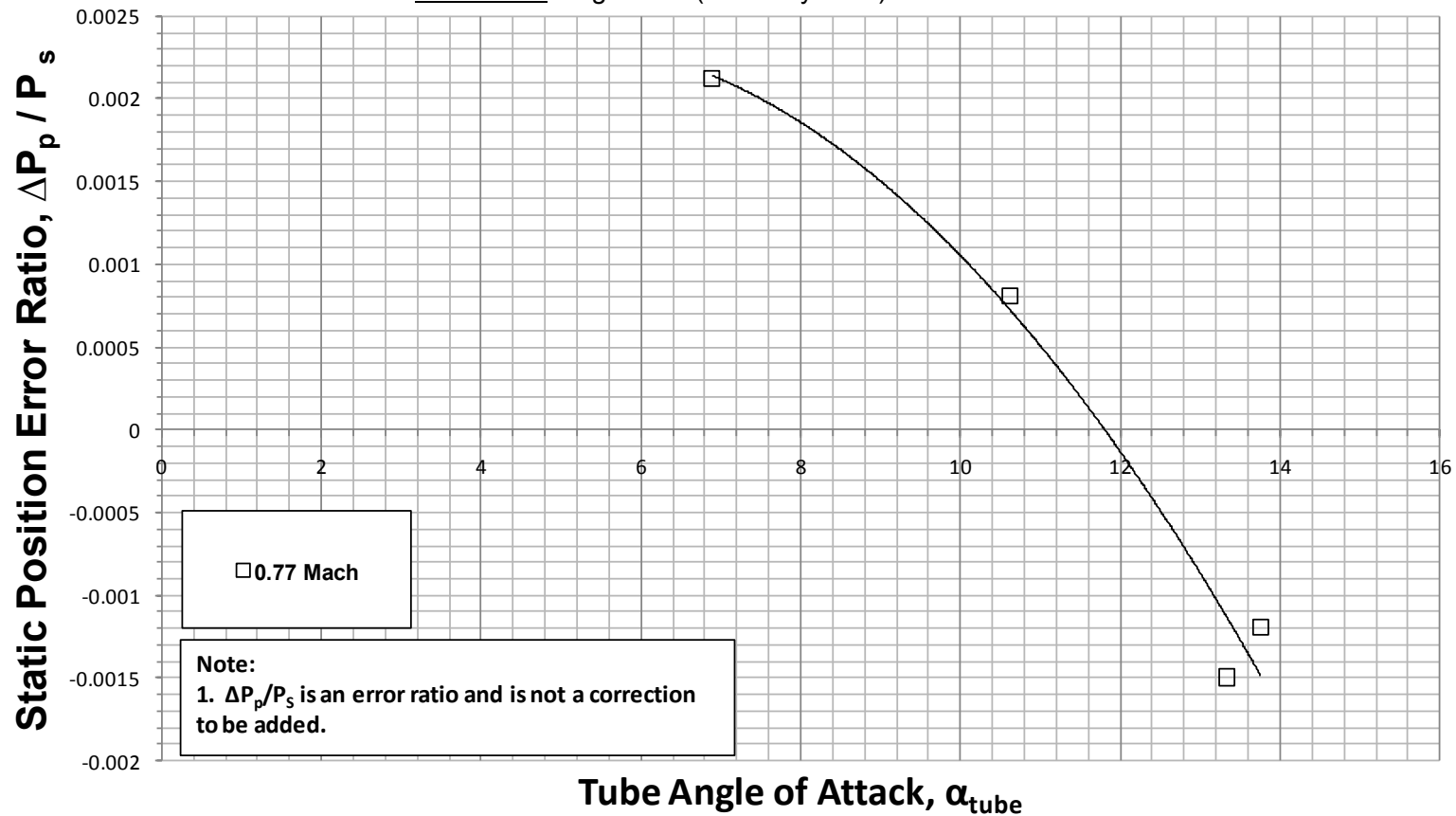


Figure A-18. Trailing Cone Static Position Error Ratio vs. Tube Angle of Attack (0.72 Mach)

# Static Position Error Ratio Trailing Cone

Aircraft: F-16D, S/N 87-0391 (ARDS Pod on Station 1 and 370 Gallon Fuel Tanks on Stations 4 and 6)

Configuration: Cruise (Gear Up / Flaps Up)

Data Basis: Flight Test (Test Day Data) / 11-31 Mar 2010

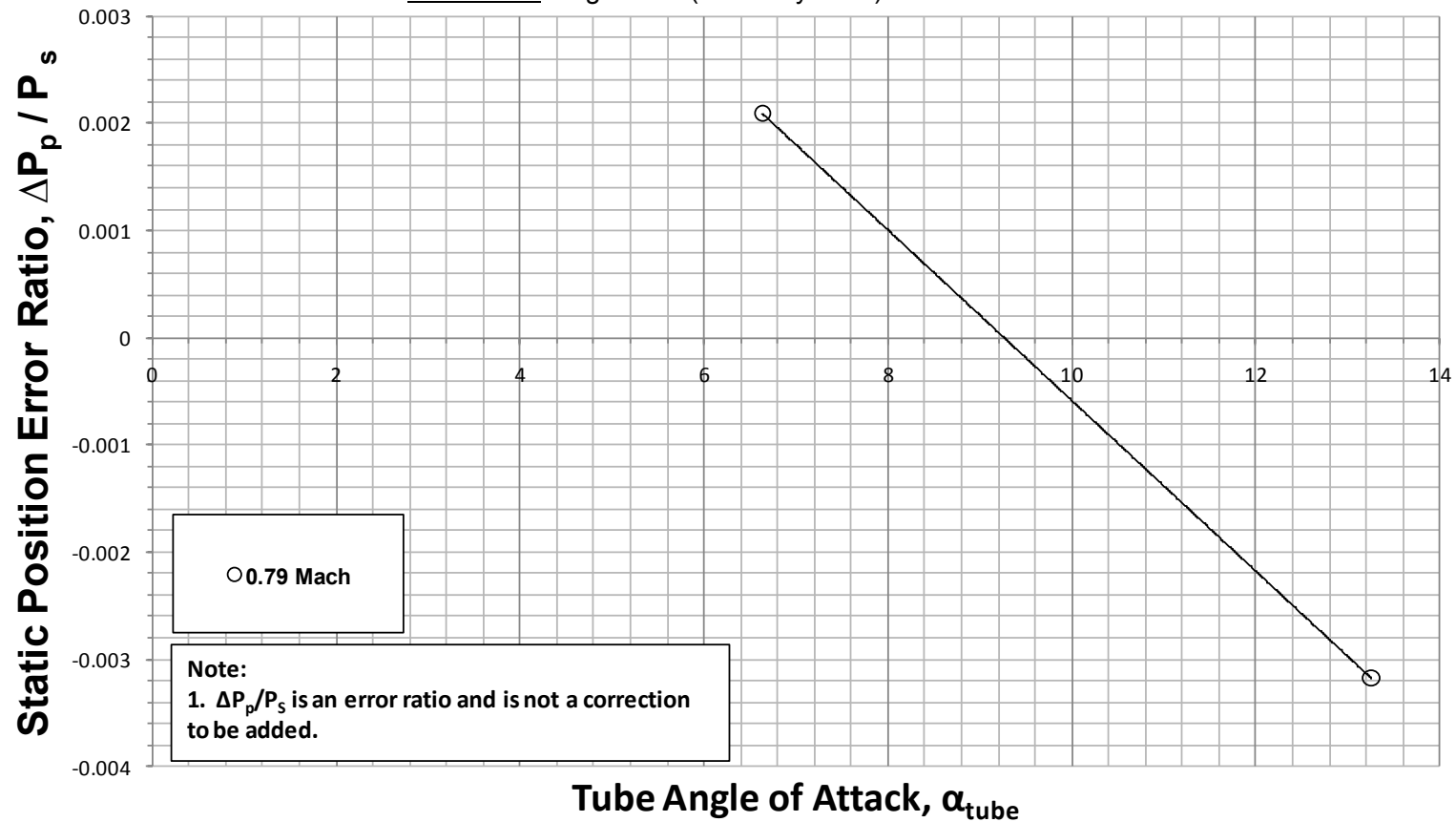


Figure A-19. Trailing Cone Static Position Error Ratio vs. Tube Angle of Attack (0.79 Mach)

# **Tube Angle of Attack Trailing Cone**

Aircraft: F-16D, S/N 87-0391 (ARDS Pod on Station 1 and 370 Gallon Fuel Tanks on Stations 4 and 6)

Configuration: Cruise (Gear Up / Flaps Up)

Data Basis: Flight Test (Test Day Data) / 11-31 Mar 2010

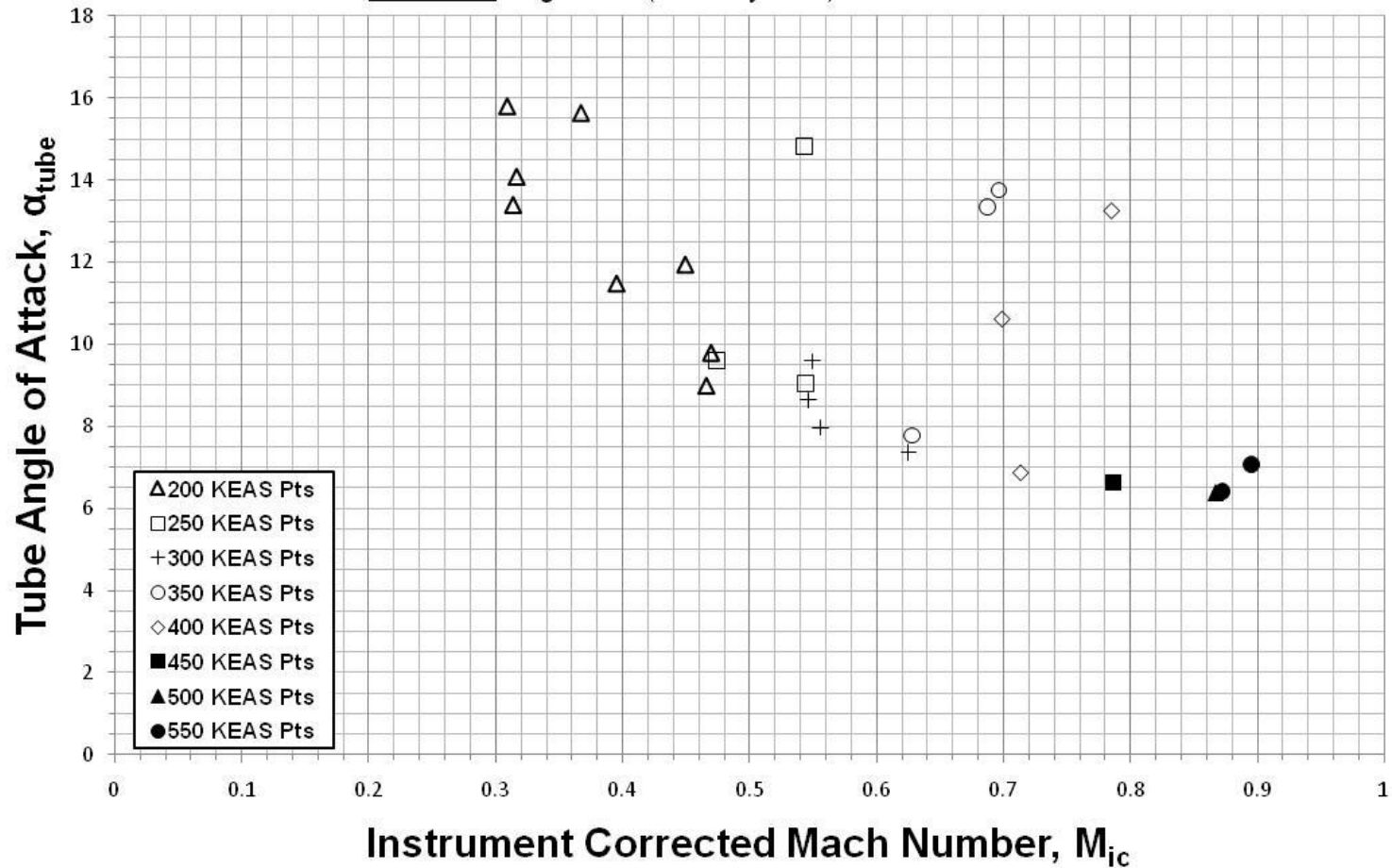


**Figure A-20. Trailing Cone Tube Angle of Attack vs. Instrument Corrected Mach Number**

# Static Source Correction Test Noseboom (Systems 1 and 2)

Aircraft: F-16D, S/N 87-0391 (ARDS Pod on Station 1 and 370 Gallon Fuel Tanks on Stations 4 and 6)

Configuration: Cruise (Gear Up / Flaps Up)

Data Basis: Flight Test (Test Day Data) / 8-31 Mar 2010

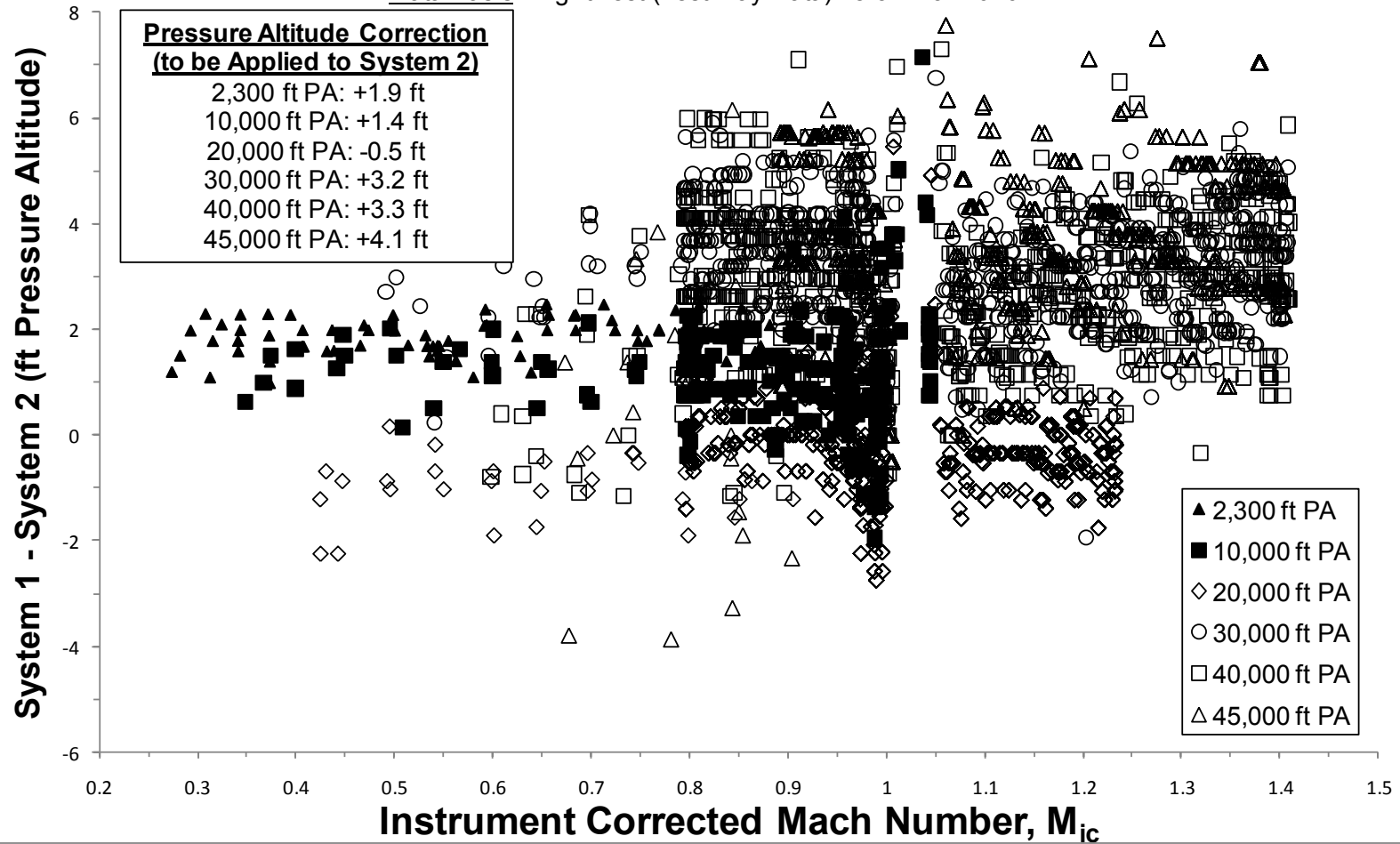


Figure A-21. Static Source Correction

# Static Position Error Pressure Coefficient 2,300 ft PA - Test Noseboom (System 1)

Aircraft: F-16D, S/N 87-0391 (ARDS Pod on Station 1 and 370 Gallon Fuel Tanks on Stations 4 and 6)

Configuration: Cruise (Gear Up / Flaps Up)

Data Basis: Flight Test (Test Day Data) / 8-12 Mar 2010

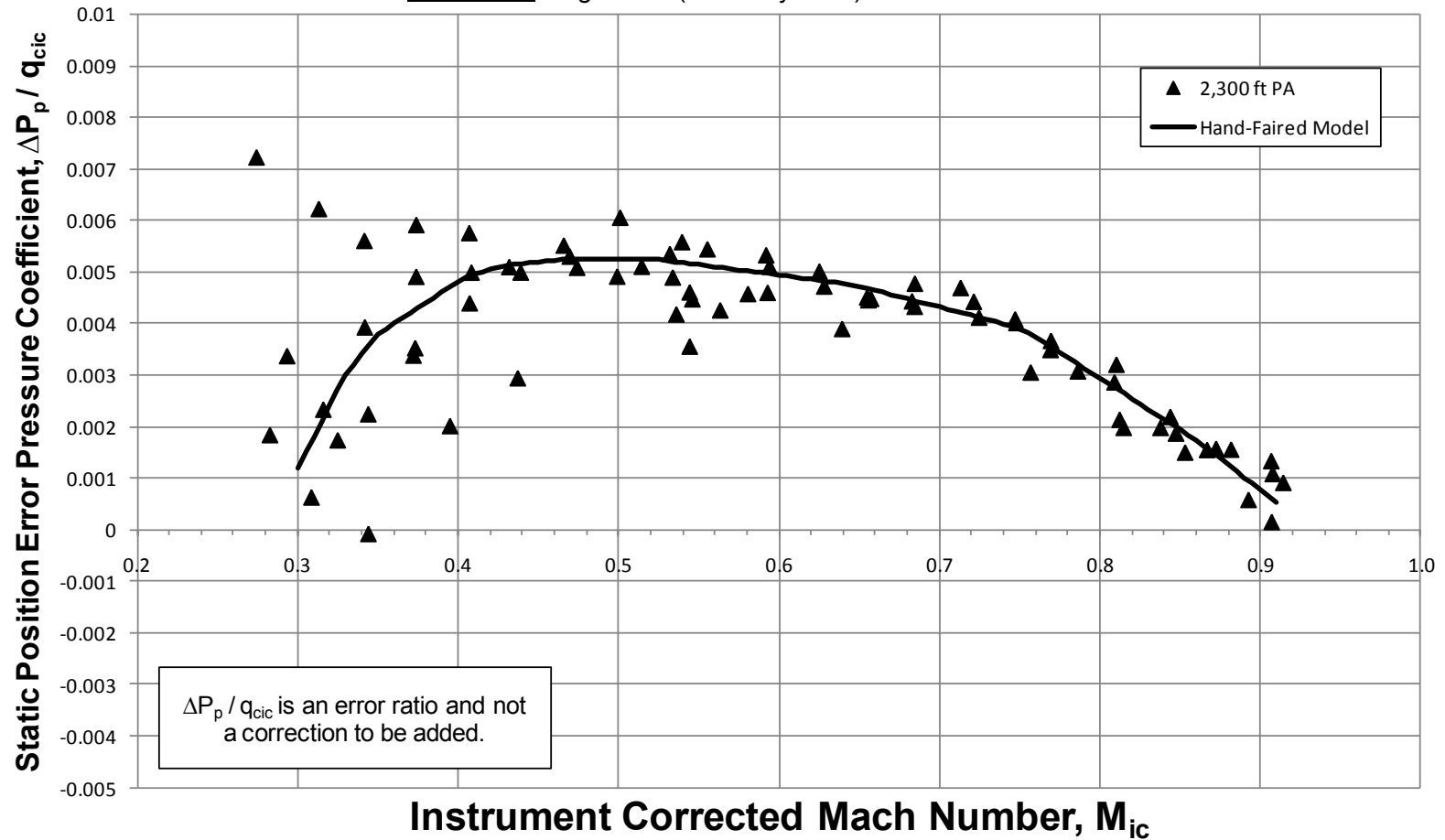


Figure A-22. Noseboom Static Position Error Pressure Coefficient (2,300 ft PA)

# Static Position Error Pressure Coefficient 10,000 ft PA - Test Noseboom (System 1)

Aircraft: F-16D, S/N 87-0391 (ARDS Pod on Station 1 and 370 Gallon Fuel Tanks on Stations 4 and 6)

Configuration: Cruise (Gear Up / Flaps Up)

Data Basis: Flight Test (Test Day Data) / 15-31 Mar 2010

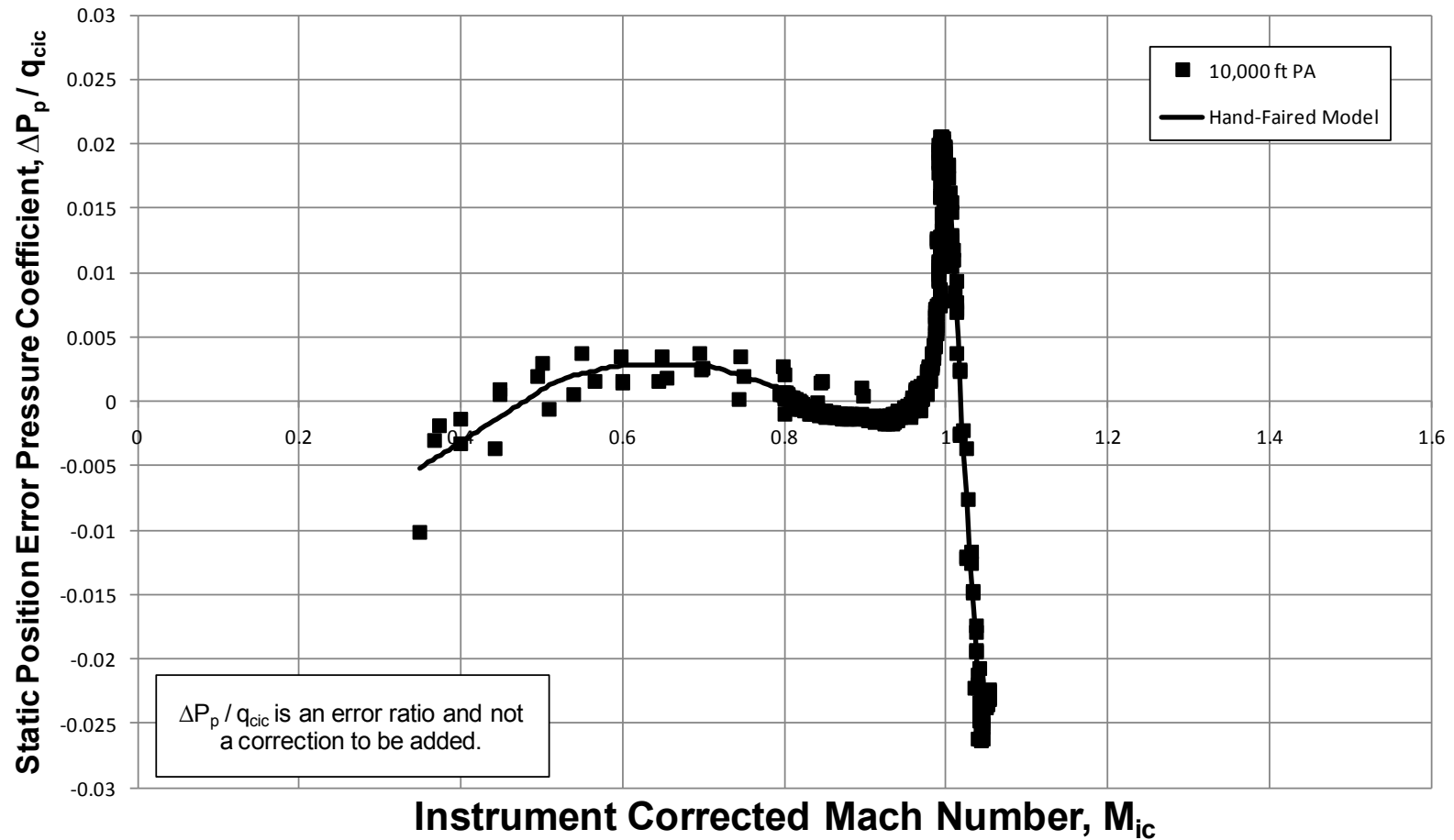


Figure A-23. Noseboom Static Position Error Pressure Coefficient (10,000 ft PA)

# Static Position Error Pressure Coefficient 20,000 ft PA - Test Noseboom (System 1)

Aircraft: F-16D, S/N 87-0391 (ARDS Pod on Station 1 and 370 Gallon Fuel Tanks on Stations 4 and 6)

Configuration: Cruise (Gear Up / Flaps Up)

Data Basis: Flight Test (Test Day Data) / 15-31 Mar 2010

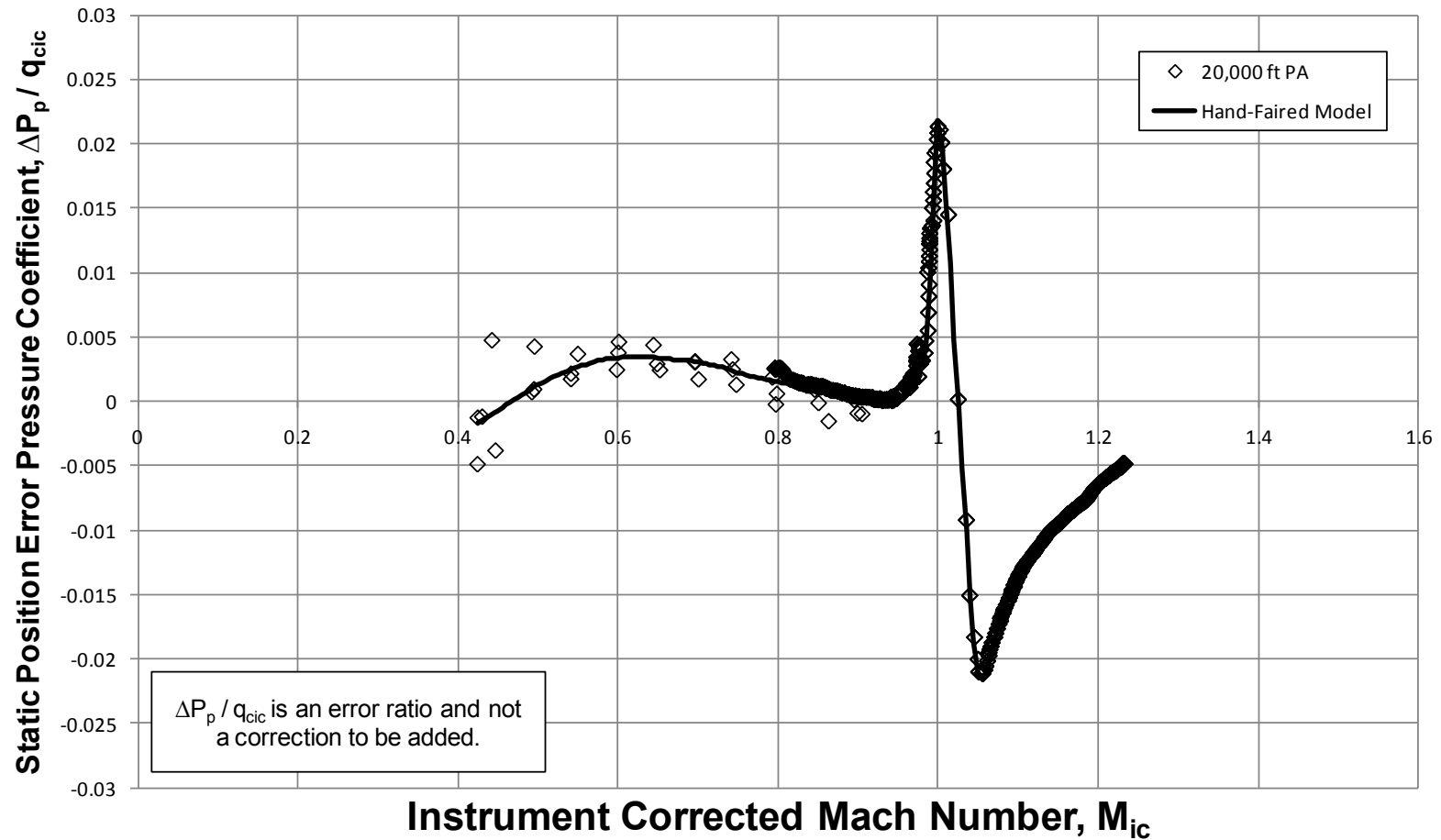


Figure A-24. Noseboom Static Position Error Pressure Coefficient (20,000 ft PA)

# Static Position Error Pressure Coefficient 30,000 ft PA - Test Noseboom (System 1)

Aircraft: F-16D, S/N 87-0391 (ARDS Pod on Station 1 and 370 Gallon Fuel Tanks on Stations 4 and 6)

Configuration: Cruise (Gear Up / Flaps Up)

Data Basis: Flight Test (Test Day Data) / 15-31 Mar 2010

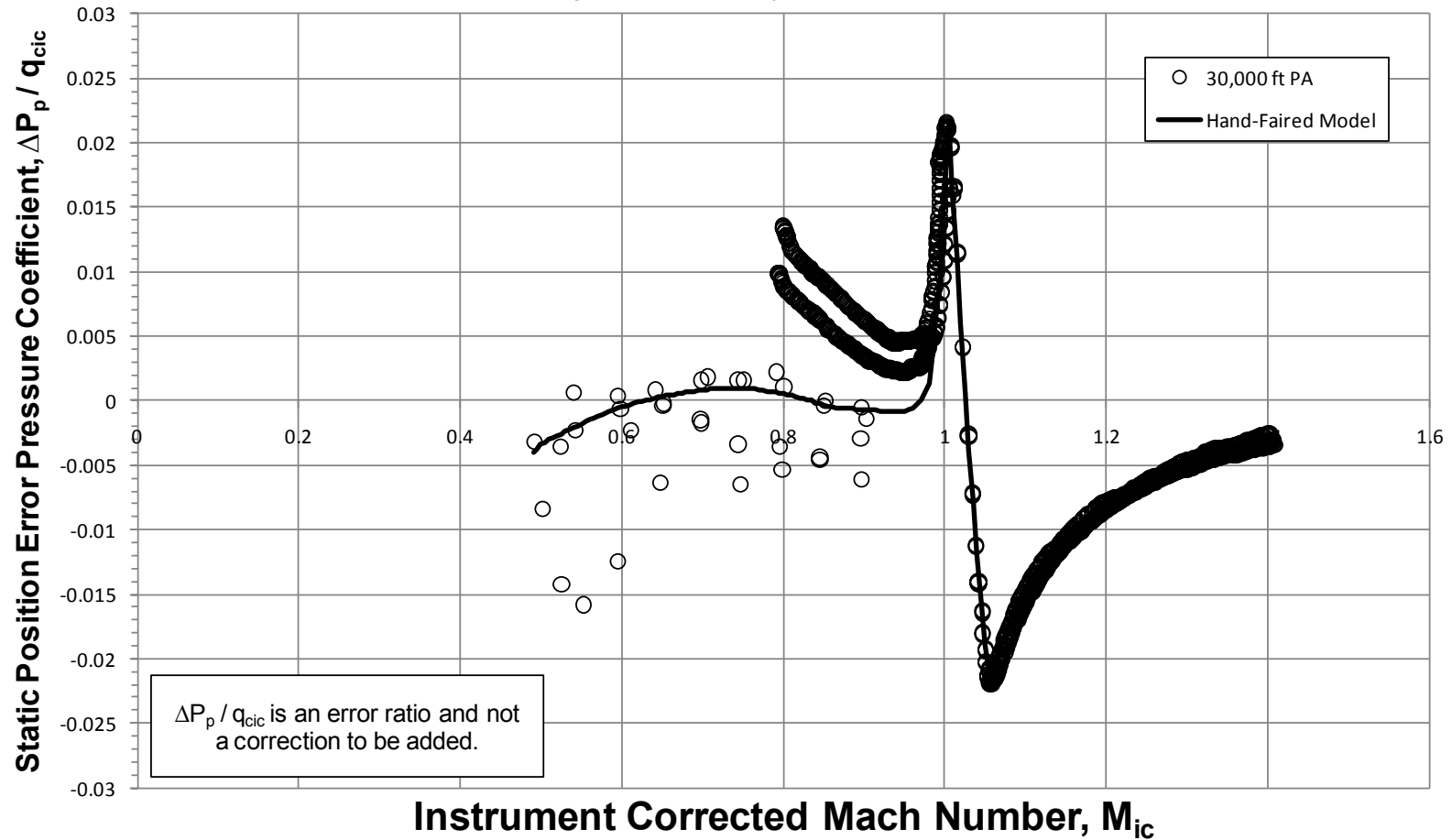


Figure A-25. Noseboom Static Position Error Pressure Coefficient (30,000 ft PA)

# Static Position Error Pressure Coefficient 40,000 ft PA - Test Noseboom (System 1)

Aircraft: F-16D, S/N 87-0391 (ARDS Pod on Station 1 and 370 Gallon Fuel Tanks on Stations 4 and 6)

Configuration: Cruise (Gear Up / Flaps Up)

Data Basis: Flight Test (Test Day Data) / 15-31 Mar 2010

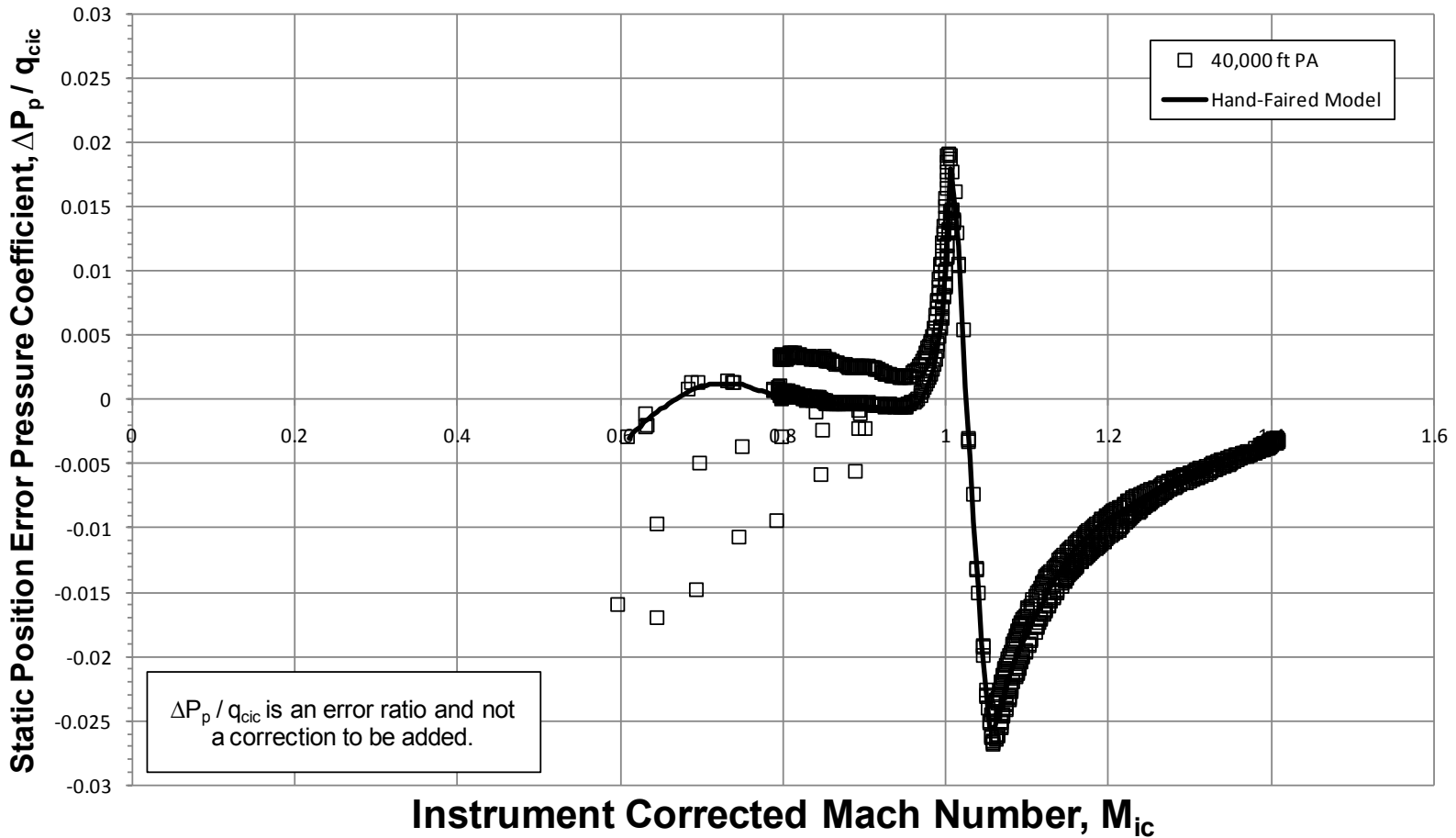


Figure A-26. Noseboom Static Position Error Pressure Coefficient (40,000 ft PA)

# Static Position Error Pressure Coefficient 45,000 ft PA - Test Noseboom (System 1)

Aircraft: F-16D, S/N 87-0391 (ARDS Pod on Station 1 and 370 Gallon Fuel Tanks on Stations 4 and 6)

Configuration: Cruise (Gear Up / Flaps Up)

Data Basis: Flight Test (Test Day Data) / 15-31 Mar 2010

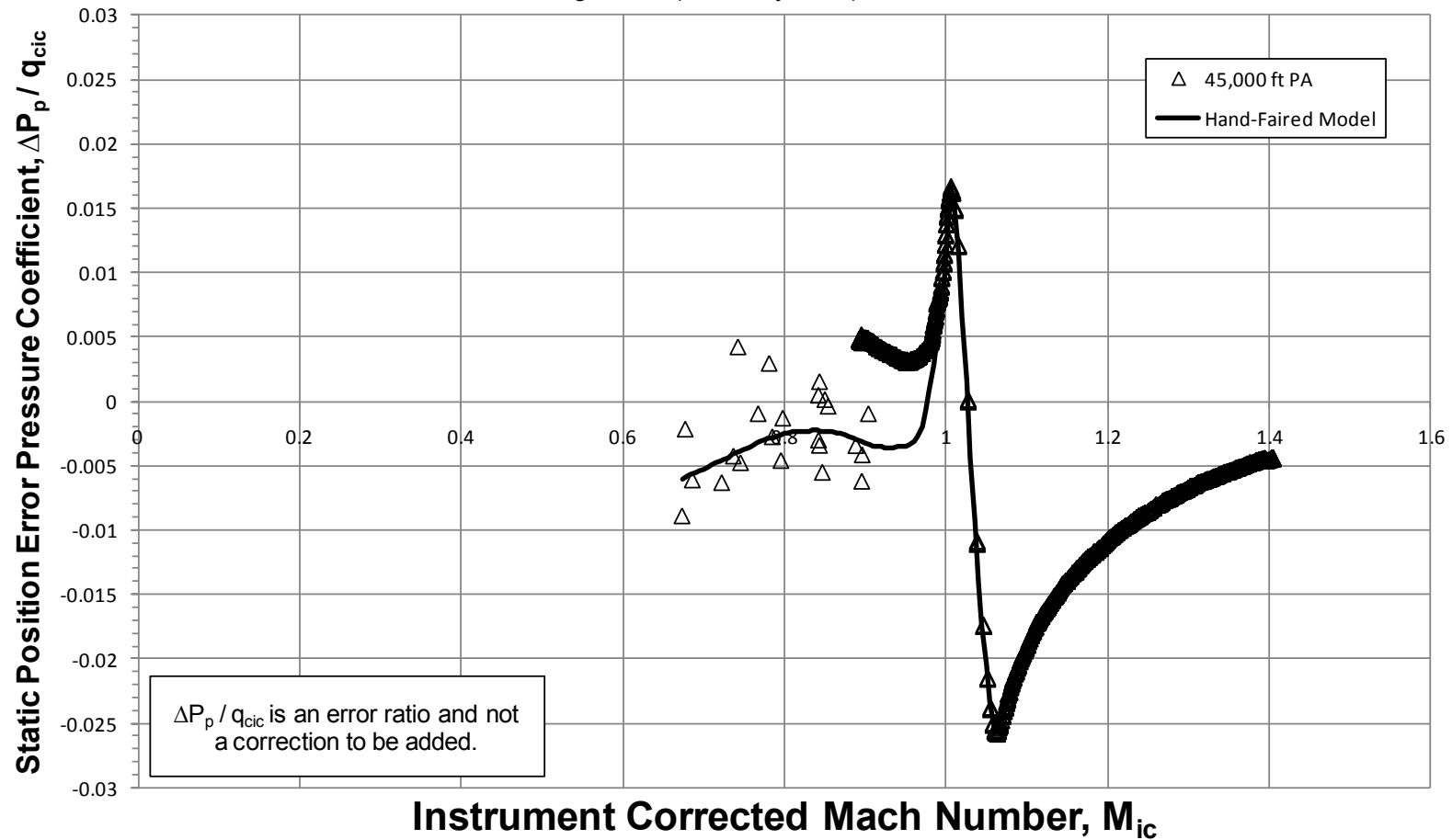


Figure A-27. Noseboom Static Position Error Pressure Coefficient (45,000 ft PA)

# Static Position Error Pressure Coefficient Models 2,300 to 45,000 ft PA - Test Noseboom (System 1)

Aircraft: F-16D, S/N 87-0391 (ARDS Pod on Station 1 and 370 Gallon Fuel Tanks on Stations 4 and 6)

Configuration: Cruise (Gear Up / Flaps Up)

Data Basis: Flight Test (Test Day Data) / 8-31 Mar 2010

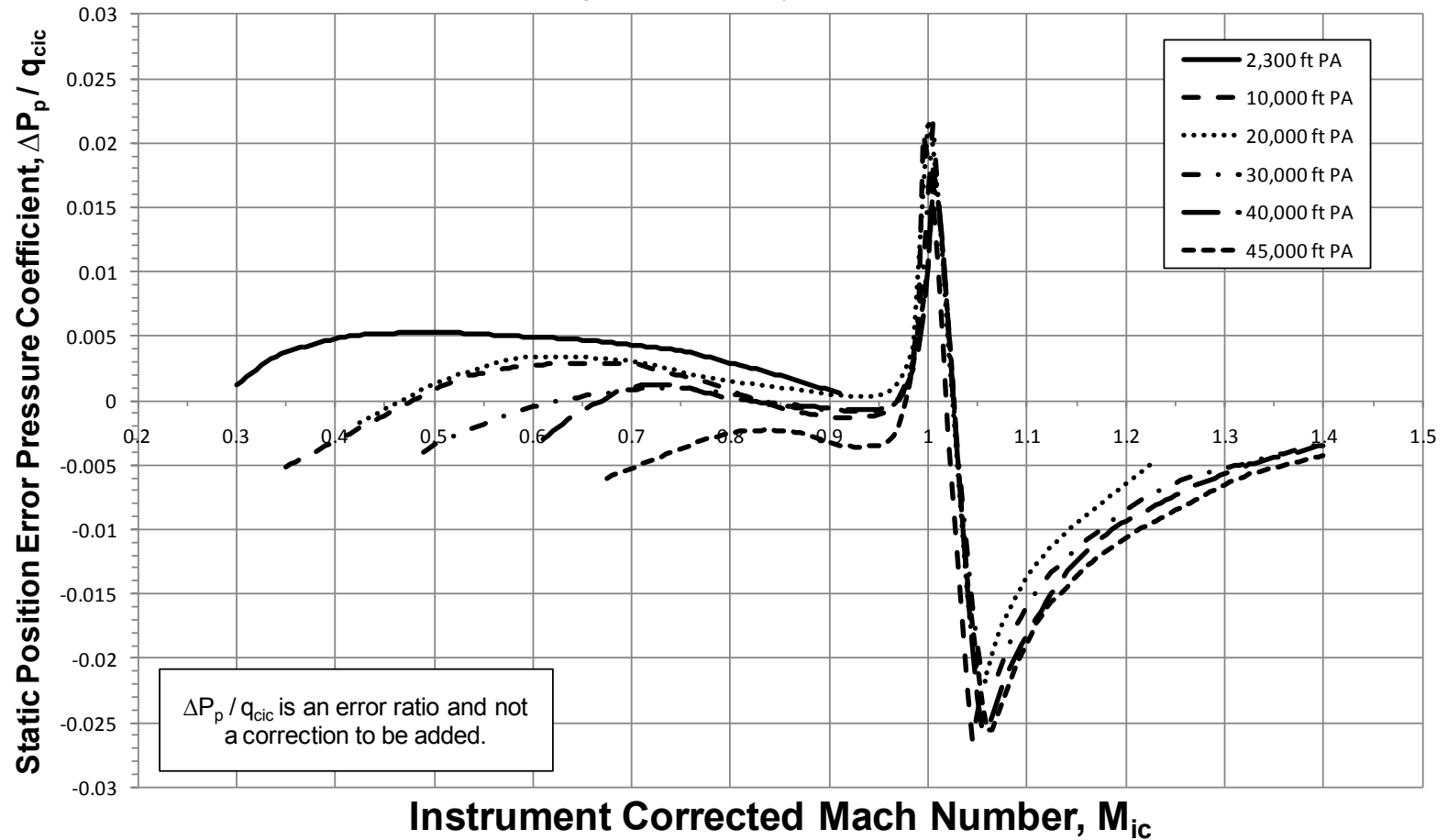


Figure A-28. Noseboom Static Position Error Pressure Coefficient Models (2,300 ft PA to 45,000 ft PA)

# Static Position Error Pressure Coefficient

## 0.40 Mach, 2,300 to 45,000 ft PA - Test Noseboom (System 1)

Aircraft: F-16D, S/N 87-0391 (ARDS Pod on Station 1 and 370 Gallon Fuel Tanks on Stations 4 and 6)

Configuration: Cruise (Gear Up / Flaps Up)

Data Basis: Flight Test (Test Day Data) / 15-31 Mar 2010

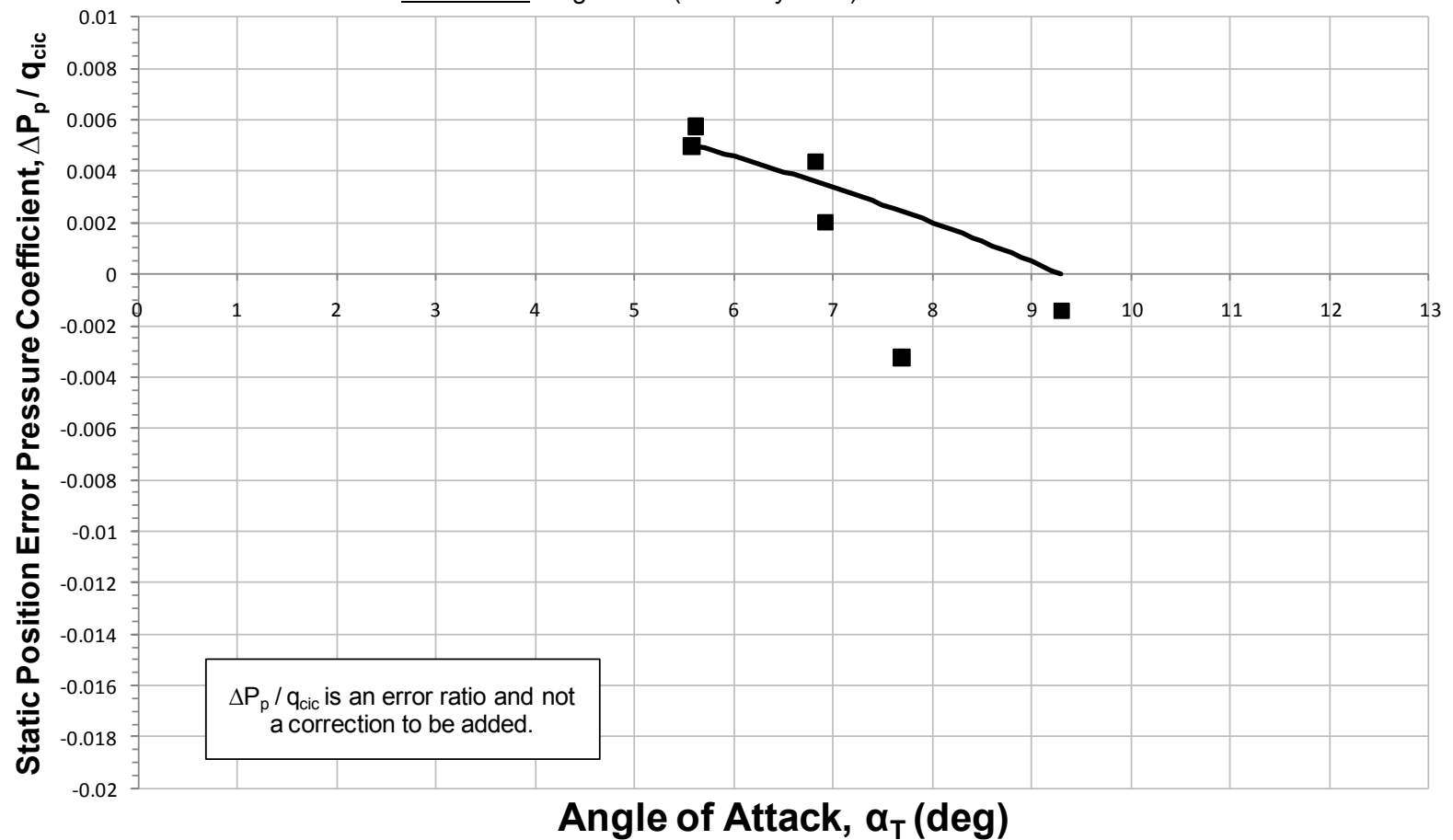


Figure A-29. Noseboom Static Position Error Pressure Coefficient (0.40 Mach)

# Static Position Error Pressure Coefficient

## 0.45 Mach, 2,300 to 45,000 ft PA - Test Noseboom (System 1)

Aircraft: F-16D, S/N 87-0391 (ARDS Pod on Station 1 and 370 Gallon Fuel Tanks on Stations 4 and 6)

Configuration: Cruise (Gear Up / Flaps Up)

Data Basis: Flight Test (Test Day Data) / 15-31 Mar 2010

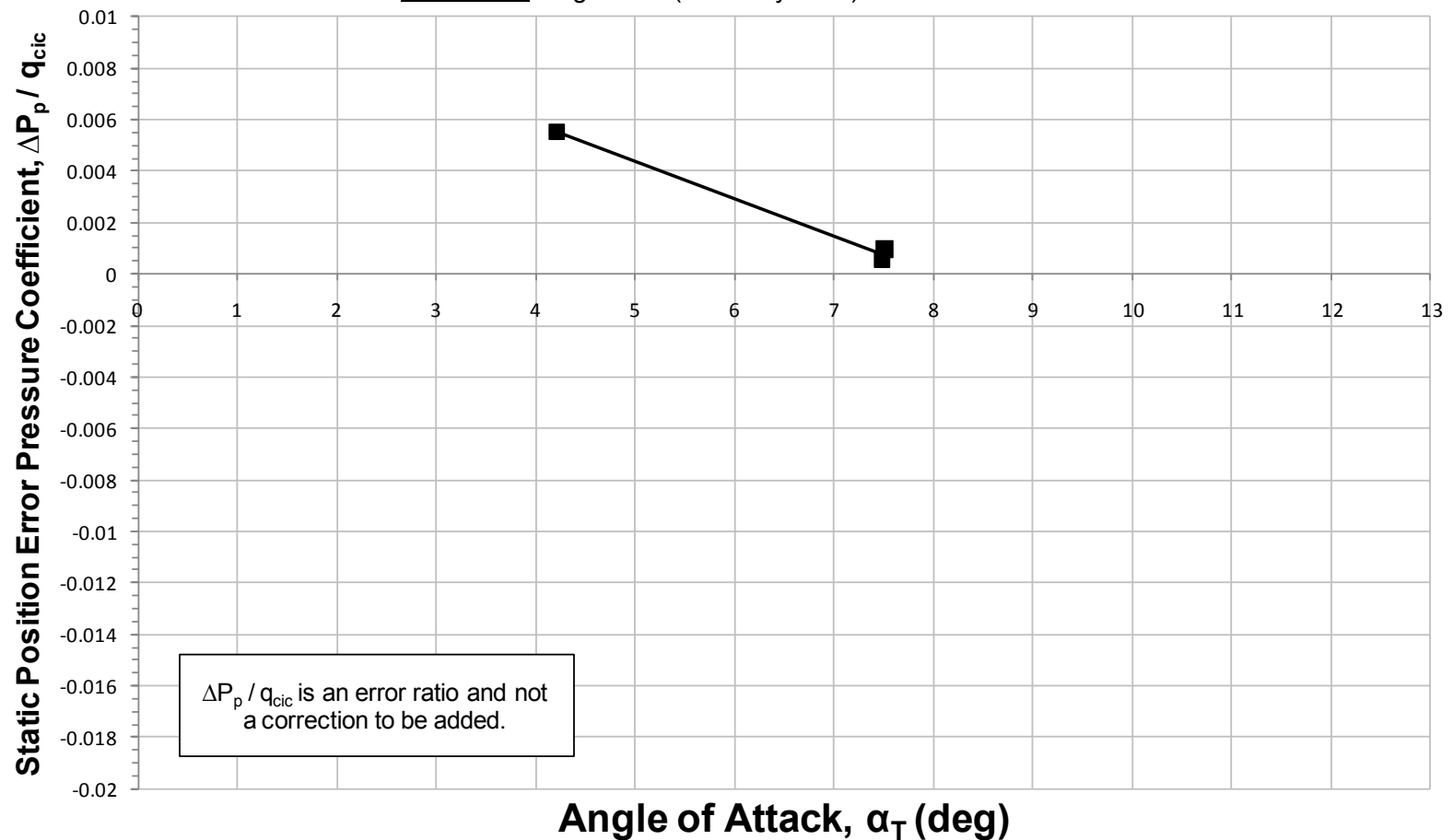


Figure A-30. Noseboom Static Position Error Pressure Coefficient (0.45 Mach)

# Static Position Error Pressure Coefficient

## 0.50 Mach, 2,300 to 45,000 ft PA - Test Noseboom (System 1)

Aircraft: F-16D, S/N 87-0391 (ARDS Pod on Station 1 and 370 Gallon Fuel Tanks on Stations 4 and 6)

Configuration: Cruise (Gear Up / Flaps Up)

Data Basis: Flight Test (Test Day Data) / 15-31 Mar 2010

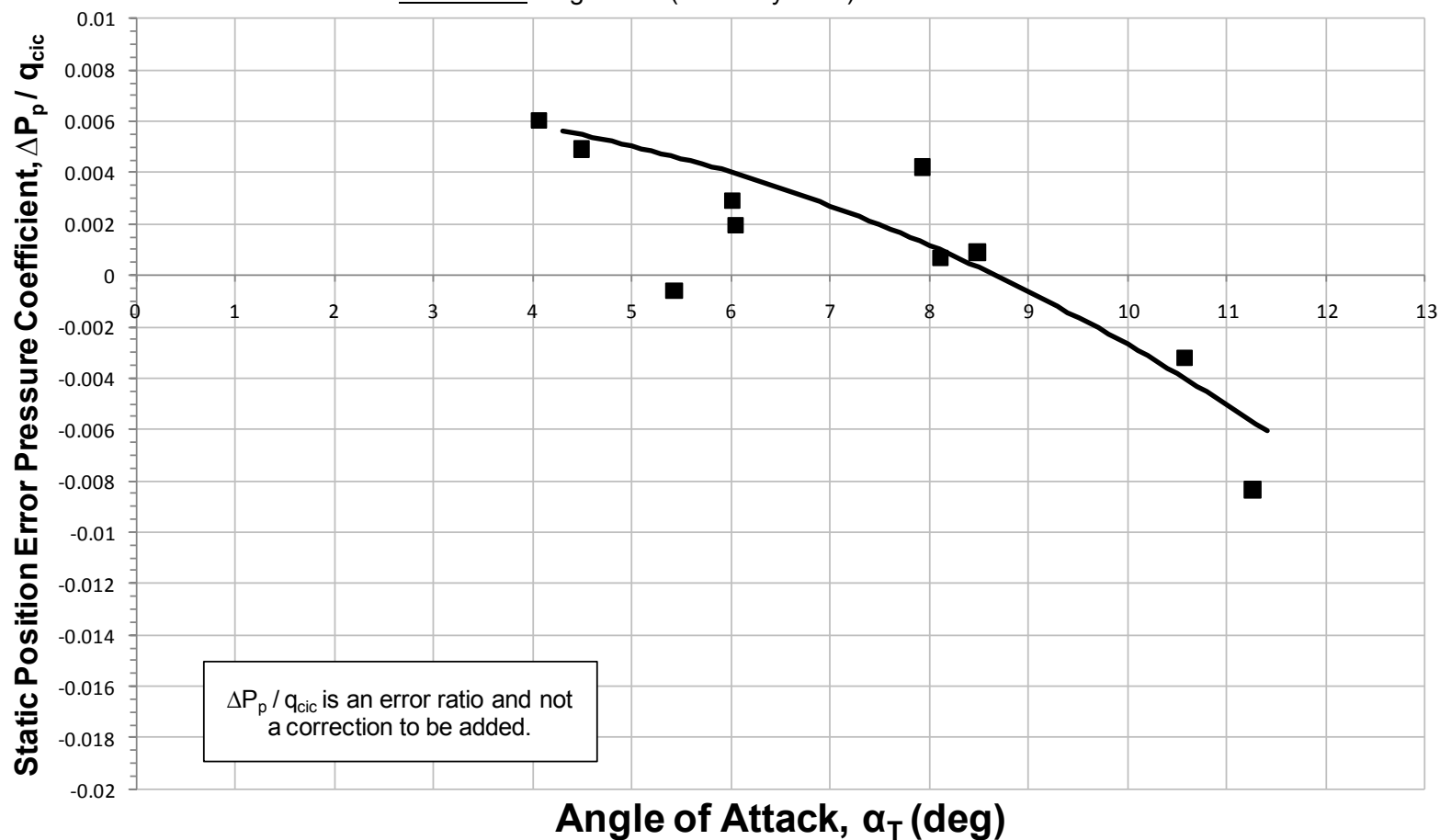


Figure A-31. Noseboom Static Position Error Pressure Coefficient (0.50 Mach)

# Static Position Error Pressure Coefficient

## 0.55 Mach, 2,300 to 45,000 ft PA - Test Noseboom (System 1)

Aircraft: F-16D, S/N 87-0391 (ARDS Pod on Station 1 and 370 Gallon Fuel Tanks on Stations 4 and 6)

Configuration: Cruise (Gear Up / Flaps Up)

Data Basis: Flight Test (Test Day Data) / 15-31 Mar 2010

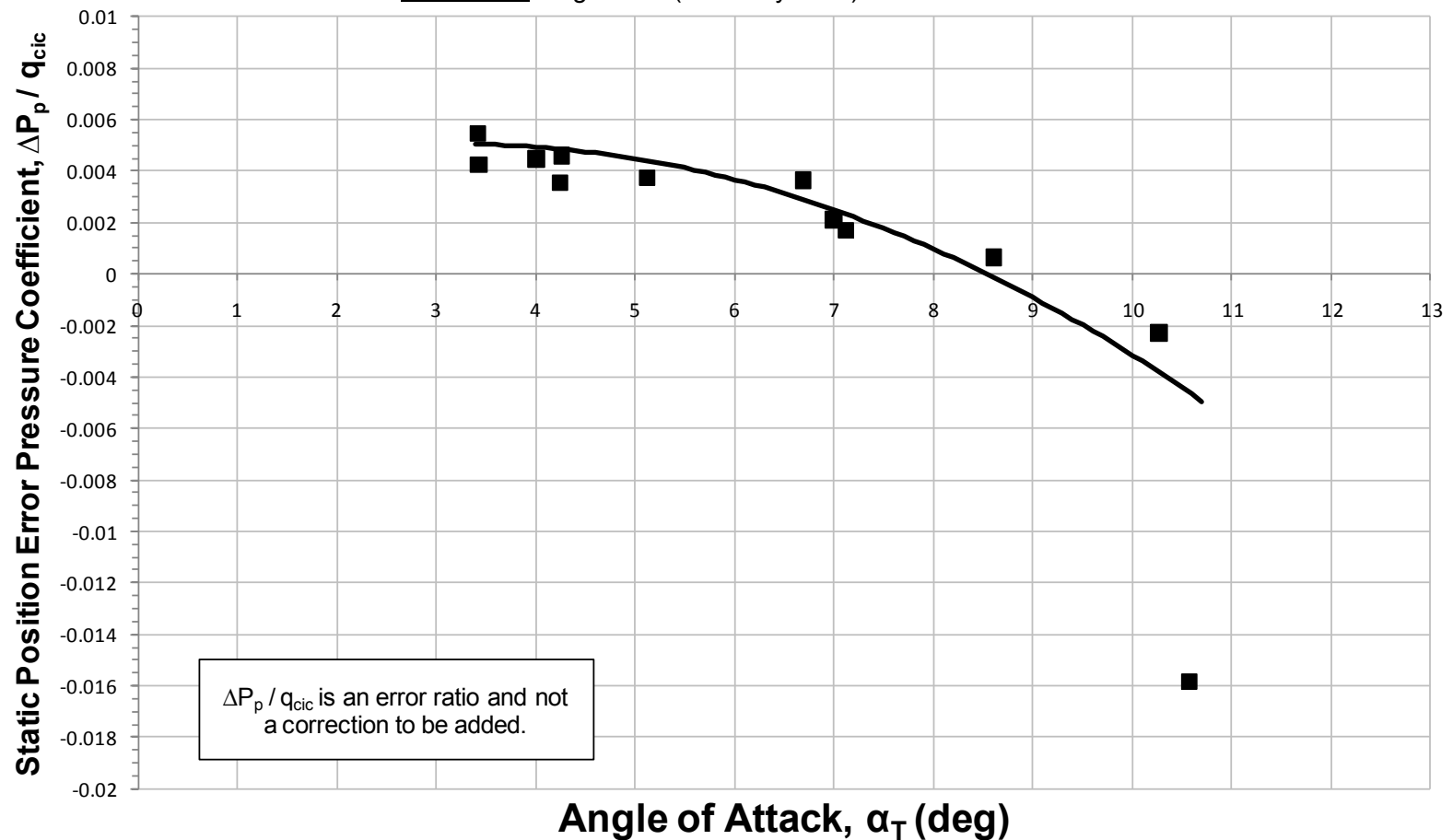


Figure A-32. Noseboom Static Position Error Pressure Coefficient (0.55 Mach)

# Static Position Error Pressure Coefficient

## 0.60 Mach, 2,300 to 45,000 ft PA - Test Noseboom (System 1)

Aircraft: F-16D, S/N 87-0391 (ARDS Pod on Station 1 and 370 Gallon Fuel Tanks on Stations 4 and 6)

Configuration: Cruise (Gear Up / Flaps Up)

Data Basis: Flight Test (Test Day Data) / 15-31 Mar 2010

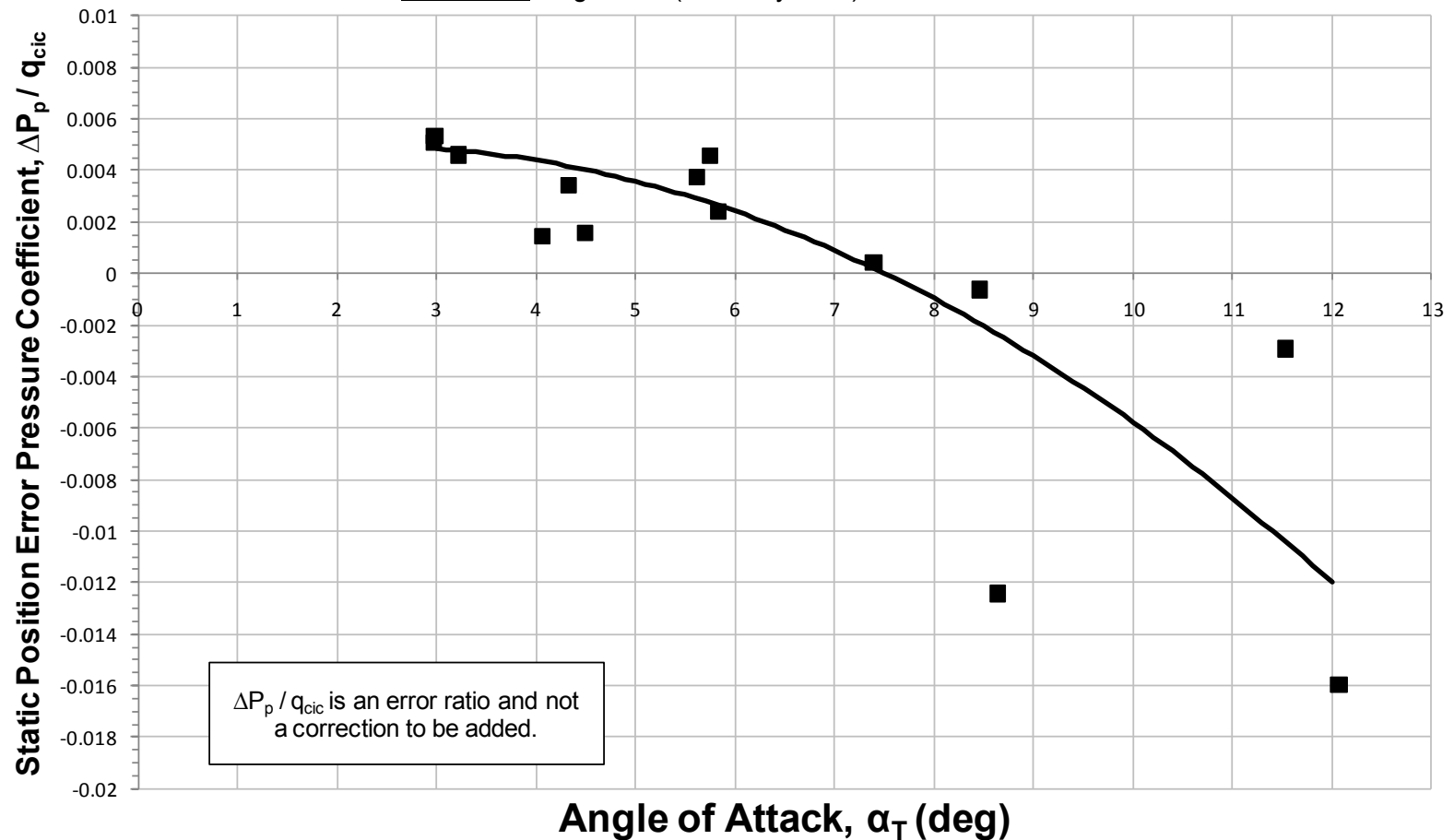


Figure A-33. Noseboom Static Position Error Pressure Coefficient (0.60 Mach)

# Static Position Error Pressure Coefficient

## 0.65 Mach, 2,300 to 45,000 ft PA - Test Noseboom (System 1)

Aircraft: F-16D, S/N 87-0391 (ARDS Pod on Station 1 and 370 Gallon Fuel Tanks on Stations 4 and 6)

Configuration: Cruise (Gear Up / Flaps Up)

Data Basis: Flight Test (Test Day Data) / 15-31 Mar 2010

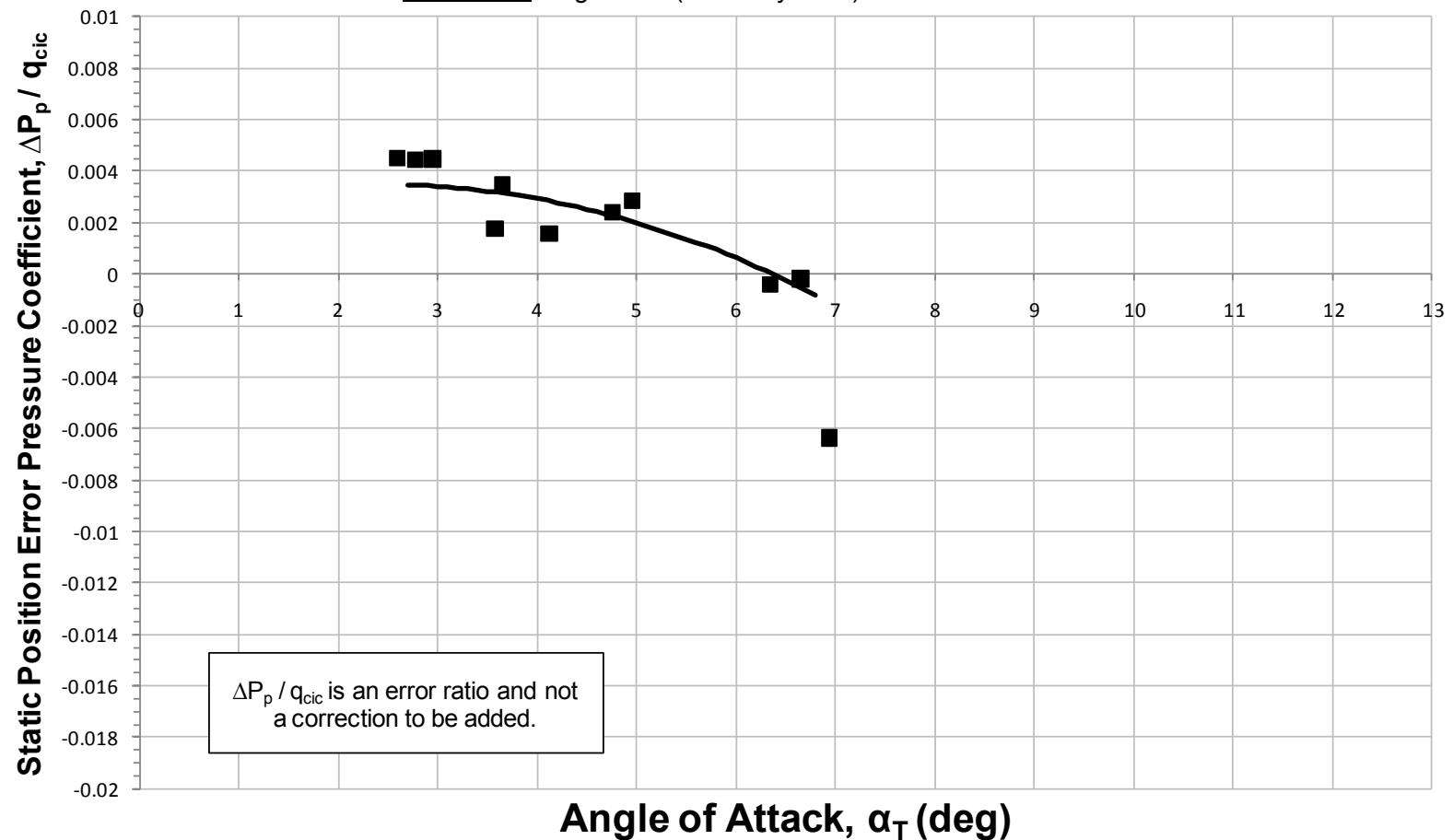


Figure A-34. Noseboom Static Position Error Pressure Coefficient (0.65 Mach)

# Static Position Error Pressure Coefficient

## 0.70 Mach, 2,300 to 45,000 ft PA - Test Noseboom (System 1)

Aircraft: F-16D, S/N 87-0391 (ARDS Pod on Station 1 and 370 Gallon Fuel Tanks on Stations 4 and 6)

Configuration: Cruise (Gear Up / Flaps Up)

Data Basis: Flight Test (Test Day Data) / 15-31 Mar 2010

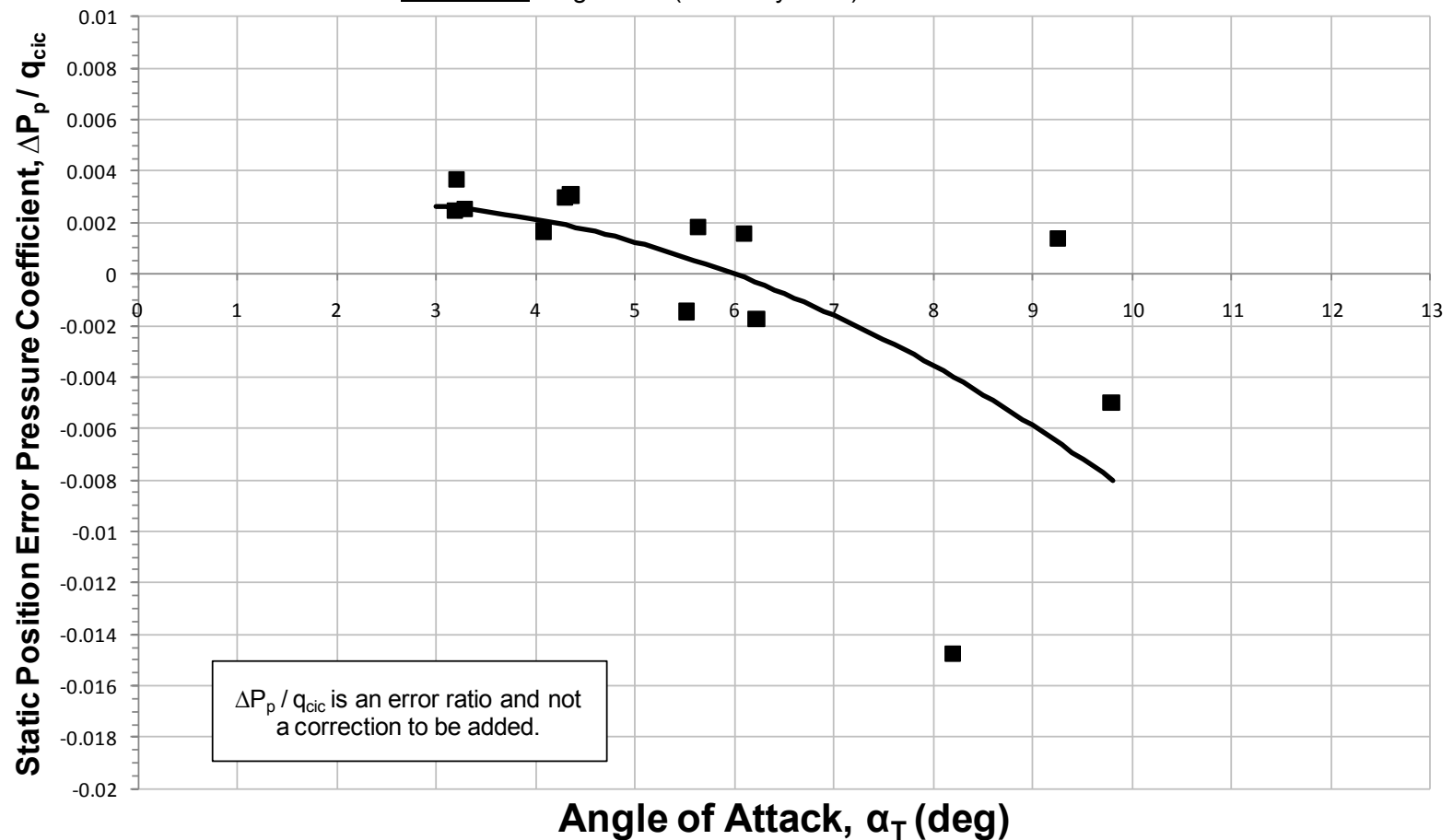


Figure A-35. Noseboom Static Position Error Pressure Coefficient (0.70 Mach)

# Static Position Error Pressure Coefficient

## 0.75 Mach, 2,300 to 45,000 ft PA - Test Noseboom (System 1)

Aircraft: F-16D, S/N 87-0391 (ARDS Pod on Station 1 and 370 Gallon Fuel Tanks on Stations 4 and 6)

Configuration: Cruise (Gear Up / Flaps Up)

Data Basis: Flight Test (Test Day Data) / 15-31 Mar 2010

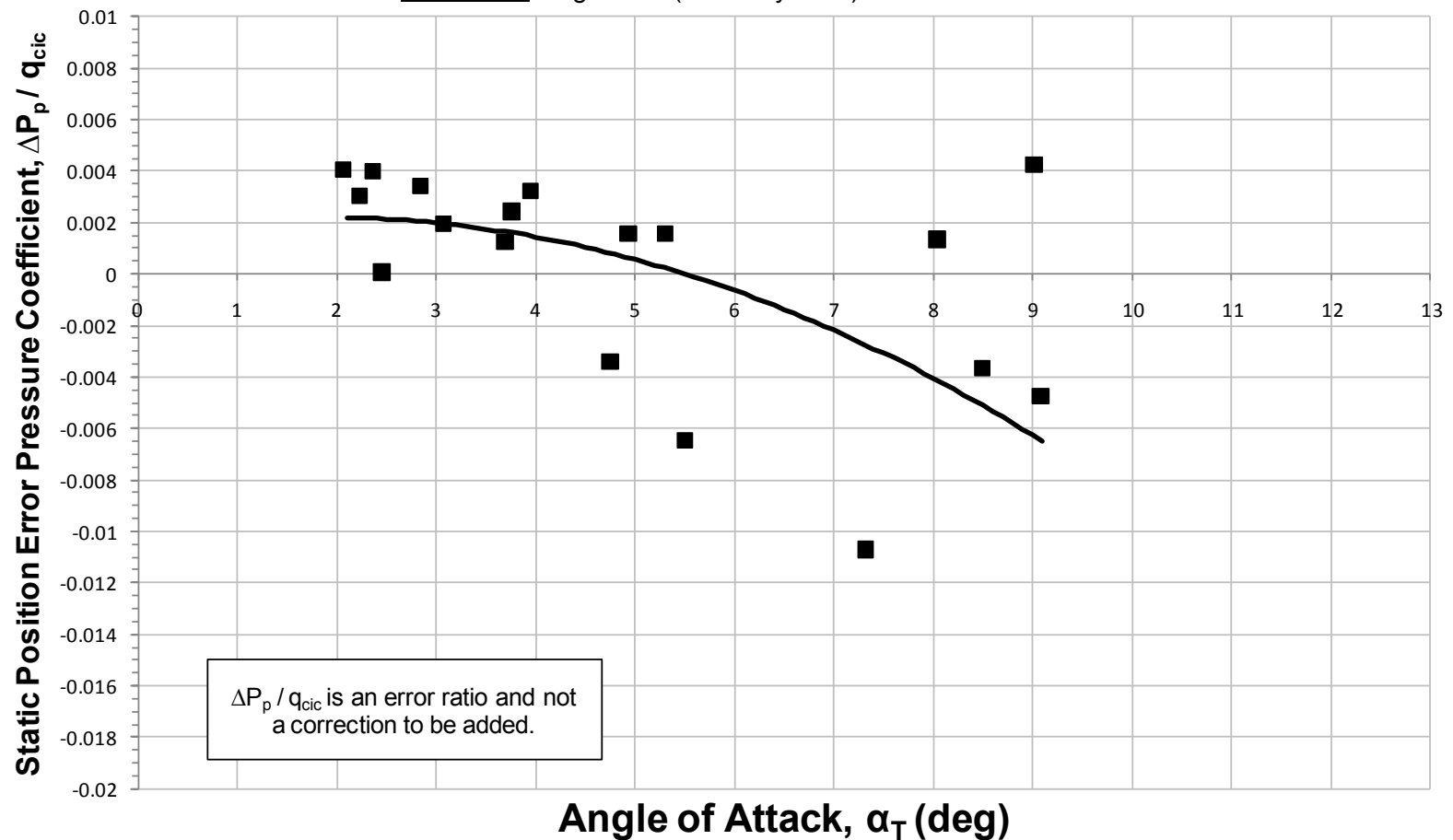


Figure A-36. Noseboom Static Position Error Pressure Coefficient (0.75 Mach)

# Static Position Error Pressure Coefficient

## 0.80 Mach, 2,300 to 45,000 ft PA - Test Noseboom (System 1)

Aircraft: F-16D, S/N 87-0391 (ARDS Pod on Station 1 and 370 Gallon Fuel Tanks on Stations 4 and 6)

Configuration: Cruise (Gear Up / Flaps Up)

Data Basis: Flight Test (Test Day Data) / 15-31 Mar 2010

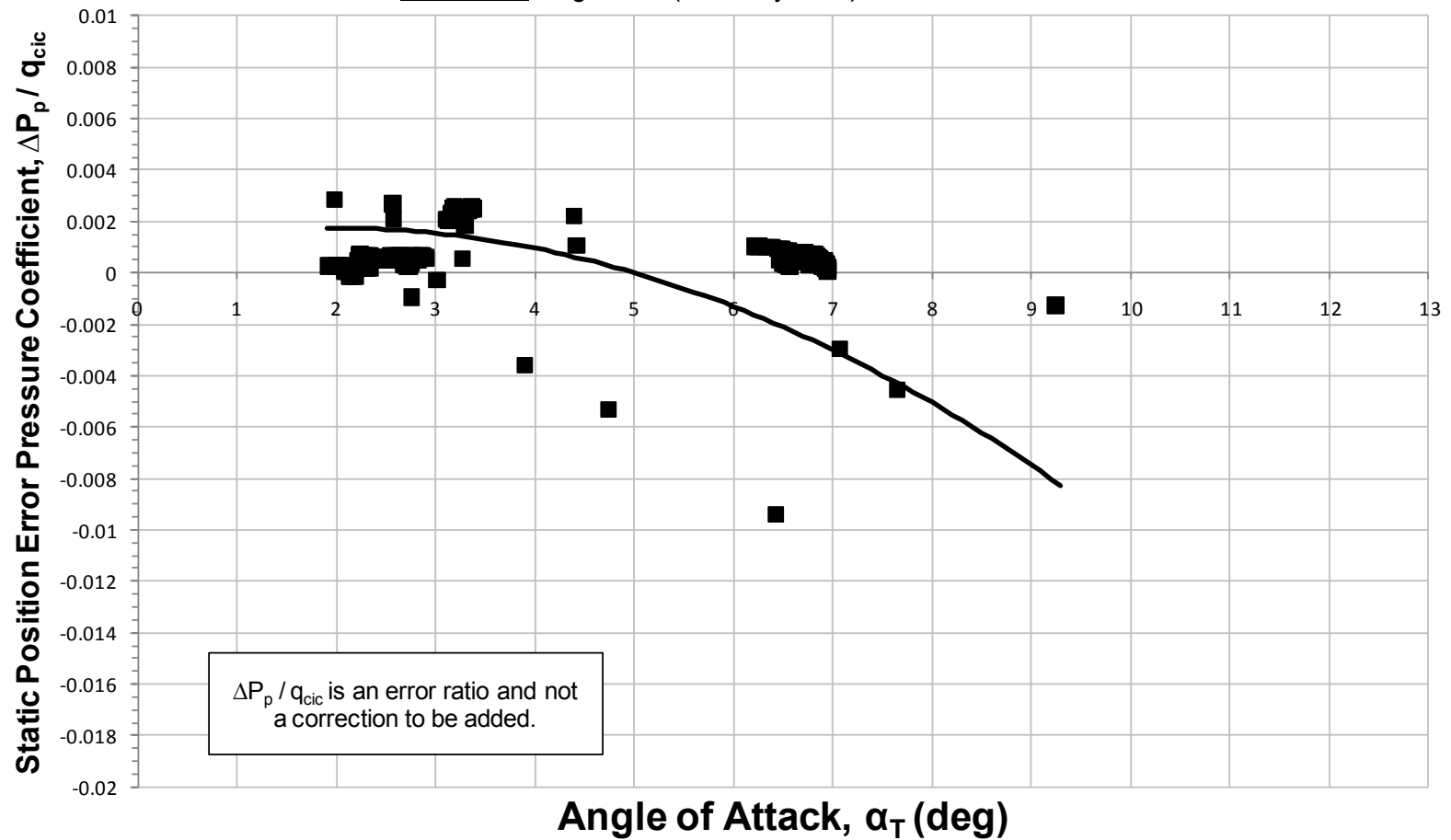


Figure A-37. Noseboom Static Position Error Pressure Coefficient (0.80 Mach)

# Static Position Error Pressure Coefficient

## 0.85 Mach, 2,300 to 45,000 ft PA - Test Noseboom (System 1)

Aircraft: F-16D, S/N 87-0391 (ARDS Pod on Station 1 and 370 Gallon Fuel Tanks on Stations 4 and 6)

Configuration: Cruise (Gear Up / Flaps Up)

Data Basis: Flight Test (Test Day Data) / 15-31 Mar 2010

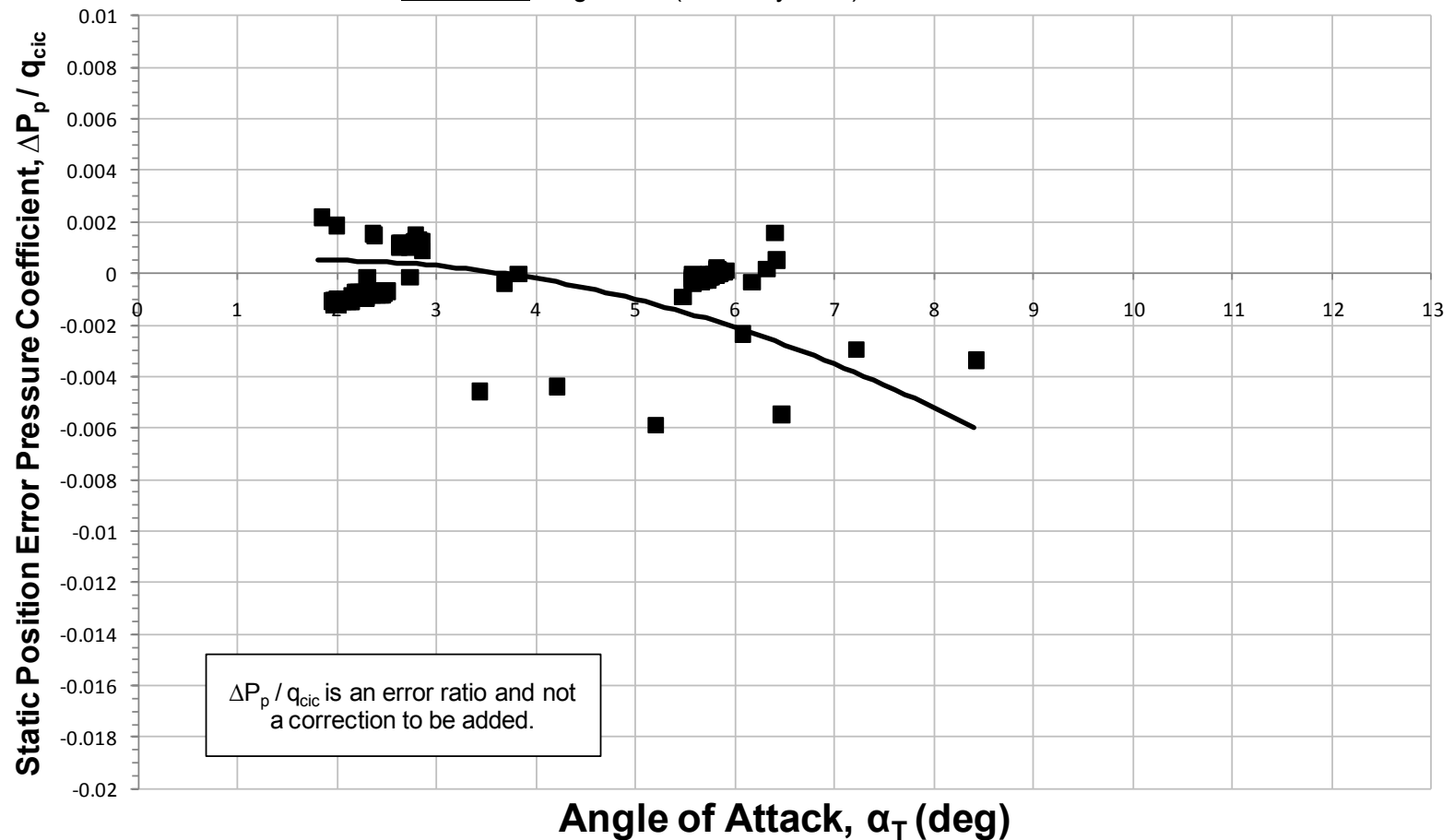


Figure A-38. Noseboom Static Position Error Pressure Coefficient (0.85 Mach)

# Static Position Error Pressure Coefficient

## 0.90 Mach, 2,300 to 45,000 ft PA - Test Noseboom (System 1)

Aircraft: F-16D, S/N 87-0391 (ARDS Pod on Station 1 and 370 Gallon Fuel Tanks on Stations 4 and 6)

Configuration: Cruise (Gear Up / Flaps Up)

Data Basis: Flight Test (Test Day Data) / 15-31 Mar 2010

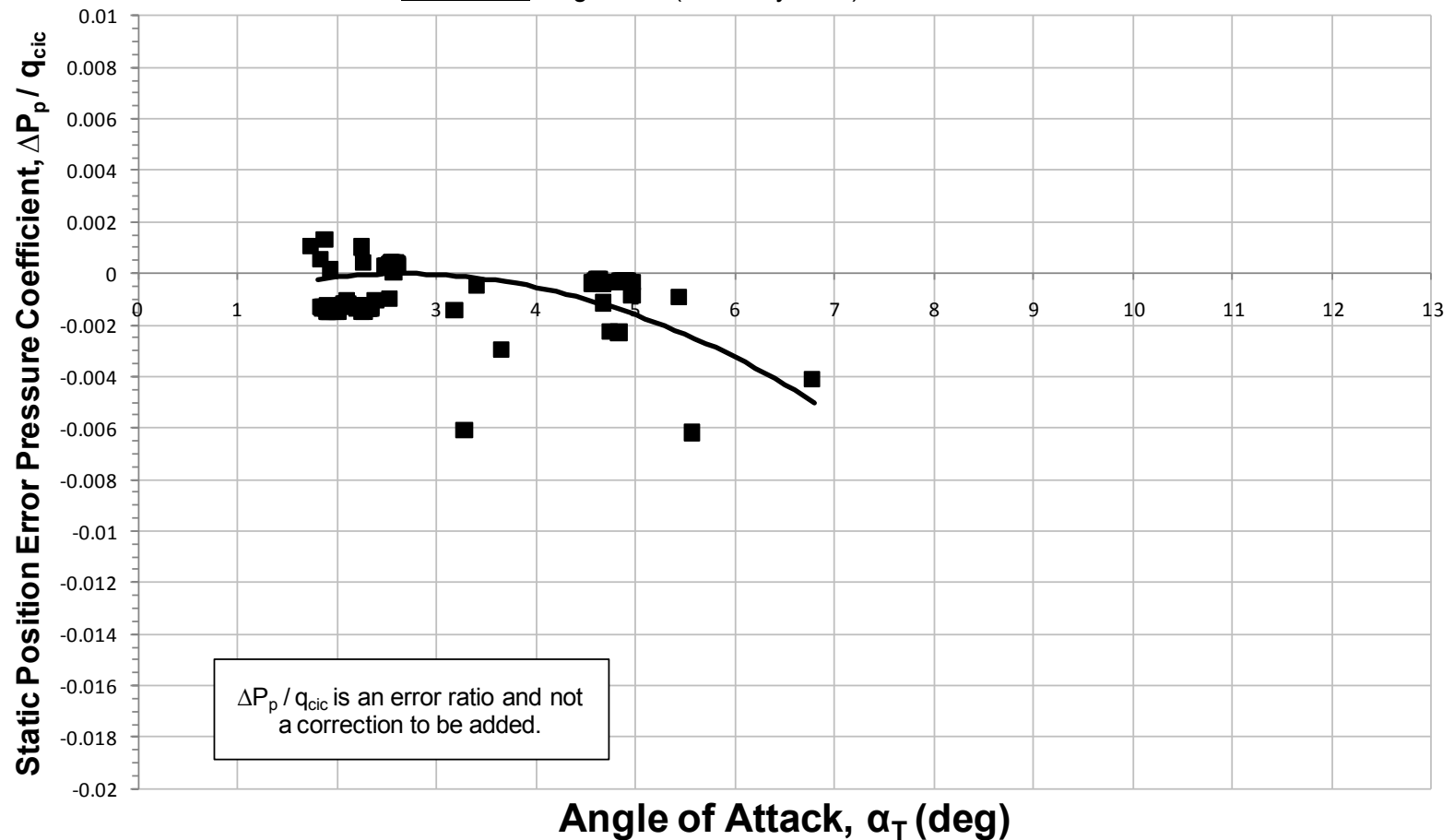


Figure A-39. Noseboom Static Position Error Pressure Coefficient (0.90 Mach)

# Static Position Error Pressure Coefficient

## 0.40 to 0.90 Mach, 2,300 to 45,000 ft PA - Test Noseboom (System 1)

Aircraft: F-16D, S/N 87-0391 (ARDS Pod on Station 1 and 370 Gallon Fuel Tanks on Stations 4 and 6)

Configuration: Cruise (Gear Up / Flaps Up)

Data Basis: Flight Test (Test Day Data) / 15-31 Mar 2010

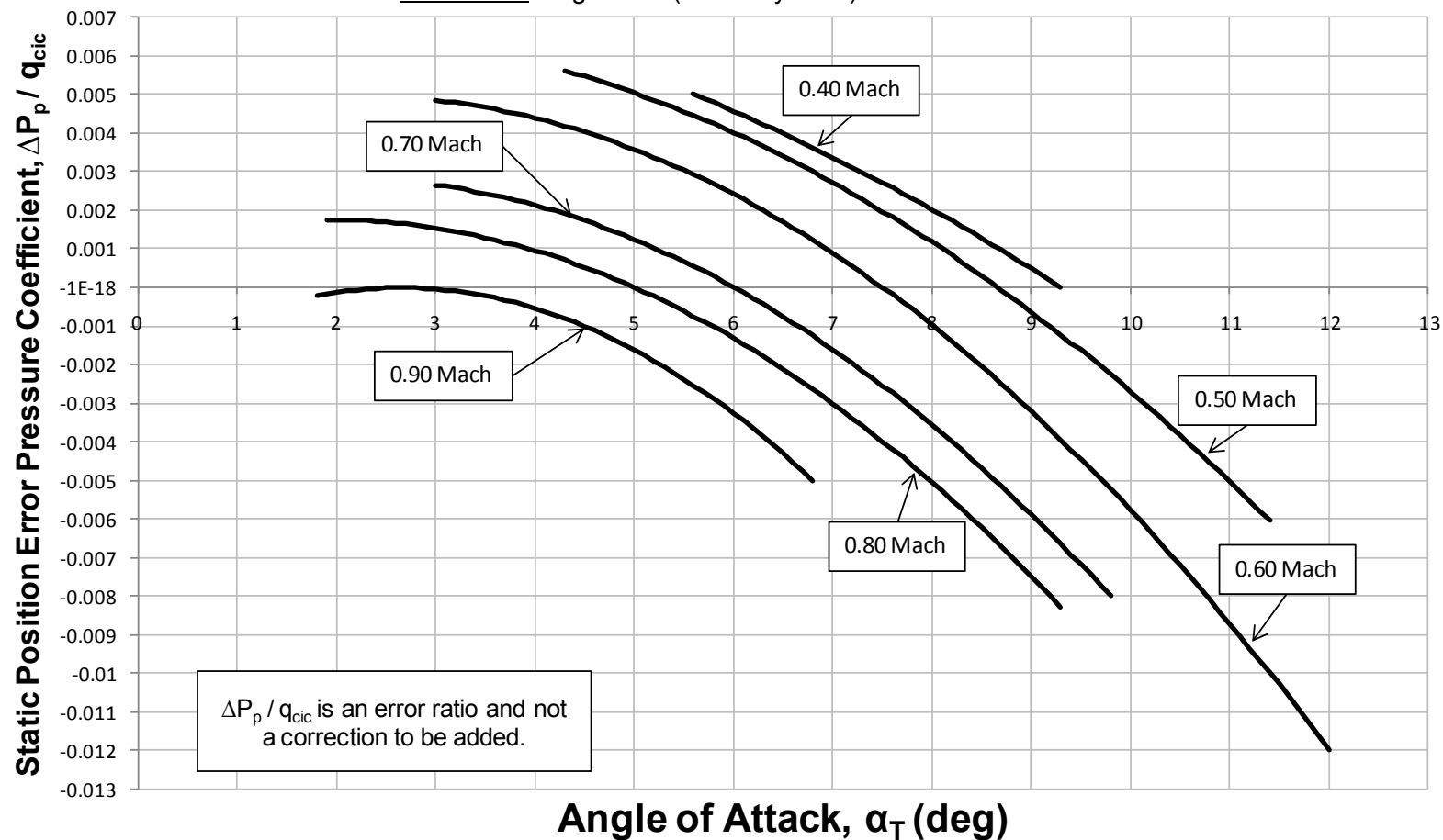


Figure A-40. Noseboom Static Position Error Pressure Coefficient Models (0.40 to 0.90 Mach)

# Static Position Error Pressure Coefficient

## 0.55 to 0.85 Mach, 2,300 to 45,000 ft PA - Test Noseboom (System 1)

Aircraft: F-16D, S/N 87-0391 (ARDS Pod on Station 1 and 370 Gallon Fuel Tanks on Stations 4 and 6)

Configuration: Cruise (Gear Up / Flaps Up)

Data Basis: Flight Test (Test Day Data) / 15-31 Mar 2010

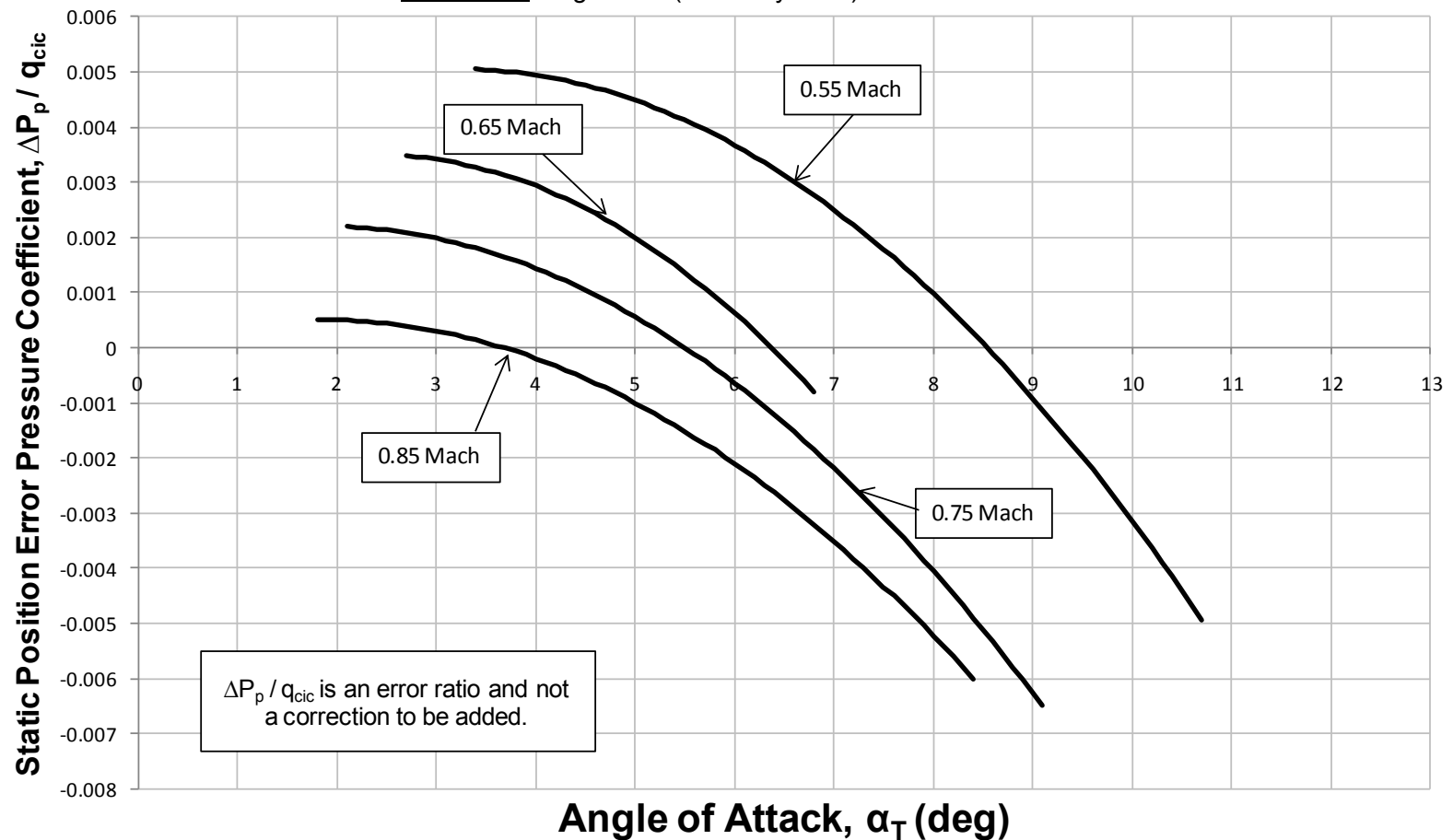


Figure A-41. Noseboom Static Position Error Pressure Coefficient Models (0.55 to 0.85 Mach)

# Static Position Error Pressure Coefficient

## 1.10 Mach, 2,300 to 45,000 ft PA - Test Noseboom (System 1)

Aircraft: F-16D, S/N 87-0391 (ARDS Pod on Station 1 and 370 Gallon Fuel Tanks on Stations 4 and 6)

Configuration: Cruise (Gear Up / Flaps Up)

Data Basis: Flight Test (Test Day Data) / 15-31 Mar 2010

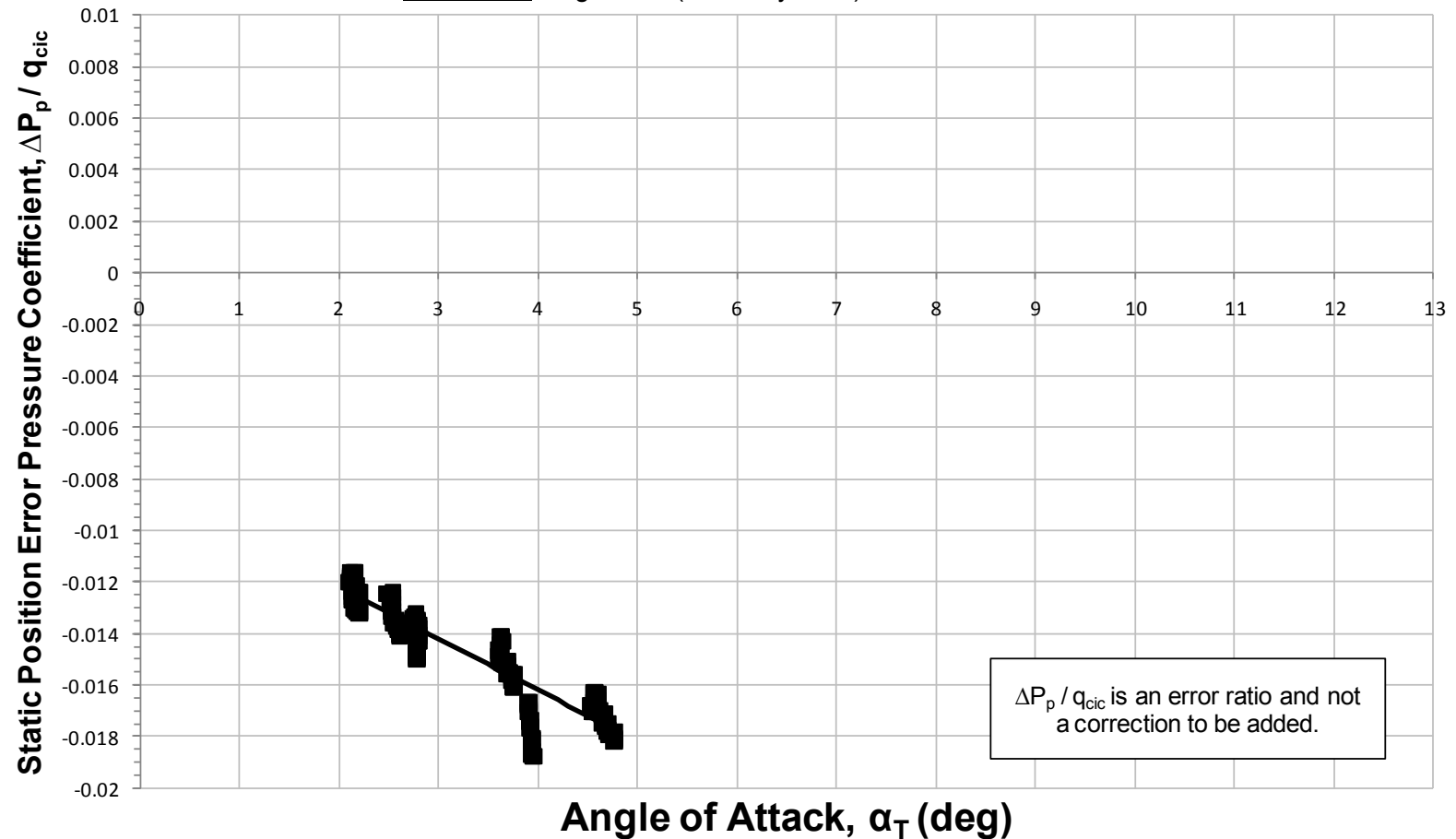


Figure A-42. Noseboom Static Position Error Pressure Coefficient (1.10 Mach)

# Static Position Error Pressure Coefficient

## 1.15 Mach, 2,300 to 45,000 ft PA - Test Noseboom (System 1)

Aircraft: F-16D, S/N 87-0391 (ARDS Pod on Station 1 and 370 Gallon Fuel Tanks on Stations 4 and 6)

Configuration: Cruise (Gear Up / Flaps Up)

Data Basis: Flight Test (Test Day Data) / 15-31 Mar 2010

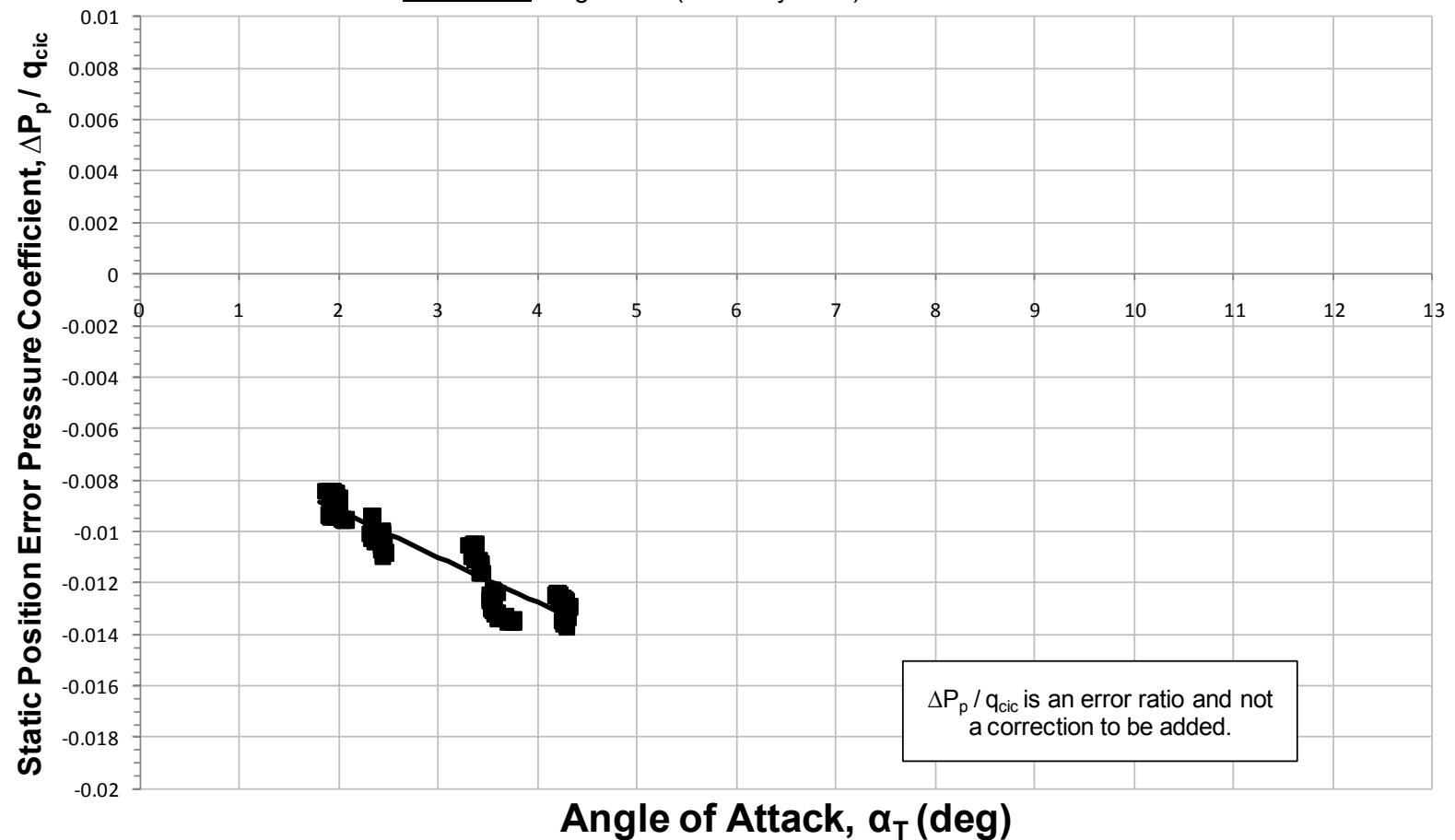


Figure A-43. Noseboom Static Position Error Pressure Coefficient (1.15 Mach)

# Static Position Error Pressure Coefficient

## 1.20 Mach, 2,300 to 45,000 ft PA - Test Noseboom (System 1)

Aircraft: F-16D, S/N 87-0391 (ARDS Pod on Station 1 and 370 Gallon Fuel Tanks on Stations 4 and 6)

Configuration: Cruise (Gear Up / Flaps Up)

Data Basis: Flight Test (Test Day Data) / 15-31 Mar 2010

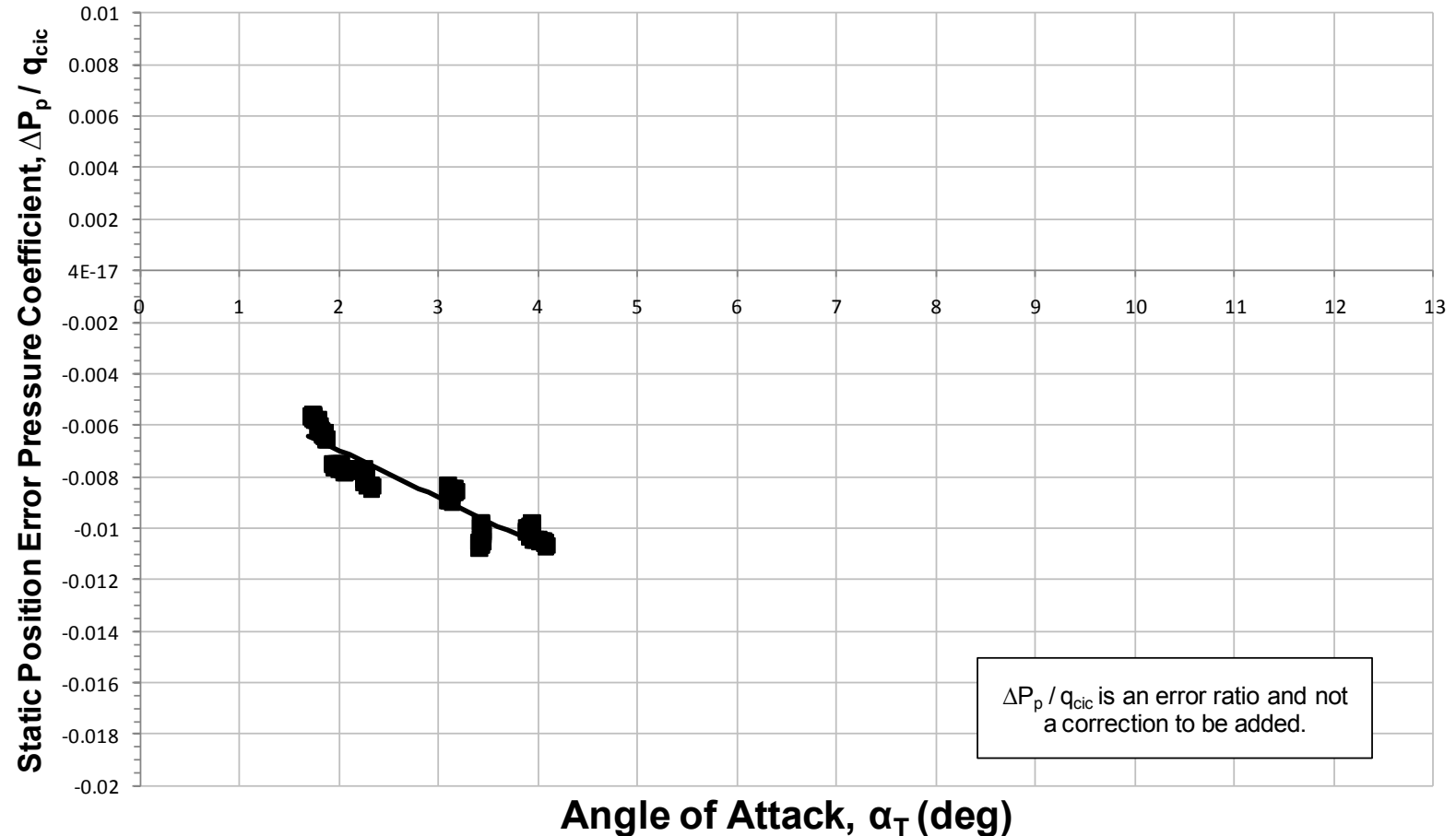


Figure A-44. Noseboom Static Position Error Pressure Coefficient (1.20 Mach)

# Static Position Error Pressure Coefficient

## 1.25 Mach, 2,300 to 45,000 ft PA - Test Noseboom (System 1)

Aircraft: F-16D, S/N 87-0391 (ARDS Pod on Station 1 and 370 Gallon Fuel Tanks on Stations 4 and 6)

Configuration: Cruise (Gear Up / Flaps Up)

Data Basis: Flight Test (Test Day Data) / 15-31 Mar 2010

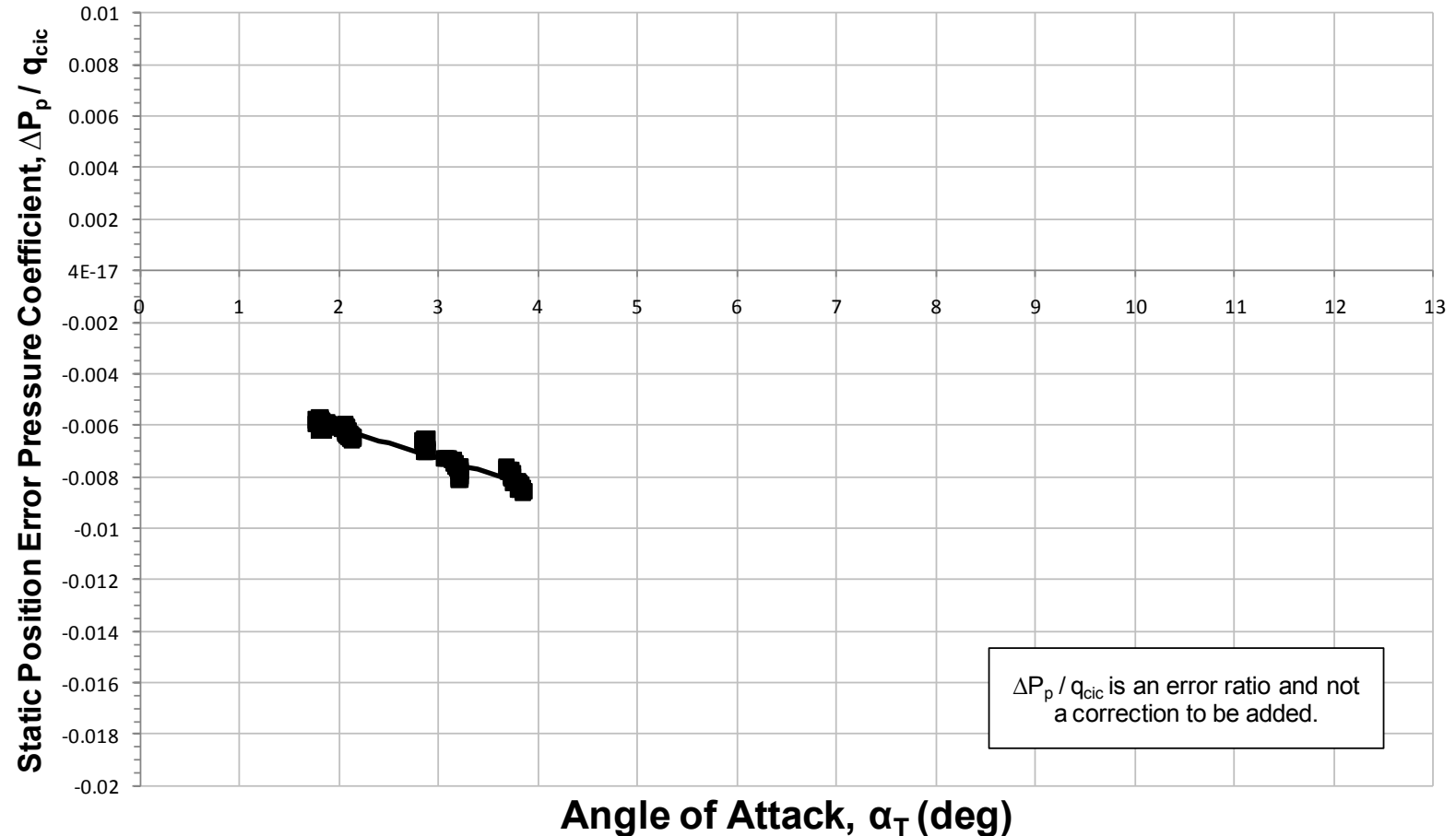


Figure A-45. Noseboom Static Position Error Pressure Coefficient (1.25 Mach)

# Static Position Error Pressure Coefficient

## 1.10 to 1.25 Mach, 2,300 to 45,000 ft PA - Test Noseboom (System 1)

Aircraft: F-16D, S/N 87-0391 (ARDS Pod on Station 1 and 370 Gallon Fuel Tanks on Stations 4 and 6)

Configuration: Cruise (Gear Up / Flaps Up)

Data Basis: Flight Test (Test Day Data) / 15-31 Mar 2010

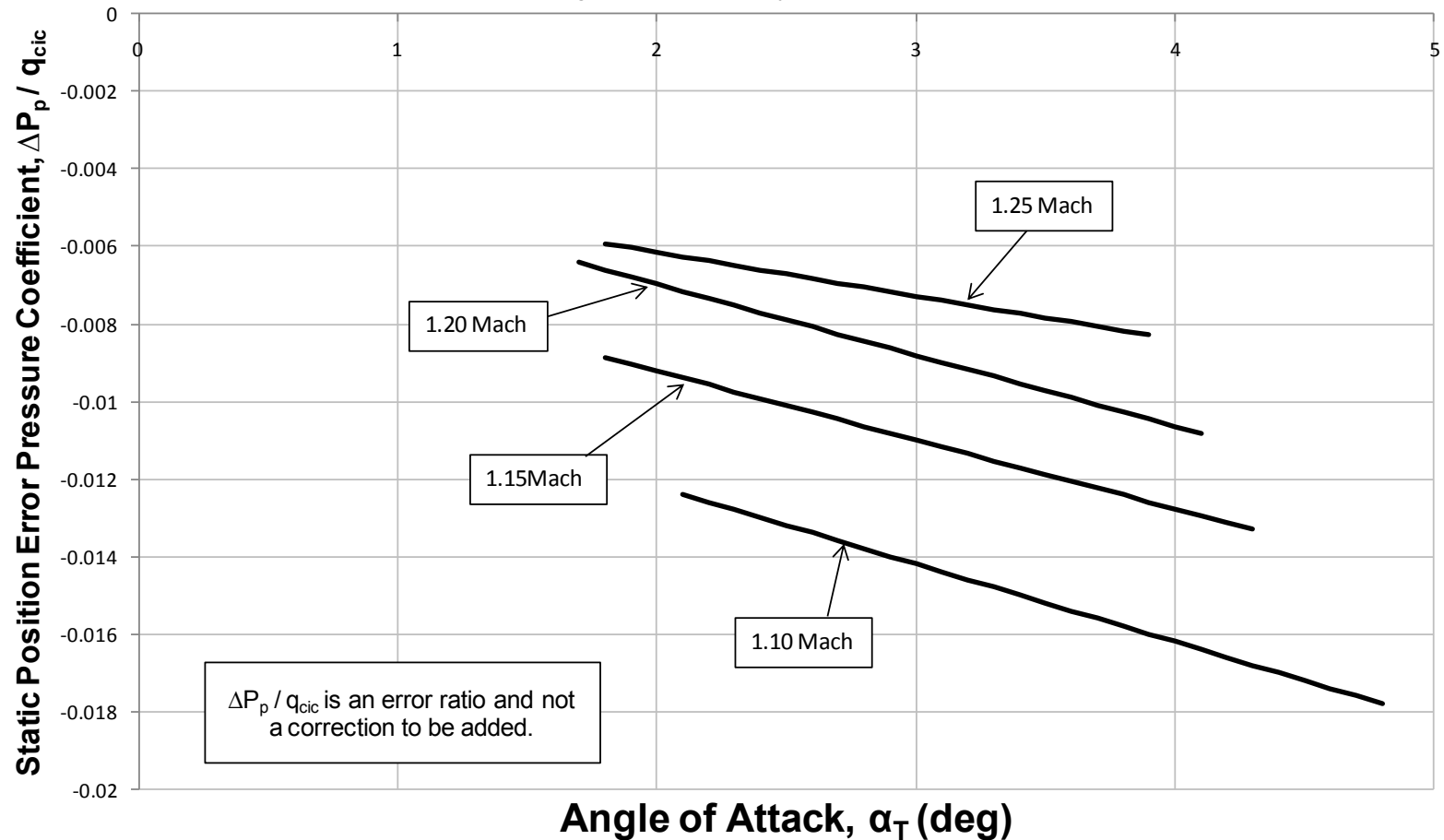


Figure A-46. Noseboom Position Error Pressure Coefficient Models (1.10 to 1.25 Mach)

# Mach Number Position Correction 2,300 ft PA - Test Noseboom (System 1)

Aircraft: F-16D, S/N 87-0391 (ARDS Pod on Station 1 and 370 Gallon Fuel Tanks on Stations 4 and 6)

Configuration: Cruise (Gear Up / Flaps Up)

Data Basis: Flight Test (Test Day Data) / 8-12 Mar 2010

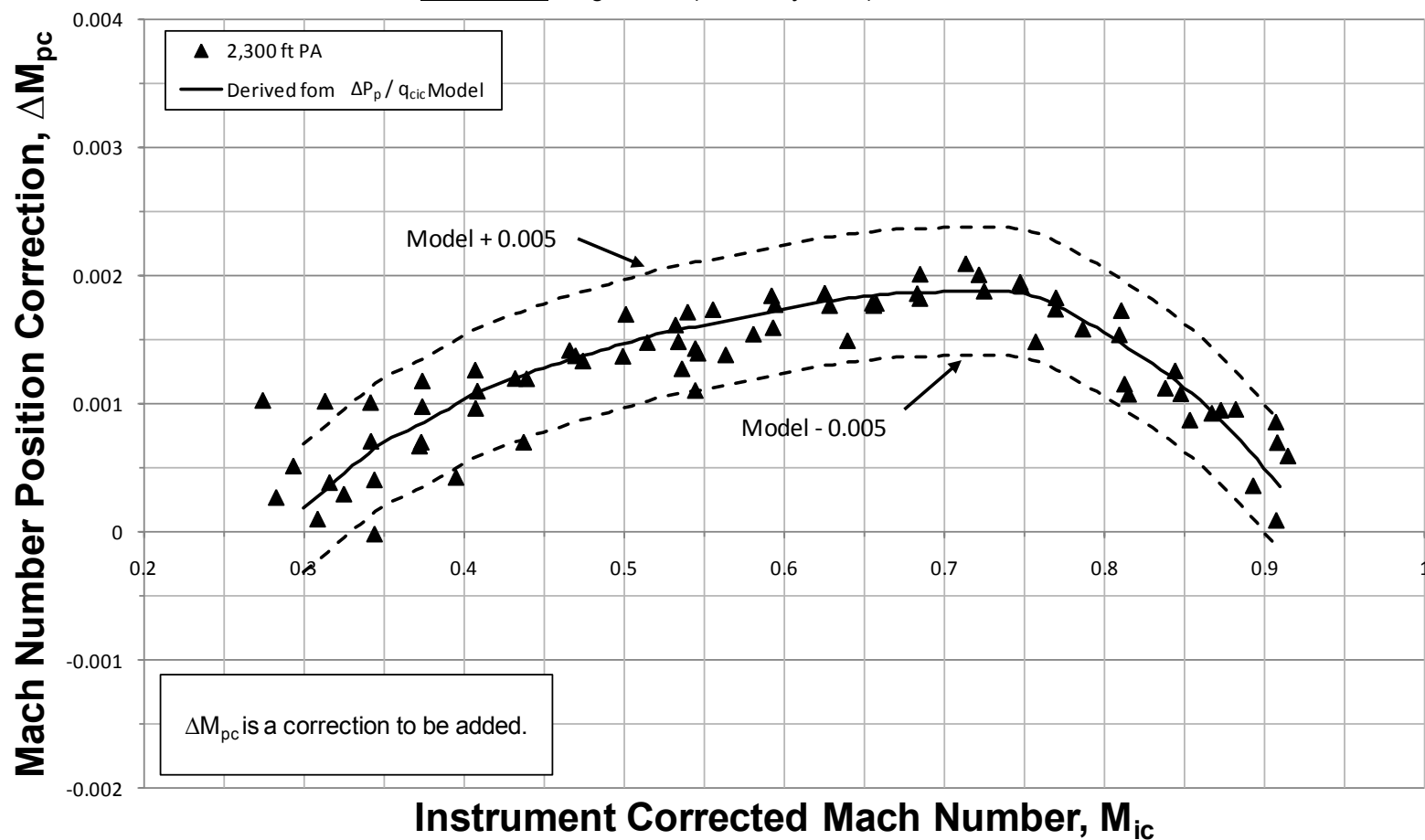


Figure A-47. Noseboom Mach Number Position Correction (2,300 feet PA)

# Mach Number Position Correction 10,000 to 45,000 ft PA - Test Noseboom (System 1)

Aircraft: F-16D, S/N 87-0391 (ARDS Pod on Station 1 and 370 Gallon Fuel Tanks on Stations 4 and 6)

Configuration: Cruise (Gear Up / Flaps Up)

Data Basis: Flight Test (Test Day Data) / 15-31 Mar 2010

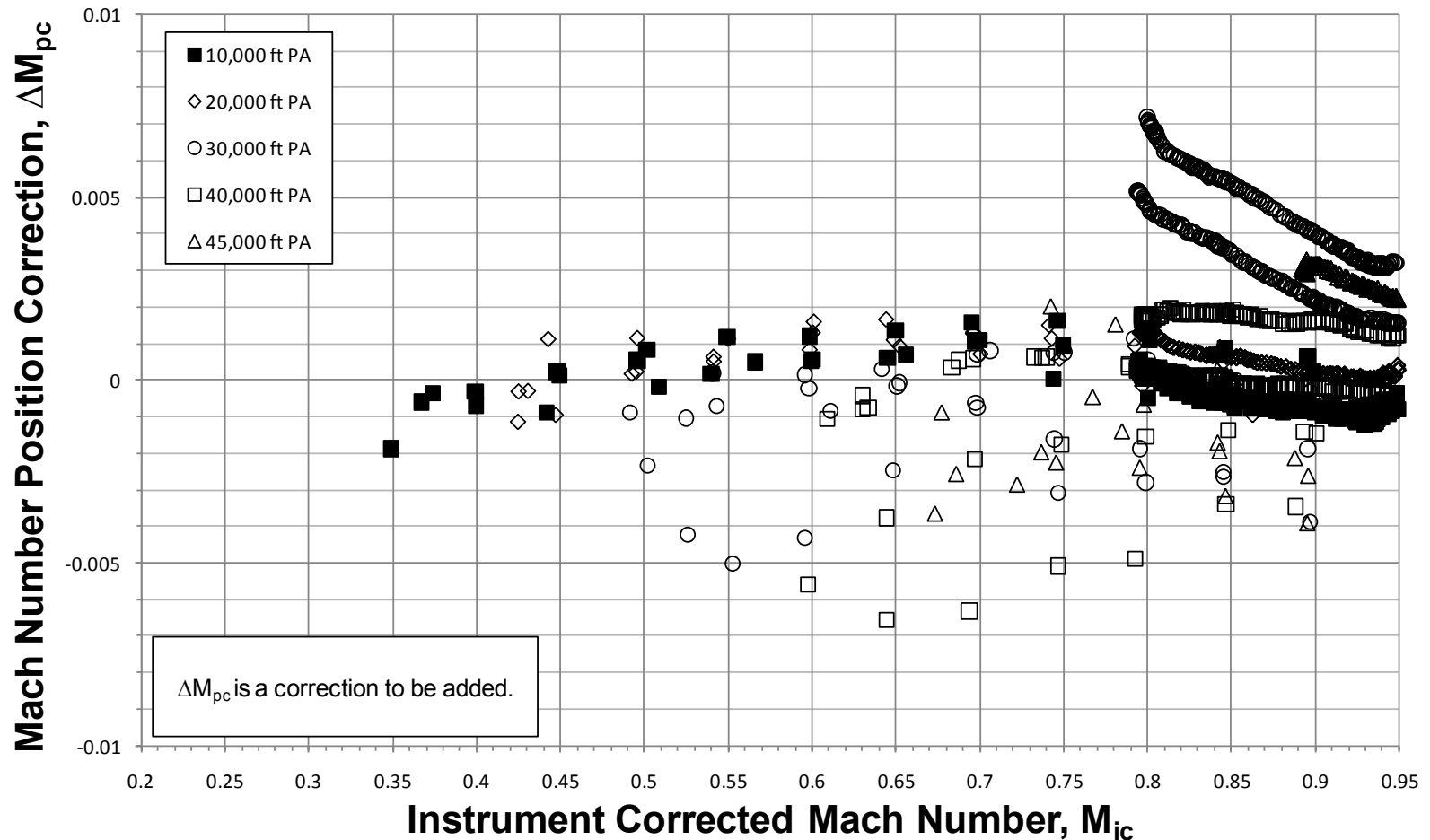


**Figure A-48. Noseboom Mach Number Position Correction (10,000 ft to 45,000 ft PA, below 0.95M)**

# Mach Number Position Correction 10,000 to 45,000 ft PA - Test Noseboom (System 1)

Aircraft: F-16D, S/N 87-0391 (ARDS Pod on Station 1 and 370 Gallon Fuel Tanks on Stations 4 and 6)

Configuration: Cruise (Gear Up / Flaps Up)

Data Basis: Flight Test (Test Day Data) / 15-31 Mar 2010

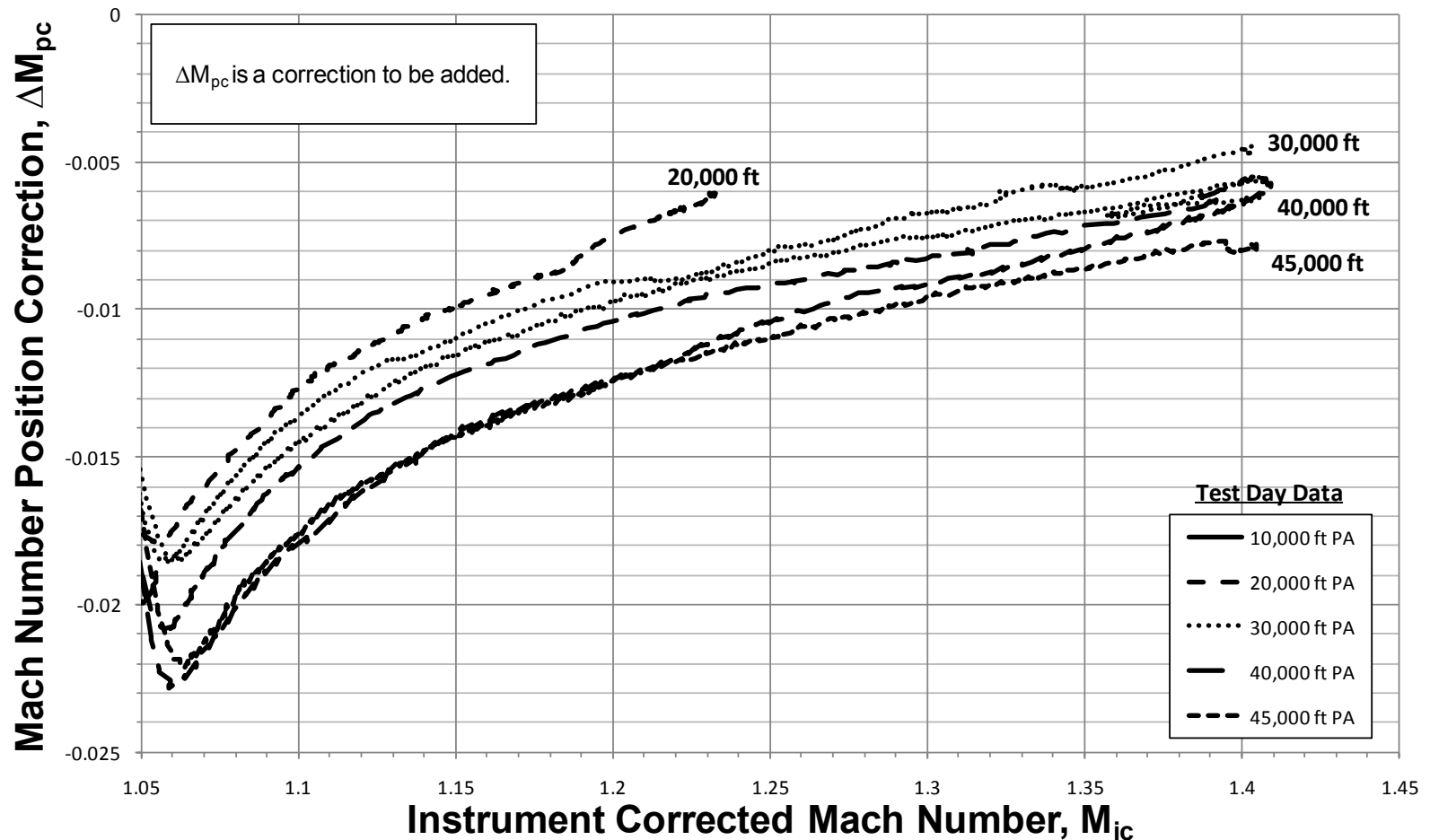


Figure A-49. Noseboom Mach Number Position Correction (10,000 ft to 45,000 ft PA, above 1.05M)

# Mach Number Position Correction Models 2,300 to 45,000 ft PA - Test Noseboom (System 1)

Aircraft: F-16D, S/N 87-0391 (ARDS Pod on Station 1 and 370 Gallon Fuel Tanks on Stations 4 and 6)

Configuration: Cruise (Gear Up / Flaps Up)

Data Basis: Flight Test (Test Day Data) / 8-31 Mar 2010

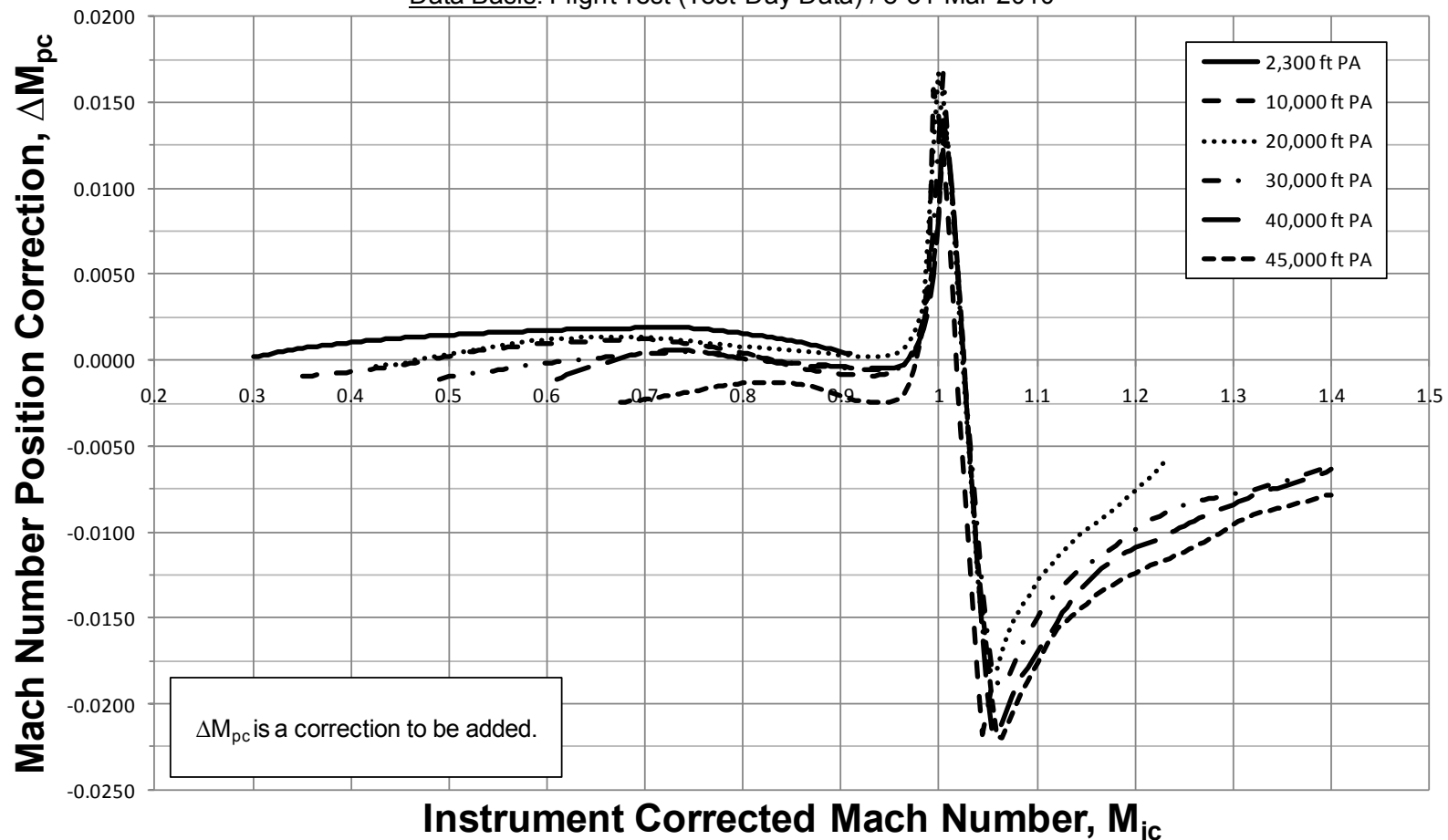


Figure A-50. Noseboom Mach Number Position Correction Models (2,300 ft to 45,000 ft PA)

# Pressure Altitude Position Correction 2,300 ft PA - Test Noseboom (System 1)

Aircraft: F-16D, S/N 87-0391 (ARDS Pod on Station 1 and 370 Gallon Fuel Tanks on Stations 4 and 6)

Configuration: Cruise (Gear Up / Flaps Up)

Data Basis: Flight Test (Test Day Data) / 8-12 Mar 2010

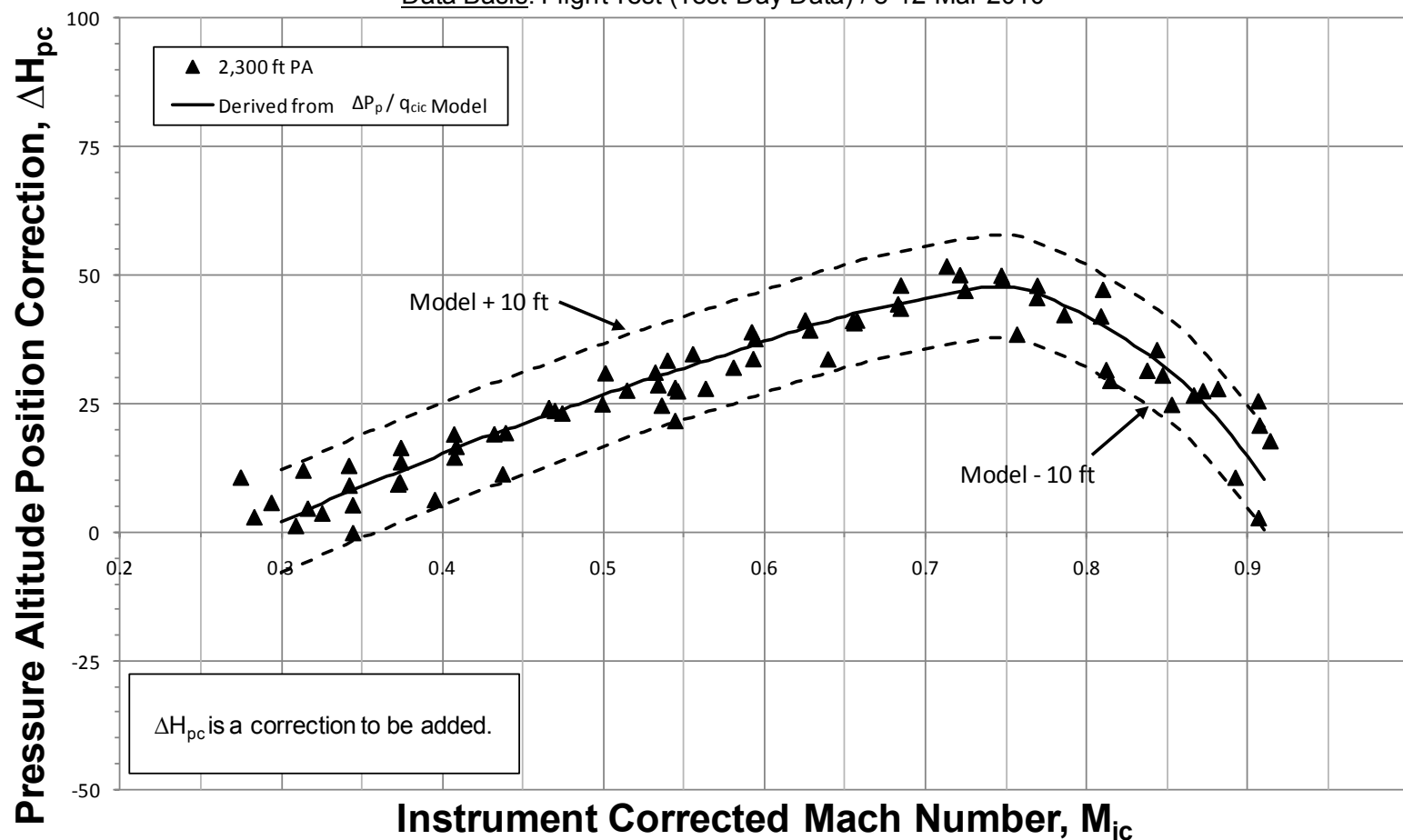


Figure A-51. Noseboom Pressure Altitude Position Correction (2,300 ft PA)

# Pressure Altitude Position Correction 10,000 to 45,000 ft PA - Test Noseboom (System 1)

Aircraft: F-16D, S/N 87-0391 (ARDS Pod on Station 1 and 370 Gallon Fuel Tanks on Stations 4 and 6)

Configuration: Cruise (Gear Up / Flaps Up)

Data Basis: Flight Test (Test Day Data) / 15-31 Mar 2010

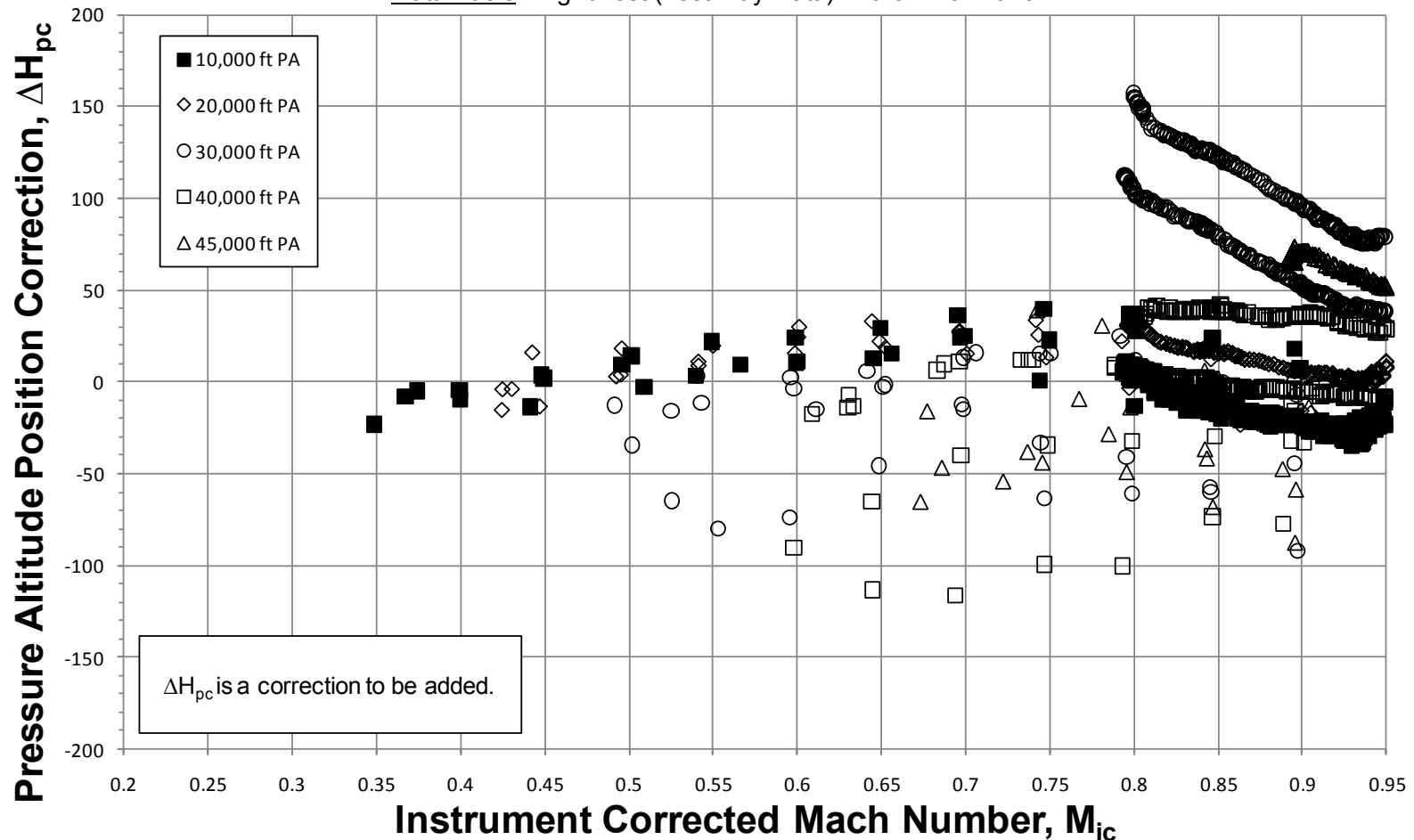


Figure A-52. Noseboom Pressure Altitude Position Correction (10,000 ft to 45,000 ft PA, below 0.95M)

# Pressure Altitude Position Correction 10,000 to 45,000 ft PA - Test Noseboom (System 1)

Aircraft: F-16D, S/N 87-0391 (ARDS Pod on Station 1 and 370 Gallon Fuel Tanks on Stations 4 and 6)

Configuration: Cruise (Gear Up / Flaps Up)

Data Basis: Flight Test (Test Day Data) / 15-31 Mar 2010

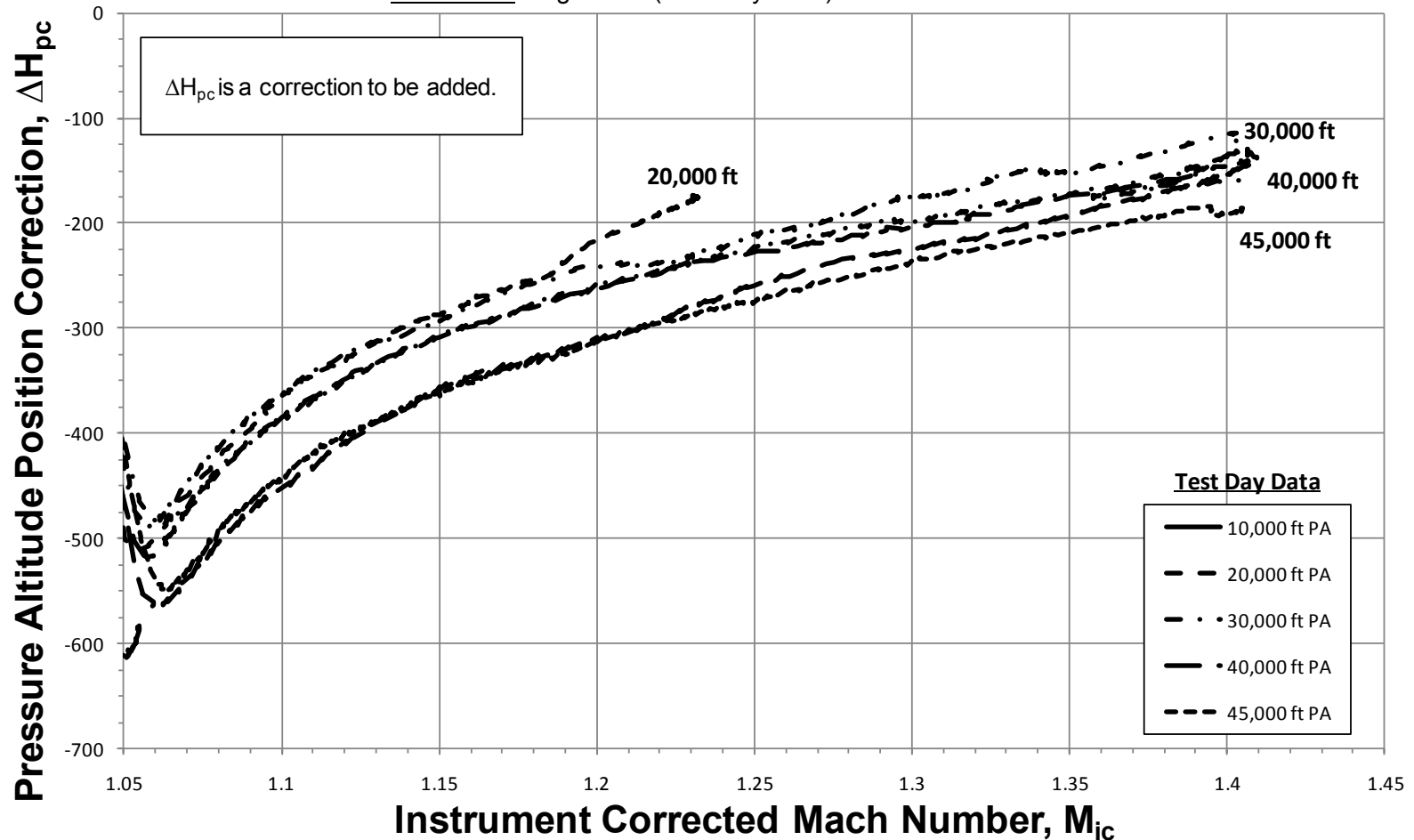


Figure A-53. Noseboom Pressure Altitude Position Correction (10,000 ft to 45,000 ft PA, above 1.05M)

# Pressure Altitude Position Correction Models 2,300 to 45,000 ft PA - Test Noseboom (System 1)

Aircraft: F-16D, S/N 87-0391 (ARDS Pod on Station 1 and 370 Gallon Fuel Tanks on Stations 4 and 6)

Configuration: Cruise (Gear Up / Flaps Up)

Data Basis: Flight Test (Test Day Data) / 8-31 Mar 2010

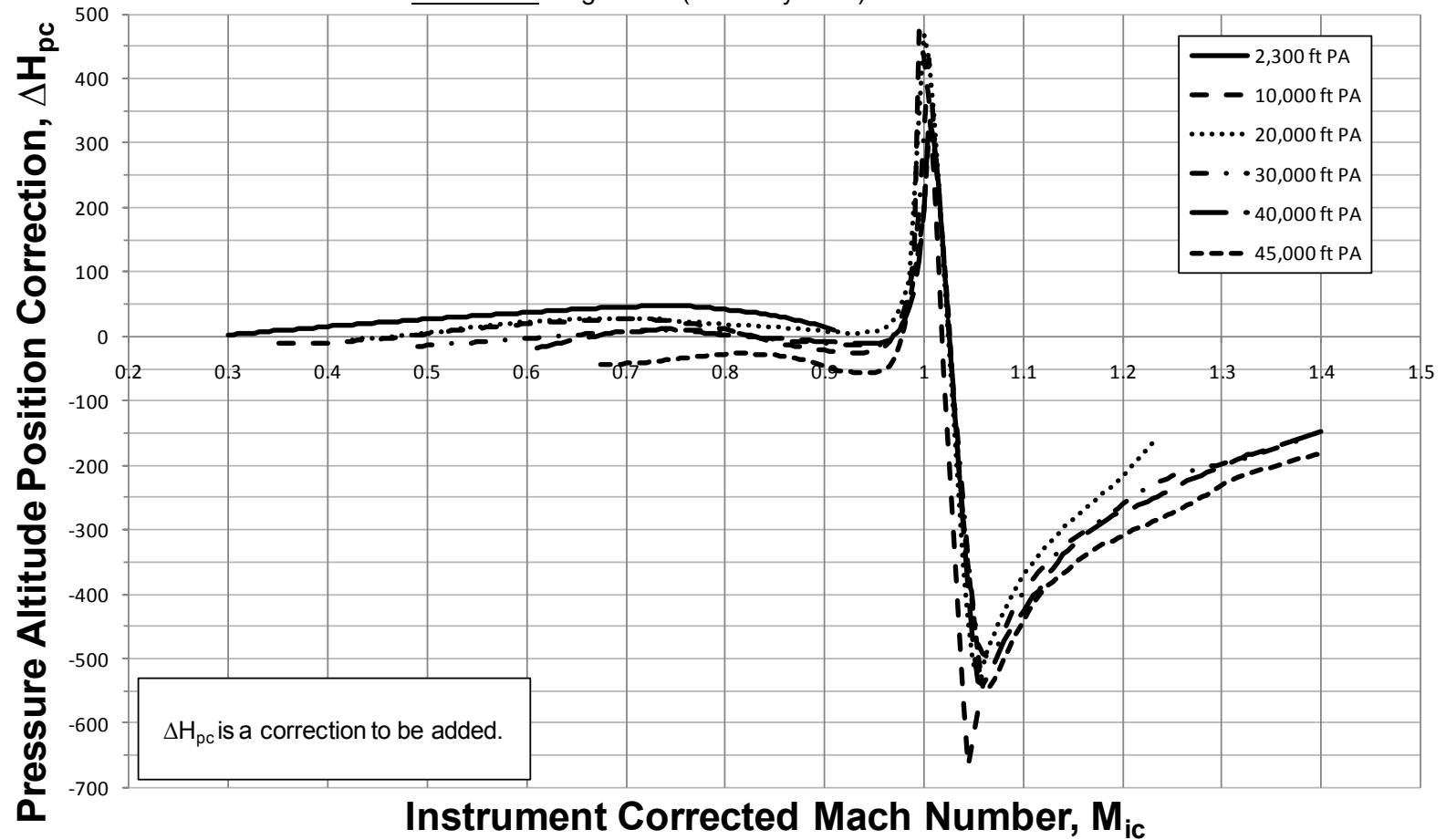


Figure A-54. Noseboom Pressure Altitude Position Correction Models (2,300 ft to 45,000 ft PA)

# Temperature Recovery Factor and Bias

Aircraft: F-16D, S/N 87-0391 (ARDS Pod on Station 1 and 370 Gallon Fuel Tanks on Stations 4 / 6)

Configuration: Cruise (Gear Up / Flaps Up)

Data Basis: Flight Test (Test Day Data) / 8 Mar 2010

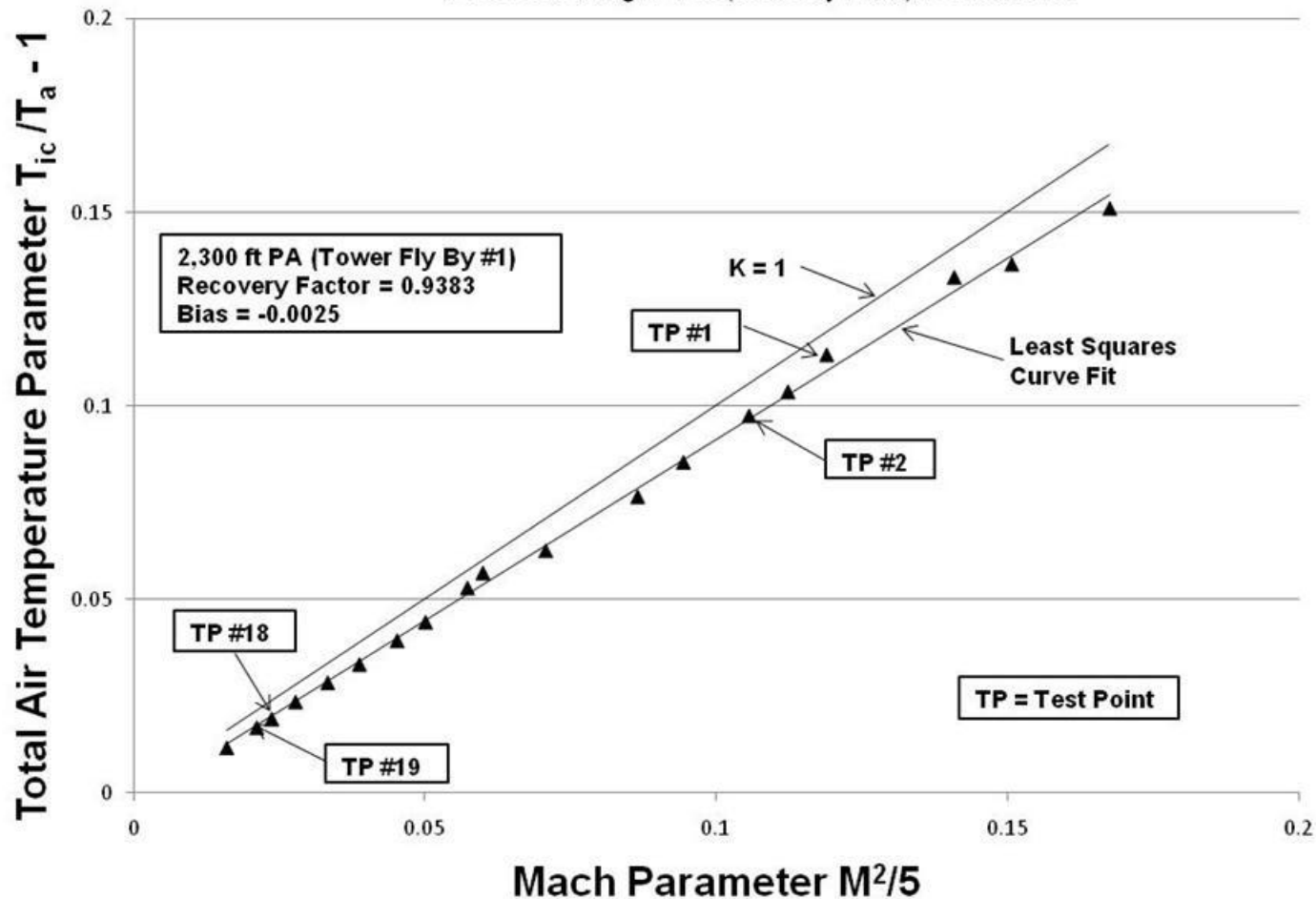


Figure A-55. Temperature Probe Recovery Factor and Bias

# Temperature Recovery Factor and Bias

Aircraft: F-16D, S/N 87-0391 (ARDS Pod on Station 1 and 370 Gallon Fuel Tanks on Stations 4 / 6)

Configuration: Cruise (Gear Up / Flaps Up)

Data Basis: Flight Test (Test Day Data) / 9 Mar 2010

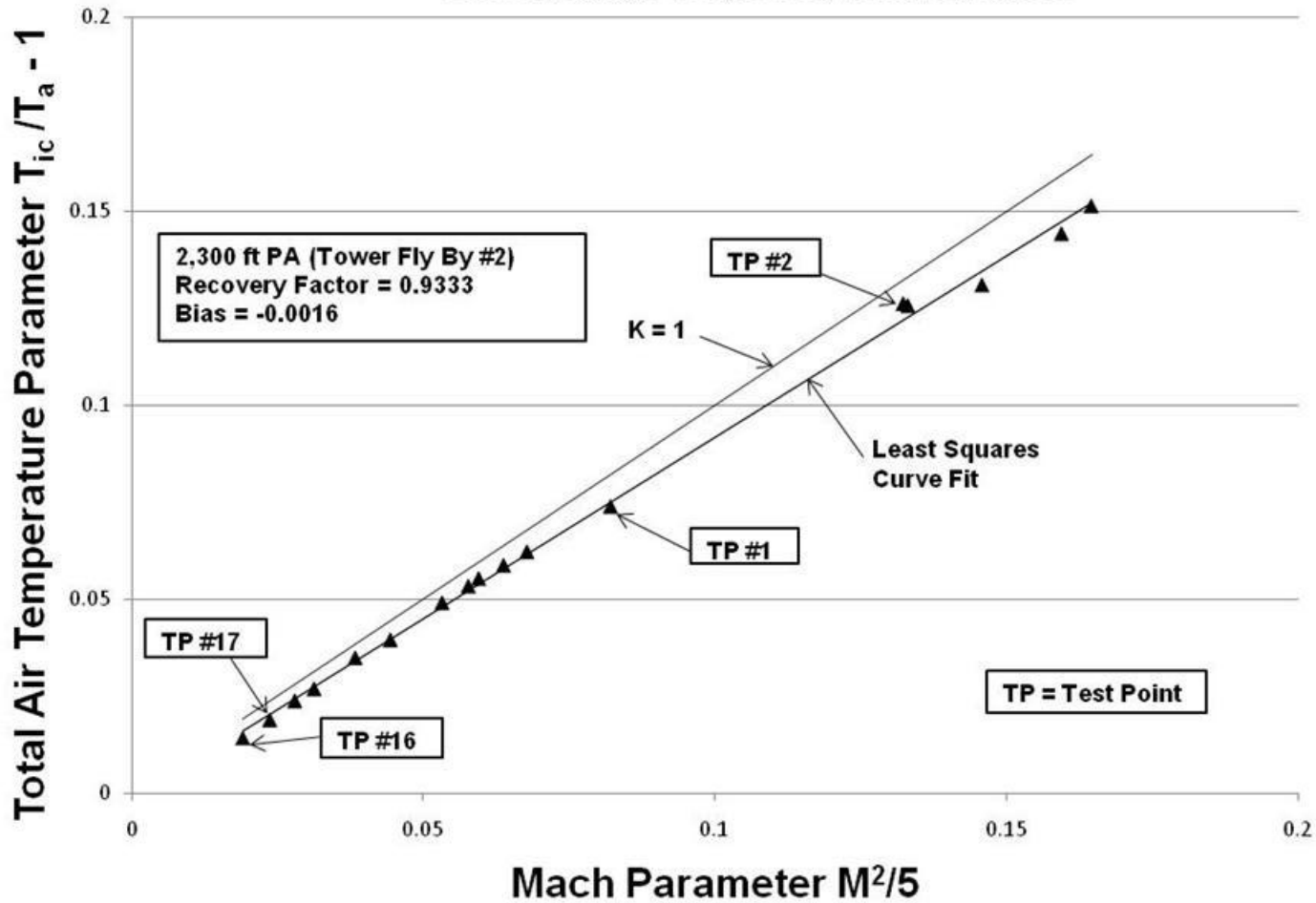


Figure A-56. Temperature Probe Recovery Factor and Bias

## Temperature Recovery Factor and Bias

Aircraft: F-16D, S/N 87-0391 (ARDS Pod on Station 1 and 370 Gallon Fuel Tanks on Stations 4 / 6)

Configuration: Cruise (Gear Up / Flaps Up)

Data Basis: Flight Test (Test Day Data) / 11 Mar 2010

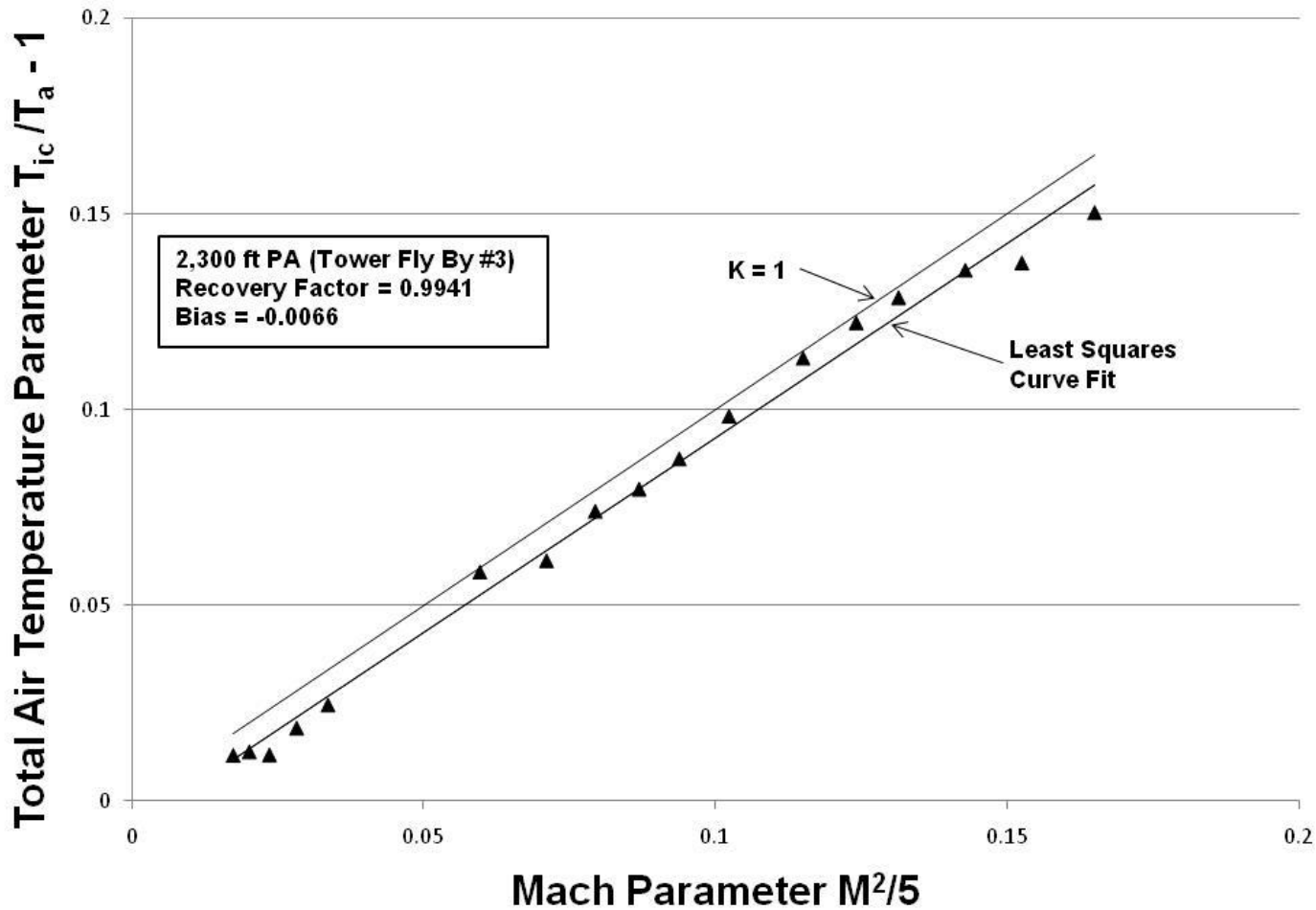


Figure A-57. Temperature Probe Recovery Factor and Bias

## Temperature Recovery Factor and Bias

Aircraft: F-16D, S/N 87-0391 (ARDS Pod on Station 1 and 370 Gallon Fuel Tanks on Stations 4 / 6)

Configuration: Cruise (Gear Up / Flaps Up)

Data Basis: Flight Test (Test Day Data) / 12 Mar 2010

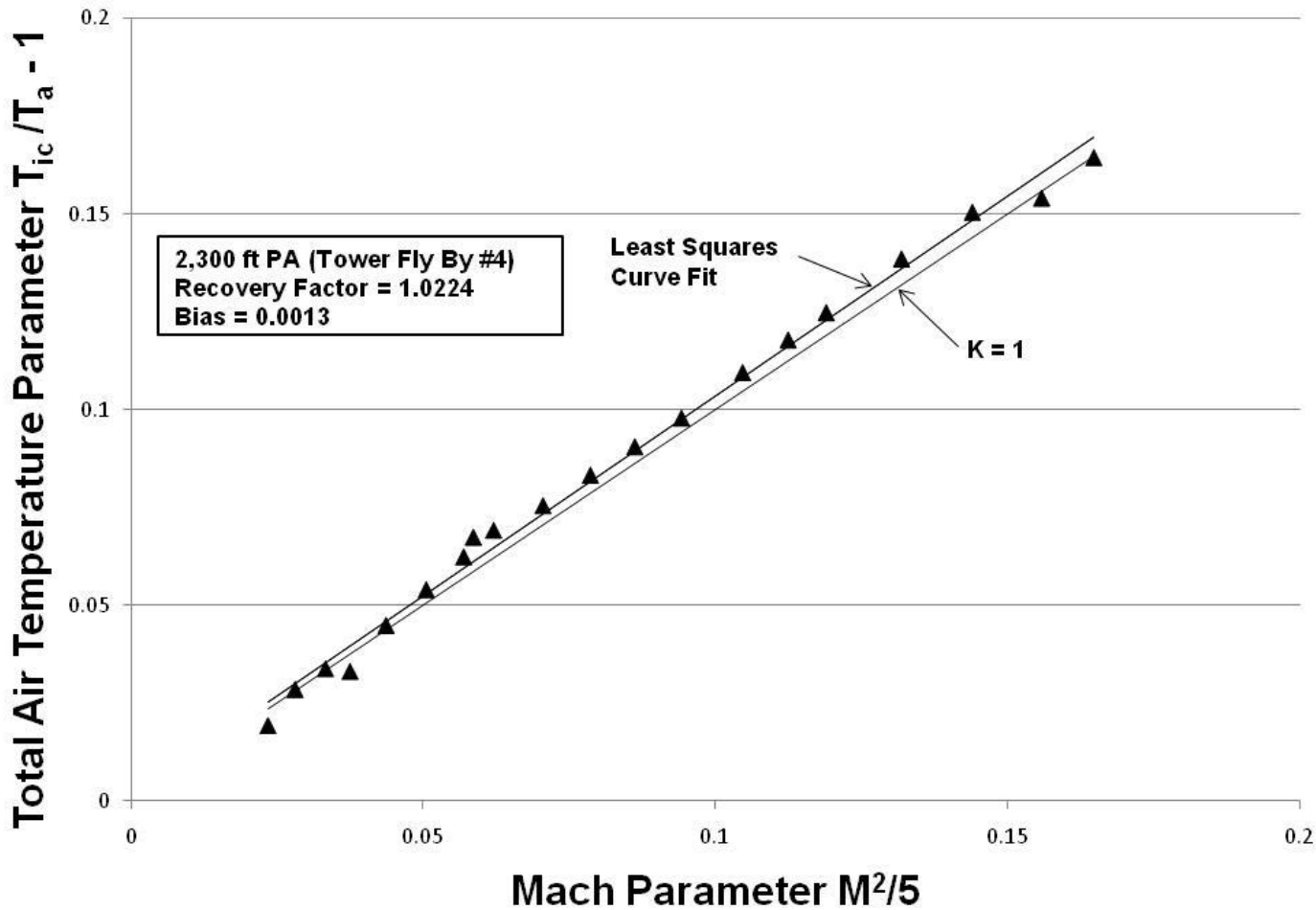


Figure A-58. Temperature Probe Recovery Factor and Bias

## Temperature Recovery Factor and Bias

Aircraft: F-16D, S/N 87-0391 (ARDS Pod on Station 1 and 370 Gallon Fuel Tanks on Stations 4 / 6)

Configuration: Cruise (Gear Up / Flaps Up)

Data Basis: Flight Test (Test Day Data) / 15 Mar 2010

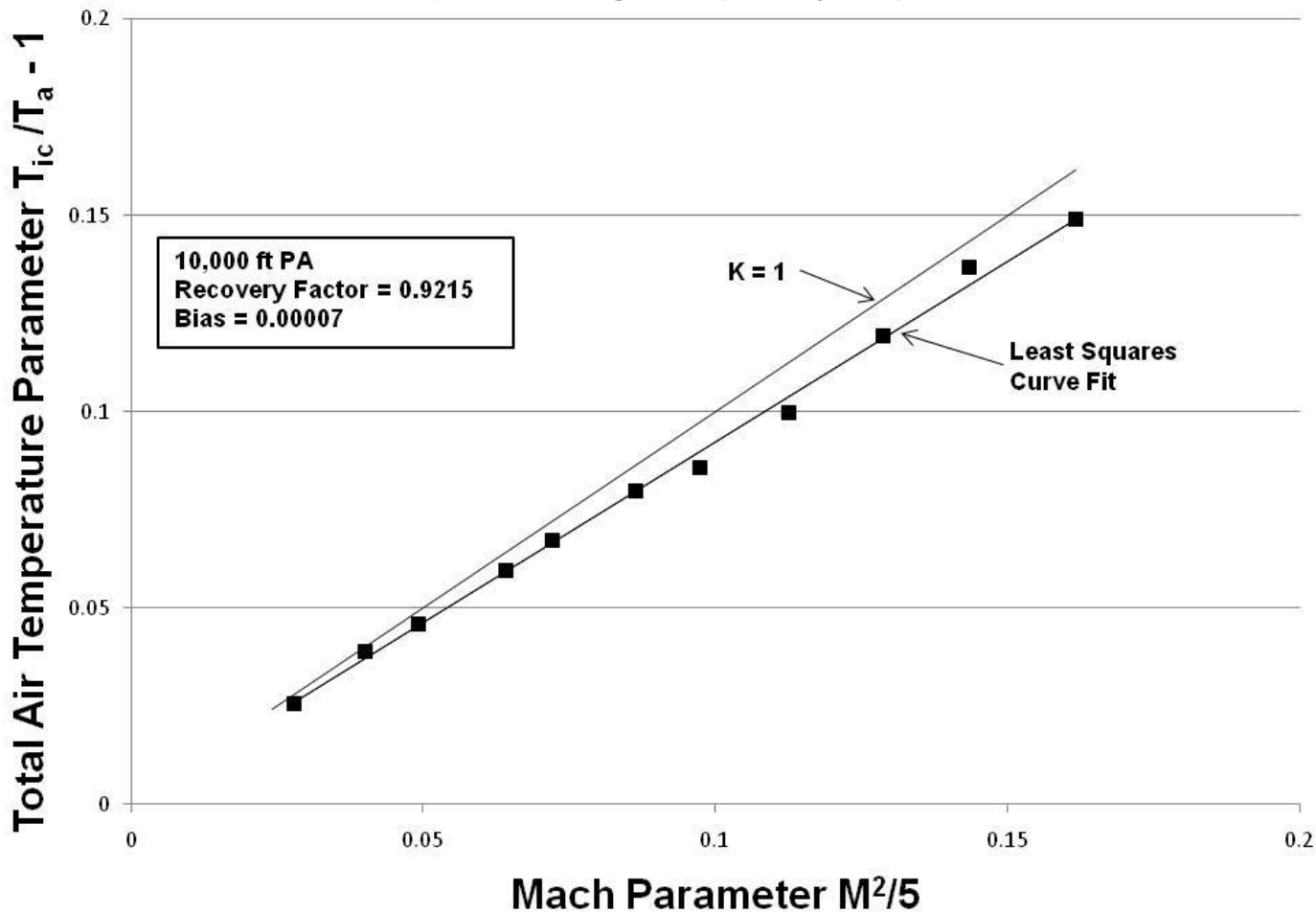


Figure A-59. Temperature Probe Recovery Factor and Bias

# Temperature Recovery Factor and Bias

Aircraft: F-16D, S/N 87-0391 (ARDS Pod on Station 1 and 370 Gallon Fuel Tanks on Stations 4 / 6)

Configuration: Cruise (Gear Up / Flaps Up)

Data Basis: Flight Test (Test Day Data) / 15 Mar 2010

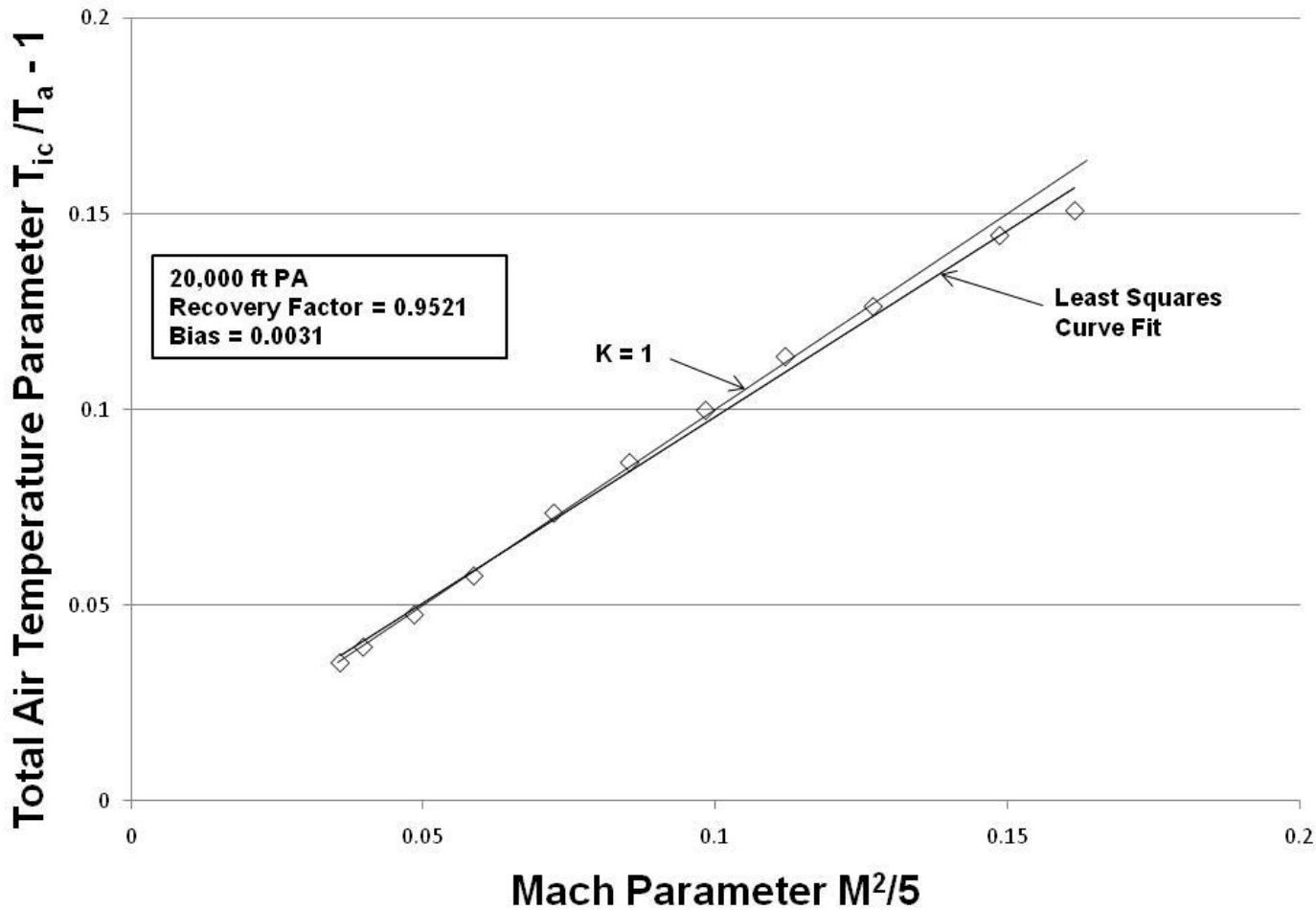


Figure A-60. Temperature Probe Recovery Factor and Bias

## Temperature Recovery Factor and Bias

Aircraft: F-16D, S/N 87-0391 (ARDS Pod on Station 1 and 370 Gallon Fuel Tanks on Stations 4 / 6)

Configuration: Cruise (Gear Up / Flaps Up)

Data Basis: Flight Test (Test Day Data) / 15 Mar 2010

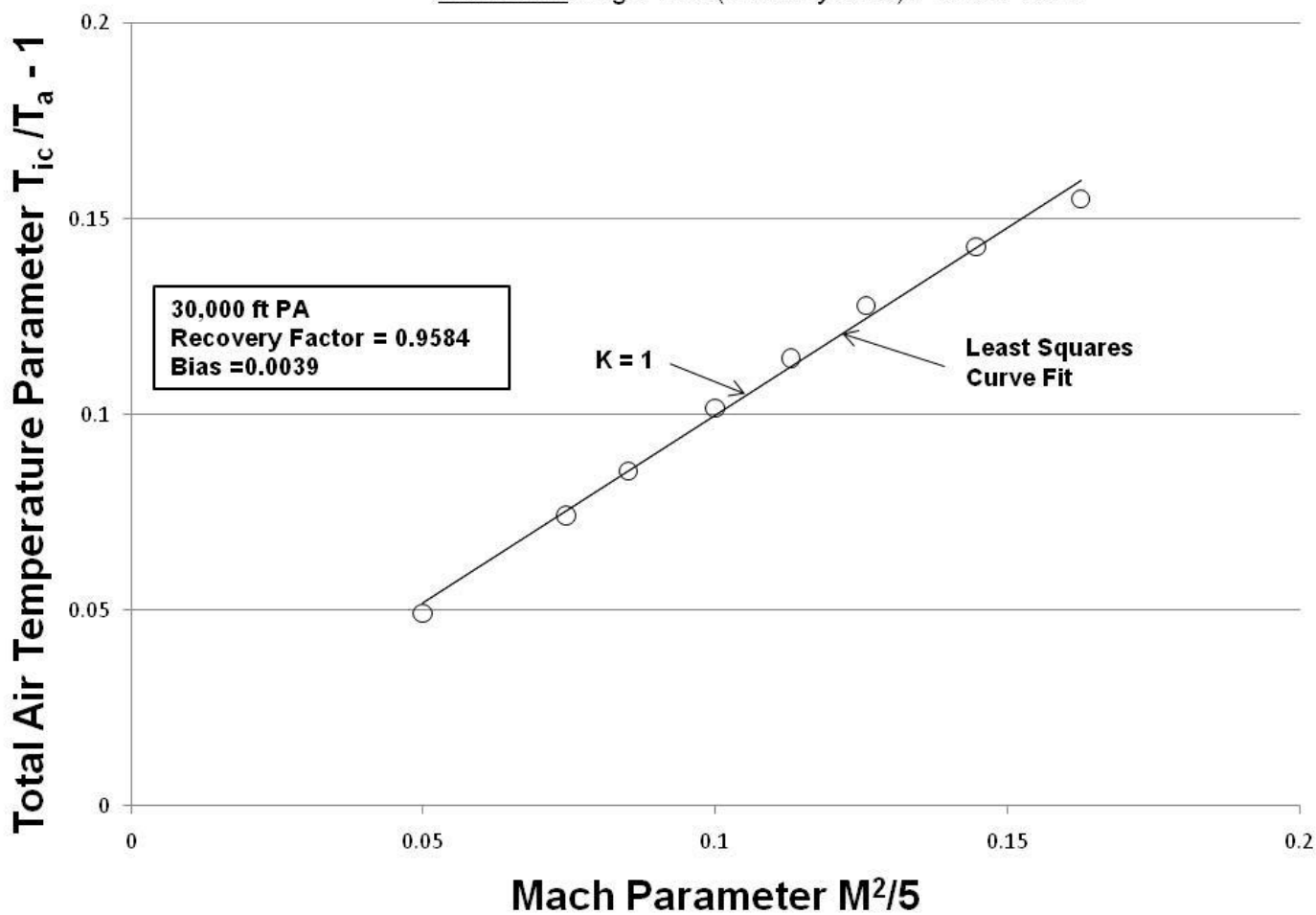


Figure A-61. Temperature Probe Recovery Factor and Bias

# Temperature Recovery Factor and Bias

Aircraft: F-16D, S/N 87-0391 (ARDS Pod on Station 1 and 370 Gallon Fuel Tanks on Stations 4 / 6)

Configuration: Cruise (Gear Up / Flaps Up)

Data Basis: Flight Test (Test Day Data) / 15 Mar 2010

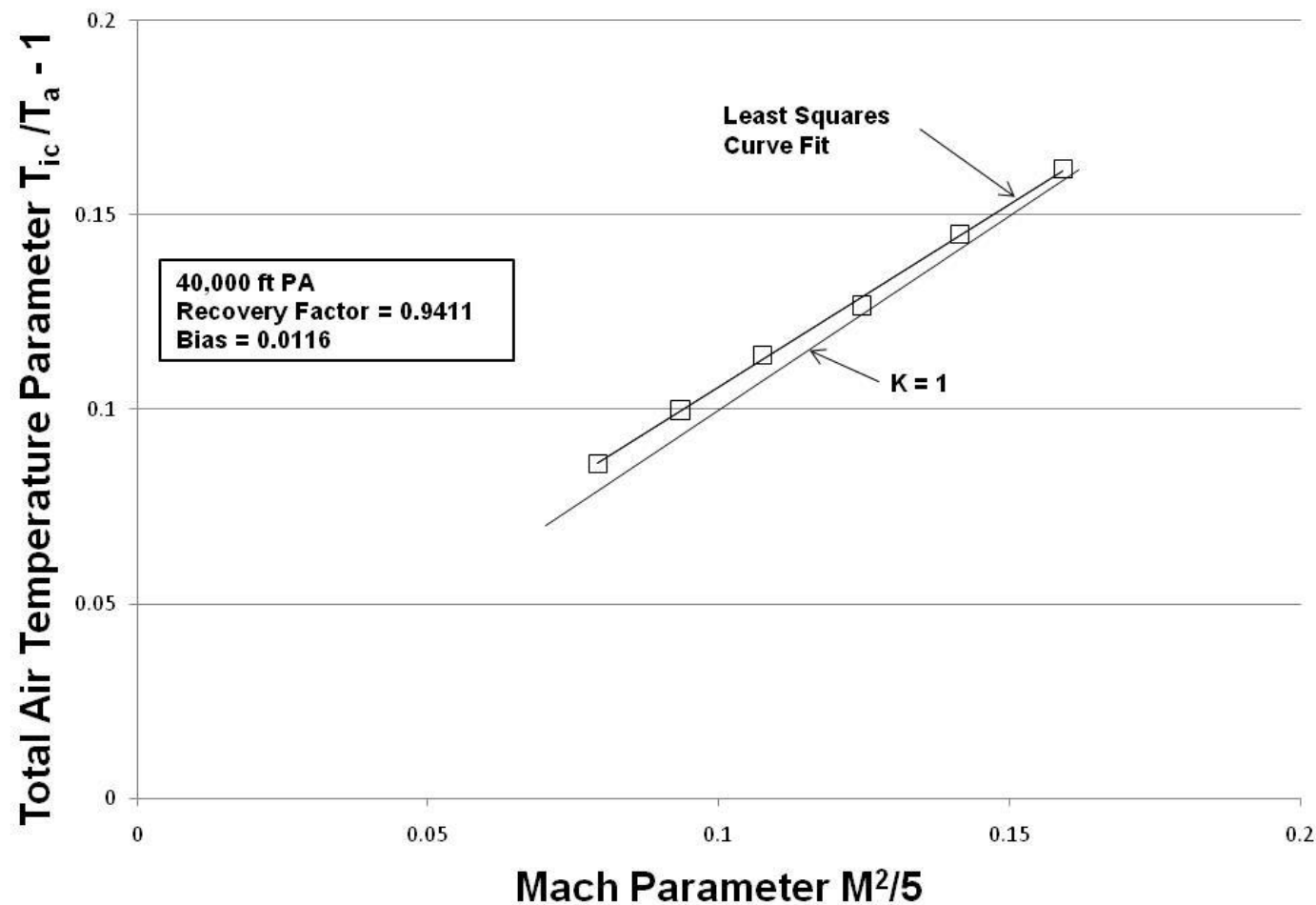


Figure A-62. Temperature Probe Recovery Factor and Bias

## Temperature Recovery Factor and Bias

Aircraft: F-16D, S/N 87-0391 (ARDS Pod on Station 1 and 370 Gallon Fuel Tanks on Stations 4 / 6)

Configuration: Cruise (Gear Up / Flaps Up)

Data Basis: Flight Test (Test Day Data) / 15 Mar 2010

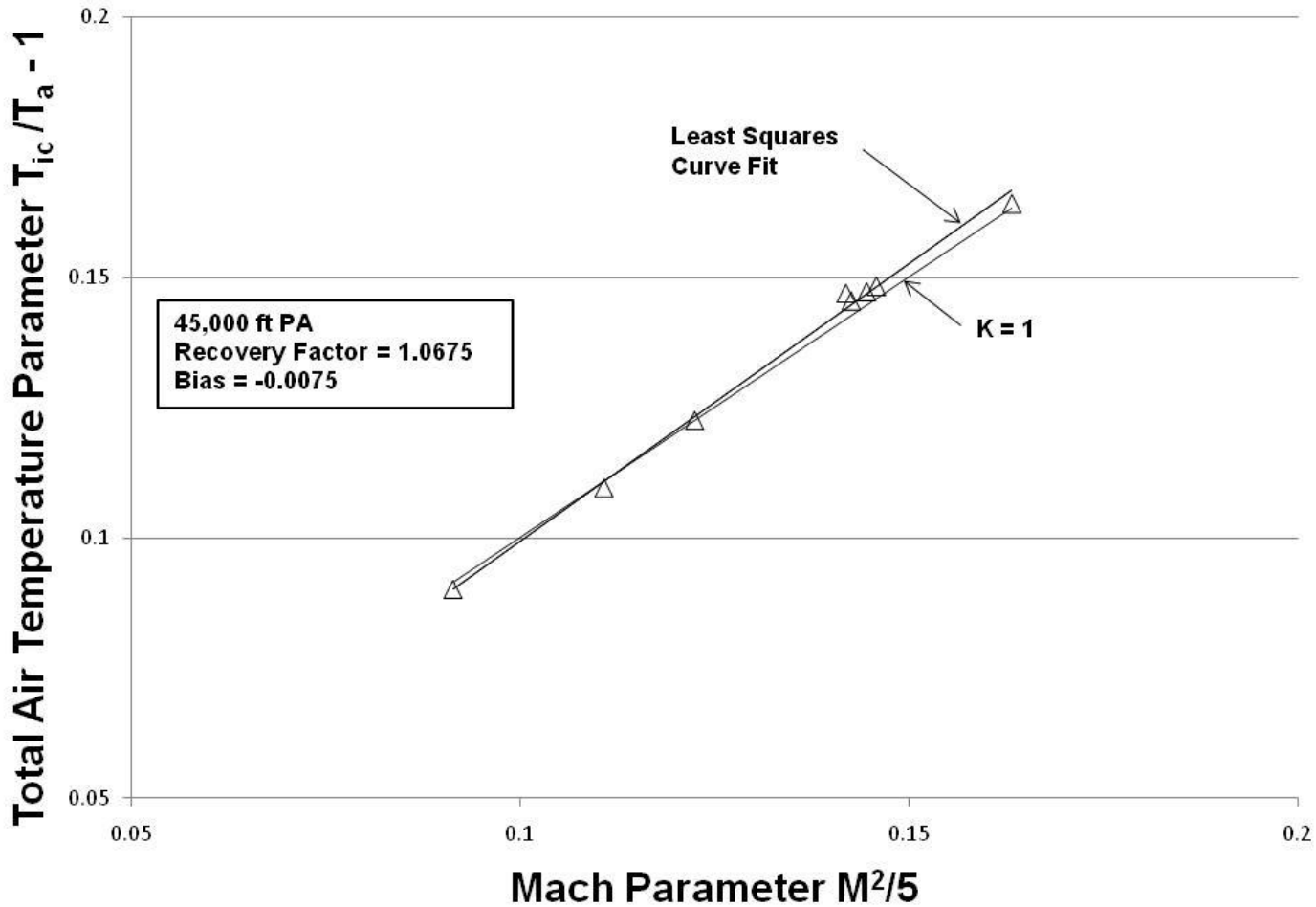


Figure A-63. Temperature Probe Recovery Factor and Bias

## Temperature Recovery Factor and Bias

Aircraft: F-16D, S/N 87-0391 (ARDS Pod on Station 1 and 370 Gallon Fuel Tanks on Stations 4 / 6)

Configuration: Cruise (Gear Up / Flaps Up)

Data Basis: Flight Test (Test Day Data) / 16 Mar 2010

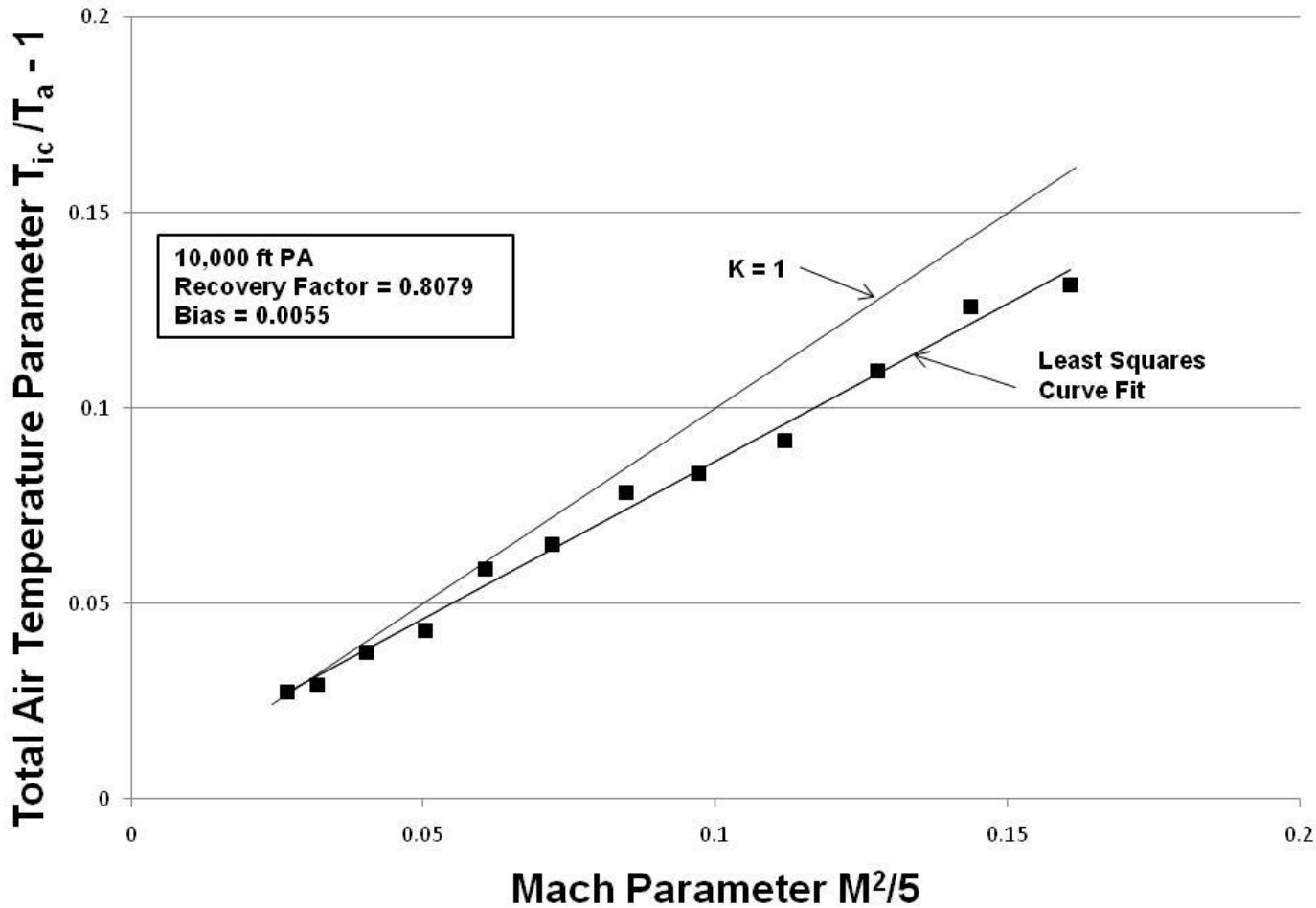


Figure A-64. Temperature Probe Recovery Factor and Bias

## Temperature Recovery Factor and Bias

Aircraft: F-16D, S/N 87-0391 (ARDS Pod on Station 1 and 370 Gallon Fuel Tanks on Stations 4 / 6)

Configuration: Cruise (Gear Up / Flaps Up)

Data Basis: Flight Test (Test Day Data) / 16 Mar 2010

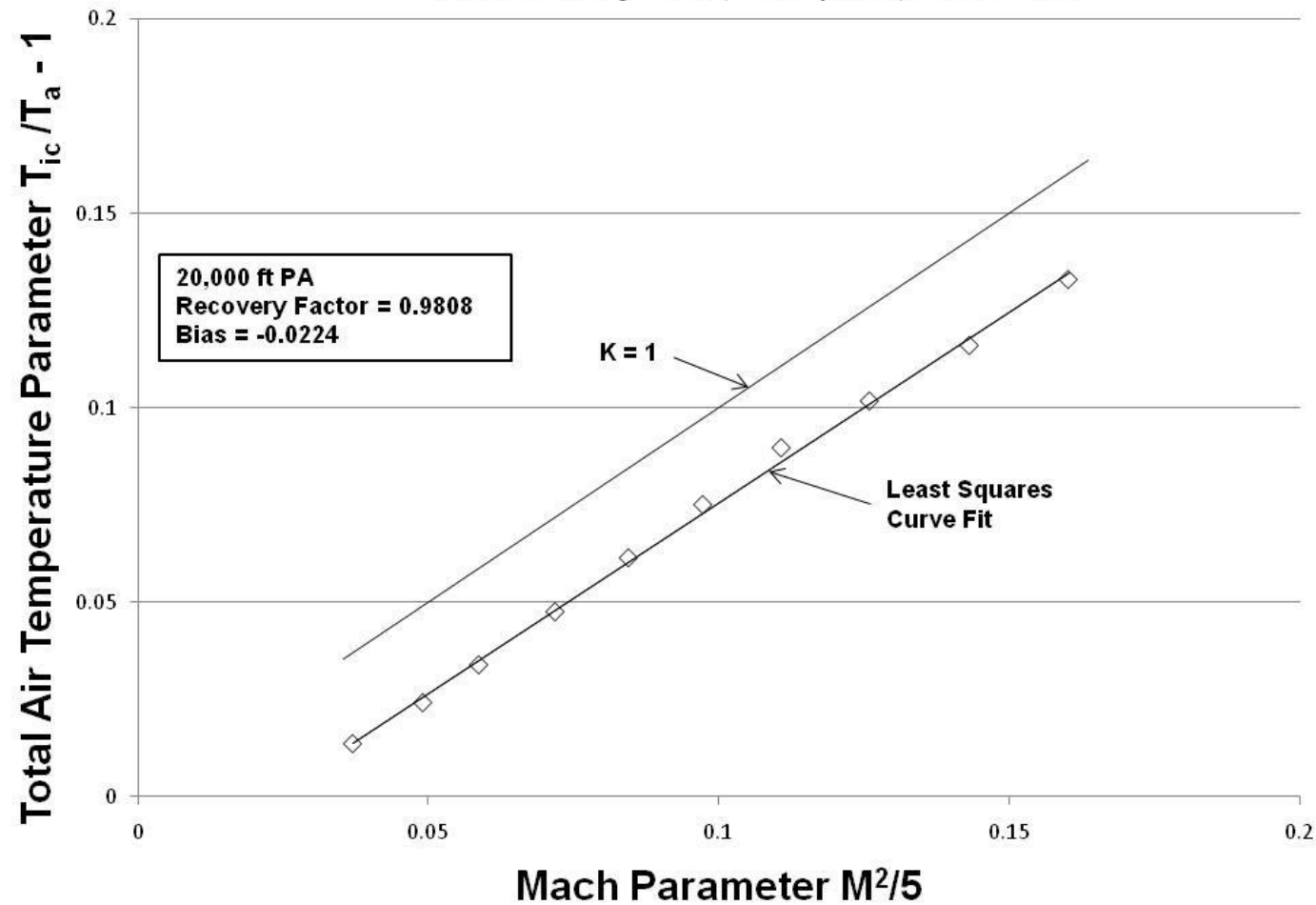


Figure A-65. Temperature Probe Recovery Factor and Bias

## Temperature Recovery Factor and Bias

Aircraft: F-16D, S/N 87-0391 (ARDS Pod on Station 1 and 370 Gallon Fuel Tanks on Stations 4 / 6)

Configuration: Cruise (Gear Up / Flaps Up)

Data Basis: Flight Test (Test Day Data) / 16 Mar 2010

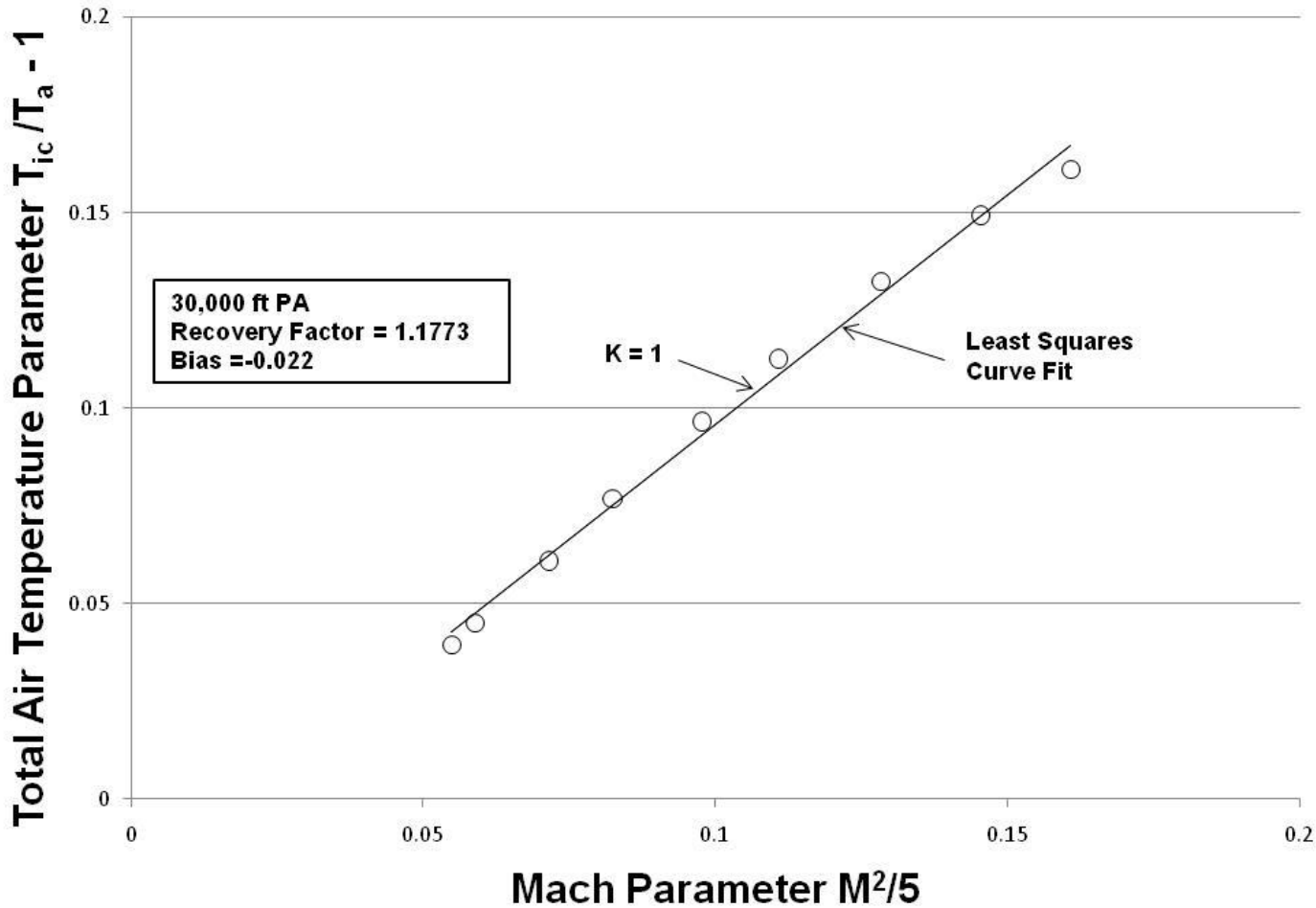


Figure A-66. Temperature Probe Recovery Factor and Bias

## Temperature Recovery Factor and Bias

Aircraft: F-16D, S/N 87-0391 (ARDS Pod on Station 1 and 370 Gallon Fuel Tanks on Stations 4 / 6)

Configuration: Cruise (Gear Up / Flaps Up)

Data Basis: Flight Test (Test Day Data) / 16 Mar 2010

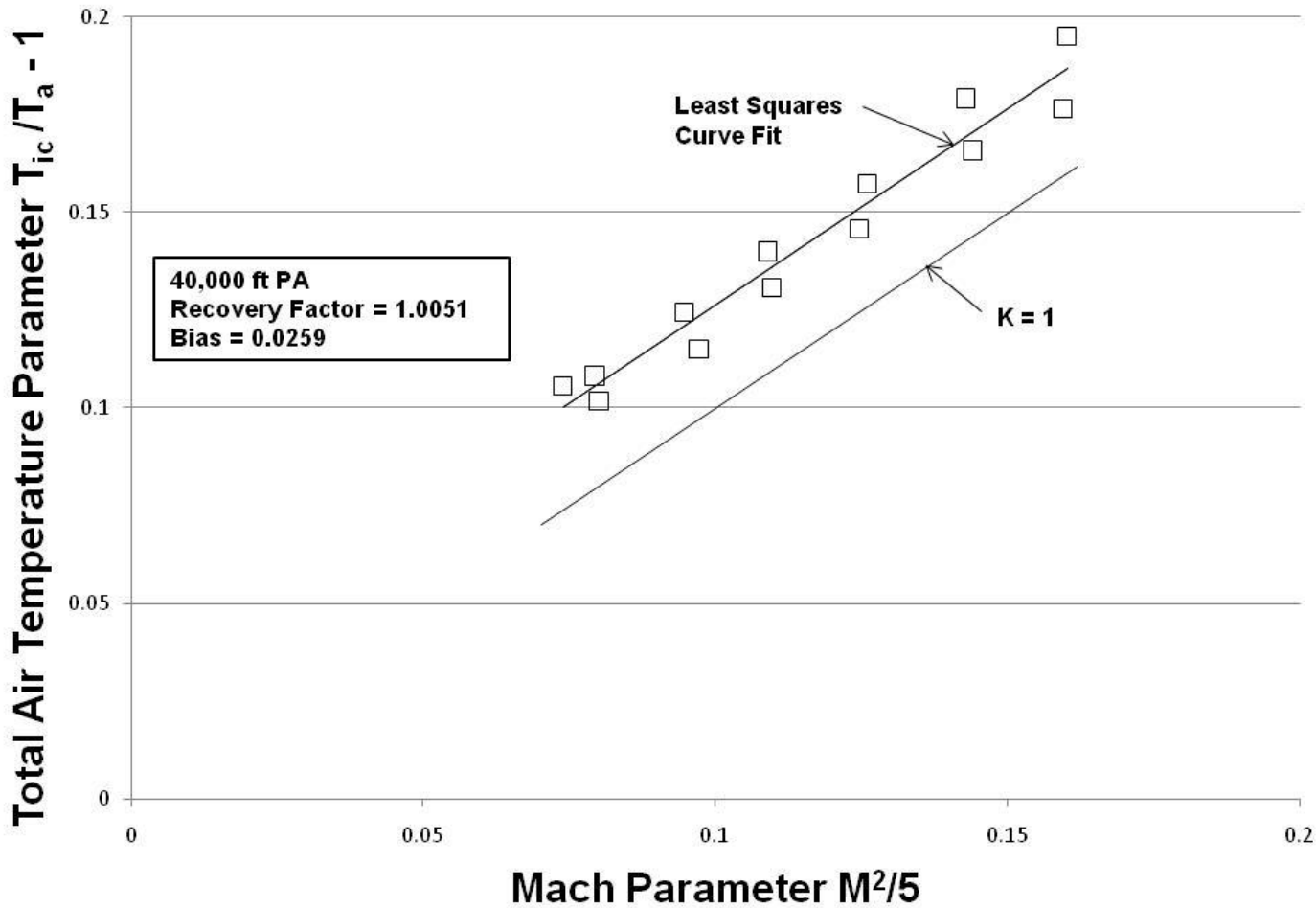


Figure A-67. Temperature Probe Recovery Factor and Bias

## Temperature Recovery Factor and Bias

Aircraft: F-16D, S/N 87-0391 (ARDS Pod on Station 1 and 370 Gallon Fuel Tanks on Stations 4 / 6)

Configuration: Cruise (Gear Up / Flaps Up)

Data Basis: Flight Test (Test Day Data) / 16 Mar 2010

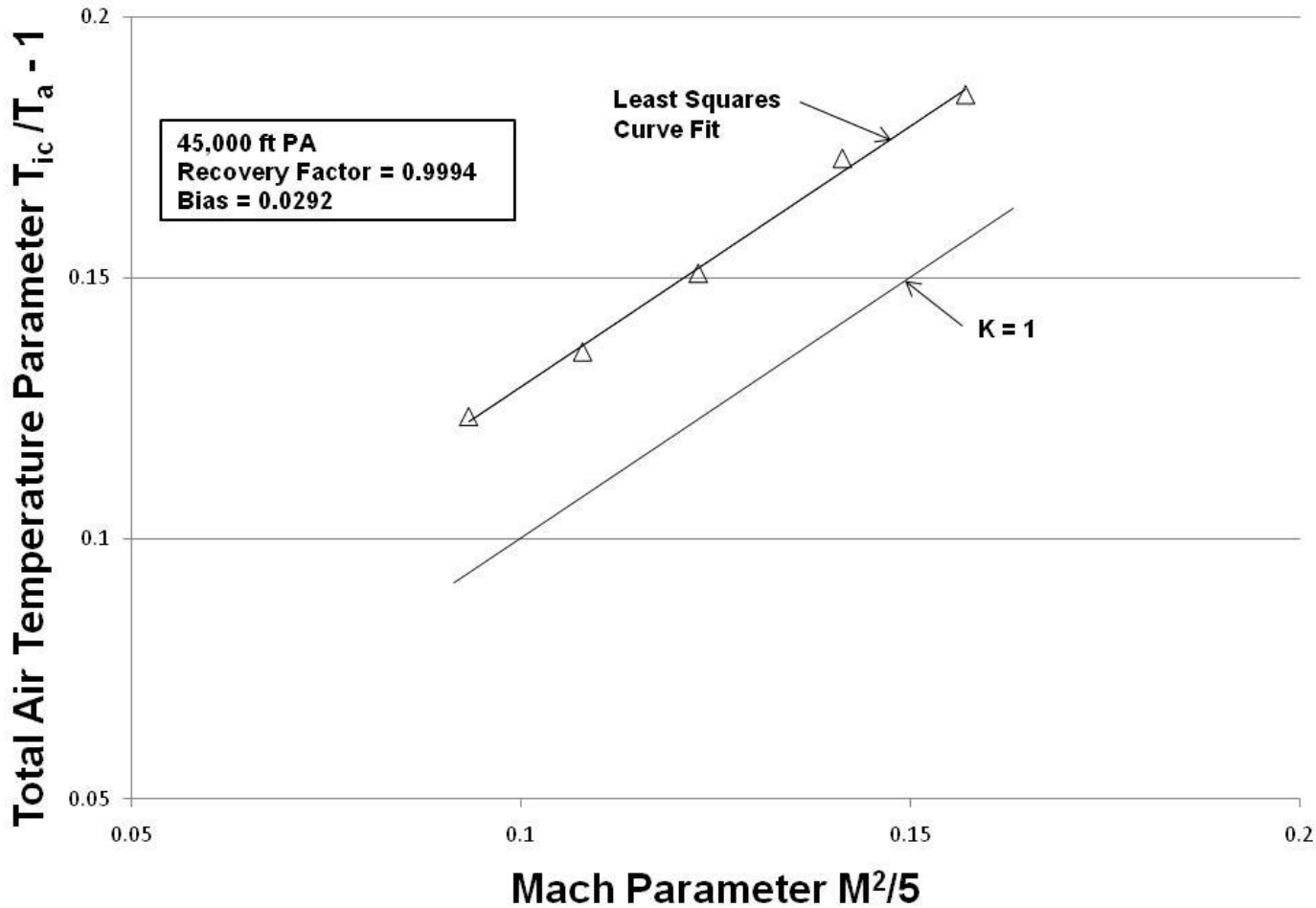


Figure A-68. Temperature Probe Recovery Factor and Bias

## Temperature Recovery Factor and Bias

Aircraft: F-16D, S/N 87-0391 (ARDS Pod on Station 1 and 370 Gallon Fuel Tanks on Stations 4 / 6)

Configuration: Cruise (Gear Up / Flaps Up)

Data Basis: Flight Test (Test Day Data) / 30 Mar 2010

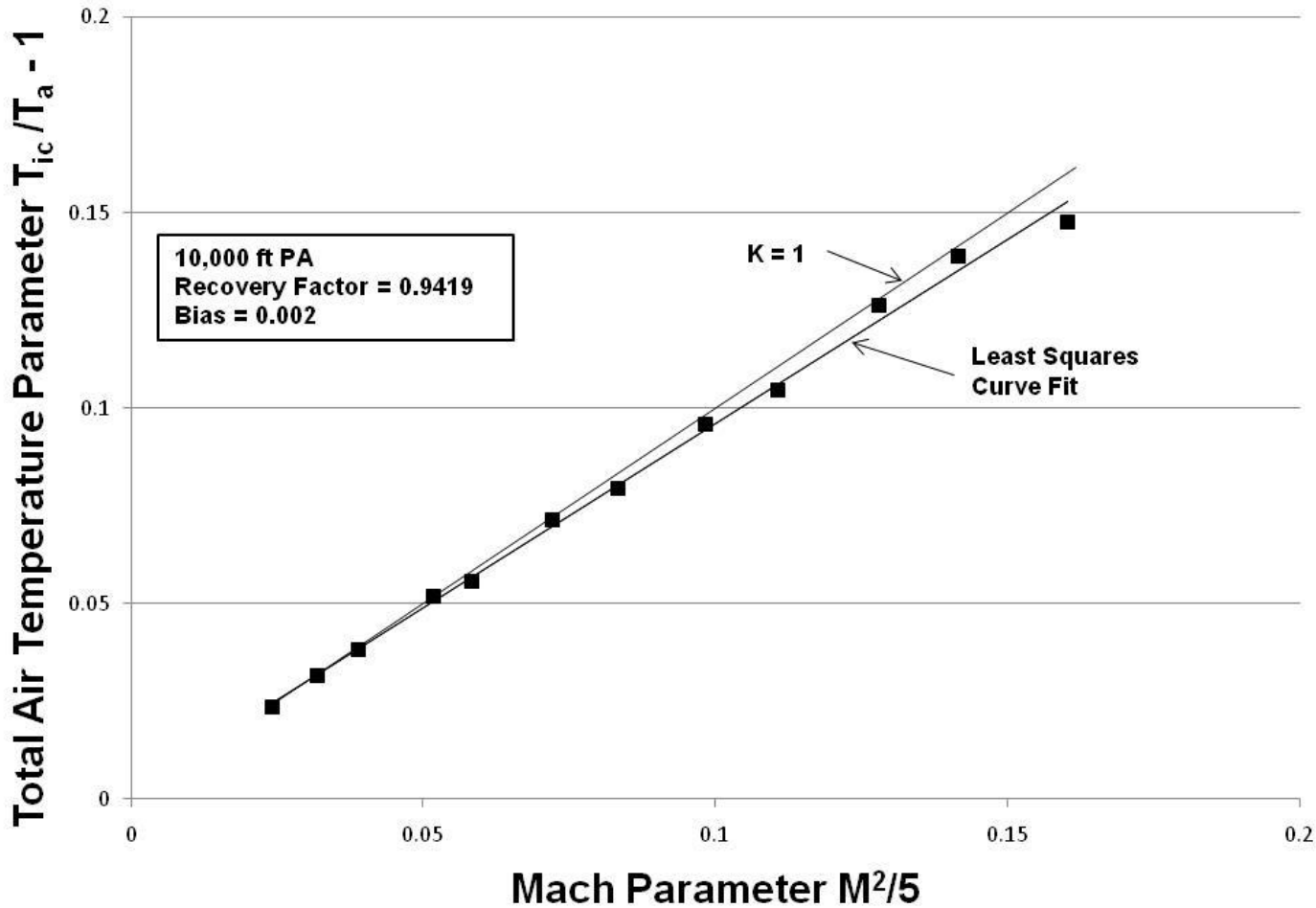


Figure A-69. Temperature Probe Recovery Factor and Bias

## Temperature Recovery Factor and Bias

Aircraft: F-16D, S/N 87-0391 (ARDS Pod on Station 1 and 370 Gallon Fuel Tanks on Stations 4 / 6)

Configuration: Cruise (Gear Up / Flaps Up)

Data Basis: Flight Test (Test Day Data) / 30 Mar 2010

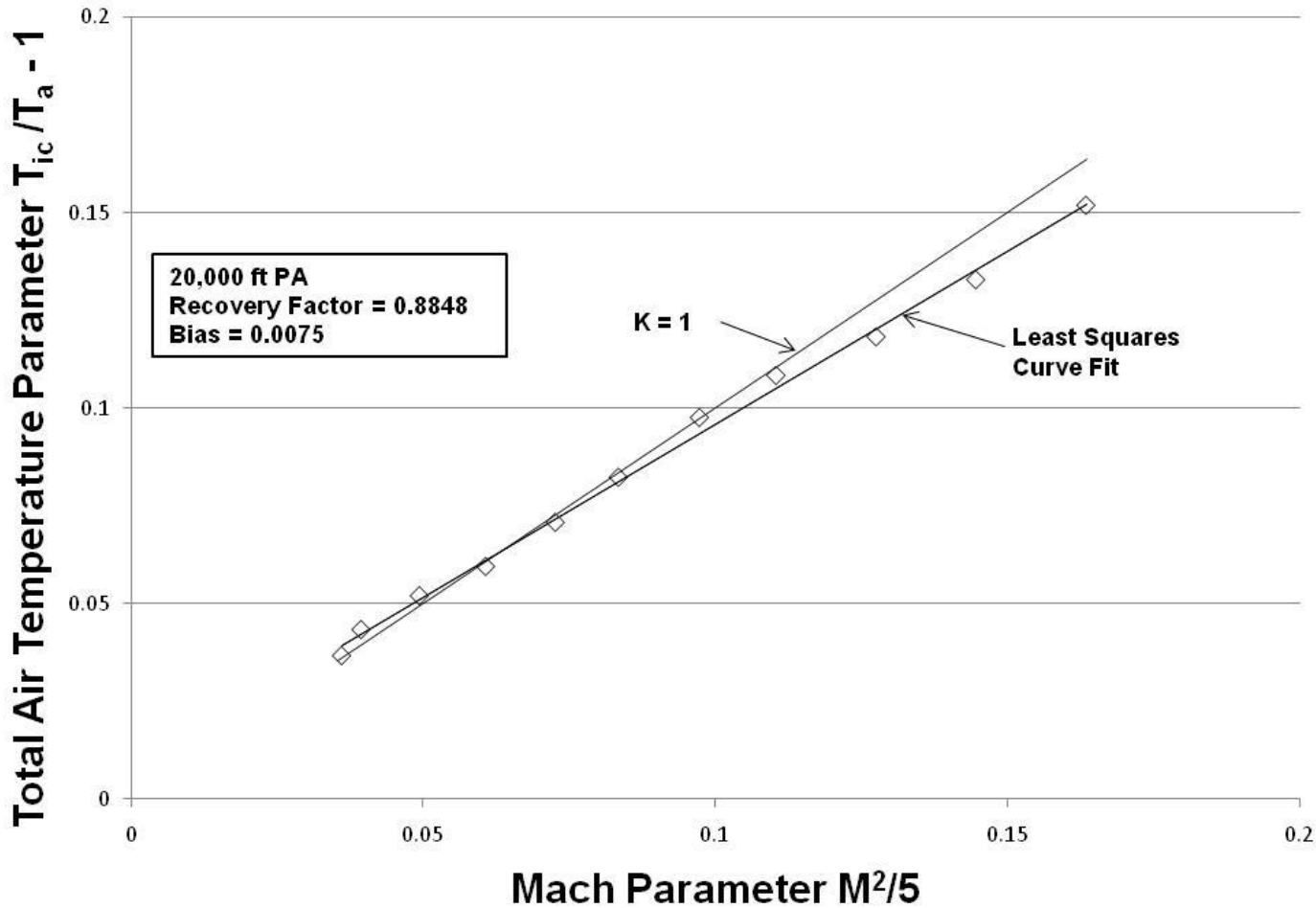


Figure A-70. Temperature Probe Recovery Factor and Bias

## Temperature Recovery Factor and Bias

Aircraft: F-16D, S/N 87-0391 (ARDS Pod on Station 1 and 370 Gallon Fuel Tanks on Stations 4 / 6)

Configuration: Cruise (Gear Up / Flaps Up)

Data Basis: Flight Test (Test Day Data) / 30 Mar 2010

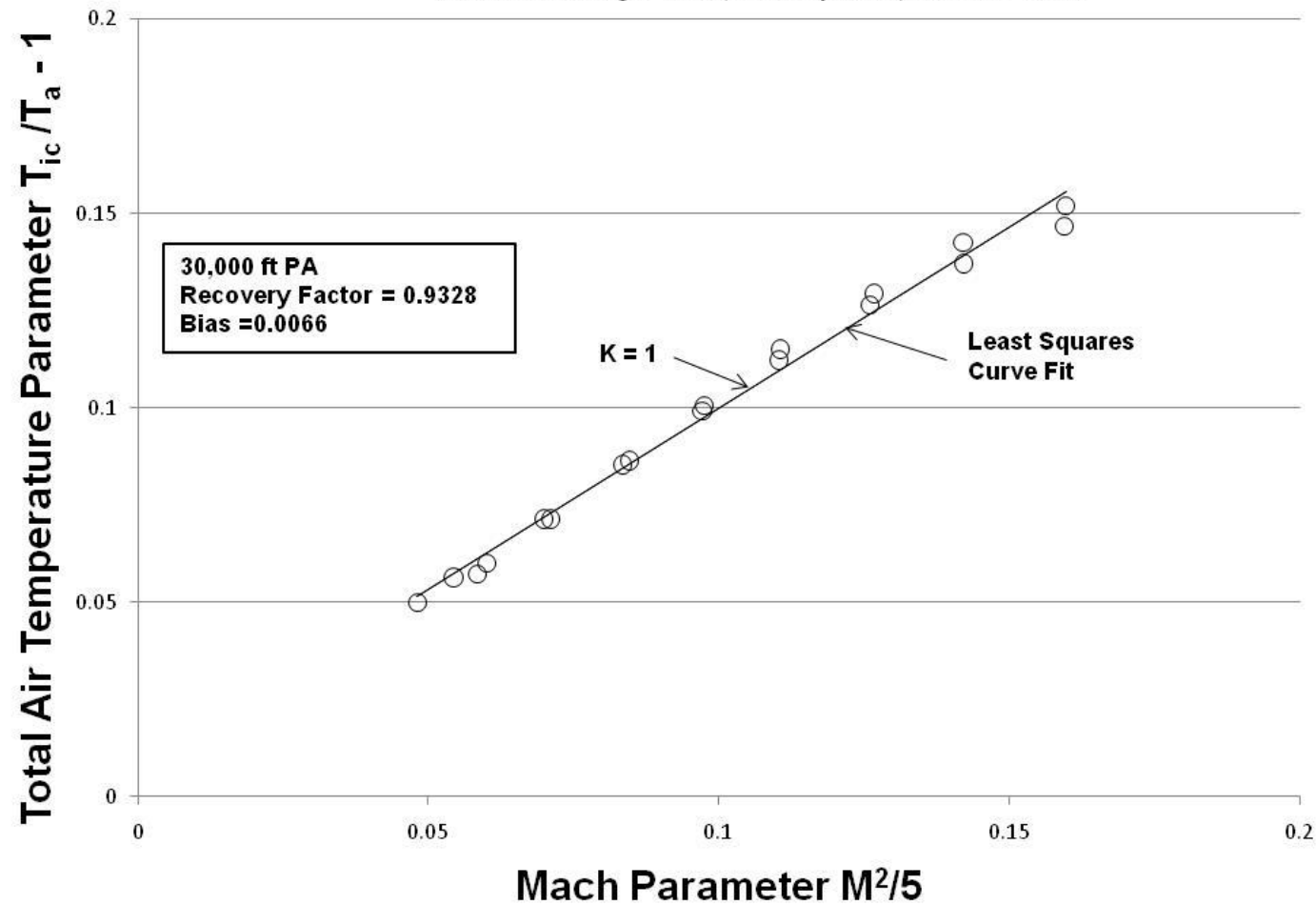


Figure A-71. Temperature Probe Recovery Factor and Bias

# Temperature Recovery Factor and Bias

Aircraft: F-16D, S/N 87-0391 (ARDS Pod on Station 1 and 370 Gallon Fuel Tanks on Stations 4 / 6)

Configuration: Cruise (Gear Up / Flaps Up)

Data Basis: Flight Test (Test Day Data) / 30 Mar 2010

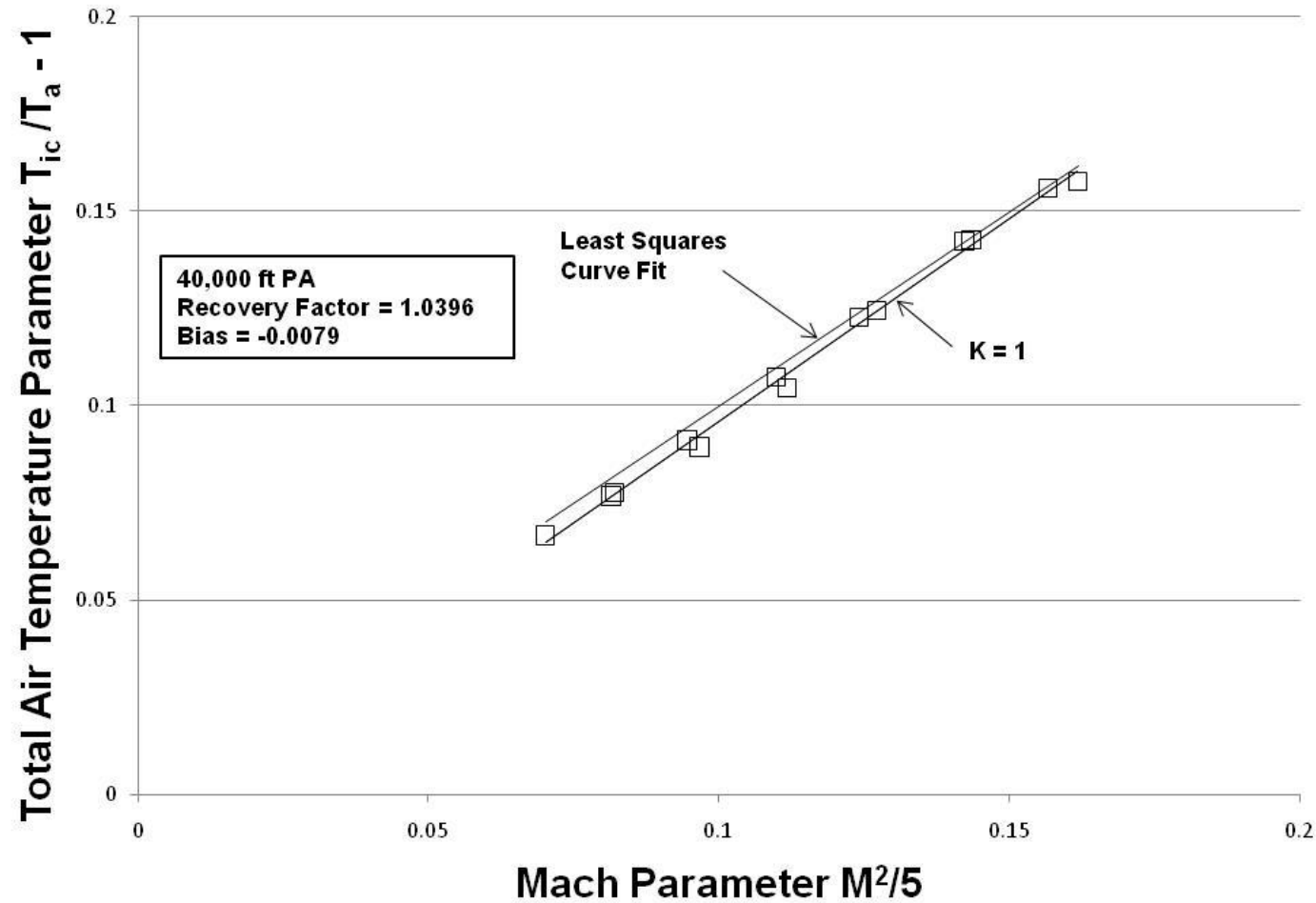


Figure A-72. Temperature Probe Recovery Factor and Bias

## Temperature Recovery Factor and Bias

Aircraft: F-16D, S/N 87-0391 (ARDS Pod on Station 1 and 370 Gallon Fuel Tanks on Stations 4 / 6)

Configuration: Cruise (Gear Up / Flaps Up)

Data Basis: Flight Test (Test Day Data) / 30 Mar 2010

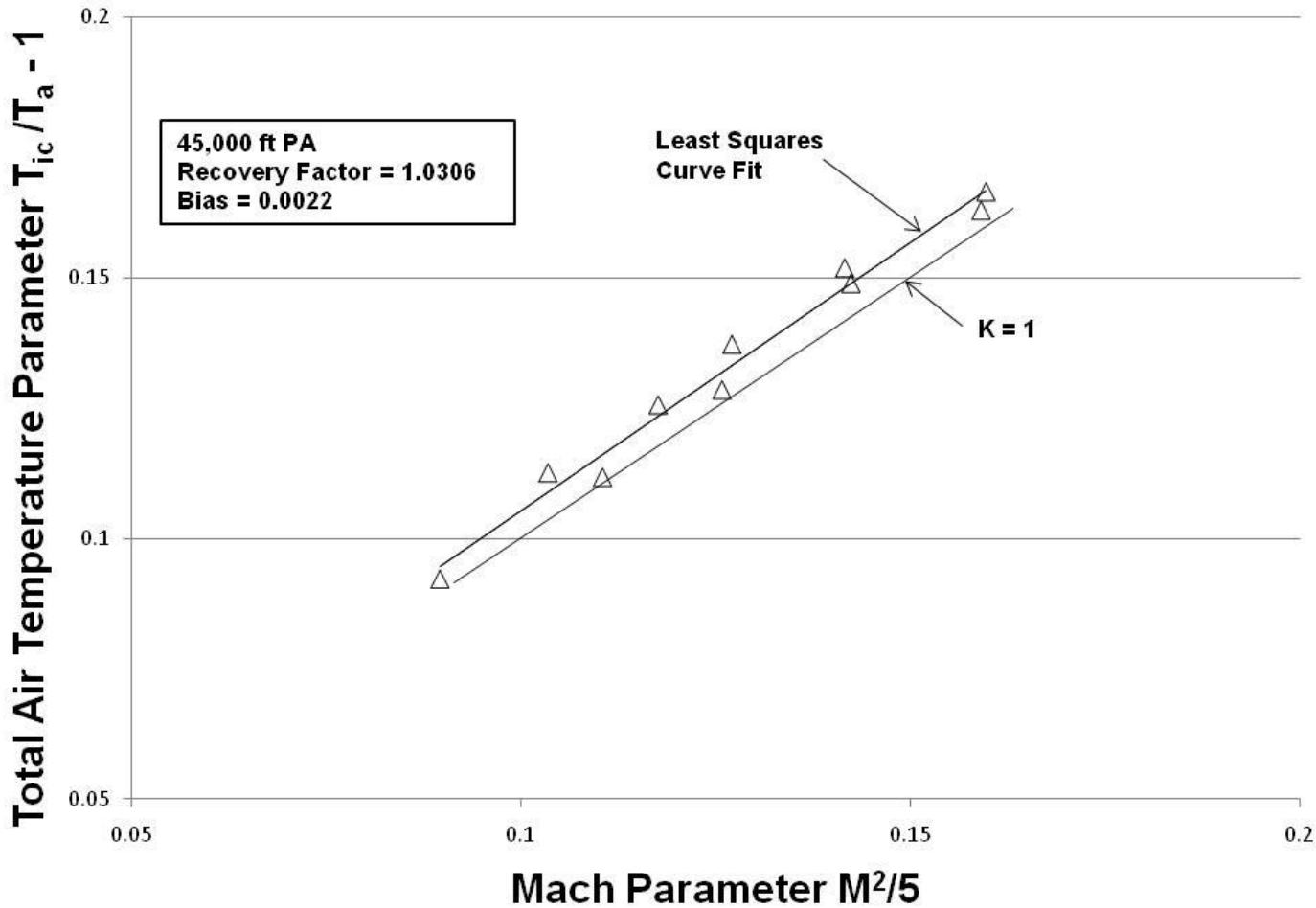


Figure A-73. Temperature Probe Recovery Factor and Bias

## Temperature Recovery Factor and Bias

Aircraft: F-16D, S/N 87-0391 (ARDS Pod on Station 1 and 370 Gallon Fuel Tanks on Stations 4 / 6)

Configuration: Cruise (Gear Up / Flaps Up)

Data Basis: Flight Test (Test Day Data) / 31 Mar 2010

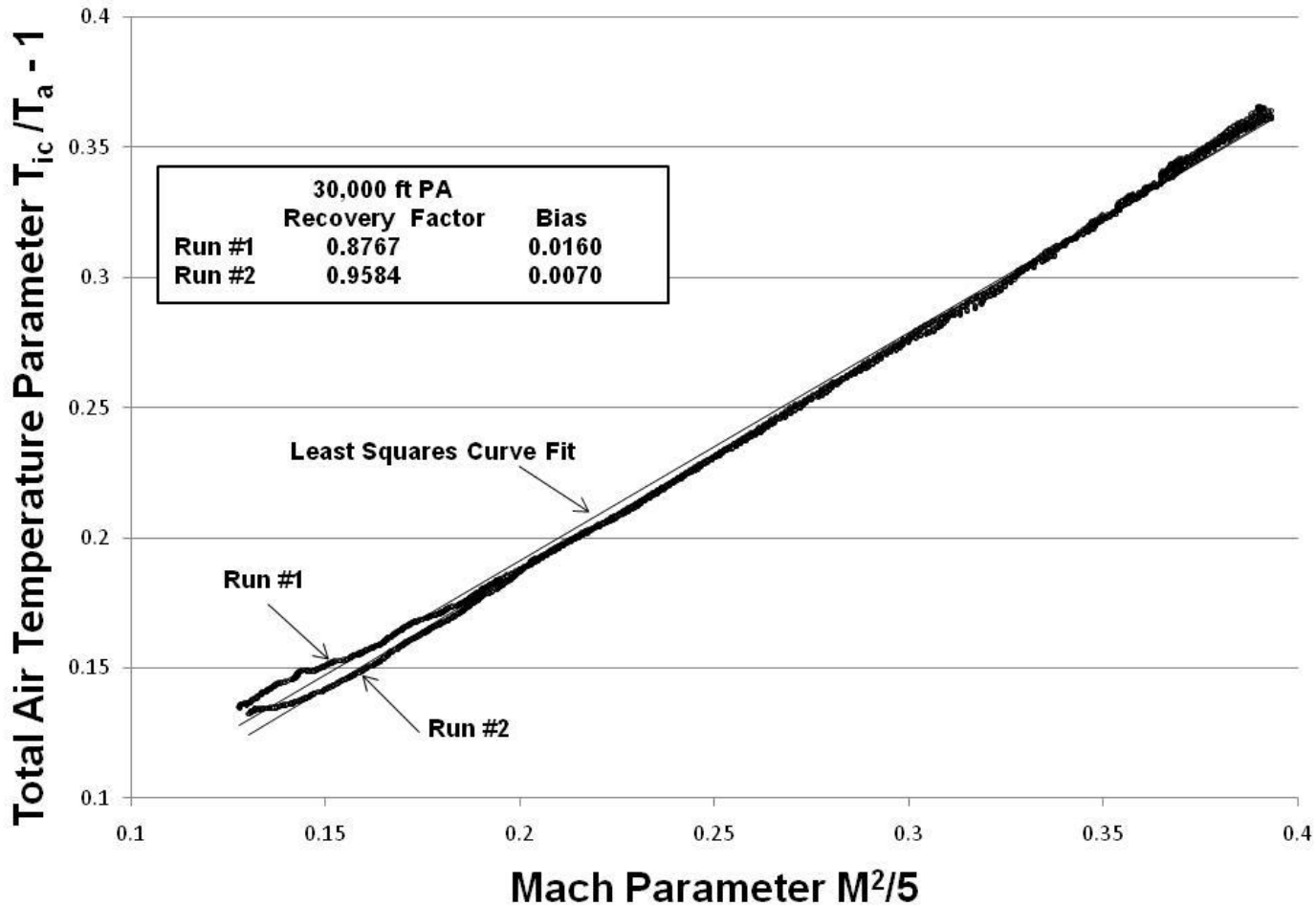


Figure A-74. Temperature Probe Recovery Factor and Bias Comparison

# Temperature Recovery Factor and Bias

Aircraft: F-16D, S/N 87-0391 (ARDS Pod on Station 1 and 370 Gallon Fuel Tanks on Stations 4 / 6)

Configuration: Cruise (Gear Up / Flaps Up)

Data Basis: Flight Test (Test Day Data) / 31 Mar 2010

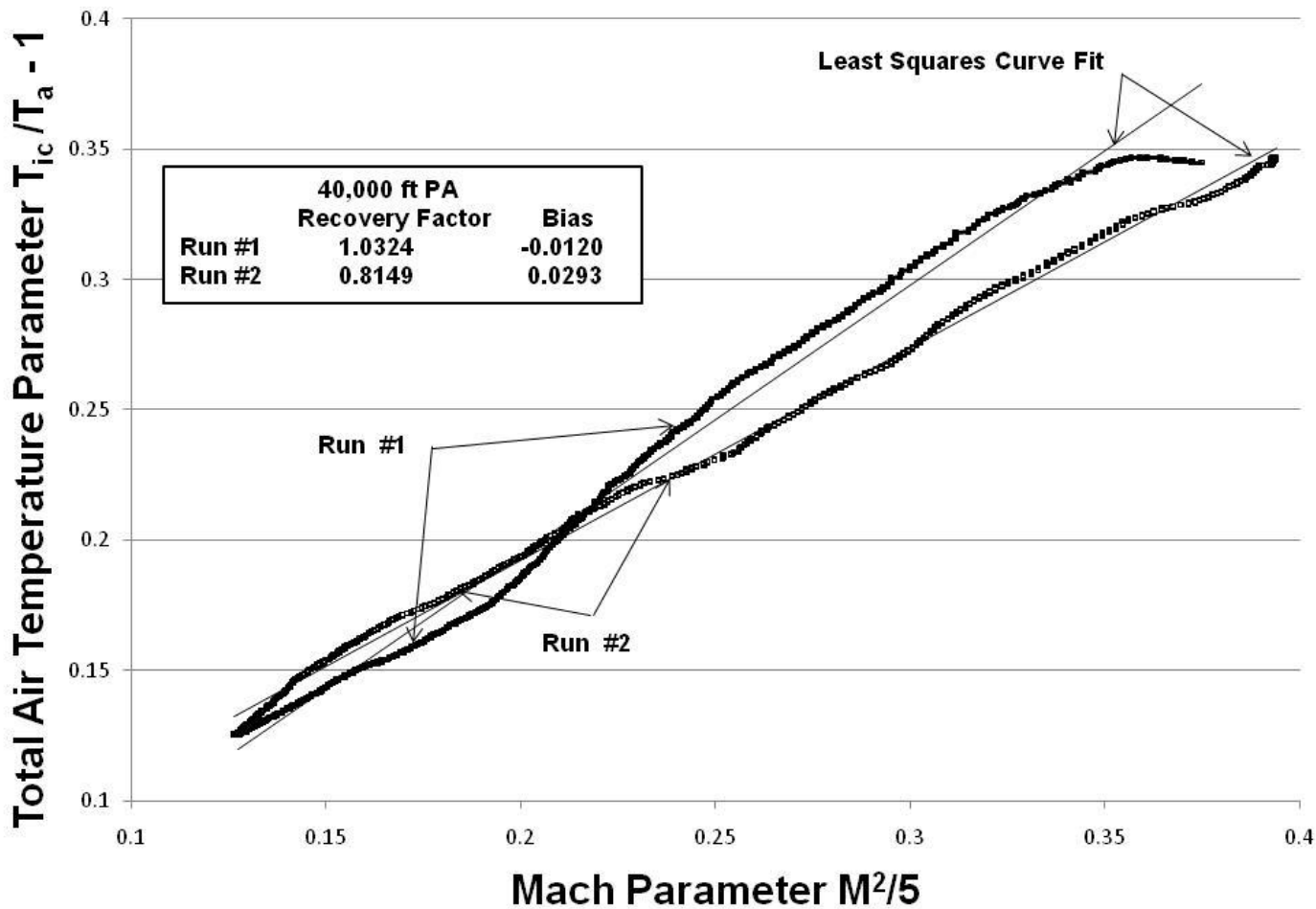


Figure A-75. Temperature Probe Recovery Factor and Bias Comparison

## Temp Recovery Factor & Ambient Temp

Aircraft: F-16D, S/N 87-0391 (ARDS Pod on Station 1 and 370 Gallon Fuel Tanks on Stations 4 / 6)

Configuration: Cruise (Gear Up / Flaps Up)

Data Basis: Flight Test (Test Day Data) / 15 Mar 2010

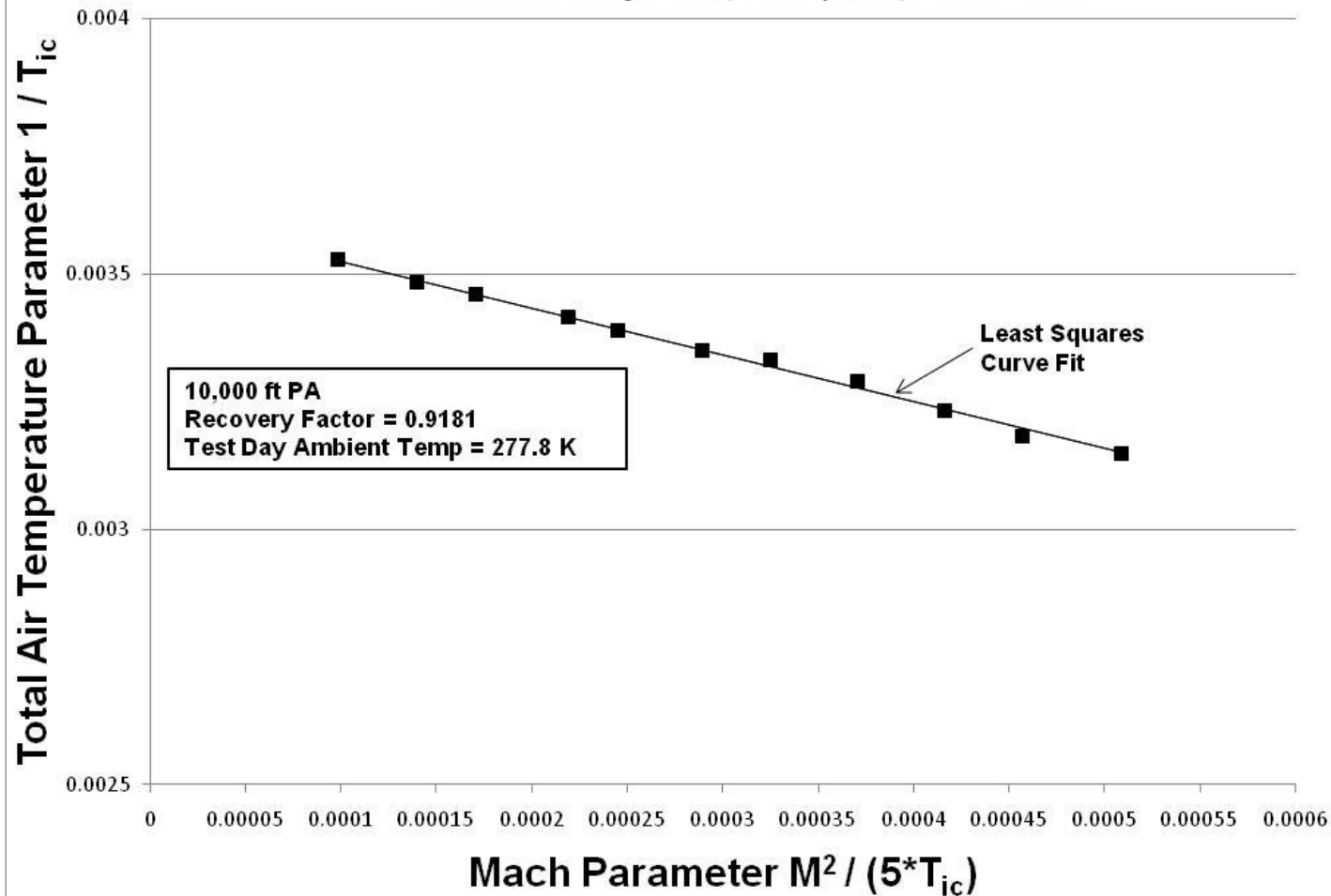


Figure A-76. Temperature Probe Recovery Factor and Ambient Temperature

## Temp Recovery Factor & Ambient Temp

Aircraft: F-16D, S/N 87-0391 (ARDS Pod on Station 1 and 370 Gallon Fuel Tanks on Stations 4 / 6)

Configuration: Cruise (Gear Up / Flaps Up)

Data Basis: Flight Test (Test Day Data) / 15 Mar 2010

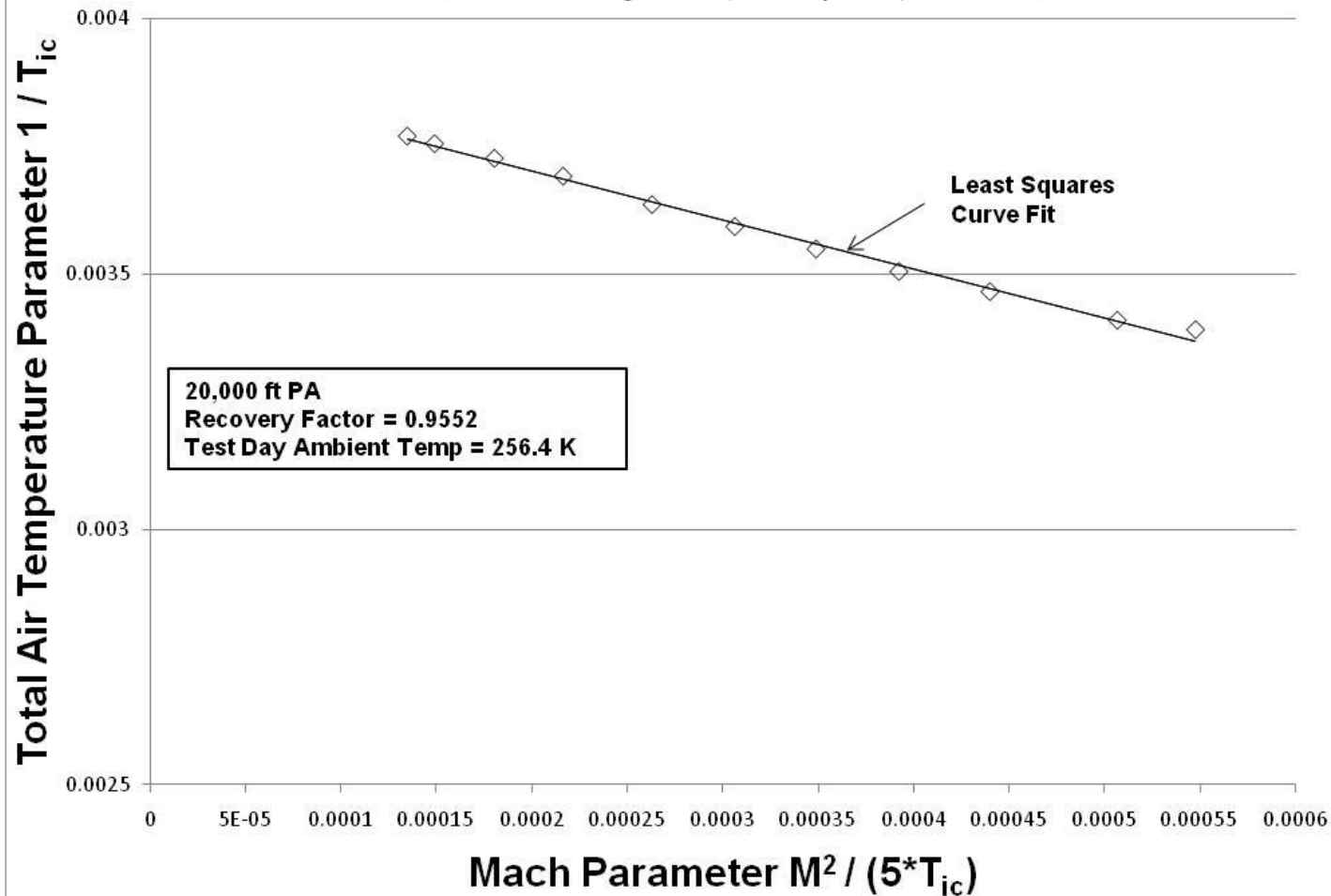


Figure A-77. Temperature Probe Recovery Factor and Ambient Temperature

## Temp Recovery Factor & Ambient Temp

Aircraft: F-16D, S/N 87-0391 (ARDS Pod on Station 1 and 370 Gallon Fuel Tanks on Stations 4 / 6)

Configuration: Cruise (Gear Up / Flaps Up)

Data Basis: Flight Test (Test Day Data) / 15 Mar 2010

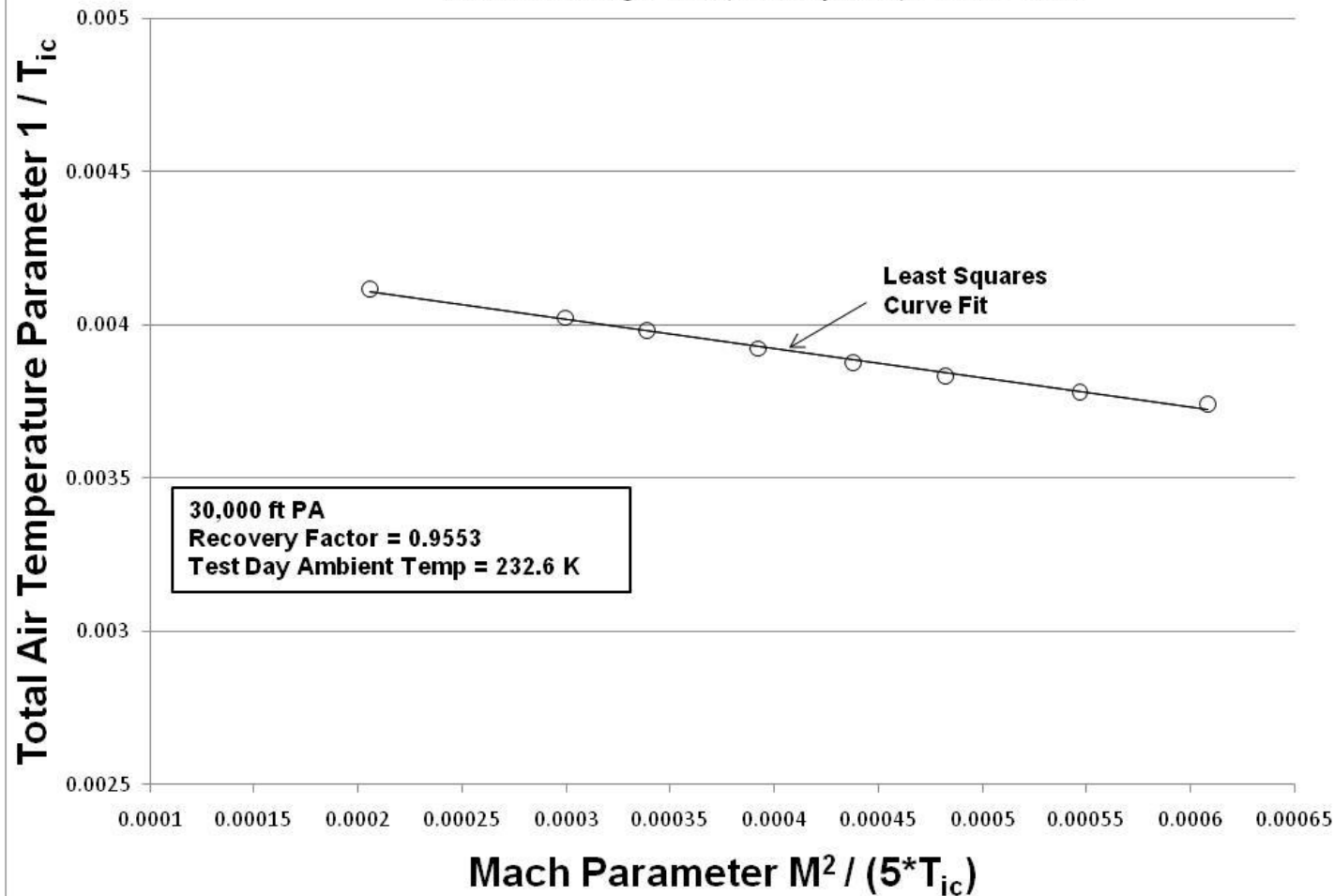


Figure A-78. Temperature Probe Recovery Factor and Ambient Temperature

## Temp Recovery Factor & Ambient Temp

Aircraft: F-16D, S/N 87-0391 (ARDS Pod on Station 1 and 370 Gallon Fuel Tanks on Stations 4 / 6)

Configuration: Cruise (Gear Up / Flaps Up)

Data Basis: Flight Test (Test Day Data) / 15 Mar 2010

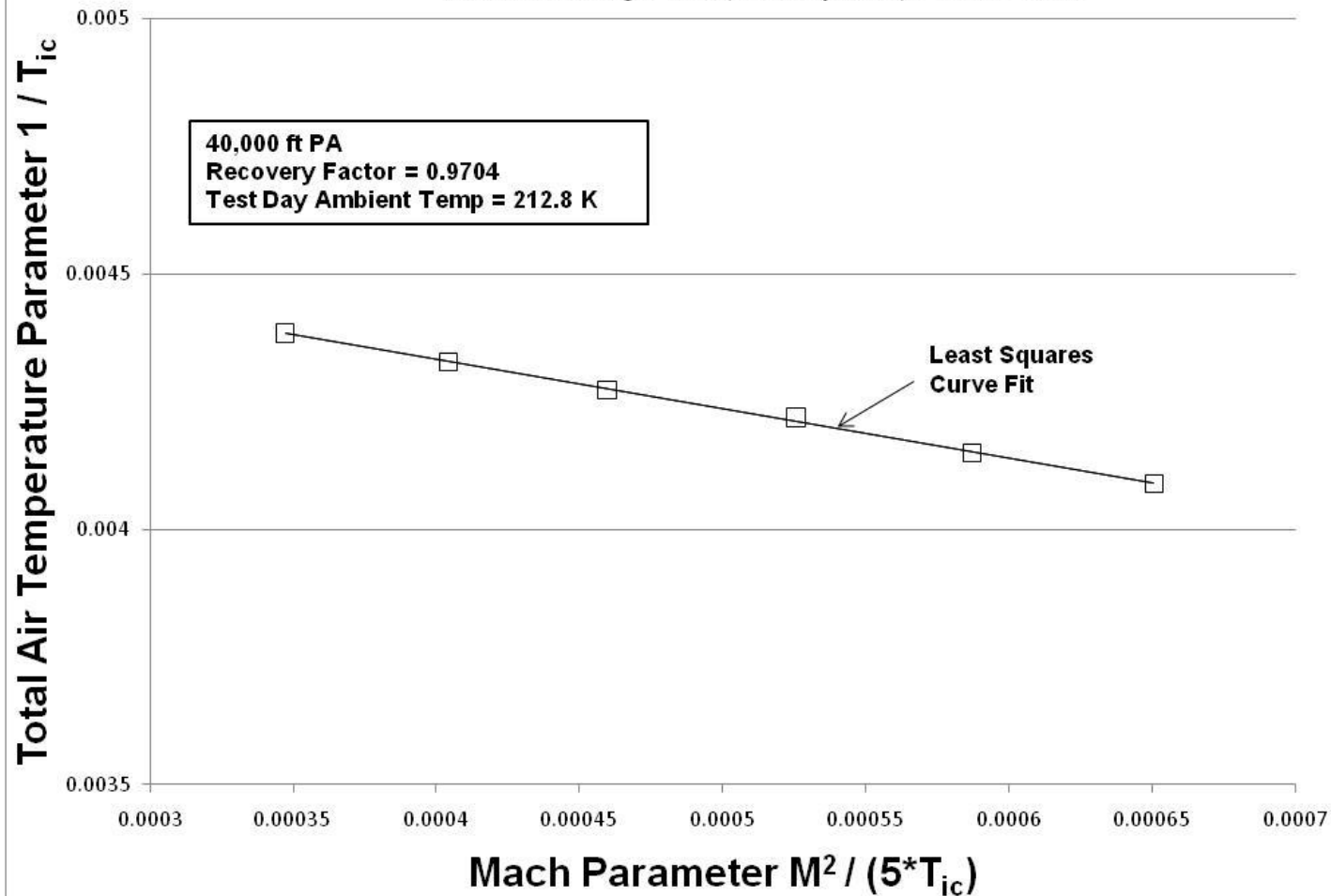


Figure A-79. Temperature Probe Recovery Factor and Ambient Temperature

## Temp Recovery Factor & Ambient Temp

Aircraft: F-16D, S/N 87-0391 (ARDS Pod on Station 1 and 370 Gallon Fuel Tanks on Stations 4 / 6)

Configuration: Cruise (Gear Up / Flaps Up)

Data Basis: Flight Test (Test Day Data) / 15 Mar 2010

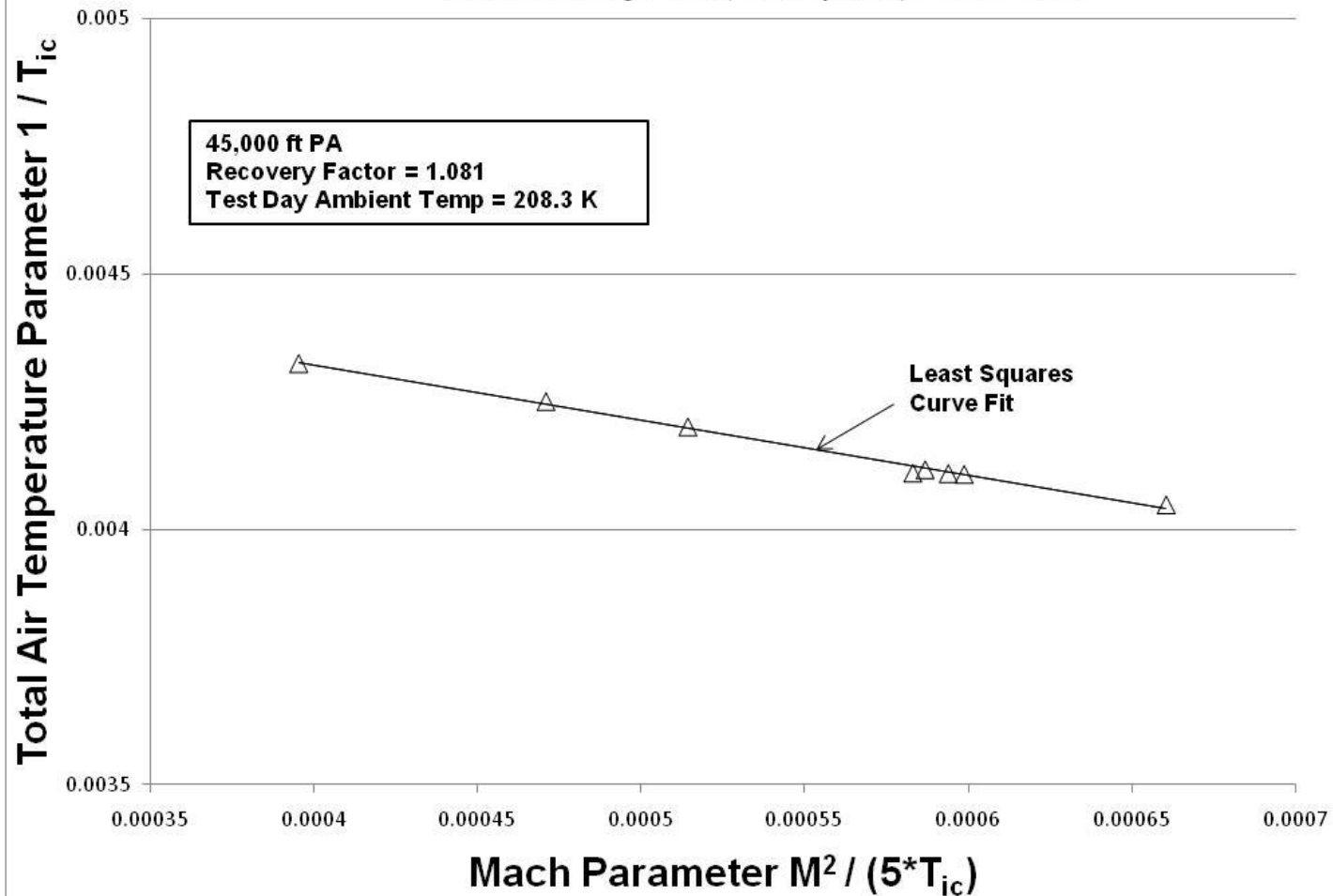


Figure A-80. Temperature Probe Recovery Factor and Ambient Temperature

## Temp Recovery Factor & Ambient Temp

Aircraft: F-16D, S/N 87-0391 (ARDS Pod on Station 1 and 370 Gallon Fuel Tanks on Stations 4 / 6)

Configuration: Cruise (Gear Up / Flaps Up)

Data Basis: Flight Test (Test Day Data) / 16 Mar 2010

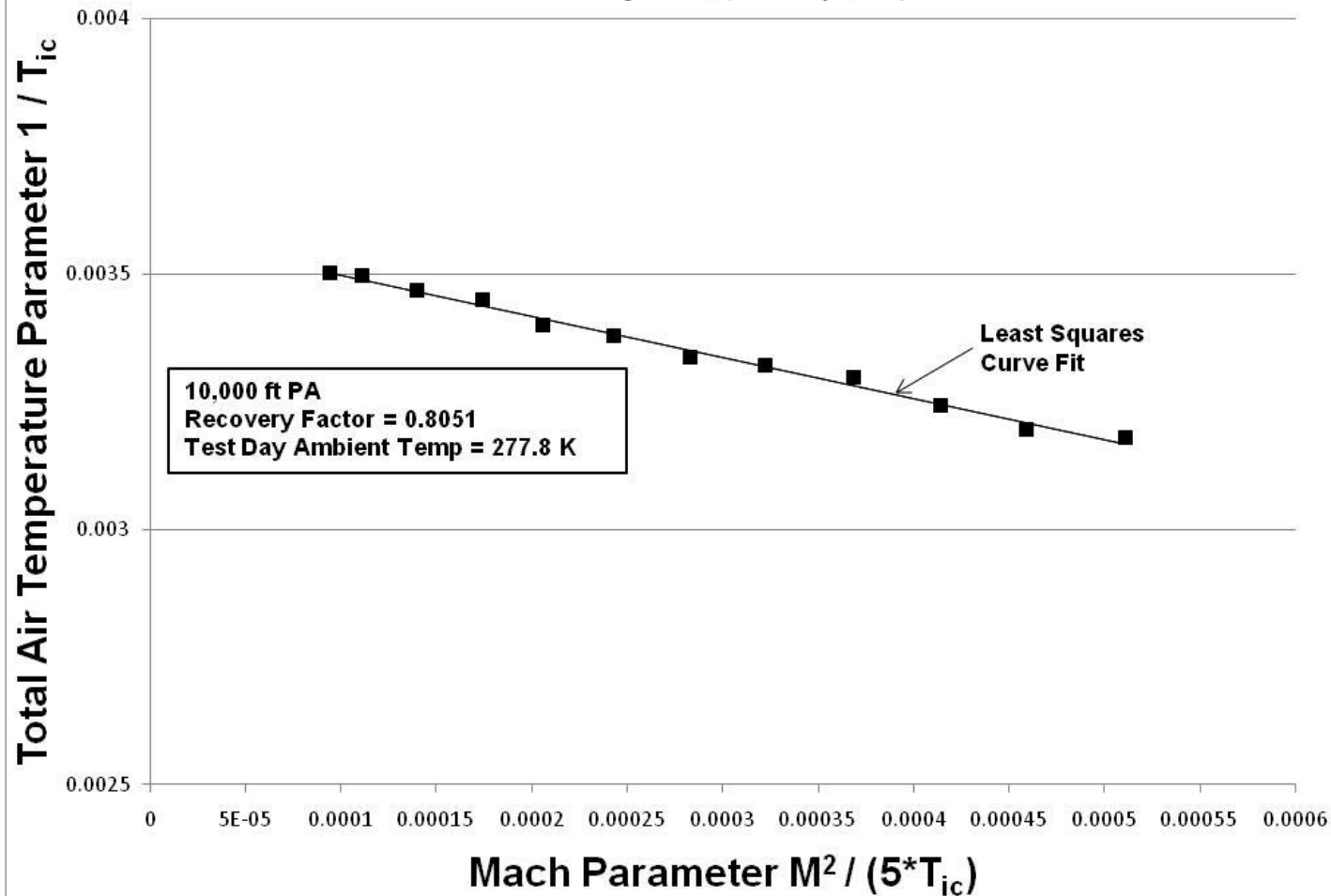


Figure A-81. Temperature Probe Recovery Factor and Ambient Temperature

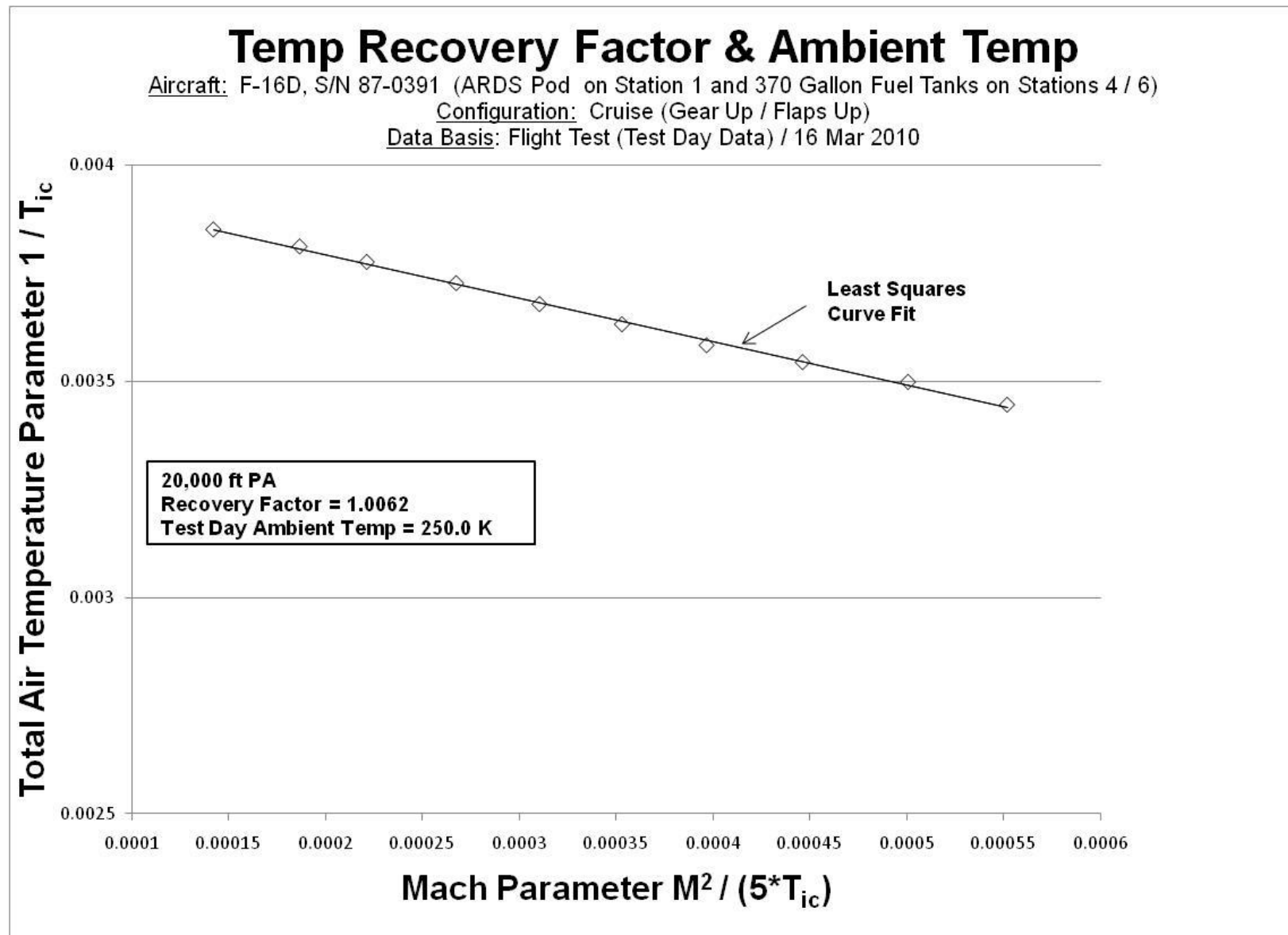


Figure A-82. Temperature Probe Recovery Factor and Ambient Temperature

## Temp Recovery Factor & Ambient Temp

Aircraft: F-16D, S/N 87-0391 (ARDS Pod on Station 1 and 370 Gallon Fuel Tanks on Stations 4 / 6)

Configuration: Cruise (Gear Up / Flaps Up)

Data Basis: Flight Test (Test Day Data) / 16 Mar 2010

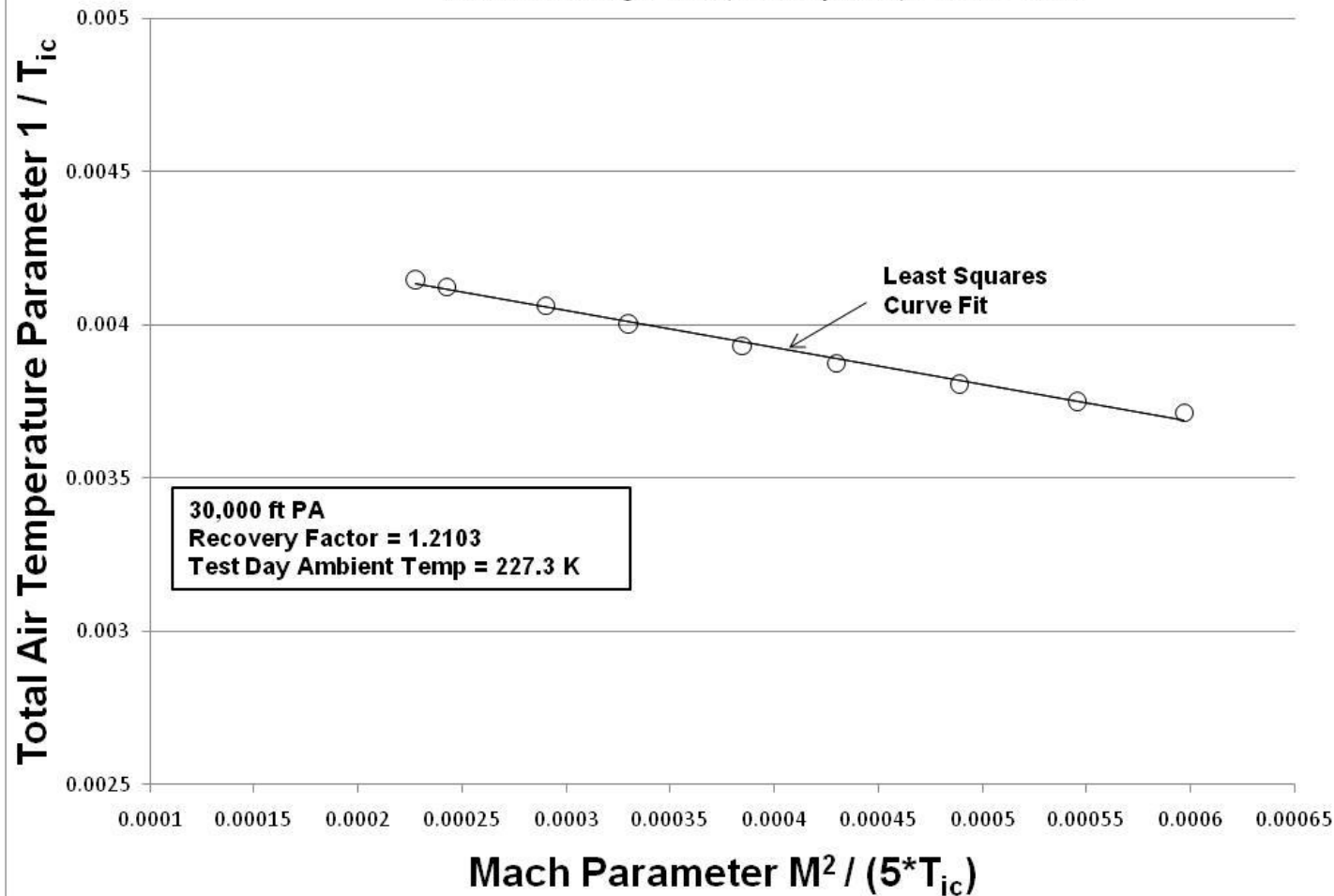


Figure A-83. Temperature Probe Recovery Factor and Ambient Temperature

## Temp Recovery Factor & Ambient Temp

Aircraft: F-16D, S/N 87-0391 (ARDS Pod on Station 1 and 370 Gallon Fuel Tanks on Stations 4 / 6)

Configuration: Cruise (Gear Up / Flaps Up)

Data Basis: Flight Test (Test Day Data) / 16 Mar 2010

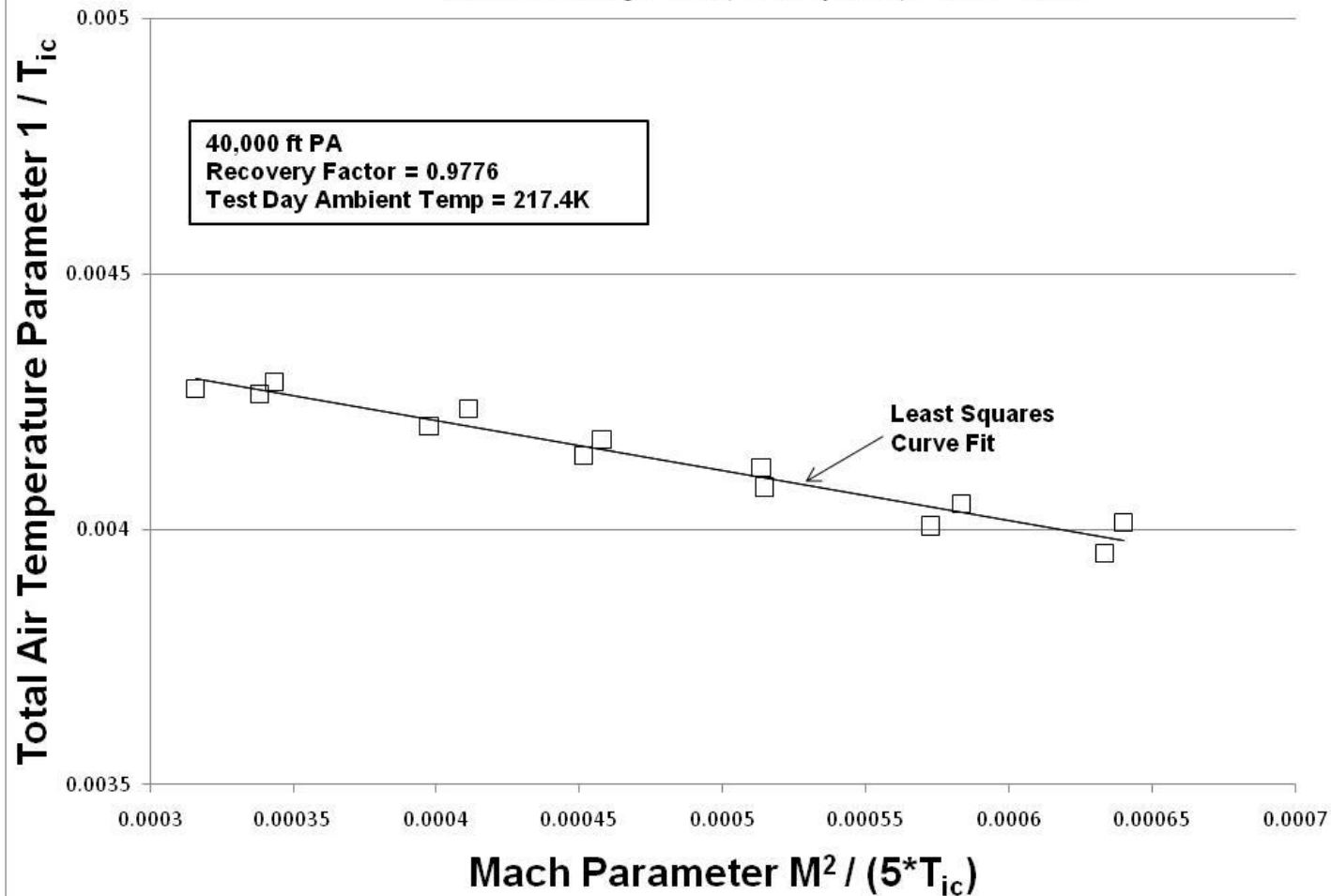


Figure A-84. Temperature Probe Recovery Factor and Ambient Temperature

## Temp Recovery Factor & Ambient Temp

Aircraft: F-16D, S/N 87-0391 (ARDS Pod on Station 1 and 370 Gallon Fuel Tanks on Stations 4 / 6)

Configuration: Cruise (Gear Up / Flaps Up)

Data Basis: Flight Test (Test Day Data) / 16 Mar 2010

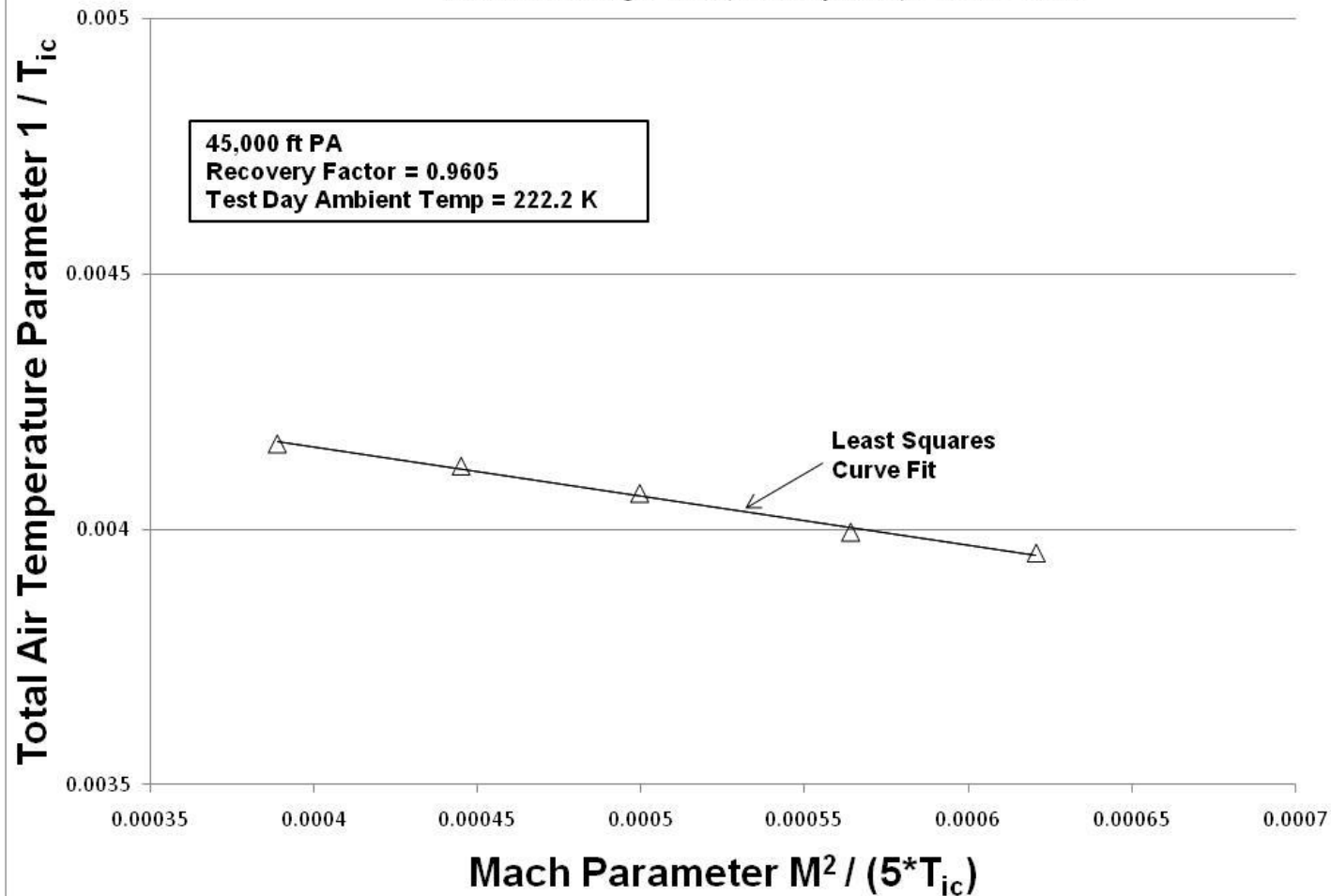


Figure A-85. Temperature Probe Recovery Factor and Ambient Temperature

## Temp Recovery Factor & Ambient Temp

Aircraft: F-16D, S/N 87-0391 (ARDS Pod on Station 1 and 370 Gallon Fuel Tanks on Stations 4 / 6)

Configuration: Cruise (Gear Up / Flaps Up)

Data Basis: Flight Test (Test Day Data) / 30 Mar 2010

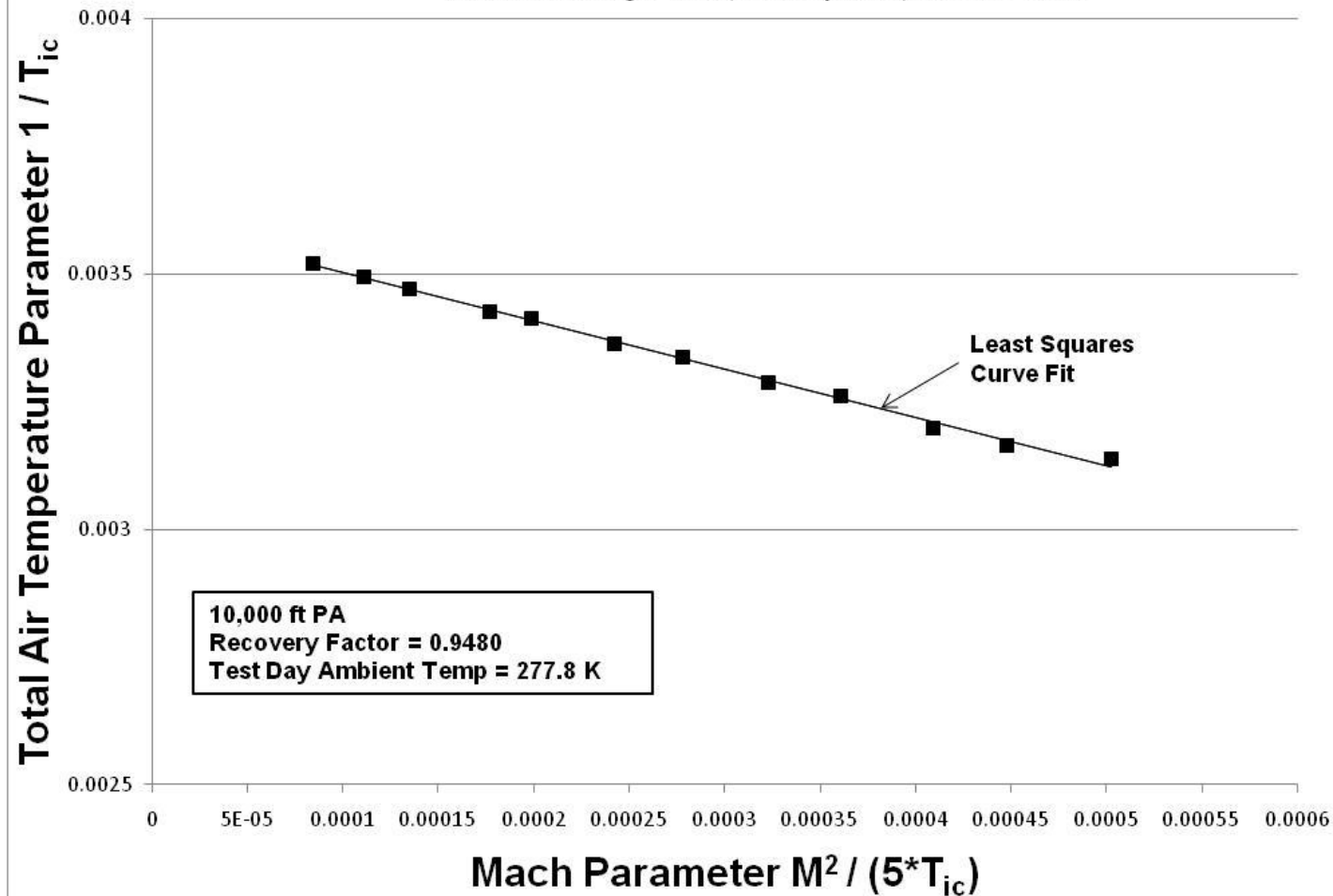


Figure A-86. Temperature Probe Recovery Factor and Ambient Temperature

## Temp Recovery Factor & Ambient Temp

Aircraft: F-16D, S/N 87-0391 (ARDS Pod on Station 1 and 370 Gallon Fuel Tanks on Stations 4 / 6)

Configuration: Cruise (Gear Up / Flaps Up)

Data Basis: Flight Test (Test Day Data) / 30 Mar 2010

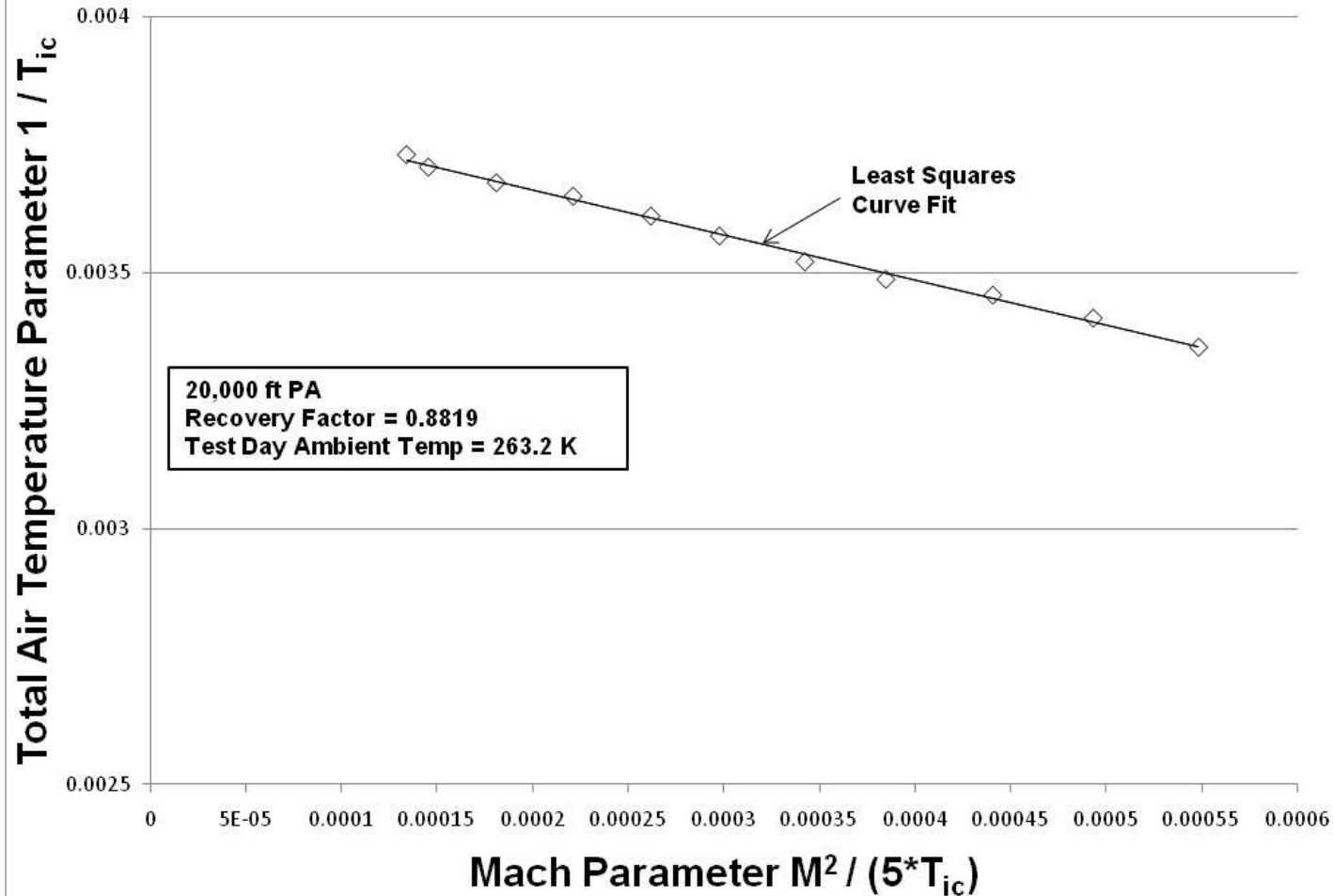


Figure A-87. Temperature Probe Recovery Factor and Ambient Temperature

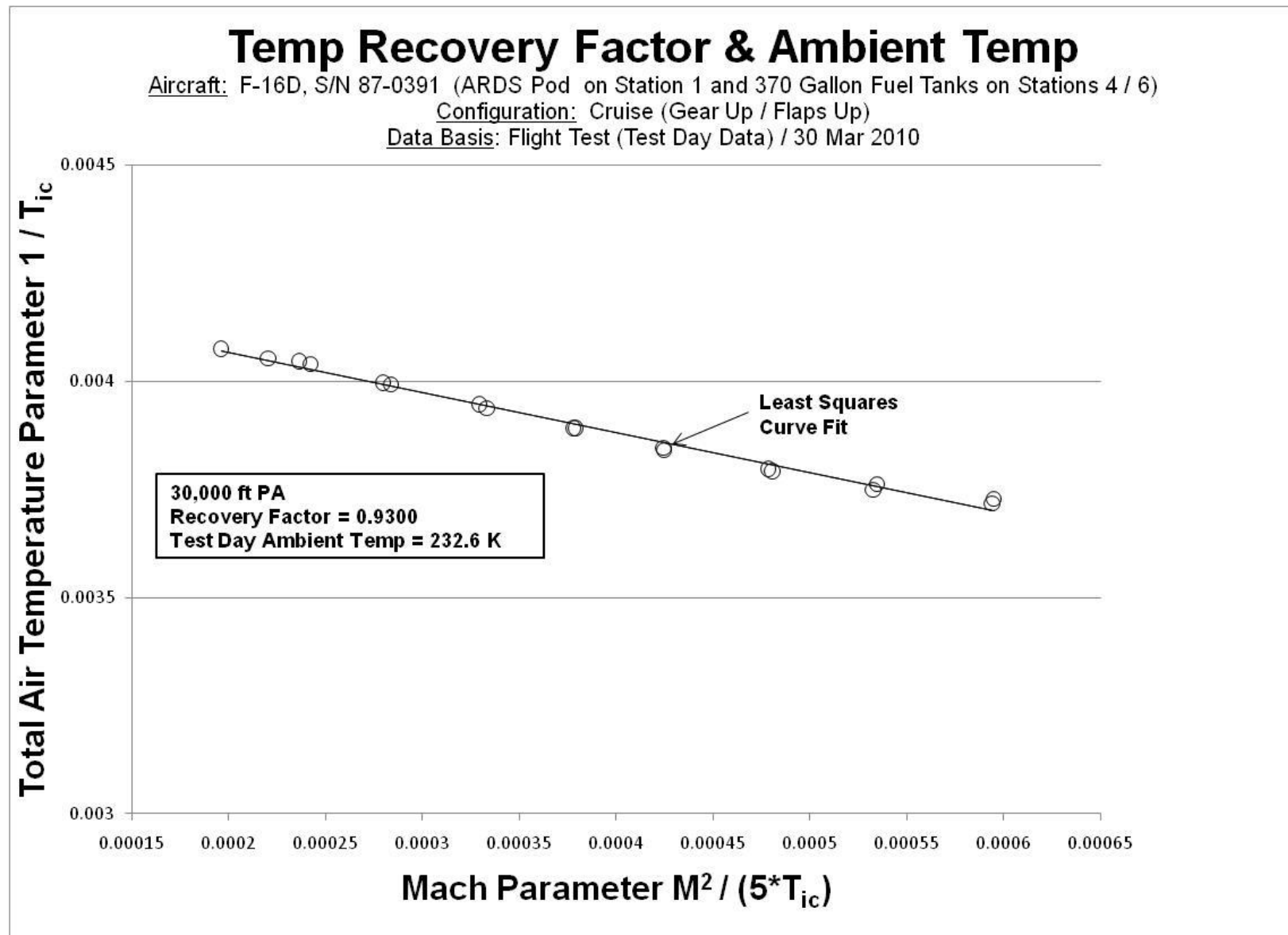


Figure A-88. Temperature Probe Recovery Factor and Ambient Temperature

## Temp Recovery Factor & Ambient Temp

Aircraft: F-16D, S/N 87-0391 (ARDS Pod on Station 1 and 370 Gallon Fuel Tanks on Stations 4 / 6)

Configuration: Cruise (Gear Up / Flaps Up)

Data Basis: Flight Test (Test Day Data) / 30 Mar 2010

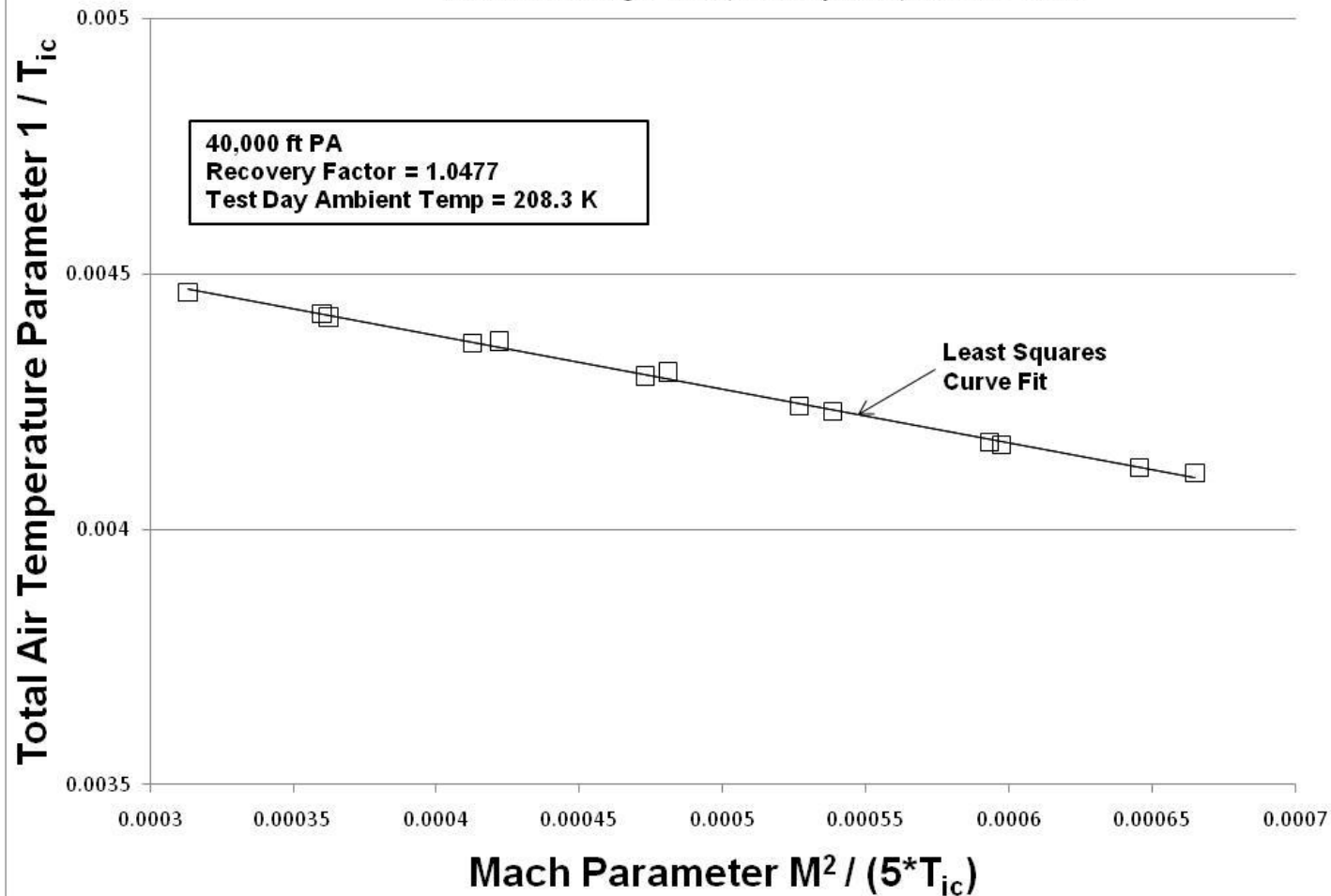


Figure A-89. Temperature Probe Recovery Factor and Ambient Temperature

## Temp Recovery Factor & Ambient Temp

Aircraft: F-16D, S/N 87-0391 (ARDS Pod on Station 1 and 370 Gallon Fuel Tanks on Stations 4 / 6)

Configuration: Cruise (Gear Up / Flaps Up)

Data Basis: Flight Test (Test Day Data) / 30 Mar 2010

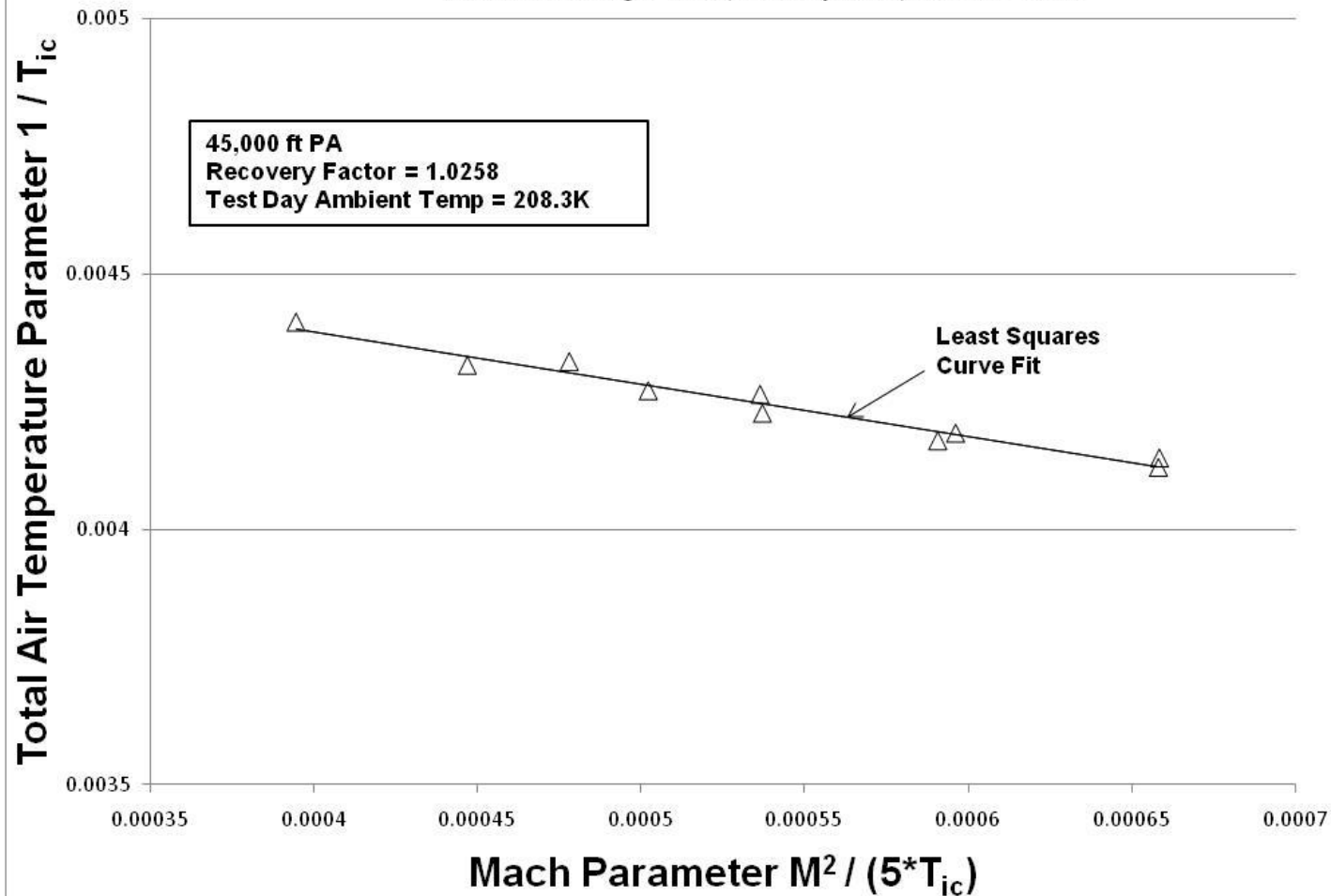


Figure A-90. Temperature Probe Recovery Factor and Ambient Temperature

## Upwash Angle at AOA Vane Test Noseboom

Aircraft: F-16D, S/N 87-0391 (ARDS Pod on Station 1 and 370 Gallon Fuel Tanks on Stations 4 and 6)

Configuration: Cruise (Gear Up / Flaps Up)

Data Basis: Flight Test (Test Day Data) / 11-31 Mar 2010

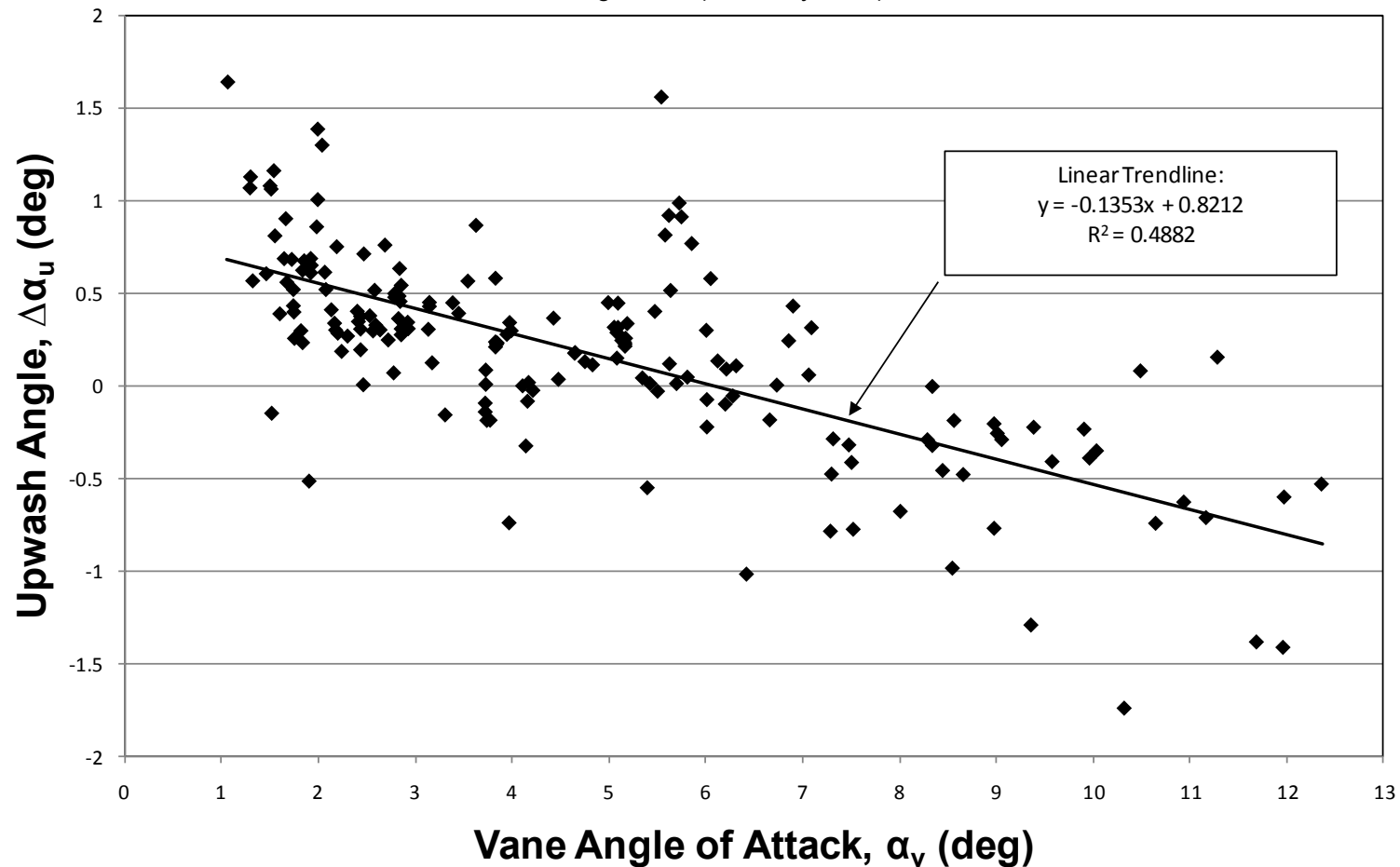


Figure A-91. Noseboom Upwash Angle at AOA Vane (2,300 ft to 45,000 ft PA)

## **APPENDIX B – DATA TABLES**

**Table B-1. Altitude-Based Noseboom Static Position Error Pressure Coefficient Model  
(0.3M to 0.48M).**

Mic	Pressure Altitude (ft)					
	2,300	10,000	20,000	30,000	40,000	45,000
<b>0.3</b>	0.0012					
<b>0.305</b>	0.0015					
<b>0.31</b>	0.0018					
<b>0.315</b>	0.0021					
<b>0.32</b>	0.0024					
<b>0.325</b>	0.0027					
<b>0.33</b>	0.003					
<b>0.335</b>	0.0032					
<b>0.34</b>	0.0034					
<b>0.345</b>	0.0036					
<b>0.35</b>	0.0038	-0.00515				
<b>0.355</b>	0.0039	-0.00495				
<b>0.36</b>	0.004	-0.00475				
<b>0.365</b>	0.0041	-0.00455				
<b>0.37</b>	0.0042	-0.00435				
<b>0.375</b>	0.0043	-0.00415				
<b>0.38</b>	0.0044	-0.00395				
<b>0.385</b>	0.0045	-0.00375				
<b>0.39</b>	0.0046	-0.00355				
<b>0.395</b>	0.0047	-0.00335				
<b>0.4</b>	0.0048	-0.00315				
<b>0.405</b>	0.0049	-0.00295				
<b>0.41</b>	0.00495	-0.00275				
<b>0.415</b>	0.005	-0.00255				
<b>0.42</b>	0.00505	-0.00235				
<b>0.425</b>	0.0051	-0.00215	-0.0017			
<b>0.43</b>	0.00512	-0.00195	-0.0015			
<b>0.435</b>	0.00514	-0.00175	-0.0013			
<b>0.44</b>	0.00516	-0.00155	-0.0011			
<b>0.445</b>	0.00518	-0.00135	-0.0009			
<b>0.45</b>	0.0052	-0.00115	-0.0007			
<b>0.455</b>	0.00522	-0.00095	-0.0005			
<b>0.46</b>	0.00523	-0.00075	-0.0003			
<b>0.465</b>	0.00524	-0.00055	-0.0001			
<b>0.47</b>	0.00525	-0.00035	0.0001			
<b>0.475</b>	0.00526	-0.00015	0.0003			
<b>0.48</b>	0.00526	0.00005	0.0005			

**Table B-2. Altitude-Based Noseboom Static Position Error Pressure Coefficient Model  
(0.485M to 0.665M).**

Mic	Pressure Altitude (ft)					
	2,300	10,000	20,000	30,000	40,000	45,000
<b>0.485</b>	0.00526	0.00025	0.0007			
<b>0.49</b>	0.00526	0.00045	0.0009	-0.004		
<b>0.495</b>	0.00526	0.00065	0.0011	-0.0037		
<b>0.5</b>	0.00526	0.00085	0.0013	-0.0034		
<b>0.505</b>	0.00526	0.00105	0.00145	-0.0032		
<b>0.51</b>	0.00526	0.00125	0.0016	-0.003		
<b>0.515</b>	0.00526	0.0014	0.00175	-0.00285		
<b>0.52</b>	0.00526	0.00155	0.0019	-0.0027		
<b>0.525</b>	0.00524	0.0017	0.00205	-0.00255		
<b>0.53</b>	0.00522	0.00185	0.00217	-0.0024		
<b>0.535</b>	0.0052	0.00195	0.00229	-0.00225		
<b>0.54</b>	0.00518	0.00202	0.00241	-0.0021		
<b>0.545</b>	0.00516	0.00209	0.00253	-0.00195		
<b>0.55</b>	0.00514	0.00216	0.00265	-0.0018		
<b>0.555</b>	0.00512	0.00223	0.00277	-0.00165		
<b>0.56</b>	0.0051	0.0023	0.00287	-0.0015		
<b>0.565</b>	0.00508	0.00237	0.00297	-0.00135		
<b>0.57</b>	0.00506	0.00244	0.00307	-0.0012		
<b>0.575</b>	0.00504	0.00251	0.00314	-0.00105		
<b>0.58</b>	0.00502	0.00257	0.00321	-0.0009		
<b>0.585</b>	0.005	0.00263	0.00328	-0.0008		
<b>0.59</b>	0.00498	0.00268	0.00335	-0.0007		
<b>0.595</b>	0.00496	0.00273	0.00338	-0.0006		
<b>0.6</b>	0.00494	0.00276	0.00339	-0.0005		
<b>0.605</b>	0.00492	0.00279	0.0034	-0.0004		
<b>0.61</b>	0.0049	0.00281	0.00341	-0.0003	-0.003	
<b>0.615</b>	0.00488	0.00282	0.00342	-0.0002	-0.0027	
<b>0.62</b>	0.00486	0.00282	0.00343	-0.0001	-0.0024	
<b>0.625</b>	0.00484	0.00282	0.00344	-3E-05	-0.0021	
<b>0.63</b>	0.00482	0.00282	0.00344	4E-05	-0.0018	
<b>0.635</b>	0.00479	0.00282	0.00344	0.00011	-0.0015	
<b>0.64</b>	0.00476	0.00282	0.00344	0.00018	-0.00125	
<b>0.645</b>	0.00473	0.00282	0.00341	0.00025	-0.001	
<b>0.65</b>	0.0047	0.00282	0.00338	0.00032	-0.00075	
<b>0.655</b>	0.00467	0.00282	0.00335	0.00039	-0.00055	
<b>0.66</b>	0.00464	0.00282	0.00332	0.00044	-0.00035	
<b>0.665</b>	0.0046	0.00282	0.00329	0.00049	-0.00015	

**Table B-3. Altitude-Based Noseboom Static Position Error Pressure Coefficient Model  
(0.67M to 0.85M)**

Mic	Pressure Altitude (ft)					
	2,300	10,000	20,000	30,000	40,000	45,000
<b>0.67</b>	0.00456	0.00282	0.00326	0.00054	0	
<b>0.675</b>	0.00452	0.00282	0.00323	0.00059	0.00025	-0.006
<b>0.68</b>	0.00448	0.00282	0.0032	0.00064	0.00045	-0.00585
<b>0.685</b>	0.00444	0.00282	0.00317	0.00069	0.00065	-0.0057
<b>0.69</b>	0.0044	0.00282	0.00314	0.00074	0.0008	-0.00555
<b>0.695</b>	0.00436	0.00282	0.00309	0.00079	0.00092	-0.0054
<b>0.7</b>	0.00432	0.00282	0.00304	0.00084	0.00102	-0.00525
<b>0.705</b>	0.00428	0.00282	0.00299	0.00087	0.0011	-0.0051
<b>0.71</b>	0.00424	0.00272	0.00292	0.0009	0.00116	-0.00495
<b>0.715</b>	0.0042	0.00262	0.00285	0.00093	0.0012	-0.0048
<b>0.72</b>	0.00416	0.00252	0.00278	0.00096	0.00122	-0.00465
<b>0.725</b>	0.00412	0.00242	0.00271	0.00099	0.00122	-0.0045
<b>0.73</b>	0.00408	0.00232	0.00264	0.00099	0.00122	-0.00435
<b>0.735</b>	0.00404	0.00222	0.00254	0.00099	0.00122	-0.0042
<b>0.74</b>	0.00399	0.00212	0.00244	0.00099	0.00122	-0.00405
<b>0.745</b>	0.00394	0.00202	0.00234	0.00099	0.00122	-0.0039
<b>0.75</b>	0.00388	0.00192	0.00224	0.00099	0.00112	-0.00375
<b>0.755</b>	0.00381	0.00182	0.00214	0.00099	0.00102	-0.0036
<b>0.76</b>	0.00373	0.00172	0.00204	0.00094	0.00092	-0.00345
<b>0.765</b>	0.00364	0.00162	0.00197	0.00089	0.00082	-0.0033
<b>0.77</b>	0.00354	0.00152	0.0019	0.00084	0.00072	-0.00315
<b>0.775</b>	0.00344	0.00142	0.00183	0.00079	0.00062	-0.003
<b>0.78</b>	0.00334	0.00132	0.00176	0.00074	0.00052	-0.0029
<b>0.785</b>	0.00324	0.00122	0.00169	0.00069	0.00042	-0.0028
<b>0.79</b>	0.00314	0.0011	0.00162	0.00064	0.00032	-0.0027
<b>0.795</b>	0.00304	0.00097	0.00155	0.00059	0.00022	-0.0026
<b>0.8</b>	0.00294	0.00083	0.0015	0.00054	0.00017	-0.0025
<b>0.805</b>	0.00284	0.00068	0.00145	0.00049	0.00012	-0.00245
<b>0.81</b>	0.00274	0.00051	0.0014	0.00044	0.00007	-0.0024
<b>0.815</b>	0.00264	0.00033	0.00135	0.00034	0.00002	-0.00235
<b>0.82</b>	0.00254	0.00016	0.0013	0.00024	-0.00003	-0.00233
<b>0.825</b>	0.00244	0	0.00125	0.00014	-0.00008	-0.00231
<b>0.83</b>	0.00234	-0.00012	0.0012	0.00004	-0.00013	-0.00229
<b>0.835</b>	0.00224	-0.00025	0.00115	-0.00006	-0.00018	-0.00227
<b>0.84</b>	0.00214	-0.00037	0.0011	-0.00016	-0.00021	-0.00227
<b>0.845</b>	0.00204	-0.00048	0.00105	-0.00026	-0.00024	-0.00229
<b>0.85</b>	0.00194	-0.00058	0.001	-0.00036	-0.00027	-0.00231

**Table B-4. Altitude-Based Noseboom Static Position Error Pressure Coefficient Model  
(0.855M to 1.035M)**

Mic	Pressure Altitude (ft)					
	2,300	10,000	20,000	30,000	40,000	45,000
<b>0.855</b>	0.00184	-0.00068	0.00095	-0.00043	-0.0003	-0.00235
<b>0.86</b>	0.00174	-0.00078	0.0009	-0.00048	-0.00033	-0.00241
<b>0.865</b>	0.00162	-0.00087	0.00085	-0.00053	-0.00036	-0.00247
<b>0.87</b>	0.0015	-0.00094	0.0008	-0.00058	-0.00039	-0.00253
<b>0.875</b>	0.00138	-0.00101	0.00075	-0.0006	-0.00042	-0.00261
<b>0.88</b>	0.00126	-0.00106	0.0007	-0.00062	-0.00045	-0.00271
<b>0.885</b>	0.00114	-0.00111	0.00065	-0.00064	-0.00048	-0.00283
<b>0.89</b>	0.00102	-0.00116	0.0006	-0.00066	-0.00051	-0.00298
<b>0.895</b>	0.0009	-0.00121	0.00055	-0.00068	-0.00054	-0.00313
<b>0.9</b>	0.00078	-0.00124	0.0005	-0.0007	-0.00057	-0.00328
<b>0.905</b>	0.00066	-0.00129	0.00045	-0.00072	-0.0006	-0.00338
<b>0.91</b>	0.00054	-0.00131	0.0004	-0.00074	-0.00063	-0.00346
<b>0.915</b>		-0.00131	0.00035	-0.00076	-0.00066	-0.00352
<b>0.92</b>		-0.00131	0.0003	-0.00078	-0.00069	-0.00356
<b>0.925</b>		-0.00131	0.0003	-0.0008	-0.0007	-0.00358
<b>0.93</b>		-0.00131	0.0003	-0.00082	-0.0007	-0.00358
<b>0.935</b>		-0.00131	0.0003	-0.00082	-0.0007	-0.00358
<b>0.94</b>		-0.00126	0.00033	-0.00082	-0.0007	-0.00356
<b>0.945</b>		-0.0012	0.00036	-0.00082	-0.0007	-0.00352
<b>0.95</b>		-0.00111	0.00041	-0.0008	-0.0007	-0.00344
<b>0.955</b>		-0.00096	0.00046	-0.00073	-0.0006	-0.00332
<b>0.96</b>		-0.00071	0.00066	-0.00063	-0.0005	-0.00312
<b>0.965</b>		-0.00036	0.00096	-0.00033	-0.00035	-0.00272
<b>0.97</b>		0.00019	0.00141	0.00007	-0.00005	-0.00192
<b>0.975</b>		0.00099	0.00216	0.00057	0.00065	-0.00072
<b>0.98</b>		0.00199	0.00306	0.00137	0.00145	0.00088
<b>0.985</b>		0.00319	0.00426	0.00357	0.00245	0.00288
<b>0.99</b>		0.00569	0.01026	0.00657	0.00395	0.00508
<b>0.995</b>		0.02069	0.01626	0.01007	0.00645	0.00758
<b>1</b>		0.01869	0.02176	0.01607	0.01045	0.01058
<b>1.005</b>		0.01569	0.01976	0.02157	0.01795	0.01658
<b>1.01</b>		0.01069	0.01576	0.01607	0.01595	0.01558
<b>1.015</b>		0.00469	0.01076	0.01107	0.01195	0.01158
<b>1.02</b>		-0.00231	0.00476	0.00607	0.00645	0.00658
<b>1.025</b>		-0.00731	-0.00024	0.00057	0.00095	0.00158
<b>1.03</b>		-0.01231	-0.00524	-0.00393	-0.00455	-0.00442
<b>1.035</b>		-0.01731	-0.01024	-0.00793	-0.00955	-0.00942

**Table B-5. Altitude-Based Noseboom Static Position Error Pressure Coefficient Model  
(1.04M to 1.22M)**

Mic	Pressure Altitude (ft)					
	2,300	10,000	20,000	30,000	40,000	45,000
<b>1.04</b>		-0.02231	-0.01524	-0.01193	-0.01455	-0.01392
<b>1.045</b>		-0.02631	-0.01874	-0.01593	-0.01905	-0.01742
<b>1.05</b>		-0.02431	-0.02124	-0.01893	-0.02305	-0.02042
<b>1.055</b>		-0.02231	-0.02154	-0.02143	-0.02555	-0.02342
<b>1.06</b>			-0.02104	-0.02193	-0.02555	-0.02562
<b>1.065</b>			-0.01964	-0.02193	-0.02455	-0.02552
<b>1.07</b>			-0.01844	-0.02143	-0.02335	-0.02452
<b>1.075</b>			-0.01744	-0.02043	-0.02225	-0.02352
<b>1.08</b>			-0.01664	-0.01943	-0.02125	-0.02252
<b>1.085</b>			-0.01584	-0.01843	-0.02045	-0.02152
<b>1.09</b>			-0.01514	-0.01743	-0.01965	-0.02052
<b>1.095</b>			-0.01444	-0.01673	-0.01895	-0.01972
<b>1.1</b>			-0.01374	-0.01603	-0.01825	-0.01892
<b>1.105</b>			-0.01324	-0.01533	-0.01755	-0.01812
<b>1.11</b>			-0.01274	-0.01483	-0.01685	-0.01732
<b>1.115</b>			-0.01224	-0.01433	-0.01635	-0.01672
<b>1.12</b>			-0.01174	-0.01383	-0.01565	-0.01612
<b>1.125</b>			-0.01134	-0.01333	-0.01495	-0.01562
<b>1.13</b>			-0.01094	-0.01293	-0.01445	-0.01522
<b>1.135</b>			-0.01054	-0.01253	-0.01385	-0.01482
<b>1.14</b>			-0.01014	-0.01213	-0.01325	-0.01442
<b>1.145</b>			-0.00974	-0.01173	-0.01285	-0.01402
<b>1.15</b>			-0.00944	-0.01143	-0.01245	-0.01362
<b>1.155</b>			-0.00914	-0.01113	-0.01205	-0.01322
<b>1.16</b>			-0.00884	-0.01083	-0.01165	-0.01282
<b>1.165</b>			-0.00854	-0.01053	-0.01125	-0.01252
<b>1.17</b>			-0.00824	-0.01023	-0.01095	-0.01222
<b>1.175</b>			-0.00794	-0.00993	-0.01065	-0.01192
<b>1.18</b>			-0.00764	-0.00963	-0.01035	-0.01162
<b>1.185</b>			-0.00734	-0.00933	-0.01005	-0.01137
<b>1.19</b>			-0.00704	-0.00903	-0.00975	-0.01112
<b>1.195</b>			-0.00674	-0.00873	-0.00955	-0.01087
<b>1.2</b>			-0.00644	-0.00843	-0.00935	-0.01062
<b>1.205</b>			-0.00614	-0.00818	-0.00915	-0.01037
<b>1.21</b>			-0.00584	-0.00793	-0.00895	-0.01012
<b>1.215</b>			-0.00554	-0.00768	-0.00875	-0.00992
<b>1.22</b>			-0.00524	-0.00748	-0.00855	-0.00972

**Table B-6. Altitude-Based Noseboom Static Position Error Pressure Coefficient Model  
(1.225M to 1.4M)**

Mic	Pressure Altitude (ft)					
	2,300	10,000	20,000	30,000	40,000	45,000
1.225			-0.00494	-0.00728	-0.00835	-0.00952
1.23			-0.00464	-0.00708	-0.00815	-0.00932
1.235				-0.00688	-0.00795	-0.00912
1.24				-0.00668	-0.00775	-0.00892
1.245				-0.00653	-0.00755	-0.00872
1.25				-0.00638	-0.00735	-0.00852
1.255				-0.00623	-0.00715	-0.00832
1.26				-0.00608	-0.00695	-0.00812
1.265				-0.00598	-0.00675	-0.00792
1.27				-0.00588	-0.0066	-0.00772
1.275				-0.00578	-0.00645	-0.00752
1.28				-0.00568	-0.0063	-0.00732
1.285				-0.00558	-0.00615	-0.00712
1.29				-0.00548	-0.006	-0.00692
1.295				-0.00538	-0.00585	-0.00672
1.3				-0.00528	-0.0057	-0.00652
1.305				-0.00518	-0.00555	-0.00632
1.31				-0.00508	-0.0054	-0.00617
1.315				-0.00498	-0.00525	-0.00602
1.32				-0.00488	-0.0051	-0.00587
1.325				-0.00478	-0.00495	-0.00572
1.33				-0.00468	-0.00485	-0.00562
1.335				-0.00458	-0.00475	-0.00552
1.34				-0.00448	-0.00465	-0.00542
1.345				-0.00438	-0.00455	-0.00532
1.35				-0.00428	-0.00445	-0.00522
1.355				-0.00418	-0.00435	-0.00512
1.36				-0.00408	-0.00425	-0.00502
1.365				-0.00398	-0.00415	-0.00492
1.37				-0.00388	-0.00405	-0.00482
1.375				-0.00378	-0.00395	-0.00472
1.38				-0.00368	-0.00385	-0.00462
1.385				-0.00358	-0.00375	-0.00452
1.39				-0.00348	-0.00365	-0.00442
1.395				-0.00338	-0.00355	-0.004345
1.4				-0.00328	-0.00345	-0.004295

**Table B-7. Noseboom Static Position Error Pressure Coefficient vs. AOA Curve Fit Equations**

Airspeed	Curve Fit Equation	Curve Fit AOA Range (0.1° increments)
0.40 Mach	$-0.00008229\alpha^2 - 0.00012517\alpha + 0.00828170$	5.6° – 9.3°
0.45 Mach	$-0.00144768\alpha + 0.01160285$	4.2° – 7.5°
0.50 Mach	$-0.00012877\alpha^2 + 0.00038308\alpha + 0.0063454$	4.3° – 11.4°
0.55 Mach	$-0.00017844\alpha^2 + 0.00114948\alpha + 0.00319724$	3.4° – 10.7°
0.60 Mach	$-0.00017667\alpha^2 + 0.00077883\alpha + 0.0041$	3.0° – 12.0°
0.65 Mach	$-0.00029349\alpha^2 + 0.00131119\alpha + 0.00206823$	2.7° – 6.8°
0.70 Mach	$-0.00017970\alpha^2 + 0.00073393\alpha + 0.00206548$	3.0° – 9.8°
0.75 Mach	$-0.00011088\alpha^2 - 0.00018674\alpha + 0.00438113$	2.1° – 9.1°
0.80 Mach	$-0.00018351\alpha^2 + 0.00070105\alpha + 0.00108246$	1.9° – 9.3°
0.85 Mach	$-0.00014725\alpha^2 + 0.00084508\alpha - 0.00054404$	1.8° – 8.5°
0.90 Mach	$-0.00028968\alpha^2 + 0.00153423\alpha - 0.00203805$	1.8° – 6.8°
1.10 Mach	$-0.00200397\alpha - 0.00818215$	2.1° – 4.8°
1.15 Mach	$-0.00178042\alpha - 0.00565330$	1.8° – 4.3°
1.20 Mach	$-0.00183429\alpha - 0.00330580$	1.7° – 4.1°
1.25 Mach	$-0.00112940\alpha - 0.00389062$	1.8° – 3.9°

**Table B-8. Tower Fly By Total Air Temperature Probe Recovery Factor and Bias**

<b>Event (2,300 ft PA)</b>	<b>K<sub>t</sub></b>	<b>T<sub>bias</sub></b>
Tower Fly By #1	0.9383	-0.0025
Tower Fly By #2	0.9333	-0.0016
Tower Fly By #3	0.9941	-0.0066
Tower Fly By #4	1.0224	0.0013

**Table B-9. At Altitude Temperature Probe Recovery Factor, Bias & Ambient Air Temperature Error**

	<b>15 Mar 2010</b>			<b>16 Mar 2010</b>			<b>30 Mar 2010</b>		
<b>Altitude</b>	<b>K<sub>t</sub></b>	<b>T<sub>bias</sub></b>	<b>T<sub>a, error</sub></b>	<b>K<sub>t</sub></b>	<b>T<sub>bias</sub></b>	<b>T<sub>a, error</sub></b>	<b>K<sub>t</sub></b>	<b>T<sub>bias</sub></b>	<b>T<sub>a, error</sub></b>
<b>10 K PA</b>	0.9215	0.00007	0.0	0.8079	0.0055	0.3	0.9419	0.002	0.1
<b>20 K PA</b>	0.9521	0.0031	0.2	0.9808	-0.0224	-1.1	0.8848	0.0075	0.4
<b>30 K PA</b>	0.9584	0.0039	0.2	1.1773	-0.022	-1.0	0.9328	0.0066	0.3
<b>40 K PA</b>	0.9411	0.0116	0.5	1.0051	0.0259	1.1	1.0396	-0.0079	-0.3
<b>45 K PA</b>	1.0675	-0.0075	-0.3	0.9994	0.0292	1.2	1.0306	0.0022	0.1

**Table B-10. Total Air Temperature Probe Recovery Factor Comparison**

	<b>K<sub>t</sub>, Traditional Method</b>			<b>K<sub>t</sub>, Alternate Plotting Technique</b>		
	<b>15 March 10</b>	<b>16 March 10</b>	<b>30 Mar 10</b>	<b>15 March 10</b>	<b>16 March 10</b>	<b>30 Mar 10</b>
<b>10 K ft PA</b>	0.9215	0.8079	0.9419	0.9181	0.8051	0.9480
<b>20 K ft PA</b>	0.9521	0.9808	0.8848	0.9552	1.0062	0.8819
<b>30 K ft PA</b>	0.9584	1.1773	0.9328	0.9553	1.2103	0.9300
<b>40 K ft PA</b>	0.9411	1.0051	1.0396	0.9704	0.9776	1.0477
<b>45 K ft PA</b>	1.0675	0.9994	1.0306	1.0810	0.9605	1.0258

**Table B-11. Calculated vs. Weather Balloon Ambient Air Temperatures**

	<b>15 March 2010</b>	<b>16 March 2010</b>	<b>30 Mar 2010</b>
	<b>T<sub>a, cal</sub> / T<sub>a, bal</sub></b>	<b>T<sub>a, cal</sub> / T<sub>a, bal</sub></b>	<b>T<sub>a, cal</sub> / T<sub>a, bal</sub></b>
<b>10 K ft PA</b>	277.8 / 276.5	277.8 / 277.9	277.8 / 277.9
<b>20 K ft PA</b>	256.4 / 256.4	250.0 / 256.2	263.2 / 259.1
<b>30 K ft PA</b>	232.6 / 231.5	227.3 / 231.8	232.6 / 233.2
<b>40 K ft PA</b>	212.8 / 211.3	217.4 / 212.1	208.3 / 209.9
<b>45 K ft PA</b>	208.3 / 213.1	222.2 / 213	208.3 / 208

**This page intentionally left blank.**

## **APPENDIX C – DAS DATA PARAMETERS**

**Table C-1. DAS Data Parameters**

<b>DAS Parameter</b>	<b>Description</b>
*AIRSPEED_SYS_1	SYSTEM 1 INSTRUMENT CORRECTED AIRSPEED (KTS)
*AIRSPEED_SYS_2	SYSTEM 2 INSTRUMENT CORRECTED AIRSPEED (KTS)
ALT_CALIB_SYS1	Instrum and Source Corrected press alt
ALT_CALIB_SYS2	Instrum and Source Corrected press alt
AMB_AIR_TEMP1	AMB_AIR_TEMP1
AMB_AIR_TEMP1_K	AMB AIR TEMP IN KELVIN
AMB_AIR_TEMP2	AMB_AIR_TEMP2
AMB_AIR_TEMP2_K	AMB AIR TEMP2 IN KELVIN
*AOA	NOSEBOOM AOA, ALIGNMENT CORRECTED (DEG)
AS_CALIB_SYS1	Instrum and Source Corrected airspeed
AS_CALIB_SYS2	Instrum and Source Corrected airspeed
C001_02B	PRESSURE ALTITUDE
C001_04B	TRUE AIR SPEED
C001_05B	MACH
C001_06B	CALIBRATED AIR SPEED
C001_07B	TRUE AOA
C001_10B_C	FREE AIRSTREAM AIR TEMP (C)
C001_10B_F	FREE STREAM AIR TEMP
C001_10B_K	FREE STREAM AIR TEMP
COCKPIT_VOICE	COCKPIT_VOICE
EVENT_MARKER	EVENT_MARKER
*FQA	AFT TANK FUEL QUANTITY (LBS)
*FQF	FORWARD FUEL QUANTITY (LBS)
*FQT	TOTAL FUEL QUANTITY (LBS)
IN001_10C	ROLL ANGLE
*IN001_10C_DEG	ROLL ANGLE
IN001_11C	PITCH ANGLE
*IN001_11C_DEG	PITCH ANGLE
IN001_12C	TRUE HEADING
IN001_12C_DEG	TRUE HEADING

\*used in data reduction for Pace Maker objectives

**Table C-1 (Continued). DAS Data Parameters**

<b>DAS Parameter</b>	<b>Description</b>
*IRIG_TIME	IRIG TIME (DDD:HH:MM:SS.S)
LOAD_CELL	LOAD_CELL
NZ	NZ FROM FC
P_A_SYS1	Ambient Air Pressure system 1
P_A_SYS2	Ambient Air Pressure system 2
*P1_PRESS_ALT	SYSTEM 1 INSTRUMENT CORRECTED PRESSURE ALT (FT)
*P3_PRESS_ALT	SYSTEM 3 INSTRUMENT CORRECTED PRESSURE ALT (FT)
PARO_1_STATIC_P	STATIC PRESSURE
PARO_1_TEMP	PARO_1_TEMP
PARO_2_TEMP	PARO_2_TEMP
PARO_2_TOTAL_P	TOTAL PRESSURE
PARO_3_STATIC_P	STATIC PRESSURE
PARO_3_TEMP	PARO_3_TEMP
PARO_4_TEMP	PARO_4_TEMP
PARO_4_TOTAL_P	TOTAL PRESSURE
*PARO_TC_PR_ALT	TRAILING CODE PRESSURE ALTITUDE (FT)
PARO_TC_PRESS	PARO_TC_PRESS
PARO_TC_TEMP	PARO_TC_TEMP
PARO_TC_TEMPF	PARO_TC_TEMPF
*PITCH_RATE	PITCH_RATE FROM FC
RL001_4D_A	RADAR ALTITUDE
ROLL_RATE	ROLL_RATE FROM FC
TAT_DEGC	TAT_DEGC
TAT_DEGF	TAT_DEGF
*TAT_K	TAT_K
TAT2_DEGC	TAT2_DEGC
TAT2_DEGF	TAT2_DEGF
*TAT2_K	TAT2_K
YAW_RATE	YAW_RATE FROM FC

\*used in data reduction for Pace Maker objectives

**This page intentionally left blank.**

# **APPENDIX D – PITOT-STATIC DATA REDUCTION METHODS**

## GENERAL

Data for the trailing cone and test noseboom were reduced in parallel, and neither was used as a truth source for the other. Identical methods were used for both systems, and a total pressure error of zero was assumed. Analysis of the trailing cone data stopped at the determination of the static position error ratio ( $\Delta P_p/P_s$ ); whereas, the test noseboom followed the entire process outlined below.

## TRUTH PRESSURE ALTITUDE DETERMINATION / PITCH ANGLE CORRECTIONS

During the analysis for both the trailing cone and the test noseboom, the static position error ratio ( $\Delta P_p/P_s$ ) and the static position error pressure coefficient ( $\Delta P_p/q_{cic}$ ) were determined by comparing indicated pressure altitude to a truth source pressure altitude. During the tower flyby sorties, grid readings were used to compute the geometric altitude of the noseboom pressure transducer, which was then corrected for ambient temperature to derive truth pressure altitude. Based on the pitch angle ( $\theta$ ) at the time of data collection (see figure 1), the trailing cone transducer pressure altitude was derived from basic rotational trigonometry. At higher altitudes, the aircraft geometric height was determined from a GPS-aided C2B G-Lite system, and noseboom and trailing-cone transducer altitudes were calculated by using the C2B as a pivot point and rotating through  $\theta$ . Those values were then compared to time-adjusted Rawisonde balloon measurements of geometric height and ambient pressure, to determine truth pressure altitude.

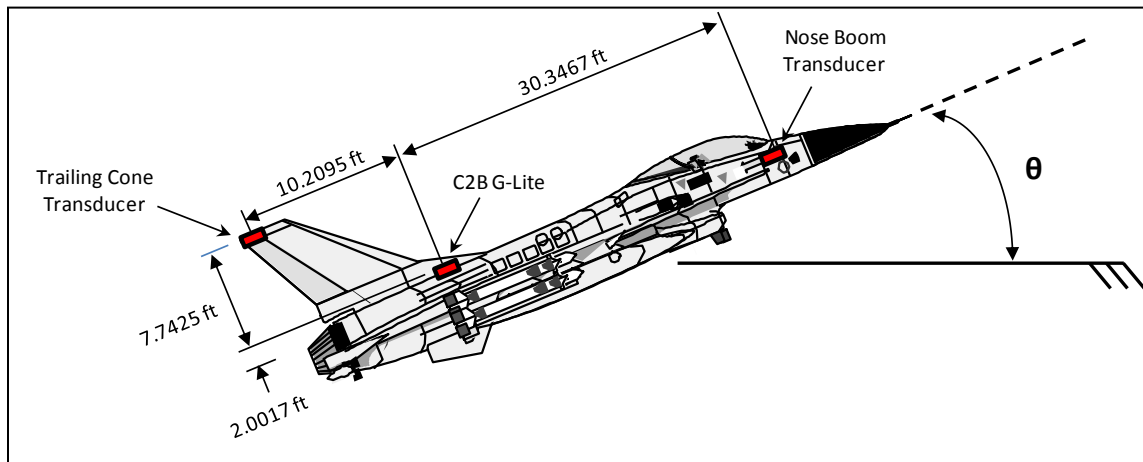


**Figure D-1. Transducer Trigonometric Relationships**

## STATIC POSITION ERROR RATIO

Given the truth pressure altitude ( $H_c$ ) and the instrument corrected pressure altitude as measured by the DAS ( $H_{ic}$ ), the pressure altitude position correction ( $\Delta H_{pc}$ ) was given by:

$$\Delta H_{pc} = H_c - H_{ic}$$

The pressure ratio ( $\delta$ ) and instrument corrected pressure ratio ( $\delta_{ic}$ ) were calculated via the following.

$$\delta = \begin{cases} (1 - 6.87559H_c \times 10^{-6})^{5.2559}, & H_c < 36,089.24 \text{ ft} \\ 0.223360e^{(-4.80637 \times 10^{-5}(H_c - 36089.24))}, & H_c \geq 36,089.24 \text{ ft} \end{cases}$$

$$\delta_{ic} = \begin{cases} (1 - 6.87559H_{ic} \times 10^{-6})^{5.2559}, & H_{ic} < 36,089.24 \text{ ft} \\ 0.223360e^{(-4.80637 \times 10^{-5}(H_{ic} - 36089.24))}, & H_{ic} \geq 36,089.24 \text{ ft} \end{cases}$$

The temperature ratio ( $\theta$ ) was derived by comparing the truth ambient temperature ( $T_A$ ) in Kelvin to the standard day ambient temperature at sea level ( $T_{SL} = 288.15 \text{ K}$ ).

$$\theta = \frac{T_A}{T_{SL}}$$

The density ratio arose from the division of the pressure and temperature ratios.

$$\sigma = \frac{\delta}{\theta}$$

The static position error ratio ( $\Delta P_p/P_s$ ) was then determined by

$$\frac{\Delta P_p}{P_s} = 1 - \frac{\delta}{\delta_{ic}}$$

## STATIC POSITION ERROR PRESSURE COEFFICIENT

The static position error pressure coefficient was determined through a series of calculations involving specific ratios of dynamic pressure ( $q_c$ ), instrument corrected dynamic pressure ( $q_{cic}$ ), standard day ambient pressure at sea level ( $P_{SL}$ ), and ambient pressure ( $P_a$ ). Different tracks were followed depending on whether the instrument corrected airspeed ( $V_{ic}$ ) was less than or greater than the speed of sound at sea level ( $a_{SL} = 661.48 \text{ knots}$ ). The method followed the sequence outlined below.

$$\frac{q_{cic}}{P_{SL}} = \begin{cases} \left(1 + 0.2 \left(\frac{V_{ic}}{a_{SL}}\right)^2\right)^{7/2} - 1, & V_{ic} < a_{SL} \\ \frac{166.921 \left(\frac{V_{ic}}{a_{SL}}\right)^7}{\left(7 \left(\frac{V_{ic}}{a_{SL}}\right)^2 - 1\right)^{5/2}} - 1, & V_{ic} \geq a_{SL} \end{cases}$$

$$\frac{q_{cic}}{P_s} = \frac{q_{cic}/P_{SL}}{\delta_{ic}}$$

$$\frac{q_c}{P_a} = \frac{\frac{q_{cic}}{P_s} + 1}{1 - \frac{\Delta P_p}{P_s}} - 1$$

$$\frac{q_c}{P_{SL}} = \frac{q_c}{P_a} \delta$$

$$\frac{\Delta P_p}{q_{cic}} = \frac{\frac{\Delta P_p}{P_s}}{\frac{q_{cic}}{P_s}}$$

### AIRSPED POSITION CORRECTION

The truth calibrated airspeed ( $V_c$ ) was then calculated from the  $q_c/P_{SL}$  ratio, in accordance with the following. When required, iteration was taken to three cycles.

$$V_c = \begin{cases} a_{SL} \sqrt{5 \left( \left( \frac{q_c}{P_{SL}} + 1 \right)^{2/7} - 1 \right)}, & \frac{q_c}{P_{SL}} < 0.89293 \\ 0.881284 a_{SL} \sqrt{\left( \frac{q_c}{P_{SL}} + 1 \right) \left( 1 - \frac{1}{7 \left( \frac{V_c}{a_{SL}} \right)^2} \right)^{5/2}}, & \frac{q_c}{P_{SL}} \geq 0.89293 \end{cases}$$

Given the truth calibrated airspeed from the above and the instrument corrected airspeed from the DAS, the airspeed position correction ( $\Delta V_{pc}$ ) was easily determined by measuring the difference.

$$\Delta V_{pc} = V_c - V_{ic}$$

### MACH NUMBER POSITION CORRECTION

True Mach number ( $M_{pc}$ ) and instrument corrected Mach number ( $M_{ic}$ ) were calculated from  $q_c/P_a$  and  $q_{cic}/P_s$ , respectively. When required, iteration was taken to three cycles.

$$M_{pc} = \begin{cases} \sqrt{5 \left[ \left( \frac{q_c}{P_a} + 1 \right)^{2/7} - 1 \right]}, & \frac{q_c}{P_a} < 0.89293 \\ 0.881284 \sqrt{\left( \frac{q_c}{P_a} + 1 \right) \left( 1 - \frac{1}{7 M_{pc}^2} \right)^{5/2}}, & \frac{q_c}{P_a} \geq 0.89293 \end{cases}$$

$$M_{ic} = \begin{cases} \sqrt{5 \left[ \left( \frac{q_{cic}}{P_s} + 1 \right)^{2/7} - 1 \right]}, & \frac{q_{cic}}{P_s} < 0.89293 \\ 0.881284 \sqrt{\left( \frac{q_{cic}}{P_s} + 1 \right) \left( 1 - \frac{1}{7 M_{ic}^2} \right)^{5/2}}, & \frac{q_{cic}}{P_s} \geq 0.89293 \end{cases}$$

The Mach number position correction ( $\Delta M_{pc}$ ) was then calculated from the difference between the two Mach values.

$$\Delta M_{pc} = M_{pc} - M_{ic}$$

# **APPENDIX E – ABBREVIATIONS AND ACRONYMS**

## LIST OF ABBREVIATIONS, ACRONYMS, AND SYMBOLS

<u>Abbreviation</u>	<u>Definition</u>	<u>Units</u>
AFFTC	Air Force Flight Test Center	---
AGE	Aircraft Ground Equipment	---
AOA	angle of attack	deg
AOB	angle of bank	deg
AOSS	angle of sideslip	deg
ARDS	Advanced Range Data System	---
CADC	Central Air Data Computer	---
CLETIS	Cone Length Extension Tube Investigative Study	---
DAS	data acquisition system	---
Degrees C	Degrees Celsius	---
EGI	Embedded GPS INS	---
FTE	flight test engineer	---
FTT	flight test technique	---
GAINR	GPS Aided Inertial Navigation Reference	---
GLite C2B	GAINR Lite – TSPI source	---
Hg	mercury	---
HUD	heads up display	---
IAW	in accordance with	---
ICP	Instrument control panel	---
IRIG time	Inter-range instrumentation group time	---
JON	Job Order Number	---
LCD	Liquid crystal display	---
MIL	military power	---
MOP	measure of performance	---
MUX	Multiplexor	---
N/A	non-applicable	---
NOTAM	Notices to airmen	---
PA	pressure altitude	---
PADI	Pacer air data instrumentation	---
PCM	Pulse code modulation	---

PCMCIA	Personal computer memory card international association	---
POC	Point of contact	---
PSIa	Pounds force per square inch absolute	---
RMCC	Ridley Mission Control Center	---
RMM	remote management module	---
RTO	responsible test organization	---
S/N	Serial number	---
SCG	Security classification guide	---
sq. feet	square feet	---
SRB	safety review board	---
STBY	standby	---
TIM	technical information memorandum	---
TM	Telemetry	---
TMP	Test Management Project	---
TPS	Test Pilot School	---
TSPI	Time, Space, Position, Information	---
TTC	Teletronics Technology Corporation	---
VMC	Visual meteorological conditions	---
YAPS	yaw angle of attack Pitot-static	---

**This page intentionally left blank.**

## **APPENDIX F – DISTRIBUTION LIST**

Onsite Distribution

	<u>Number of Copies</u>	
	Color Hard Copy	CD ROM (PDF)

USAF TPS/EDT  
220 South Wolfe Ave  
Edwards, CA 93524

1	1
---	---

USAF TPS/CS (Attn: Dottie Meyer)  
220 South Wolfe Ave  
Edwards, CA 93524

1	1
---	---

USAF TPS/EDP (Attn: Russell Erb)  
220 South Wolfe Ave  
Edwards, CA 93524

8	8
---	---

USAF TPS/SI (Attn: Vinh Pham)  
220 South Wolfe Ave  
Edwards, CA 93524

1	1
---	---

Rohmann Services (Attn: Chad Bellay)  
305 E Popson Ave, Bldg 1405  
Edwards, CA 93524

1	1
---	---

Frank Brown  
773TS/ENFB  
Room 102  
Building 1400  
Edwards, CA 93524

2	2
---	---

412 TW/ENTL (AFFTC Technical Library)  
307 E Popson Blvd, Bldg 1400, Room 110  
Edwards AFB, CA 93524-6630

1	1
---	---

AFFTC/HO  
305 E Popson Ave, Bldg 1405  
Edwards AFB CA 93524-6630

1	1
---	---

Offsite Distribution

40 FLTS  
Captain James Pate  
505 W Choctawhatchee Ave Ste 1  
Eglin AFB, FL 32542

1	1
---	---

---

Total

17	17
----	----